The VLT White Book

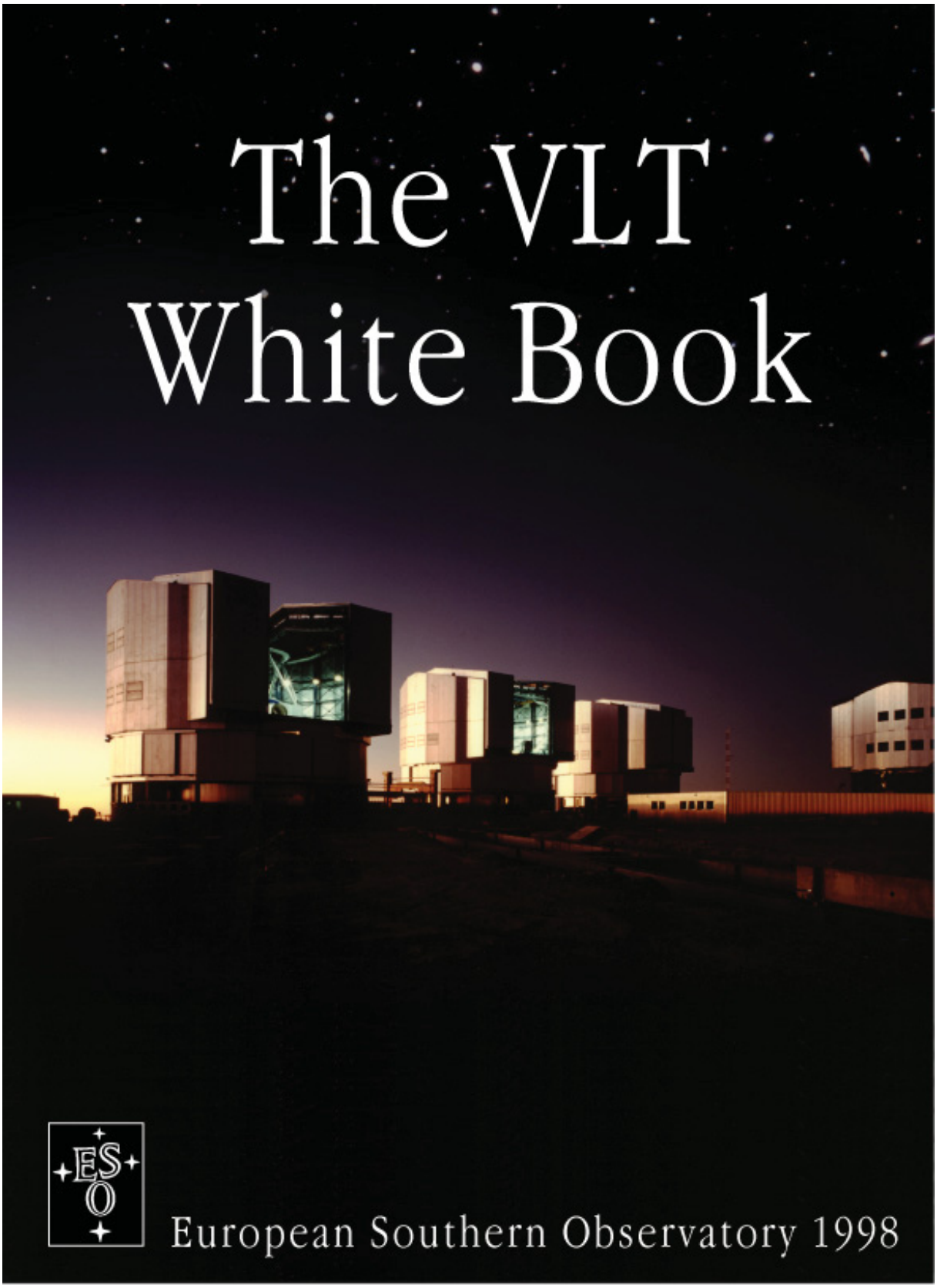

European Southern Observatory 1998

VLT Whitebook - List of Contents

VLT Whitebook: Introduction

The publication of the VLT Whitebook is part of a general effort by ESO to inform the astronomical user community of the member states about the basic concepts which have guided the design and development of the hardware and operating systems of the VLT/VLTI project and of the new observatory on Paranal.

As the complexity of individual telescopes and their related instrumentation keeps growing, it is difficult even for the professional astronomer to be intimately conversant with all of the details which will permit the most effective utilization of the facility. In addition to direct experience at the telescopes used in all their different modes, it will be necessary to develop, both in the ESO Staff and in the user community, an in-depth working knowledge of the most effective observing strategies.

While this overall description of VLT/VLTI and Paranal can not be carried out to the depth required by the specialist, it is intended to give a solid overview of the baseline configuration of telescopes, instruments and operating systems.

We conceive of the VLT/VLTI telescope array and all auxiliary facilities on Paranal as the observing element of an institutional structure intended to offer European Astronomers up-to-date facilities to do science. Some of the elements necessary for the operation of this structure are embodied by operational units at ESO's Headquarters in Germany as well as in Chile.

In particular, proposal solicitation and evaluation, program selection, initial programme schedule, as well as observing block preparation and transmittal to Paranal for execution are carried out at Garching. Detailed scheduling, support to astronomers in either service or visitors mode, real time diagnostics and optimization of the observations occur on Paranal. ESO in Chile also provides logistic support including transportation and housing for visiting astronomers. Data are reduced and stored in the ESO archive at Garching and from there distributed to the observers. This distributed approach to the execution of the functions is common to the La Silla and Paranal observatories. Also common is the development of detectors, instruments and software. This permits a very efficient use of our resources. Communications between the different functional groups is essential for the effective and successful completion of the scientific programmes. It is important for the best results that not only the ESO Staff, but the full user community, be appraised of our procedures and schedules.

This new powerful facility on Paranal clearly gives the European Astronomical Community a fully competitive tool in ground based optical astronomy for the first time in this century. It is the result of literally thousands of man-years of effort by ESO, European Institutions and European Industry. The impact which it will have on all branches of astronomy will hopefully only be limited by our ability to use it to its full potential.

Riccardo Giacconi
Director General
ESO

Chapter 1: VLT Concepts and Performance

The ESO Very Large Telescope (VLT) provides the European scientific community with a ground-based telescope of collecting power greater than currently available facilities, offering basic imaging and spectroscopic capabilities at visible and infra-red wavelengths. The concept selected is an array of four identical, independent 8.2-metre *Unit Telescopes* (*UTs*). When joined with several 1.8-m *Auxiliary Telescopes* (*ATs*) into an interferometric array, this facility will achieve very high spatial resolution at unequalled sensitivity.

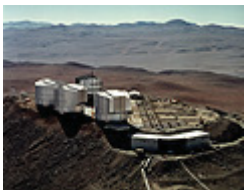

Figure 1.1 [JPG: 256k]. An aerial view of the Paranal summit in mid-April 1998 with the large observatory platform on which the many components of VLT were being installed. The four enclosures (telescope `domes') are seen, three of which have been closed. The long, subterranean interferometric tunnel is in the middle. The concrete supports for the smaller, moveable telescopes of the VLT Interferometric Array are located all over the platform, together with the foundations for the tracks. The VLT control building, from where the observations with the four large telescopes will be made, is placed on a smaller and slightly lower platform in the foreground.

The VLT is located on **Cerro Paranal** in Northern Chile (70 o 24' 11" W; 24 o 37' 31" S) at an altitude of 2635 meters. It operates at wavelengths ranging from 0.3 to 25 µm, combining very high sensitivity with very high angular resolution over adequate fields-of-view (FOV).

Its four identical 8.2-meter diameter telescopes (known as **Unit Telescopes** , or UTs) and its three smaller **Auxiliary Telescopes** (or ATs) can be used in several different modes:

- the **Independent Telescope Mode** using each UT separately, each feeding one of its four foci (one Cassegrain, two Nasmyth and one coudé),
- the **Combined Coherent Mode** , or **VLT Interferometer (VLTI)** , in which two or more UTs, two or more ATs, or UTs and ATs together are combined interferometrically to give an angular resolution equivalent to a telescope with up to 200 meters diameter. The interferometric modes are equipped with their own set of scientific instruments. In addition, it is in principle also possible to implement
- a **Combined Incoherent Mode** , combining light from the four UTs into one telescope with a 16-meter equivalent collecting area.

This chapter discusses the main concepts and overall performance of the VLT, based on the scientific objectives.

1.1 Scientific Objectives and Technical Requirements

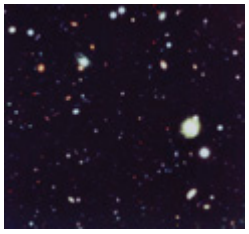

Figure 1.2 [JPG: 456k]. NTT SUSI Deep Field (linear intensity scale). This colour image was obtained in 1997 at the 3.5-m New Technology Telescope. It shows objects as faint as 26th magnitude and illustrates well the performance in deep imaging at good angular resolution with a relatively modest investment in exposure time at a 4m-class ground-based telescope. Of the approximately 500 galaxies detected in this field, the largest fraction are expected to be at redshifts smaller than z = 1 and about 20 percent to have higher redshifts, up to z = 4 and possibly beyond. Spectra of many such objects can be obtained efficiently with the VLT.

Thanks to its flexibility, the VLT is able to quickly respond to new scientific challenges raised by the rapid advances of astronomical knowledge. While it is difficult to anticipate what such challenges will be ten or more years ahead, the astronomical community has identified some **basic scientific issues** which have been used in driving the design of the VLT, its scientific instrumentation, and operational modes, e.g.:

- Measure the fundamental parameters of the Universe;
- Push as far as possible the search for the emergence of the first light in the Universe;
- Detect and study galaxies in the act of their formation;
- Unravel the evolution and metamorphosis of galaxies with cosmic time, from their formation to the present;
- Map the emergence and growth of large scale structures;
- Elucidate the connection between galaxy formation and the present physical conditions in the nuclei of galaxies, both active and inactive;
- Study the birth of stars and protoplanetary systems, out of the interstellar medium;
- Refine our understanding of the evolution of single and binary stars all the way to their final stages;
- Discover extrasolar planetary systems and characterize them to prepare for their further study from space; and
- Expand our knowledge of solar system bodies.

The **concepts and performance** of the VLT stem from top guidelines that were established to accommodate the diverse scientific needs of the wide ESO community. According to these, the VLT should have:

- the largest possible collecting area, given the available resources;
- the widest wavelength coverage, to fully exploit all atmospheric windows;
- Maximum flexibility and wide instrumental diversification, allowing multiple use of the facility including simultaneous multi-wavelength observations;
- Diffraction-limited capability over the largest possible baseline; and
- Optimization of science operation procedures, to allow full, real time exploitation of the astronomical quality of the site and guarantee maximum scientific return.

1.2 Implementation and Future Optimization

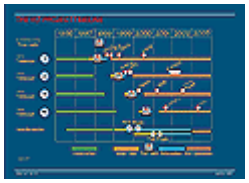

Figure 1.3 [JPG: 492k]. The VLT Project Timeline (status February 1998).

The VLT and its many subsystems are in the process of being implemented. First Light at UT1 is expected in May 1998. Some of the subsequent milestones are indicated in Figure 1.3.

The **lifetime** of the VLT is expected to exceed 25 years. During this lifetime the VLT, its instrumentation and data systems are expected to undergo major upgrades to ensure that the facilities remain fully competitive as technology improves and as science requirements evolve.

Each of the VLT focal instruments will generally remain fixed at one specific focus of a UT. This will ensure that all instruments operate in a stable environment, reducing overheads. This also allows a minimum of 12 focal instruments (3 at each UT) to operate, with the possibility of switching rapidly from one to another.

The instruments will be modified, upgraded, and eventually replaced, maintaining state-of-the-art technology and following the evolving scientific needs. The lifetime of each scientific instrument is expected to be in the range of 7 to 12 years.

Within the constraint of sufficient optical identity of the four UTs to ensure the interferometric mode, it is planned to optimize three UTs in the IR, by adopting appropriate coatings and reducing the obstruction emissivity.

1.3 Performance Requirements

This chapter summarizes some of the main features of the VLT that are required to perform the various front-line scientific investigations to be undertaken with this facility.

Outstanding **angular resolution** has the highest scientific priority for the VLT. For this, UT1 will have **Adaptive Optics (AO)** correction both at Nasmyth and at Cassegrain foci. UT1 will also host a **Sodium Laser Guide Star Facility** for Adaptive Optics.

For the non-AO telescope operation, the global image quality criterion for the VLT is the **Central Intensity Ratio (CIR)** which is the ratio of the central intensity of the point-spread-function of the actual telescope to that of a perfect telescope. For the 5 percentile best seeing condition, corresponding to a seeing of 0.4 arcsec FWHM (Full Width Half Maximum) for long exposures towards zenith and at 500 nm wavelength, the CIR for 60 minutes exposures at all foci exceeds 50% at first light and 80% within three years thereafter. This CIR includes the effects of optical quality, telescope and enclosure seeing, wind buffeting of the mirrors and the telescope structure, tracking and differential seeing motions between the guide star and the science object. The CIR criterion will be met for the 90 percentile wind velocity at 0.4 arcsec seeing for all usable wavelengths and zenith angles, with the appropriate adjustment for wavelength and zenith distance variation of the 5 percentile seeing FWHM. This CIR criterion is met without the aid of adaptive optics or fast guiding.

It is essential for the VLT to have a **wide field-of-view (FOV)** to achieve several of its primary scientific goals. To this end, the maximum allowable deterioration of the image quality (CIR) compared to the on-axis performance is less than 10% over a 10 arcmin diameter flat FOV, or over a curved FOV of 20 and 30 arcmin diameter, respectively for the Cassegrain and Nasmyth foci. At the coudé focus, the CIR for diffraction limited images does not deteriorate by more than 5% over the size of the isoplanatic patch for all wavelengths.

Atmospheric dispersion is corrected up to zenith angles of 50 o for instruments requiring high image and spectrophotometric quality. The image quality deterioration does not exceed 10% for images taken through broad-band filters, and spectrophotometric errors do not increase by more than 5%.

High throughput over the entire 0.3 - 25 μm spectral range is essential for the VLT to achieve its scientific goals. To this end, the transmission in the unobscured areas of the pupil at all times is better than 76%, 66% and 50%, at the Cassegrain, Nasmyth, and coudé foci, respectively, at 0.32 μm. For the IR-optimized telescopes the throughput at 0.85 μm will not drop below 91%, 86%, and 65% for Cassegrain, Nasmyth, and coudé, respectively.

The IR optimized telescopes have a **thermal emissivity** above 2 μm that is less than 4%, 5% and 10% at the Cassegrain, Nasmyth and coudé foci, respectively. For the UV-optimized telescopes, 3 times higher values are acceptable.

Accurate pointing and tracking of the telescopes is essential for maximizing the efficiency of the VLT. All UTs and ATs are able to acquire in less than 3 minutes any target to within 70 o zenith distance. Offset pointing of 45 o and 60 o in elevation and azimuth respectively is possible within 35 seconds, to within 0.1 arcsec accuracy relative to the telescope encoders. A pointing model provides the absolute pointing coordinates of the acquired target to within 3 arcsec RMS at first light and within 1.5 arcsec RMS 3 years thereafter.

Using offset pointing UTs and ATs will achieve an **absolute RMS pointing accuracy** of 0.10 arcsec RMS at 0.5 μm, provided a suitable reference star is available within 1 o 20' (10' for the ATs). The absolute pointing procedure takes no more than 20 seconds.

The UTs will **track** to better than 0.05 arcsec RMS over any 15 seconds period without using guide-star position information, and over a one hour period when using guide-star tracking. If the guide star falls within the isoplanatic patch for wavefront tilts, rapid guiding is provided to reduce the guide star motions by at least a factor of 5.

The secondary mirrors of the IR-optimized UTs allow **chopping of the image** with a throw on the sky varying from 0.1 to 30 arcsec in any sky direction, a frequency of at least 5 Hz at a duty cycle of 80%. Short (< 10 seconds) and long term (> 10 seconds) throw reproducibilities are respectively 0.12% RMS and 0.3% RMS for throws above 10 arcsec, and 0.012 arcsec RMS and 0.030 arcsec RMS for throws less than 10 arcsec.

The UTs can operate at **zenith distances** ranging from 0.5 o to 70 o. Any obstruction by adjacent enclosures is limited to zenith angles larger than 60 o.

UT1 will be equipped with **adaptive optics** designed to give a Strehl Ratio larger than 70% at wavelength 2.2 μm for 0.6 arcsec seeing at 0.55 μm when using a natural guide star brighter than V = 13. The Adaptive Optics system bandwidth is high enough to maintain this performance down to 1 μm for 0.45 arcsec seeing at 0.55 μm. An artificial reference star will be implemented to extend the sky coverage to at least 35% in the K-band, while allowing for a decrease in Strehl Ratio by at most a factor of two.

An important feature of the VLT project has been the development of an **end-to-end model** of the UTs, cf. Chapter 2.9. It encompasses many of the subsystems (optical, mechanical, control hard- and software), as well as environmental parameters (atmospheric, seismic). This very useful tool allows to predict the telescope performance under different conditions.

1.4 The VLT Interferometer (VLTI)

The VLT possesses unique interferometric capabilities in the **Combined Coherent Mode (VLT Interferometer; VLTI)** (cf. Chapter 9). In particular, with its unequalled mirror area, this will allow imaging and spectral observations at very high angular resolution (milliarcsec level) with the **highest sensitivity** available at any facility.

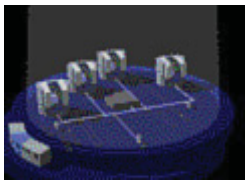

Figure 1.4 [JPG: 160k]. Schematic representation of the VLTI components. It shows the underground paths of the collimated beams from the telescopes to the long, centrally located delay-line tunnel and onwards to the centrally located Interferometric Laboratory. The VLT Control Building is to the left.

For instance, the VLTI will be able to detect and characterize low mass companions around main sequence and pre-main sequence stars, to image the circumstellar environment of stars in nearby star forming regions, to resolve the star cluster at the centre of our Galaxy and to probe the broad line region of nearby Active Galaxy Nuclei (AGNs).

In terms of **technical performance** , the VLTI facility will

- achieve an effective angular resolution of 1 milliarcsec (mas) at wavelength 1 μm,
- cover the wavelength region from 0.5 to 25 μm with spectral resolutions of up to 10000 at 2.2 μm,
- reach a narrow-angle astrometric precision of 10 μarcsec accuracy,
- allow simultaneous operation of at least two UTs and three ATs for proper uv-plane coverage and phase retrieval,
- reach an overall sensitivity corresponding to a limiting magnitude of K = 23 while fringe tracking on a reference source, and
- provide the capability to reference on a source of brightness greater than K = 16 located within 30 arcsec from the primary target anywhere at zenith distances less than 60 o.

These requirements are satisfied when the VLTI is capable of delivering to the focal instrument a proper fringe contrast efficiency which is defined as the maximal fringe contrast obtainable at the coherent combined focus when observing a monochromatic point source. It includes all atmospheric, telescope and instrumental effects down to the interferometric laboratory. This implies, in particular, that all coudé foci will incorporate an Adaptive Optics corrector.

Two major **modes of observation** are distinguished: a **Co-phased Mode** , in which the image is diffraction limited (mono-speckle) and the interferometer is co-phased by fringe tracking, and a **Blind Mode** , in which the interferometer is not co-phased.

In the first case, the instrument can integrate over long exposure times while, in the second, it performs short duration exposures to freeze the atmospheric effects while the delay lines track the estimated mean geometric delay. For both these modes, the **environmental conditions** are assumed to be 0.66 arcsec atmospheric seeing at 0.5 μm, 8 msec atmospheric coherence time at 0.5 μm, less than 10 m/s wind speed, and no occurrence of significant seismic events.

The **fringe contrast efficiency in the co-phased mode** will exceed 60% at an observing wavelength of 2.2 μm for a source brighter than K = 8. This fringe contrast criterion includes effects due to optical design, optics imperfections, polarisation effects, internal seeing, Adaptive Optics residuals, fringe tracking residuals, differential image guiding, unequal beam intensities and vibrations. Calibration of the fringe contrast will enable to recover the actual fringe contrast to 5% accuracy.

The **fringe contrast efficiency in the blind mode** (within each speckle) will exceed 70% at any wavelength. This fringe contrast criterion includes effects due to residual high frequency atmospheric and internal seeing effects, polarisation effects, unequal beam intensities and vibrations. Calibration of the fringe contrast will enable to recover the actual fringe contrast to 5% accuracy.

The VLTI optics will be provided with **coatings** which optimize the VLTI transmission in the 0.5-20 μm wavelength region with more than 97% average efficiency per reflection. All UT coudé trains and all AT optics will have the same coatings.

The VLTI has an **unvignetted field-of-view** of 2 arcsec diameter on axis at 0.5 μm for the UTs, and 1.4 arcsec diameter on axis at 0.5 μm for the ATs. The same field will be available for a reference source located within 30 arcsec off axis.

1.5 Instrumentation

To achieve its scientific goals, the VLT is equipped with **first class, innovative, fullycompetitive, high-performance focal instruments** that are mounted quasi-permanently at the respective foci.

Figure 1.5 [JPG: 400k]. The VLT Instruments and their locations at the Unit Telescope foci. The numbers in parenthesis indicate the expected year that they will enter into operation.

The instrumental complement of the VLT (cf. Chapter 8) has been designed to fully exploit the quality of the Paranal site in its entire range of conditions, and to achieve an optimal, largely non-redundant coverage of the parameter space (field of view and spatial resolution, spectral range and resolution, multiplexing and sky coverage). Moreover, it will be optimized globally as well as instrument by instrument. One VLT focus (other than coudé) will be left free to accommodate small, highly innovative visitor instruments on a non-permanent basis.

Specific **science drivers** specify the scientific performance of each instrument, defining its throughput, quantum efficiency, photometric accuracy, field of view, multiplexing capability, calibration, quick look, documentation, data analysis and data archiving.

Long term monitoring of instrument performance ensures that such performance is maintained.

Without compromising significantly the scientific performance of individual instruments, ESO is seeking **maximum standardization** of main components, including computers, detector controllers, cryogenics, control software, and data flow system.

1.6 Science Operations

The most efficient, possible use of the VLT/VLTI facilities is of prime concern. To this end, **new operation modes** have been developed, allowing telescopes, instruments, and data flow to work together in a fully coordinated fashion and to adapt quickly to the prevailing atmospheric conditions.

Operations have been designed to minimize the global overhead for target selection, telescope pointing, target and guide star acquisition, instrument set up, read-out time, data acquisition and storage and real time display.

Operation of the VLT Observatory includes activities at the telescope site on Paranal and the ESO Headquarters in Garching. VLT operation activities at the two sites are organized in a coordinated fashion.

The VLT facility is offered in two modes: one with the astronomer present at the telescope, overviewing and guiding the activities of the observatory staff (**Visitor Mode**), and one where observations are acquired by observatory staff on the basis of predetermined sequences of operations (**Service Mode**). The operational modes of the instruments may differ in Visitor and Service observing. However, in both modes telescopes and instruments will be operated by ESO staff.

Observations in Visitor and Service mode alike follow a **Phase 1/Phase 2 process** , with Phase 1 approved proposals being admitted to Phase 2. As a result of Phase 2 proposal preparation, all observations will be specified as **Observation Blocks** using template configurations for all available instrument modes. Support for observations outside the available templates must be justified on the basis of exceptional scientific merits.

To maximize the scientific return of the VLT in Service mode, **flexible scheduling** will ensure the capability of taking advantage of the best `astro-meteorological' conditions, e.g., moments with the best seeing or lowest water vapour.

To this end the VLT site houses an **Astronomical Site Monitor (ASM)** recording all relevant meteorological and astronomical site parameters, and forecast capabilities shall be implemented.

The **final scheduling** is aimed at obtaining the most valuable astronomical data, given the prevailing observational conditions. The astronomer users will always receive the raw science data together with the raw calibration data in addition to any data products ESO may provide.

In Visitor observing mode ESO provides the astronomer with all **logistic support** for the observing of their approved programmes on Paranal. Visiting astronomers are allowed to submit alternative programmes along with their primary programmes, so as to make a scientifically most effective use of their VLT time were the meteorological conditions different from those adequate to execute the primary project.

VLT operations will ensure appropriate **calibration of all VLT data** taken in Service mode. A calibration plan will be designed for each VLT instrument and pipeline reductions will be implemented for standard instrument modes.

Visiting astronomers will have the opportunity of using the same calibration procedures. ESO will provide a quality control of the data taken in Service mode, ensuring that the observations were performed as requested and the calibrations meet the accuracy requirements.

1.7 Data Archive and Distribution

The **VLT observations will be systematically archived** along with the calibration data and those engineering and environmental data that may be required for the subsequent scientific analysis (cf. Chapter 10). Such data are distributed to the Principal Investigators (PIs) promptly, i.e., with the goal of delivering at least 90% of the data within one month and 100% within six months. Quick-look data will be available during the observations.

All VLT data products will be accessible by the major **astronomical data reduction tools** . In addition to the raw science and calibration data, astronomers will receive data products which are the result of pipeline reductions carried out by ESO.

All archived data are accessible to the community after expiration of a **proprietary period of 12 months** from the delivery to the PI. Extensions to this period may be granted by the Director General upon justified request.

VLT Whitebook Chapter 2: The Main Elements

As the foremost observational facility of the European Southern Observatory, the **VLT facility forms an integral part of the organisational set-up** . While the most visible components of the VLT are installed at Paranal, many related activities take place at the ESO Headquarters in Garching, to which Paranal is permanently connected via high-capacity data links. In particular, the data handling, the development of instruments, initiation of new programmes, the allocation of observing time all take place at the ESO HQ.

The main elements of the VLT at Paranal are:

- The four 8.2-metre Unit Telescopes (UTs) with their enclosures;
- The VLT Interferometer and its Auxiliary Telescopes (VLTI);
- The incoherent beam combination including the combined coudé laboratory;
- The optical and infrared astronomical instruments;
- The control system of the telescopes and instruments consisting of a network of computers and local control units with their software, and the communications system, consisting of local area networks, access to wide area network and intercontinental links to support remote observing;
- The astronomical monitoring facility to allow sky monitoring and meteorological data collection;
- The telescope area infrastructure which includes a control and operation building, the necessary local facilities and technical equipment necessary for the operation of the VLT;
- The hotel area which provides facilities necessary for the accommodation of staff; and
- The general technical facilities necessary for the operation and maintenance of the observatory such as power generators, water storage, warehouse, a mirror maintenance building containing the coating plant for the primary mirrors, workshops, laboratories, etc.

This chapter introduces the main components of the VLT at Paranal, incuding an overview of the Paranal Observatory infrastructure. More details about some of these subsystems, especially about the underlying technical issues, will be found in the following Chapters. The operations at the ESO Headquarters in Garching are described in Chapter 10.

2.1 VLT Unit Telescope

Figure 2.1 [JPG: 128k]. Mechanical structure of UT4 during pre-assembly at Ansaldo (Milan, Italy).

The ESO Very Large Telescope incorporates an **array of four 8.2-metre Unit Telescopes (UTs)** which can work in single or in combined mode. In the latter, the VLT provides the total light collecting power of a 16-metre single telescope. The telescopes may also be used in interferometric mode providing high-resolution imaging. The useful wavelength range extends from the near UV (near 3000 A) up to the mid-infrared (about 25 µm).

The main structures of the VLT were designed, produced and assembled by an Italian consortium composed of *Ansaldo Energia* (Genova), *European Industrial Engineering* (Venice) and *SOIMI* (Milan). Fig. 2.1 provides an overall view during the pre-assembly phase at the factory.

Schematic views of one VLT Unit Telescope in its enclosure,with indication of the main telescope components, are shown in Figs. 2.2 and 2.3.

Figure 2.2 [GIF: 31k]. Schematic side view of VLT Unit Telescope in its enclosure.

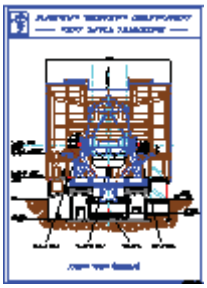

Figure 2.3 [GIF: 32k]. Schematic front view of VLT Unit Telescope in its enclosure.

The VLT Unit Telescope has **alt-azimuth mount** . In such a mount the telescope tube moves around a horizontal axis (the *elevation axis*). The two bearings which support the tube are mounted on a fork rotating around a vertical axis (the *azimuth axis*) thus enabling it to poin over the entire sky.

The **telescope tube** itself consists of a steel structure supporting at the bottom the primary mirror (M1) in its cell, and at the top the M2 Unit (with the secondary mirror) by means of metallic beams called "spiders".

Each Unit Telescope is protected from the external environment by an **enclosure** . The enclosure also provides access for operation and maintenance to certain areas of the telescope

and a protection against the wind during observations. The telescope is mounted on a concrete foundation, the telescope pier.

The VLT Unit Telescope **optical layout** is of the Ritchey-Chrétien type. Each of the four telescopes can operate in either **Cassegrain, Nasmyth** or **Coudé Focus** . The stellar light is collected by the primary mirror (M1), concentrated by the combination of the primary and the secondary mirror (M2), either directly to the Cassegrain focus located below the primary or to one of the two Nasmyth foci. The coudé focus is obtained by transferring one Nasmyth focus to another location in the telescope basement by means of an optical relay system. From the coudé focus, the light can be sent to the **Combination Mode Focus** or to the **Interferometric Focus** .

The Unit Telescopes are equipped with **active optics** . The optical quality of the image is continually monitored by an image analyser using a reference star and the contributions of the various optical aberrations (defocus, astigmatism, coma, etc.) are computed.

To achieve the best **optical quality** , discrete correction commands are given to the primary mirror support system, controlling the shape of the thin and flexible M1 mirror, and to the M2 Unit, which controls the position of the M2 mirror along 5 degrees of freedom.

The **astronomical instruments** are mounted at the Nasmyth foci, as well as below the main mirror at the Cassegrain focus. These foci are accessible from the Nasmyth platforms and from the azimuth platform at the base of the telescope (the *fork base floor*), respectively.

When changing between Cassegrain and Nasmyth/coudé operation, the curvature of M1 must be changed (by means of *active optics*) and M2 must be refocused.

For **maintenance** , e.g. coating, the complete M1 Unit (cell and mirror; about 50 tons) is removed from the telescope and transported over the fork base floor out of the enclosure.

2.2 The Main Mirrors (M1, M2 and M3)

The VLT Unit Telescopes have a complex system of optical mirrors.

Each Unit Telescope has a **Primary Mirror (M1)** of 8.2-metre diameter, supported by a structure (the **M1 Cell**), attached to the telescope tube. The telescope tube is closed at the bottom by the M1 Cell which also supports the **M3 Tower** with the **Tertiary Mirror (M3)** . At the top, the telescope structure supports the **M2 Unit** with the **Secondary Mirror (M2)** .

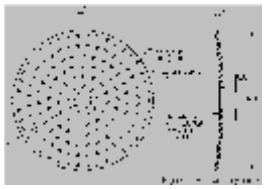

Figure 2.4 [GIF: 10k]. Geometry of the VLT Primary Mirrors (M1).

Figure 2.5 [GIF: 32k]. First VLT M1 after polishing at the REOSC factory.

The 8.2-m Zerodur primary mirrors (Fig. 2.4) are 175 mm thick and their shape is actively controlled (**active optics**) by means of 150 axial force actuators, the necessary active corrections being obtained from wavefront sensors located off-axis on the image surface.

The 23-tons mirror blanks were manufactured by spin-casting at the *SCHOTT Glaswerke* (Mainz, Germany) and the optical figuring (Fig. 2.5) was performed at *REOSC* (Saint Pierre du Perray, France), together with the interfaces with the mirror cell and auxiliary equipment such as transport containers. Dedicated facilities were built by the two companies to execute their respective contracts.

The successful production of these mirrors represents a major breakthrough, not only in terms of manufacturing processes but also in terms of metrology. Indeed, the accurate and reliable measurement of a thin, flexible 50 m 2 optical surface constitutes a serious technological challenge.

The **M1 Cell** that supports the primary VLT mirror was manufactured by *GIAT* (St. Etienne, France). It is a 3D metallic welded structure which is attached by twelve flanges to the main telescope tube. The primary mirror is positioned on the upper side of the cell and held in place by axial and lateral supports. On the bottom side of the cell there is an attachment flange for the Cassegrain Adapter/Rotator.

Figure 2.6 [JPG: 419k]. The first VLT M2 Beryllium Mirror in the test laboratory of DASA (Ottobrunn near Munich, Germany), during the determination of its inertia and center of gravity. The mirror is covered by a peelable protective layer. (September 1997).

Figure 2.7 [GIF: 125k]. The lightweighted M3 mirror.

The light-weight, **M2 mirror** is made of Beryllium and weighs 51 kg (Fig. 2.6). It measures 1.12-m in diameter and is 50 mm thick. The form is convex and hyperbolic. By changing its position and orientation it is possible to correct some optical aberration of the telescope (defocus and decentring coma) and to change the pointing. The first blank was produced by *Brush Wellman* (USA) and the polishing was done by *REOSC* (Saint Pierre du Perray, France.

The **M2-Unit** is an opto-mechanical system consisting of the M2 mirror and the mechanical and electronic components used to control its position along 5 degrees of freedom. Physically, the M2-Unit is comprised of the M2 mirror assembly, the electro-mechanical assembly, and an external electronic cabinet. It was built by the *Dornier Satellitensysteme* (Friedrichshafen, Germany).

The 45 o , flat and elliptically shaped, **tertiary mirror M3** (Fig. 2.7) is mounted on top of the **M3 Tower** that is fixed in the center of the M1 Cell. The tower can rotate along its axis (ideally coincident with the azimuth axis of the telescope) and extends from the M1 Cell up to the level of the altitude axis through the central hole of the primary mirror. A mechanism at the top of the M3 Tower is used to move the mirror away from the optical path when the instrument at the Cassegrain focus is used. This mechanism also allows a remote, fine adjustment of the M3 position. The M3 Unit was made by *Carl Zeiss* (Jena, Germany) who also polished the M3 mirror. It was 80% lightweighted by *SCHOTT Glaswerke* (Mainz, Germany).

The **main mirror parameters** (nominal values) are summarized in Table 2.1.

Table 2.1: Main Mirror Parameters

Parameter	**M1**	**M2**	**M3**
Material	Zerodur	Beryllium	Zerodur
Diameter	8200 mm	1116 mm	1242 x 866 mm (elliptical)
Thickness	177 mm	130 mm	140 mm
Weight	23,000 kg	44 kg	105 kg
Shape	Concave	Convex	Flat
Curvature (radius)	+28,975 mm	-4550 mm	> 63,000 m

2.3 Active and Adaptive Optics

The VLT **Active Optics System** is based on the experience gained with the ESO 3.5-m New Technology Telescope at La Silla and ensures that the primary (M1) and secondary (M2) mirrors are kept in optimal shape and alignment.

The VLT is also equipped with **Adaptive Optics Systems** in several places. The first to be installed will be the *Nasmyth Adaptive Optics System (NAOS)* , cf. Chapter 8.5. Others will follow at the coudé foci and will support observations with the VLT Interferometer. MACAO (Chapter 8.6) is planned for the Cassegrain focus of UT1, as a subsystem of SINFONI (Chapter 8.3.5).

2.3.1 Active Optics

Due to the low ratio between their thickness and diameter, the VLT primary mirrors are rather flexible and sensitive to various disturbances, thus requiring permanent control of their optical shape.

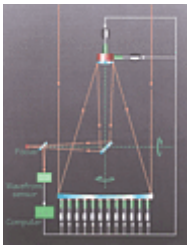

Figure 2.8 [GIF: 31k]. Schematic view of the VLT Active Optics System.

Active Optics consists in applying controlled forces to the primary mirror and in moving the secondary mirror in order to cancel out the optical errors. This scheme was developed by ESO for its 3.5-m New Technology Telescope (NTT) and is now applied to the VLT. The system must essentially compensate for static or slowly varying deformations such as manufacturing errors, thermal effects, low frequency components of wind buffeting, telescope inclination, etc.

The **elements** of the active optics system of the VLT are the *primary mirror* , with its active support system located within the M1 Cell structure, the *M2 unit* , the *CCD Shack-Hartmann wavefront sensor (WFS)* located in the sensor arm of the adapter, and the *computer* analysing the wavefront sensor data.

There are three **modes of operation** : Baseline, Fast Corrections , and Open Loop Corrections

2.3.1.1 Baseline

The active optics baseline operation is the correction of wavefront aberrations generated by the optics of the telescope and by slowly varying temperature inhomogeneities in or near the building. The corrections are based on an image analysis.

The active optics system constantly monitors the optical quality of the image using an offset reference star as it is picked up in the field by the wavefront-sensor CCD in the adapter sensor arm. The same offset star is also used by the acquisition and autoguiding CCD.

The system controls the relative position and the shape of the optical elements. The primary mirror shape can be actively controlled by varying the force pattern applied by means of its support system. The latter consists of 150 computer controlled axial actuators, applying a distribution of forces at the back of the mirror.

Periodically the image analyzer calculates the deviation of the image from the best quality. The image analysis typically requires about 30 seconds (1/30 Hz) in order to integrate out the effect of atmospheric seeing. The computer decomposes the deviation into single optical contributions (defocus, astigmatism, coma, etc.) and calculates the force correction which each active element has to perform to achieve the optimal quality. The set of 150 correction forces, one for each axial actuator, is computed and transmitted to the local control of the M1 Cell-M3 Tower for execution. The focus and coma terms are corrected by displacements of the secondary mirror.

2.3.1.2 Fast Corrections

The feedback scheme is the same as above but here the maximum frequency for fast corrections is 1 Hz. These shorter integration times reduce the signal to noise ratio of measurements and affect both the sky coverage (requirement of brighter guide stars in the field) and the number of aberrations which can be corrected (only the lowest spatial frequency ones).

2.3.1.3 Open Loop Corrections

This mode does not use feedback information from the image analyser.

The open loop mode is used in the absence of any sufficiently bright guide star, or in the case of image analysis failure, or as initialization for baseline operation after a new telescope preset. For this type of operation accurately predicted forces on M1 (dependent on telescope tube inclination) and predicted positions (dependent also on temperature) are required.

2.3.2 Adaptive Optics

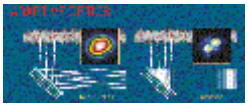

Figure 2.9 [GIF: 53k]. General principle of Adaptive Optics.

Adaptive Optics (AO) (Fig. 2.9) is capable of correcting fast-changing wavefront aberrations, with speeds up to several tens of Hz at 0 dB gain. It needs a reference signal from a **Guide Star** , which may be either natural or artificial, e.g., implemented with a Sodium Laser projected on the mesospheric layers, cf. Chapter 8.7.

Sources of **image quality degradation** within the telescope include the residual errors of the telescope control system, deflection of the telescope structure induced by gravity, thermal expansion and wind buffeting and the atmospheric distortions. Slowly varying errors, for example due to gravitational flexure and thermal effects, are corrected by the Active Optics system, but that system cannot correct transient errors. The Adaptive Optics systems, on the other hand, will correct also all these sources of error.

An Adaptive Optics system consists of three main functional elements: **a wavefront sensor (WFS)** to measure the distortions of the wavefront coming from a source (measured either in the visible or in the IR), a **correction device** (deformable mirror and tip-tilt assembly) and a **real-time control computer** . A dichroic mirror or beam-splitter element splits the light towards the WFS (in transmission) and towards the astronomical instrument (in reflection).

Adaptive Optics systems have been in operation at ESO since 1992 at the 3.6-m telescope on La Silla. The latest instrument is **ADONIS** which has served as a basis for the design of the VLT systems, and is routinely offered to the astronomers.

ESO is planning the implementation of several Adaptive Optics systems at the VLT, all optimized for Near-Infrared (NIR) operation and for the particular instrument to be fed. They will allow to reach the **diffraction limit resolution** in the NIR bands, and to increase the photon concentration in the spectrograph slits.

One of these is a Shack-Hartmann system for the Nasmyth focus, **NAOS** (a detailed description is available in Chapter 8.5), which will feed the CONICA instrument.

The other, planned AO systems belong to the **Curvature systems class** , cf. **MACAO** (Chapter 8.6). They will be cloned from a master breadboard, assembled in-house and customized to the VLT standards. Two 35-element curvature AO systems are planned for the spectrographs, SINFONI and CRIRES. Four 60-actuator curvature systems are planned for the coudé foci, to feed also the beam combiners of the VLTI for single speckle interferometry.

A **Laser Guide Star Facility** that will create an artificial guide star is planned for UT1, cf. Chapter 8.7.

2.4 Array Configuration

The elements of the **VLT Interferometer (VLTI)** are the 8.2-m diameter VLT Unit Telescopes (UTs) and the 1.8-m diameter Auxiliary Telescopes (ATs); for a detailed discussion of the VLTI, cf. Chapter 9. While the location of the UTs is fixed, the ATs can be moved between a limited number of stations. Light is directed underground from the telescopes to the central interferometric tunnel where the delay lines are installed and onwards to the beam combination laboratory, where interferometric fringes are produced and detected.

The interferometric array consisting of solely the UTs is called the **VLT Interferometer Main Array (VIMA)** . The interferometric array consisting solely of the ATs is called the **VLT Interferometer Sub-Array (VISA)** .

The location of the UTs on the telescope platform has been determined by a number of factors other than optimum placement for interferometric imaging. Major constraints in this connection were the limited dimensions of the site, and influence between UTs due to sky and wind obstruction.

The definition of the locations of the AT stations has been the subject of thorough studies and has resulted in optimum performance of the resulting combination of UT and AT units, as well as of the AT units alone, from the point of view of **interferometric imaging** . The major guidelines in achieving satisfactory performance is this respect are **efficient coverage of the UV plane** and **high-precision calibration** .

The following guidelines have served to define the **optimum placement of AT stations** at the areas northwards and southwards of the interferometry tunnel:

1. An optical interferometer combines highest sensitivity with a reasonable potential for creating images with good fidelity when the number of elements is less than ten. These elements should be arranged in a non-redundant configuration such as to maximize the amount of available information. The imaging performance of an interferometer can be well assessed by examining the UV coverage of the array, in both snapshot mode and Earth-rotational synthesis mode.
2. Baselines between the UTs provide the interferometric signal with the highest sensitivity. The four UTs should therefore be placed to optimize interferometric imaging performance, which makes a two-dimensional configuration necessary.
3. The UTs are the largest structures on the site. They must be placed such that they do not obstruct each other down to a zenith distance of 60 o , and down to a zenith distance of 75 o for sources 1 1/2 hours from the meridian. The influence between telescopes due to obstruction of free air flow must be minimized for the major wind directions. This requirement leaves practically only the northern rim of Paranal as suitable location for the UT. Also, placement of the UTs depends critically on the soil conditions, which further limit the available locations.
4. A number of AT stations should provide baselines which combine a UT and an AT, and which cover holes and blind azimuth angles present in the VIMA configuration. These baselines provide enhanced sensitivity in comparison with purely AT based baselines for a number of observing modes.

5. AT stations should provide very close spacings to enable coverage of the UV plane at short baselines which are inaccessible to the UT array as well as to combinations of UT and AT elements. This lack of coverage is due to obstruction by the domes of UTs. The resulting "central hole" in UV coverage is of the order of 20 m in radius.
6. A configuration with good UV coverage should be possible with AT elements exclusively. A VISA with a minimum of three ATs can be operated as an independent imaging array.
7. The placement of stations should permit studies with linear, non-redundant and partially redundant configurations, possibly at various angles with the NS-direction. These configurations allow for application of redundant spacings calibration methods.

Figure 2.10 [GIF: 38k]. Layout of the individual VLTI elements. Unit Telescopes are shown as large, filled circles, the location of VISA stations are indicated by small, filled circles. These circles represent the diameters of the primary mirrors when pointed at the zenith. Solid lines show the location of tracks for transporting ATs between stations. Dotted lines show the subterranean light ducts.

The resulting layout of the VIMA and VISA arrays is shown in Fig. 2.10 along with the interferometric tunnel and the interferometric laboratory. The Unit Telescopes are located along an arc covering the north edge of the site. The long structure rotated by 19 o.55 anti-clockwise from the E-W direction represents the interferometric tunnel and the interferometric laboratory. This orientation of the tunnel and the location of the interferometric laboratory is chosen, such that the optical paths are as similar as possible for all Unit Telescopes.

The resulting maps of the UV coverage for the VIMA and VISA configurations are shown in Figs. 2.11 and 2.12, respectively.

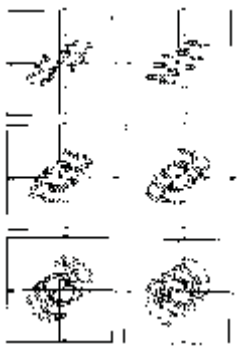

Figure 2.11 [GIF: 112k]. UV plane coverage of the VIMA.

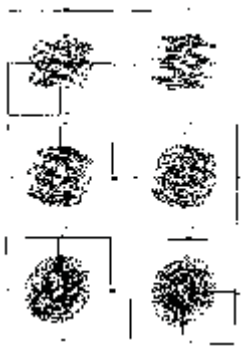

Figure 2.12 [GIF: 168k]. UV plane coverage of the VISA.

2.5 Beam Combination and Interferometry

A detailed discussion of the VLTI is found in Chapter 9.

The beams from the individual telescopes of the VLT array are combined coherently by means of a number of subsystems:

- **UT Coudé Trains** , located below each UT and including the necessary mirrors (M4 - M8) to direct the beam from the Nasmyth platform to the coudé focus, as well as the Adaptive Optics systems (Chapter 2.3.2), located there. From here the beams are guided to the 140-metre long underground, Interferometric Tunnel and the Delay Lines installed there;
- There will be similar **AT Coudé Trains** (Chapter 9.4);
- **Delay Lines** to equalise optical path length differences (OPD) and to transfer a pupil at a fixed location inside the Interferometry Laboratory (Chapter 9.5); and the
- The **Beam Combination Laboratory** at the center of the Paranal platform where the fringes are detected (Chapter 9.6) by the interferometric instruments (Chapter 9.7).

The option to combine the beams incoherently is open and will be decided later.

2.6 Instrumentation Package

The VLT is equipped with a number of mostly **multi-mode instruments** with imaging and spectroscopic capabilities, covering the spectral range from the atmospheric UV-limit (300 nm) to the mid-IR (25 μm). Each of these is described in some detail in Chapter 8.

Three foci (*one Cassegrain, two Nasmyth*) are available from the beginning of operations at each of the four UTs, i.e., a total of 12 foci. The full complement of first generation, general-use instrumentation at the VLT encompasses **11 instruments** . In addition, one *Nasmyth Visitor focus* is reserved for standalone innovative instruments brought by external teams.

Each UT also has *one coudé* focus. Two coudé foci are initially available to feed the VLTI, and ultimately all four coudé foci will be opened with some adaptive optics capability. However, no (non-interferometric) instruments have yet been approved for them.

Imaging and spectroscopic instruments are also foreseen at the interferometric focus. They are discussed in Chapter 9.7 and will not be mentioned further here.

2.6.1 VLT Instrumentation Projects

Table 2.2 gives an overview of the approved VLT Instrumentation projects, arranged in order expected date of operation.

Table 2.2: VLT Instrumentation Projects

Acronym	Built by	Observing Modes	Installation
ISAAC	ESO	Imaging, polarimetry & long-slit spectroscopy (1-5 µm)	1998
FORS1/2	Heidelberg, München, Göttingen, ESO	Imaging, MOS * , polarimetry (300-1000 nm), long-slit spectroscopy	1998/1999
NAOS	ONERA, Paris, Grenoble, ESO	Adaptive Optics Adapter for CONICA	2000
CONICA	MPIA Heidelberg & MPIE Garching	High angular resolution imaging, polarimetry and spectroscopy (1-5 µm)	2000
UVES	ESO, Trieste	High resolution cross dispersed spectrography (300-1000 nm)	1999
FLAMES	Genève, Paris, Toulouse, Australia, ESO	MOS * (fiber) & Integral field spectrograph (370-1000 nm)	2001 (?)
VISIR	Saclay, ASTRON	Imaging & long-slit spectroscopy (8-25 µm)	2000
VIMOS	Paris, Marseille, OHP, Toulouse, Bologna, Milano, Napoli, ESO	Wide Field Imaging & MOS * (370-1000 nm)	2000
NIRMOS	Paris, Marseille, OHP, Toulouse, Bologna, Milano, Napoli, ESO	Wide Field Imaging & MOS * (1-1.7 µm)	end 2001
CRIRES	ESO	High resolution echelle spectroscopy (1-5 µm)	2002
SINFONI	MPE-Garching, ESO	A.O.-based Integral field spectroscopy (1-2.5 µm)	2001

* MOS = Multi-Object Spectroscopy

2.6.2 Observational Strategy

The VLT instruments have been conceived and constructed according the requirements imposed by scientific goals and the various observational modes.

The following operational strategy has been adopted. All observations with the VLT instruments will be carried out by an instrument operator, according to **Observing Blocks** developed by the proposer/observer (cf. Chapter 10). Two different observing modes are offered: the conventional **visitor mode** , with the astronomer present (physically or electronically) on the site to lead his/her program, and a **service mode** , performed directly by the operator with the help of an ESO astronomer. It is envisaged that at most 50% of the observations will be performed in service mode.

Special observations requiring real-time choices presumably will be performed in the conventional visitor mode, while survey programmes or regular monitoring may profit most from service observations.

An important aspect for the operation of the VLT observatory is the increased efficiency from **flexible scheduling** of the observations. Many programmes will require exceptional environmental conditions, e.g. extremely good seeing for imaging spectroscopy, very low vapor content for some infrared windows, slow turbulence for observations near the diffraction limit of the telescope with adaptive optics corrections, etc. Flexible scheduling allows such observations to be obtained optimally, with a guaranteed scientific quality.

This strategy ultimately requires a **full complement of automated, multi-mode instruments** for the VLT. Switching of instruments, when needed, is then easily achieved, with minimal loss of time, just by working at another telescope focus.

In addition, one Nasmyth focal station remains free for **visitor instruments** . This facility will provide fast access to innovative instruments.

With the development of the VLT Interferometry facility, initially at least two UT coudé foci will be available for potential instruments. While no decision has yet been taken, two possible instruments are being discussed: a **very high spectral resolution visible spectrograph** and a **visible speckle camera** . In addition, one coudé focus could possibly be opened for visitor instruments, if and when the need is felt.

When the full interferometric capability will be in place, use of the **combined incoherent coudé focus** may also be contemplated; this would offer the full light collecting power of a 16-metre equivalent diameter telescope.

2.6.3 Observational Domains

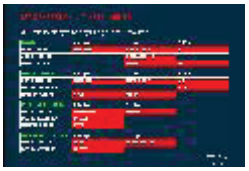

Figure 2.13 [JPG: 384k]. The domains of the first-generation instruments in terms of spectral region and resolution, as well as type of observation (imaging; long-slit, multi-object or integral-field spectroscopy).

As can be seen in Fig. 2.13, the VLT Instrumentation will enable different types of observations, from singly objects, to integral fields. They also cover large domains, in terms of **spatial and spectral resolution** as well as **wavelength** . Moreover, the VLTI will bring much higher spatial resolution capabilities and the spectral resolution limit of 100,000 may be surpassed with potential instruments under discussion for a Nasmyth and/or a coudé focus.

2.6.4 Detectors

The integration of state-of-the-art detectors and their associated electronics is essential for the success of the VLT instrumentation. ESO actively pursues the following strategy:

- **Optical Detectors** : CCDs plus controllers are mainly provided by ESO. The baseline is 2k x 4k 15 µm pixels, high quantum efficiency (thinned), very low noise chips. The **FIERA** controller has been developed with the goal of not limiting performance of the chip, neither in terms of noise, nor in speed.
- **Near Infrared Detectors:** The IR-arrays plus the controller system are mainly provided by ESO. Presently available chips are the 1k x 1k 1-2.5 µm, 18.5 µm pixel Rockwell Array (HAWAII) and the 1k x 1k 1-5 µm, 27 µm pixel Santa Barbara Research Corporation Array (ALADDIN). A 2k x 2k 1-25 µm Rockwell array is under development. The IRACE controller does not limit either the noise or speed performance of the present chips.
- **Medium Infrared Detectors:** The IR-array plus the controller will be provided by the VISIR Consortium. Again, the performances will not be limited by the electronics.

2.6.5 Spectroscopic Modes

The recognition that different classes of astronomical objects may have strikingly different spatio-spectral 3-dimensional (apparent) shapes has lead to the end of the "monopoly" of the long-slit spectrograph. A wide variety of instrument modes, finely tuned to the 3D characteristics of their sought-for targets, has been developed. The VLT instrumentation package is no exception with its overall goal to cover efficiently most astronomical objects (see Fig. 2.13). Main such classes are:

- **Extended "Continuum" Objects** (Regions of Star Formation, Open and Globular clusters, Nearby Galaxies, etc.): There is no optimum solution available, as their 3D (x, y, lambda) volume far exceeds what can be mapped with present 2D-only detectors. Long-Slit Spectroscopy is by far the simplest, most efficient and most used way, but it covers only a thin spatial slice at a time. By virtue of its simplicity, it is also still widely used on less than optimum cases. Almost all VLT instruments feature this mode.
- **Extended "Monochromatic" Objects** (Galactic and Extragalactic HII regions, SNRs, etc.): This is done with Scanning Imaging Spectrographs. For low spectral resolutions, up to 100, interference filters are generally used. Higher spectral resolution, up to a few 10,000, is typically the province of the Scanning Fabry-Perot Spectrograph, which covers the entire region in space, but only a thin spectral slice at a shot. Lack of convenient tunable order-sorter filters limits its use to kinematical surveys of ionized Interstellar Matter. At the VLT, it is represented with CONICA and coupled with the Adaptive Optics capability (NAOS).
- **"Single Point" Object** (stars, quasars, etc.): Their thin, but very long, "beam" shapes along the wavelength axis are perfectly mapped on a 2D detector by the crossed-dispersed echelle spectrograph. Three VLT instruments feature that mode, UVES and FORS2 in the visible and CRIRES in the IR.
- **"Multiple Point" Objects** (galactic or extragalactic star clusters, galaxies in distant clusters, etc.): Multi-object spectrographs, either of the multi-slit or of the multi-fiber flavor, permit efficient surveys of these loose collections of objects. This, arguably second most popular mode, is well represented on the VLT, with FORS1/2, VIMOS, NIRMOS and FUEGOS.
- **"Single Small" Individual Objects** (e.g. compact HII regions, galactic cores, interacting galaxies, radiogalaxies, etc.): This recent addition to the instrumental arsenal , under the trade name of *Integral Field Spectroscopy* , efficiently maps the full 3D volume on the detector in one single exposure, provided the spatial field is small (typically 40 x 40 pix only). They are based on a classical spectrograph fed by an image slicer, made from a multi-lens, multi-fiber or multi-mirror array. On the VLT, there are two "wide-field" (about 40 arcsec diameter) systems on VIMOS and NIRMOS, one "medium-field" (about 12 arcsec) on FUEGOS and one "small-field" (about 4 arcsec), coupled with Adaptive Optics, on SINFONI.

2.6.6 Imagery

Many of the present VLT Instruments, e.g. FORS, CONICA, ISAAC and VISIR, are spectro-imagers which, in addition to their spectroscopic capabilities, provide direct imagery through sets of broadband and/or interference filters.

In addition, the two **VLT test cameras** , which are used extensively during the commissioning of the Unit Telescopes, provide a well sampled, imaging capability in an approx. 1 x 1 arcmin field, down to the atmospheric UV limit, with a thinned 2k x 2k CCD

2.7 The Enclosures

Four enclosures have been built for the four VLT UTs by the *SEBIS-consortium* (Italy). The installation at Paranal began in 1994 and will be finished in 1998.

2.7.1 Basic Functions

Each VLT telescope is enclosed in a building (the **enclosure**), with the following main functions:

- In the closed position, to **protect the telescope** and its instrumentation against adverse weather conditions, dust, lightning and lightning electromagnetic pulses and to preserve its thermal environment.
- In the open position, to **allow the telescope a free field of view** by means of a large slit in a rotating dome. At the same time the enclosure provides wind protection and the right amount of ventilation and air circulation in the enclosure to create optimum observing conditions for the telescope during night-time astronomical observations

In addition to these main functions, each enclosure provides:

- a circular floor in continuation of the fork base azimuth platform as required for the main mirror transport and Cassegrain instruments;
- a large access door for the Main Mirror Cell on its carriage (diameter 9.5 metres);
- platforms allowing access to all telescope levels where instruments are to be installed and operated;
- a crane for the lifting and transporting of instruments onto the telescopes; and
- access to platforms and floors

2.7.2 Design

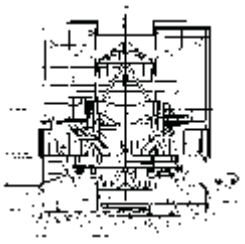

Figure 2.14 [GIF: 152k]. Front view of enclosure.

Figure 2.15 [GIF: 128k]. Horizontal cut through VLT enclosure at level +11044 (Nasmyth platform).

Figs. 2.14 and 2.15 show vertical and horizontal cuts that illustrate the design of the enclosures

The VLT enclosure is designed as a building of cylindrical shape, constructed as a steel structure with both roof and facades covered with weather-tight and thermally insulating cladding panels. Each enclosure consists of:

- A **fixed cylindrical part** rising from 5.144 m (above the nominal 0.0 Telescope Area level) up to approximately the level of the Nasmyth platforms of the telescopes. This fixed part of the enclosure surrounds the lower part of the telescope and has a floor at the same level as the telescope azimuth platform. At this level the large main mirror door is situated, as well as some large ventilation doors. The fixed part has a second floor, the *Nasmyth access area* , situated at the same level as the Nasmyth platforms of the telescope. The fixed part of the enclosure furthermore contains the lift and staircases between fork base floor and Nasmyth access area. Moreover, on the fixed part a circumferential walkway to access and maintain the rotation system is installed.
- An **upper rotating part** (the dome), of a cylindrical shape with a 9.50 m wide **observing slit** that can be closed by two doors. The observing slit is equipped with a windscreen with variable permeability, and louvers are installed in the walls around the circumference of the dome. The dome has the same rotation axis as the telescope azimuth axis and is able to rotate independently of the telescope, without any physical interference at any position of the telescope. The dome includes a crane for a variety of handling tasks, and ladders and access platforms as required for the maintenance of all mechanisms.

2.7.3 Environmental Control

The VLT enclosures feature advanced **environmental control** in order to provide the best possible local conditions for the astronomical observations. Given the meteorological forecast for the coming night, the operational model of the telescope will enable the control system to optimize the observing conditions. The decision criteria are:

- Temperature differences with the ambient air inside the enclosure have to be minimized;
- Maximum flushing has to be ensured; and
- Wind buffeting on the telescope and the primary mirror has to be kept within an acceptable range.

These requirements aim at minimizing mirror and dome seeing due to temperature inhomogeneities, while the third one is connected to dynamic pressure fluctuations which cause image degradation.

To be able to satisfy these requirements, a number of active and passive systems are available which ensure **thermal control** and **air flow control** .

2.7.3.1 Thermal Control

Active thermal control in the VLT enclosures is effected by **air conditioning** , **active cooling** of heat sources inside the telescope enclosure (electronic cabinets, etc.) and the **mirror back plate cooling system** .

The **air conditioning** concerns the inner volume of the enclosure during the day when the dome is closed. The cooled air is distributed and mixed homogeneously in the entire volume of the enclosure by means of air exhausts distributed along the entire inner surface, including the top part of the dome when the dome itself is locked in the parking position.

The air conditioning system consists of a secondary chilled water circuit which feeds a number of air treatment units. This circuit is interfaced by means of a mixing bottle to the central (primary) chilled water circuit of the VLT Telescope Area. The air cooling control system is integrated in the general enclosure control system.

The heat load of the interior of the closed enclosure has been evaluated considering all components, namely:

- the heat transfer due to input and infiltration of external air into the enclosure. The latter, in particular its seals and connections, are designed with the aim of achieving an internal maximum air renewal rate of 1 volume per hour in the closed enclosure, taking into account the slight pressurization requirement of about 5 mm H 2 O;
- the conductive heat transfer from the external surface;
- the heat generation of occupants;
- the heat generation of lighting and motors in the enclosure; and
- an additional heat load from the telescope.

The **passive thermal control** in the VLT is effected by:

- minimizing by adequate insulation and seals the heat input both from the external environment and from the lower enclosure basement; and
- appropriate coating for radiative exchange with the cold sky.

A model-based optimization method is used for thermal control of the telescope. Given the meteorological forecast for the coming night, the system adjusts the air conditioning temperature set point and the mirror back plate cooling system such that we can optimize the seeing conditions during the night. The procedure is repeated continuously using temperature sensor readings as initial values in the model.

2.7.3.2 Air Flow Control

Air flow inside the enclosure at night is determined by the following:

- the ventilation doors in the fixed part of the telescope enclosure, i.e. the large mirror door (10 m width, 4.2 m height) and four smaller doors around the periphery (each 5 m width, 4.2 m height);
- the louvers on the rotating part of the enclosure (representing about 150 m 2); and
- the windscreen placed behind the vertical part of the large slit doors.

Extensive wind tunnel tests and computational fluid dynamics simulations were performed to determine the optimal air flow control strategy in order to satisfy the requirements. A 1:64 model was used to measure the pressure fluctuations on the primary mirror, turbulence intensities near the secondary mirror unit, wind speeds in selected locations, and flushing times, all this for a large number of opening configurations and wind directions. Flow visualizations using a special oil mixture were recorded on tape for later use during telescope commissioning for optimization. The wind tunnel tests were performed at the *Department of Wind Engineering of the Institute for Steel Construction at the RWTH Aachen* (Germany).

2.8 The Paranal Observatory

Figure 2.16 [JPG: 188k]. Map of the Paranal Observatory area.

Figure 2.17 [JPG: 232k]. Aerial view of the Paranal Observatory area.

The Paranal Observatory is located in the Atacama desert, some 120 km south of the city of Antofagasta. The area belongs administratively to the II Region, the administrative center of which is Antogasta. During the search for the optimal VLT site, this mountain early became one of the candidate locations and extensive site testing took place here in the 1983 - 1991 period.

The surrounding area (approx. 725 km 2) was donated to ESO by the Chilean Government in 1988 on the condition that ESO would commence the construction of the VLT Observatory here within five years.

The ESO Council took the decision to install the VLT at Paranal in December 1990. The construction started in 1991 and involved the removal of of more than 300,000 cubic metres of rock and soil from the Paranal peak (thereby lowering it by 28 metres) to create the large platform needed for the many components of the VLT.

At the same time, a **Base Camp** at the foot of the mountain was created with the main technical installations for the telescopes not needed at the top (Mirror Maintenance Building, etc.) as well as offices, dormitories and other installations (watertanks, power plants, etc.).

2.8.1 Infrastructure

The Paranal Observatory is divided into two main areas, the **Telescope Platform** at the top of the mountain (altitude 2635 m), and the **Base Camp** at the foot (altitude 2360 m). The distance by the 12-m wide access road is about 2 km.

The observational activities take place at the Telescope Platform, while the Base Camp contains staff quarters, maintenance facilities and other functional entities, including a visitors' centre for the public.

2.8.1.1. Main Facilities

The main facilities available at the VLT Observatory are as follows:

- **Telescope Platform** :
  - The four 8.2-m Unit Telescopes (UT1 - 4) and their enclosures;
  - Interferometric Laboratories and incoherent combined focus;
  - 1.8-m Auxiliary Telescopes (ATs) which feed the interferometric laboratory;
  - Telescope Control Building with instrument integration facilities, separated from the telescope enclosures; and
  - Time Reference System and Astronomical Site Monitors.

- **Base Camp** :
  - Mirror Maintenance Facility;
  - Mechanical and electronic workshops;
  - Facilities for the supply of electrical power, compressed air, cooling liquid, and communications;
  - Warehouse and storage facilities;
  - Facilities for the storage of liquid nitrogen;
  - Standard vehicles for the handling and on-site transportation of equipment, transportation of personnel, food, water, etc.; and
  - Hotel accommodation for site personnel; and
  - A Visitors' Centre for the public.

Figure 2.18 [GIF: 160k]. Map of the Telescope Area.

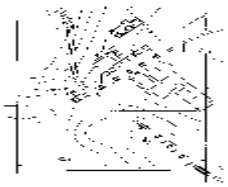

Figure 2.19 [GIF: 79k]. Map of the Base Camp and Maintenance Area.

Maps of the two areas are shown in Figs. 2.18 and 2.19, respectively.

2.8.1.2 Time Reference System

The VLT Observatory has a central **Time Reference System** which distributes Universal Time information to the telescope and instrument control systems, as well as other systems that require this information.

For general time setting requirements, **UTC** is available to instrument control software via the Instrument LAN. For applications requiring a high accuracy time reference, the UTC signal is distributed directly to the individual instrument LCUs by means of a dedicated fibre-optic Time-Bus. In this case a standard electronic module (Time Interface Module - TIM) within the LCU decodes the full UTC signal and provides a high accuracy local time reference for instruments. The absolute time accuracy of this reference, measured from the moment at which a processor interrupt is generated, is 10 μsec or better.

UT1 time is also available to instruments via the Instrument-LAN. For more demanding applications, the correction terms to convert UTC to UT1 is available via the Nasmyth Instrument LAN for precise local computation of UT1 in the instrument LCU.

Sidereal Time is computed centrally and is available to instrument LCUs via the Nasmyth Instrument LAN. This is not intended for high accuracy applications, however.

The Time-Bus also allows processes in different LCUs to be sychronised with a precision of 10 μsec or better. Asynchronous synchronisation between the LCUs of different sub-systems is possible in some situations through the LAN system

2.8.1.3 Astronomical Site Monitors

The observatory has a central **Astronomical Site Monitor (ASM)** to provide continuous monitoring of the prevailing astronomical conditions at Paranal as well as meteorological data and predictions. This information is available to the instrument control software via the LAN system. The facility also provides an archiving system to allow the accumulation of statistics for modelling and prediction.

2.8.2 Geographical Data

The **location** is characterized in Table 2.3:

Table 2.3: VLT Location

Altitude above sea level	2635.43 m
Distance from coast	12 km
Highest neighboring peak	Cerro la Chira, 2569 m, 11 km to the NNE
Road distances	130 km to Antofagasta
	Appr. 1200 km to Santiago
	Appr. 600 km to La Silla

The **geographical coordinates** of the four Unit Telescopes are given in Table 2.4:

Table 2.4: UT Geographical Coordinates

Telescope	Latitude	Longitude
UT1	-24 deg 37 min 33.117 sec	70 deg 24 min 11.642 sec W
UT2	-24 deg 37 min 31.465 sec	70 deg 24 min 10.855 sec W
UT3	-24 deg 37 min 30.300 sec	70 deg 24 min 09.896 sec W
UT4	-24 deg 37 min 31.000 sec	70 deg 24 min 08.000 sec W

2.8.3 Observing Conditions

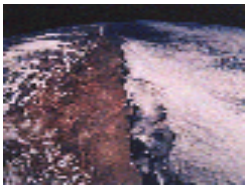

Figure 2.20 [GIF: 376k]. View of the Atacama desert, taken during Shuttle repair mission to the Hubble Space telescope. The cloud-free strip between the Pacific Ocean (cold Humboldt stream along the coast) and the Andean mountains (Cordillera) is obvious and clearly indicates this area's dry climate.

The Paranal area in the Chilean Atacama desert is believed to be the best site for astronomical observations in the southern hemisphere.

2.8.3.1 Meteorological Data

The main meteorological and climatic data are given in Table 2.5, with graphical representations of the main parameters in the figures.

Table 2.5: Meteorological Data for Paranal

Parameter	Value	Comment
Air pressure	750 mbar	±50 mbar
Density	0.96 kg/m³	Typical
Temperature	-8° to 25°C	Measured 1985-1990
Temperature gradient during night	-0.4°C/h	Typical
Humidity	5-20%	Typical
Rainfall	100 mm/year	Max.
Snow	Once or twice per year	Typical
Ice buildup	5 cm	Maximal
Day and night averaged solar radiation	cf. Fig. 2.21	
Daily maximum	1120 W/m²	Summer
	800 W/m²	Winter
Ozone	180 mg/m³	Maximal
Wind distribution	>10 m/s	25% of the nights
	>20 m/s	50 nights per year

	cf. Fig. 2.22	
Wind long-term extremes	47.2 m/s	50 years return period
	50.7 m/s	100 years return period
	54.2 m/s	200 years return period
Wind Direction (Wind rose)	cf. Fig. 2.23	Typical
Pollution	NO < 3 ppb	Typical
	NO2 < 2 ppb	Typical
	SO2 < 4 ppb	Typical

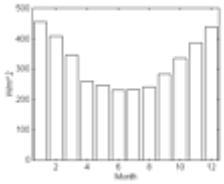

Figure 2.21 [GIF: 5k]. Day and night averaged solar radiation at Paranal.

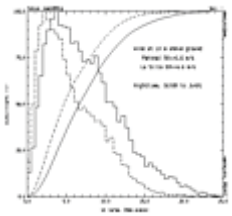

Figure 2.22 [GIF: 6k]. Wind velocities at Paranal and La Silla.

Figure 2.23 [GIF: 3k]. Paranal windrose.

2.8.3.2 Sky Data

Photometric Nights: The sky is photometric in 77 % of the night time (Fig. 2.24).

Seeing: The 50 % fractile 0.66" FWHM (Fig. 2.25).

Water Vapour: The precipitable water vapour is less than 1 mm for 8.2 % of the night time. (Fig. 2.26).

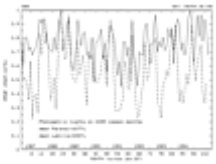

Figure 2.24 [GIF: 15k]. Average monthly percentages of photometric nights at La Silla and Paranal for the period 1987-1995.

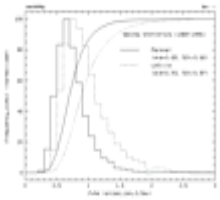

Figure 2.25 [GIF: 8k]. Seeing statistics on the basis of one hour equivalent exposures at La Silla (dotted Line) and Paranal (full line) from 1989 to 1995.

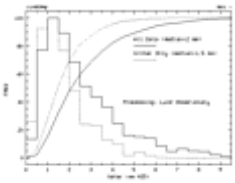

Figure 2.26 [GIF: 5k]. Distribution of integrated water vapour content in the atmosphere above Paranal for the period July 1992 to December 1994. The distribution, in percent, is given for the amount of precipitable water, expressed in millimeters.

2.8.4 Seismics

Paranal is located in a **seismic area** where the South American tectonic plate is being subducted under the Pacific plate. The main seismic data are given in Table 2.6.

ESO has carried out extensive studies of the influence of this activity on the various components of the VLT. A number of **anti-seismic (e.g., damping and shock-absorbing) elements** have consequently been introduced into the telescope foundations and the enclosures in order to ensure minimum damage to essential elements under given circumstances. Several moderately strong events have ocurred during the construction phase, during which the validity of these concepts was confirmed.

Table 2.6: Seismic Data for Paranal

Type of event	**Value**	**Comment**
Moderate earthquake:	Some times per year	Mg < 7.75
Operating basis earthquake (OBE) :		
Peak horizontal acceleration	0.24 g	Typical
Probability of excedance	50 %	
Repetition period	25 years	
Magnitude	7.75	Richter
Hypocentral distance	100 km	
Duration	65 s	
Max. likely earthquake (MLE) :		
Peak horizontal acceleration	0.34 g	Typical
Probability of excedance	10 %	
Repetition period	100 years	

Magnitude	8.5	Richter
Hypocentral distance	150 km	
Duration	200 s	

2.9 The VLT End-to-End Model

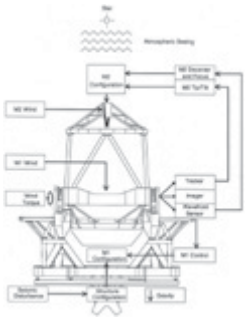

Figure 2.27 [GIF: 175k]. The VLT End-to-End Telescope Model.

The VLT end-to-end model is a complex system application that represents the **critical performance aspects** of the VLT UT through the Nasmyth and Cassegrain foci. The model provides interactive systems and analysis of the integrated mechanical, controls, and optical performance of a single UT. The individual or combined effect of atmospheric turbulence, environment, and elevation configuration is included to support disturbance analysis of the system. The model provides ESO with the ability to perform analysis, evaluation of design alternatives, and investigation of various operational aspects of the VLT. The diagram of the telescope model is shown in Fig. 2.27.

Inherent in the VLT model is **close coupling between optical, controls, and structural design configurations** . Analysis of nested sensor, servo, and actuator loops combined with various optical designs or structure definitions is possible. The combined effect of the entire system to each of the VLT sensors is available to the user. Questions concerning the system radiometric sensitivity under different observing conditions can be addressed as well as the effect of atmospheric turbulence between multiple objects and sensors as a function of line-of-sight angle. Assumptions regarding primary mirror response to wind loading and the mitigating effect of the Active Optics control loop can also be investigated.

Included in this model is a representation of structural dynamics through to the telescope fork, optical dynamics through to the Nasmyth and the Cassegrain foci, closed-loop control of the primary mirror shape, secondary tip/tilt/decenter/defocus, and limited environmental effects, including wind load, turbulence, gravity, and seismic disturbances. Typical analyses run with the model have included:

- Response of primary mirror hydraulic support to wind load;
- Limiting magnitude performance with full disturbances;
- Contribution of local seismic disturbances on overall telescope performance;
- Control bandwidths required to meet desired error rejection with full disturbance;
- Observation of a star for long periods;
- Tracking performance with and without atmospheric turbulence

2.9.1 Components

The **telescope optics** is modeled through to the Cassegrain and Nasmyth foci. The approach is to calculate all the geometrical system aberrations, and to build up a description of the complex electromagnetic field in an equivalent pupil and then propagate this pupil to the image plane using a Fraunhofer single Fourier transform propagator. This method, by far the least computationally intensive, is extremely accurate in reasonably well-designed imaging systems such as the VLT.

The **atmosphere** is modeled with up to three phase screens, each with its own wind speed and altitude. The object and guide star are geometrically propagated through the phase screens to obtain an equivalent representation in the pupil place, i.e., the phases from the portions of the phase screens that geometrically coincide with the entrance pupil are added in the pupil.

Three sensors are modeled: the *image sensor* which represents the scientific instrument, the *track sensor* used to measure the image motion in the field stabilization loop and the *wavefront sensor* used by the Active Optics loop. The image and track sensors are CCD detector arrays, and the wavefront sensor is of the Hartmann Shack type. All three sensors model shot noise, readout noise, detector quantum efficiency, and fill factor. The CCD model also includes dark current noise and the effects of pixel-to-pixel non-uniformity, least significant bit, and well capacity. High-frequency disturbance effects on the image are collected on three sensors by sampling the incident intensity at a higher rate than the sensor frame.

The **VLT structural model** is linear and is derived from mass/stiffness matrices. The telescope structure is segmented into two components: *the fork* (or pier) on one hand, *the tube* with the M1 Mirror and Cell on the other hand. This latter FE model includes the lateral supporting system of the primary mirror, but not the axial support interface between the mirror and its cell. The M1 axial supporting system is defined outside the FEMs by the hydraulic support model.

The primary axial support consists of 150 evenly spaced hydraulic pistons that apply each a force on the rear of the primary. The pistons chambers are connected together thanks to an **hydraulic network** , of which a representation is implemented in the model.

Mechanical disturbances modeled in the VLT end-to-end model are the **seismic, gravity and wind disturbances** , with the latter divided into three categories: wind on the primary mirror, wind on the M2 unit and wind on the elevation axis. Except for the gravity, each of these disturbances is specified by its mean value and a PSD given in terms of poles, zeroes and a gain. A time series is then generated, based on the time step and the simulation duration. The simulation time step is selected in such a way that aliasing is avoided.

The **Active Optics** function is to compensate for the low-frequency aberrations by deforming the primary and defocusing and/or decentering the secondary. The Active Optics control loop uses the wavefront sensor to measure these aberrations.

The model also includes a system to **stabilize the image motion** . This system makes use of the M2 tip/tilt function to compensate for image translations measured by the tracker. The jitter to be corrected by this system is a combination of tilt due to telescope excitation by wind and of atmospheric tilt. The stabilization control loop also includes the M2 dynamics.

2.9.2 Model Architecture

Figure 2.28 [GIF: 47k]. Functional flow diagram of the VLT end-to-end model.

The model functional flow diagram is illustrated in Fig. 2.28.

The telescope structure consists of the pier, the fork, the tube, the primary, its cell and the hydraulics. These can be acted upon by either a wind force, a wind pressure field, gravity or a seismic excitation. The user may observe the dynamics of any node defined within the structure or generate a modal representation if desired.

The state and position of the M1 optical surface is then generated for the complex field calculation. Next, the complex field at the pupil is calculated with contributions from atmospheric turbulence, irradiance from selected objects at the telescope entrance aperture with obscurations, and high order errors resulting from misalignments within the UT. The misalignment-induced high order wavefront error is derived from sensitivity coefficients input by the user and computed from ray-tracing during the initialization. Image translation and/or tip/tilt is handled separately in each sensor leg to allow different effective focal lengths for the sensors.

Wavefront propagation to either the tracker or imager is accomplished independently with sensor frame rates as specified by the user. The track sensor generates tip/tilt error signals to M2. The wavefront sensor provides correction forces to M1 and focus/decenter commands to M2.

VLT Whitebook Chapter 3: The Optics

The current design of the VLT optical systems is the outcome of a long evolution, dating back to the 1970's, when the first ideas about a *giant telescope* were beginning to circulate within the astronomical community. The question of the most desirable telescope configuration (single or multiple elements) was open until the mid-1980's.

The decision to include a Cassegrain focus, in addition to the Nasmyth and coudé foci, was taken during the design phase, after the beginning of the VLT project.

3.1 Concept

Figure 3.1 [GIF: 59k]. Optical lay-out of the VLT with dimensions indicated.

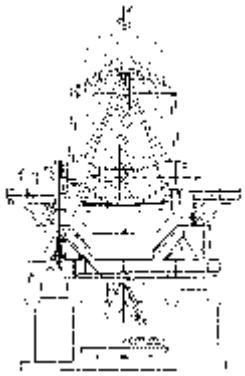

Figure 3.2 [GIF: 94k]. Lay-out of the VLT optics, superposed on the mechanical structure, thus showing the location of the individual elements.

The four individual VLT 8.2-m telescopes each have **four foci** : *two Nasmyth, one Cassegrain* and *one Coudé* . The optical lay-out, including eight mirrors (M1 to M8) and with the main dimensions, is shown in Fig. 3.1. Adding the interferometric focus (cf. Chapter 9), brings the total number to 17. The location of the individual optical elements within the telescope structure is seen in Fig. 3.2.

In the Nasmyth configuration, the design is of the **Ritchey-Chrétien type** , i.e., the telescopes are nominally free of field coma. However, the Cassegrain focus is not of the Ritchey-Chrétien type. Conversion between the two foci implies a repositioning of the secondary mirror and a change of the conic constant and radius of curvature of the primary mirror.

The **coudé focus** is located below the main telescope structure. It also serves to send on the beam towards the interferometric delay lines and the interferometric focus.

The nominal values of the **main optical parameters** at the VLT foci are contained in Table 3.1.

Table 3.1: VLT Foci Main Optical Parameters			
Parameter	**Cassegrain**	**Nasmyth**	**Coudé**
No. of reflections	2	3	8
Focal length	108,827 mm	120,000 mm	378,400 mm
Focal ratio	13.41	15.0	47.3
Scale	0.53 mm/arcsec	0.58 mm/	1.84 mm/
Object FOV (total)	15 arcmin	30 arcmin	1 arcmin
Object FOV (unvignetted)	2.7 arcmin	7.2 arcmin	1 arcmin
Image FOV (total)	475 mm	1044 mm	110 mm
Image FOV (unvignetted)	85 mm	250 mm	110 mm

The **optical performance** of the VLT is expressed in terms of peak intensity in a long-exposure image at a given wavelength and with a given atmospheric seeing. The basic assumptions are:

1. the **atmospheric turbulence** can be presented by a free atmosphere model;
2. **scintillation** is neglected, i.e., the modulus of the electromagnetic field is assumed to be constant over the whole area of the entrance pupil; and
3. **background noise** is neglected.

3.1.1. Optical Quality

The **optical quality requirement** is based on diffraction theory and takes into account atmospheric turbulence. Only long-exposure images are considered, which means that speckle patterns are averaged out. On the other hand, it is assumed that the seeing conditions are stable within the exposure time.

Resolution and **sensitivity** are kept at a level where the limitation is given by the atmosphere rather than by the optical quality of the telescope. To a large extent the telescope aberrations are hidden by atmospheric seeing. To stay on the safe side, the quality requirement assumes excellent seeing.

The parameter which represents the actual optical quality of the telescope is the decrease of the central intensity in the long-exposure image of an unresolved star. The key parameter is the **Central Intensity Ratio (CIR)** . Thus, the optical quality requirement for the VLT unit telescopes that:

CIR > 0.80

i.e., the maximum allowable decrease of the peak intensity in the long exposure image is 20% with r o = 250 mm at wavelength 500 nm, where r o is the *atmospheric coherence length* .

The requirement applies to the Nasmyth and Cassegrain foci. It includes all errors which affect the phase of the wavefront, with the sole exception of the turbulence of the free atmosphere, i.e., surfaces, guiding, alignment and control errors are included, as well as the local air turbulences and the effect of wind pressure.

The geometrical parameter which can most reliably quantify the actual optical quality of a large ground-based telescope is the **rms radius** of the geometrical image; geometrical energy concentration and total image size are much less representative. The current goal for the VLT at Nasmyth focus should lead to a **rms radius of the geometrical image in the order of 0.1 arcsec** , including guiding errors.

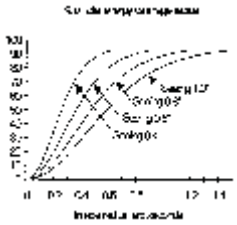

Figure 3.3 [GIF: 9k]. Predicted energy concentration of the VLT optics.

At this level, the full width at half maximum (FWHM) of the long-exposure image is virtually the same as the FWHM of the seeing disc. With 0.4 arcsec seeing at wavelength 500 nm, the FWHM of the long-exposure point spread function is expected to be in the 0.45 arcsec range and the diameter of 80% encircled energy in the 0.80 arcsec range, with a seeing of 0.40 arcsec (*r o* = 250 mm) at wavelength 500 nm.

The expected energy concentration with seeing angles varying between 0.4 and 1.0 arcsec FWHM is shown in Fig. 3.3.

3.1.2. Operating Conditions

The optical quality of the VLT unit telescopes at Nasmyth and Cassegrain foci will be maintained under the following operating conditions:

- Temperature range 0 to 15 o C
- Average wind speed 18 m/s ± 2 m/s at 1 Hz
- Zenithal distance between 0 o and 70 o

A deterioration of image quality is accepted outside this range. The variation of the CIR with temperature is very limited anyhow.

3.2 The Primary Mirror

Figure 3.4 [JPG: 441k]. The M1 Zerodur mirror, installed at the UT1 and with the protective cover removed. At this time, it was still uncoated. (April 1998).

The primary mirrors of the VLT UTs are the largest ever made. They are actively supported, thin Zerodur menisci, 8.2-m diameter. The mirror blanks were produced by *Schott Glaswerke AG* (Mainz, Germany); the optical figuring, manufacturing and assembling of interfaces and auxiliary equipment were done by *REOSC* (St. Pierre du Perray, France).

Following completion and testing, the first VLT primary mirror was ready at REOSC in November 1995.

This chapter provides information about the manufacturing specifications, a brief account of the long production procedure and tables with the actually achieved parameter values.

3.2.1 Specifications

The essential requirement for the optical performance of the VLT primary mirror is that it shall not impair the image quality permitted by atmospheric turbulence, even under the very best seeing conditions which may occur at the observatory site and at any wavelength. Hence the mirror specifications take into account the disturbing role played by atmospheric turbulence.

Since the mirror is actively controlled, low spatial frequency terms can be subtracted from the overall wavefront error. In the telescope, these terms are dealt with by an appropriate offset of the support forces. For the VLT primary mirrors, active optics is achieved by modal corrections, i.e., the measured deformation is fitted with the mirror's eigenmodes (up to 16) and the necessary correction forces are deduced linearly from the eigenmodes' coefficients.

The total active forces budget for the active optics correction capability of the unit telescopes is in the 800 N range (compression forces only). Of these, a budget of ±120 N has been allocated for the figuring errors of the primary mirrors. The support system in the M1 cell has been designed to reach an accuracy of a few grammes. The support system used by the optical manufacturer for the purposes of manufacturing and testing does not require an accuracy better than about 2 N, which is sufficient to allow accurate wavefront measurements.

The optical quality specification after active correction is in-line with the formalism developed at ESO to assess telescope performance. In particular, it can be shown that *a loss of optical quality* or of reflectivity of the surfaces reduce signal throughput in the same manner as would a *reduction of collecting area* .

The specification for high spatial frequencies requires that after a perfect active correction with the 16 first eigenmodes, the remaining errors do not degrade the peak intensity in the long-exposure Point Spread Function by more than 18%, at a wavelength of 500 nm and an atmospheric coherence length r 0 of 500 mm (seeing angle 0.2 arc second FWHM). Hence the optical quality specification for the primary mirror is that the Central Intensity Ratio **CIR = 0.82 with r o = 500 mm (seeing angle 0.2 arcsec) at = 500 nm** , after perfect active correction of the 16 lowest spatial frequency eigenmodes of the mirror. Under more frequent and still excellent seeing conditions, e.g. 0.4 arcsec, the CIR should be higher than 0.95.

3.2.2 The Manufacturing Process

The manufacturing process at Schott starts with the casting of approximately 45 tons of glassy Zerodur into a concave mold. Thereafter the mold is transported onto a rotating platform where it is spun until solidification. When the temperature has decreased to about 800 o C and the viscosity is such that the blank will retain its meniscus shape, it is brought into an annealing furnace where it is cooled down to room temperature in about 3 months.

The critical operation of unmolding required the design of a sophisticated handling tool with an array of 18 actuated suction cups that allow the mirror to be handled within extremely low external stresses. The first surface to be machined is the convex surface, onto which a thin crystalline layer has built up during annealing. This layer has a different thermal expansion coefficient than the bulk of the substrate; it may endanger the integrity of the blank and must be removed first. Therefore the first operation after unmolding is to turn the mirror convex surface up and lay it down onto the machine. The blank is then turned back concave surface upwards and the concave surface machined, following which it is brought back into the furnace for the ceramization cycle, that takes approximately 9 months. Then it is machined down to final shape unless a fine-annealing cycle is still required to achieve the extremely low residual stresses needed of the final product.

The blanks were transported in a special transport container via the Rhine river, along the coast to Calais and up the Seine river to Evry, from where the transport to the REOSC premises was done by road, on a hydraulic platform. Once at REOSC, it is positioned on the figuring machine on an array of 150 pneumatic supports with the same distribution and interface with the mirror as the support system of the M1 cell.

The mirror is ground spherical with large, stiff tools, then aspherical with flexible tools of diameters ranging from 1 to 4 meter. The computer-controlled figuring process of REOSC consists in adjusting the tool speed to provide the wear pattern corresponding to the material to be removed, in accordance with the measured surface deviations. At the grinding stage, the mirror surface is mapped by spherometry to sub-micron accuracy. At the end of this phase, the mirror surface is within approximately 1 µm RMS of the final shape. At this point, lateral interface pads are glued onto the outer edge of the mirror and the mirror is transferred onto the polishing machine. The latter is identical to the figuring machine and is located at the bottom of a 30-m high optical test tower.

At the early stage of polishing the mirror is controlled by infrared interferometry at 10.6 µm through an infrared null-lens. Thereafter it is tested by interferometry at 633 nm through a visible null-lens.

Inspections and quality assurance verifications occurred periodically during the manufacturing processes. Verification of the mirror blanks compliance with the specifications was performed through a series of dimensional measurements, together with measurements of material properties, e.g. Young's modulus, average value and dispersion of the coefficient of thermal expansion, and internal characteristics, e.g. mapping of inclusions, stress birefringence at the edges and at inclusions. At the final verification, the polished mirror assembly was inspected for physical characteristics (weight, dimensions), for interfaces (geometry, distribution, safety with respect to overload) and optical quality. A number of cross-checks were made to ensure that no systematic error (e.g., matching error) had escaped detection.

The mirrors were measured at different orientations to track possible asymmetries, e.g. in the alignment of the set-up. The sampling of the full aperture test covered 250 x 250 measurement points on the mirror, which limits the minimum period of detectable wavefront errors to 64 mm. Higher spatial frequencies were sampled by sub-pupil interferometric tests providing 250 x 250 points on circular sub-pupils of 2.5-m diameter.

3.2.3 Mirror Characteristics

Table 3.2 lists the characteristics of the mirror blanks, as compared to the specifications. The geometrical characteristics are **well within the specifications and the homogeneity of material properties is simply outstanding** . Inclusions (including bubbles) content is particularly low. Residual stresses, as predicted by modeling and measured by birefringence, are negligible.

Table 3.2: Characteristics of VLT Main Mirror Blanks

Parameter	**Specified**	**Blank 1**	**Blank 2**	**Blank 3**	**Blank 4**	Unit
Geometrical dimensions						
Outer diameter	8200 ± 2	8201.52	8201.74	8201.72	8201.74	mm
Diameter of center hole	1000 ± 0.5	999.81	999.93	999.87	999.72	mm
Concentricity	±1	0.01	0.01	0.01	0.01	mm
Thickness	177+2-0	177.9	177.7	177.5	177.7	mm
Concave surface						
Curvature	28975	28975	28975	28975	28975	mm

Profile tolerance	2	0.12	0.08	0.08	0.06	mm
Convex surface						
Curvature	28977	28977	28977	28977	28977	mm
Profile tolerance	2	0.05	0.07	0.06	0.07	mm
Material properties						
Density	2.53	2.534	2.534	2.534	2.535	
CTE	0 ± 0.15 10 -6	-0.043 10 -6	-0.032 10 -6	-0.040 10 -6	-0.017 10 -6	K -1
Homogeneity	< 0.05 10 -6	0.009 10 - 6	0.011 10 - 6	0.024 10 - 6	0.028 10 - 6	K -1
Young's modulus	91000	90000	90000	90400	90300	Mpa
Poisson's ratio	0.24	0.243	0.243	0.243	0.243	
Internal quality						
Inclusions in critical volume						
Mean size	< 5	< 0.5	< 0.5	< 0.6	< 0.6	mm
Max. size	< 8	2.3	3.5	1.1	XX	mm
Average number	< 0.5	< 0.01	< 0.01	< 0.01	XX	cm -3
Max. in 10 cm 3	< 8	< 4	< 4	< 4	< 4	
Stress birefringence caused by inclusions						
in critical volume	< 25	21	<12	0	0	nm
outside critical volume	< 50	30	<12	27	0	nm

Permanent stress at outer edge (compressive)						
Mean value	> -10	-6.2	- 9.3	-6.5	-8.0	nm/cm
Max. value	> -20	-7.0	-10.4	-8.3	-9.5	nm/cm

Interferometric tests have revealed that in the active mode the first three mirrors are diffraction-limited at H-alpha (wavefront RMS error of 48 nm, 39 nm and 35 nm, respectively).

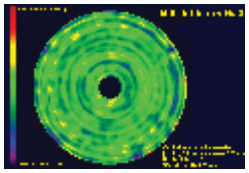

Figure 3.5 [GIF: 120k]. Wavefront map of the third primary mirror, as measured at REOSC, and after perfect active correction (16 first eigenmodes).

As an example, Fig. 3.5 shows the wavefront error map of the first mirror. Note that care must be taken in interpreting the data shown. High spatial frequencies visible on the interferogram and wavefront maps correspond to periods comparable or larger than the atmospheric coherence length (25 cm for a seeing of 0.4 arcsec in the visible). Indeed the surface is relatively smooth at very high spatial frequencies; sub-pupil interferometric tests with 250 x 250 points on 2.5-m diameter areas reveal that the wavefront variation for spatial periods below ~20 cm is in the 5 nm RMS range and decreasing at even higher spatial frequencies.

Table 3.3 lists the essential results obtained with the first mirrors. In this table the curvature and the conic constant are obtained from the direct Hartmann test. The correlation with other measurements such as spherometry and distance measurement mirror-to-null-lens is about 2 mm on the curvature and below measurement noise on the asphericity. Hence there is an exceptionally good agreement between all tests aimed at tracking errors of matching. Correction forces determined from each series of interferometric measurement are stable within ~5 N. These variations are likely to be due to drifts of the force settings as well as support inaccuracy and variations of thermal conditions. Vertical thermal gradients in the test tower were found to be of the order of 2 ºK or less, and horizontal gradients below 0.1 ºK.

Table 3.3: Optical Properties of VLT Main Mirrors

Parameter	**Specified**	**Mirror 1**	**Mirror 2**	**Mirror 3**	**Mirror 4**	**Unit**
Radius of curvature	28800 ± 100	28762.9	28760.0	28762.6	N/A	mm

Conic constant (passive mode)	-1.004616	-1.004457	-1.005089	-1.004392	N/A	
Active forces	±120	-83 +52	-80 + 82	-84 +81	N/A	N
RMS Wavefront (active mode)	N/A	48	39	35	N/A	nm
RMS Slope (active mode)	N/A	0.055	0.038	0.057	N/A	arcsec
Strehl ratio at 500 nm	0.25	0.722	0.791	0.826	N/A	
CIR (= 500 nm, r o = 500 mm)	0.820	0.852	0.884	0.889	N/A	
Microroughness	N/A	15-25	8-15	20	N/A	Å

The production of the VLT primary mirrors proceeded according to schedule and requirements, and within budget. No major difficulty has been encountered, and the experience gained with the first mirror allowed to streamline the process to such an extent that the production rate at REOSC is in the range of one year, from blank to finished mirror.

In conclusion, the optical quality of the VLT primary mirrors is fully adequate for the very best observing conditions encountered at any ground-based astronomical site.

3.3 The Secondary Mirror

Figure 3.6 [JPG: 432k]. The M2 mirror, installed at the top of the UT1 tube, together with the M2 Unit (April 1998).

The M2 mirror is a **convex, hyperbolic mirror** with an external diameter of 1.1 metres. It is supported by the M2 Unit at the top of the telescope tube and reflects the light from the M1 mirror towards the M3 plane mirror. By modifying its position and orientation, it is possible to correct some optical aberration of the telescope (defocus and decentring coma) and to change the pointing.

The mirror cell is a ring type element, interfacing the mechanics of the electromechanical assembly.

3.3.1 Specifications

The M2 mirrors of the VLT are convex hyperbolic mirrors whose optical design parameters and physical dimensions are given in Table 3.4:

Table 3.4: Specifications of M2 Mirrors

Parameter	Specified	Measured/Comment
Minimum optical diameter	1116 mm	ca. 1119.8 mm
Maximum mechanical diameter	1120 mm	1119.98 mm
Bevel	Minimised, < 2 mm	< 0.1 mm
Internal obscuration diameter	46 mm	45.9 mm
Blank material	Beryllium	Structural grade I-220H

Cladding	Electroless Nickel coating	
Mirror mass	Minimised; < 50 kg	43 Kg
Total mass (including cell)	Minimised, < 56 kg	52.5 kg
First eigenfrequency (free-free)	ca. 800 Hz	798.4 Hz
First eigenfrequency mounted	ca. 400 Hz	370 Hz
Internal residual stresses	< 40 MPa	< 10 Mpa (estimated)
Radius of curvature	-4553.57 mm	-4554.62 mm
Conic costant	-1.66926 ± 0.003	-1.69980
Passive mode (all surface errors)	0.7 arcsec RMS	0.3 arcsec RMS after removal of defocus and 3rd order Spherical Aberration
High spatial frequency errors	CIR >= 0.98	0.98
Microroughness	< 2 nm RMS	<= 1.5 nm RMS

The optical quality requirements depend on whether the mirror is in the **active** mode (active optics correction in operation, removing low spatial frequency errors) or in the **passive mode** (active optics correction not in operation):

- In the **passive mode** (all surface errors included): The RMS slope error of the surface of the mirror after removal of the effects of curvature error (focus error) and conic constant (third order spherical aberration) is less than 0.7 arcsec; and
- In the **active mode** (only high spatial frequency errors considered): The variation of peak intensity in the PSF of the telescope at the Nasmyth focus (induced by the high spatial frequency errors of the mirror) are less than 2 % i.e., the Central Intensity Ratio is larger than or equal to 0.98, with an atmospheric coherence length of 250 mm at a wavelength 500 nm.

The **micro-roughness** of the polished surface is random and < 2 nm RMS. There are a minimum of surface flaws (scratches, pits and sleeks), and the mirror is stable with respect to ageing, at least over a period of 25 years.

3.3.2 The Manufacturing Process

Figure 3.7 [GIF: 112k]. The M2 mirror (back side) at *Loral* during the manufacturing phase.

The **mechanical characteristics of the mirror** , listed in Table 3.4, are no less important than the optical ones. The mirror must be stiff and light to limit the actuators forces and power dissipation, to achieve a high closed loop bandwidth and to minimise the stresses.

To achieve this performance, the blank, exhibiting an open back flat structure, is made of **lightweighted, Nickel-plated Beryllium** . The optical figuring is done on the Nickel layer. The support system uses three flexural bipods located at approximately two thirds of the radius and fastened onto the blank in reinforced areas. The mirror cell is made of Titanium.

The **manufacturing technology** can be considered to represent the state-of-the-art for large Beryllium optics. The requirements set on the secondary mirror, especially in mechanical terms, led to a selection of structural-grade Beryllium (I-220H), rather than optical-grade. Starting from Beryllium powder obtained by impact grinding in order to overcome the natural anisotropy of Beryllium, a billet of 1.2-m diameter is produced by Hot Isostatic Pressing (HIP). The billet exhibits a density > 99.7% of the nominal density. After radiographic inspection, the blank is light-weighted and the interfaces for the supports are generated by machining.

The procedure of grinding to the aspherical shape also includes a certain number of **thermal annealing cycles** for the removal of internal stresses and to stabilise the mirror. The blank is then electroless nickel plated. Due to the large surface of the structural pockets and ribs at the back of the blank, a thinner layer of nickel is put on the back face than on the front face to

avoid unnecessary weight increase. This is a critical process, because the deposited Nickel must have a thermal expansion coefficient very similar to that of the Beryllium in order to avoid bimetallic effects.

The minimum thickness of Nickel on the front surface is dictated by the polishing process.

Since the mirror is slightly undersized, it must be polished up to the rim and mus not have a turned-down edge. A sharp edge is necessary for minimised infrared emissivity.

The first of the four blanks was slightly oversized to avoid edge effects during polishing. After polishing, the edge of the mirror was cut by electro-machining, which produced a sharp edge and the right external dimension, but demanded some further polishing. The external edge was then protected with a chemical Nickel layer.

Blanks 2, 3 and 4 are cut prior to Nickel plating and final polishing. Afterwards, they are polished up to the edge.

Throughout the manufacturing process, great care must be exersized to avoid any figure change induced by release of internal stresses or by the removal of material. For this purpose, a large number of thermal cycles are foreseen at each manufacturing stage and also during the polishing phase. The objective is to achieve internal residual stresses that are well below the microyield strength of the material, thus guaranteeing the long-term stability of the blank.

3.3.3 Mirror Characteristics

After coating and installation at UT1 in late April 1998, the reflectivity of the surface of the first M2 mirror was measured as 92.3 ± 0.5 % at wavelength 670 nm. The microroughness was 11 ± 5 Å (mean value of 9 measurements).

3.4 The Nasmyth Mirror

Figure 3.8 [GIF: 398k]. The M3 mirror and its cell (CAD).

Figure 3.9 [GIF: 171k]. Beam paths near the M3 Mirror, during operation at the Nasmyth foci (left) and at the Cassegrain focus (right).

The **Tertiary Mirror Assembly** is an opto-mechanical system constituted by the Tertiary Mirror (M3) and its support Cell (Fig. 3.8). In Nasmyth configuration, the mirror deflects the light beams reflected by the secondary mirror towards the scientific instrument located at one or the other Nasmyth focus. In Cassegrain configuration, the M3 Mirror Assembly is remotely flipped in towed position, parallel to the axis of M3 Tower (Fig. 3.9).

The tertiary mirror assemblies for the VLT UTs consist of **optical flats** (elliptical shape, 890 x 1260 mm 2). The achieved design is challenging since it provides a 70 Hz first Eigenfrequency for a total mass of 180 Kg for the complete unit. The lightweight Zerodur blanks are produced by *Schott Glaswerke AG* (Mainz, Germany).

The completion and testing of the first tertiary mirror at *Carl Zeiss* (Jena, Germany) was ready in June 1998.

This chapter provides information about the manufacturing specifications and a brief account of the production sequence.

3.4.1 Specifications

Because the M3 is fairly close to the Nasmyth foci of the telescope, compensation of the mirror misfigure by means of active optics is limited to curvature errors only. Since the wavefront sensors of the active optics system are located off-axis, they receive light beams which have been intercepted by different areas of the M3. Nevertheless, the active optics corrections apply to the entire FOV. Therefore, off-axis surface deviations of the M3 can impair the on-axis optical quality. As a consequence, the optical quality specification limits the sum of the surface deviations for the off- and on-axis footprints of the light beams.

The Tertiary Mirror Assembly being located on the M3 Tower 2.5-metres above the Primary Mirror, the mass of the Assembly is kept low to minimize centering errors of the Mirror.

The optical quality specifications cover the effect of all deviations of the actual surface of the Mirror, with respect to an ideally plane surface, on the imaging performance at the Nasmyth foci. It includes:

1. the minimum radius of curvature of the Mirror (best fitting sphere over the useful area of the mirror): R > 63000 meters;
2. the maximum allowable mid- to low spatial frequency wavefront slope errors at Nasmyth focus are less than 0.023 arcsec;
3. the maximum allowable high spatial frequency errors at Nasmyth foci: < 5 nm RMS and < 20 nm PTV (mirror mechanical surface); and
4. the microroughness over the useful optical area is < 2 nm RMS.

3.4.2 M3 Hydraulic Support System

The M3 is a Zerodur lightweight mirror, 140 mm high, supported by 13 axial and 6 lateral supports, connected to a passive hydraulic system to provide the required stiffness. To prevent the mirror from falling from its Cell, 12 additional pads (safety pads) have been installed. The Cell is a welded stainless steel structure, 90 mm high. Reference marks for the fine adjustment of the mirror position with respect to the cell and an alignment target for the future adjustment of the tertiary mirror have been integrated.

3.4.3 Manufacturing of the M3 Blanks

Figure 3.10 [GIF: 268k]. The lightweighted M3 mirror.

The production of the M3 blanks at Schott comprises the **casting and grounding out** of an elliptical Special Zerodur substrate, and **lightweighting up to a 65% ratio** by means of machined cores on the rear side of the blank (Fig. 3.10). The complete blank is etched after grinding. Cage lapping and polishing of the mirror is done with the optical face down. Fine polishing is achieved by computer controlled polishing, to bring the mirror surface into specification, especially as far as the edge is concerned.

A test tower was erected for interferometric testing. An algorithm was developed for processing the data from the tests in two positions.

3.4.4 Mirror Characteristics

Table 3.5 shows some data for the two first M3 mirrors. Note that the second mirror is not yet finished (TBC: to be continued).

Table 3.5: Charactistics of M3 Mirrors

Parameter	Specified	Unit 1	Unit 2
Radius of curvature	> 63,000 meters	2,500,000 m	> 230,000 m TBC
Mid-to-low spatial frequency errors	< 0.023 arcsec; < 200 nm PTV	0.009 arcsec; 155 nm PTV	0.018 arcsec TBC; 350 nm PTV TBC
High spatial frequencies	< 20 nm PTV; < 5 nm RMS	19.5 nm PTV; 2.2 nm RMS	TBD
Microroughness	< 2 nm RMS	1 nm RMS	TBD

3.5 Sky Baffling and Pupil Alignment

Figure 3.11 [GIF: 180k]. The Sky Baffle at the M2 Unit during tests.

Stray light reduction is basically accomplished on two levels: in the telescope tube and in the focal plane instrument.

At the telescope level, the direct sky radiation that would otherwise reach the focal plane is prevented from doing so by means of the **M2 Sky Baffle** (Fig. 3.11).

When looking, e.g., from the Cassegrain focus towards the secondary mirror (M2), an annular portion of the sky will be visible around the M2. A similar area of the sky can be seen from the other foci. The sky background radiation from this area would be imaged directly onto an instrument detector and would therefore contribute significantly to the registered signal, increasing the number of irrelevant photons received, i.e., decreasing the signal-to-noise ratio of the recorded information.

The M2 Sky Baffle eliminates this radiation. However the baffle cannot, and is not intended to provide a complete protection against straylight. It is rather designed to complement the general light baffling within the instruments by eliminating an important source of parasitic light.

The Sky Baffle is located on top of the M2 Unit and has a diameter of 1500 mm when deployed. The baffle segments are **selectively coated** (by a special "Maxorb" foil) on the visible, lower side. The coating has the characteristics of a black coating in the visible spectral range and of a low-emissivity coating in the infrared range. Moreover, the segments are temperature controlled in order to prevent local seeing effects; they are maintained at the same temperature as the surrounding air.

The M2 Unit is furthermore equipped with a so-called **Multipurpose Interface (MPI)** at the centre of the mirror. It allows to accommodate either an alignment target (for the telescope alignment) or a light source. This source (e.g., via an optical fibre connected to a light emitting diode) will be used, in particular, by the VLTI instruments for their **pupil alignment** . This provision also includes some space reserved for the necessary electronic equipment and the related cable routings within the M2 Unit.

3.6 The Cassegrain Focus

3.6.1. Optical Design

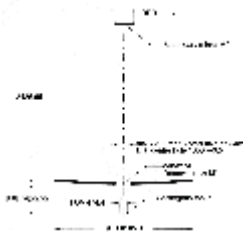

Figure 3.12 [GIF: 51k]. Optical design of the Cassegrain focus. The diameters diameters indicated are those of the reflective surfaces

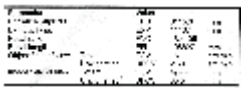

Figure 3.13 [GIF: 39k]. Nominal optical design data at Cassegrain focus.

The nominal **optical design** of the VLT Unit Telescopes at the Cassegrain focus is shown in Fig. 3.12 and the corresponding data given in Fig. 3.13. The pupil is on M2 and the unvignetted field of view is the maximum field of view without vignetting by the primary mirror.

The **backfocal distance** is 2500 mm; it is measured from the vertex of the primary mirror down to the Cassegrain focus. The vertex of the primary mirror is about 4.34 mm below the plane defined by the edge of the nominal centre hole, dia. 1000 mm. The distance between the vertex of the primary mirror and the intersection point of the elevation axis with the optical axis is 2500 mm.

Because of the field curvature **the image scale** is not constant. Figure 3.14 gives the distance from the optical axis to the centroid on the image surface (curved field) with respect to the sky angle.

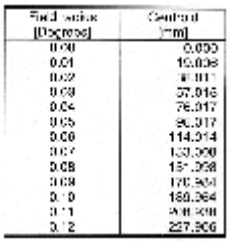

Figure 3.14 [GIF: 40k]. Image scale of the curved image plane at the Cassegrain focus.

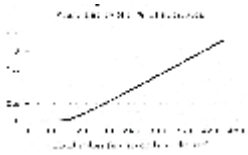

Figure 3.15 [GIF: 32k]. Vignetting by the primary mirror at the Cassegrain focus.

Vignetting by the primary mirror occurs when the aperture beam extends outside the reflective area of the primary mirror. With the nominal optical design and nominal M1 bevel size the unvignetted field of view is 2.68 arc minutes in diameter. There is no vignetting by the central hole. The vignetting by M1, in percents of the area of the entrance pupil (inner diameter 1120 mm, outer diameter 8115 mm) is plotted in Fig. 3.15.

The **field aberrations** on the curved Cassegrain image are third order coma and astigmatism. The coma term of the wavefront error is increasing linearly with the distance to the optical axis. The term of astigmatism is increasing linearly like the square of the distance to the optical axis.

3.6.2. Adapter/Rotator

The Cassegrain Adapter/Rotator is almost completely equivalent to the Nasmyth Adapter/Rotator that is discussed in detail in Chapter 3.7.2 ; please consult that chapter. It has the same functions, except that it does not include the deflection of light (to the coudé, etc. foci, as well as the feeding of light from a peripheral reference star into the coudé field.

3.6.3 Instrument Interface

Cassegrain instruments with a total mass not exceeding 3000 kg can be attached to the Rotator flange.

The moment applied by the instruments to the Rotator flange with a moment vector perpendicular to the optical axis, must not exceed 20 kNm. Instruments attached to the Rotator flange must not apply a total moment to the Rotator flange due to imbalance and friction, with a moment vector parallel to the optical axis, exceeding 500 Nm in any telescope altitude. The maximum torque component due to friction alone, for example from the instrument cable wrap mechanism, must not exceed 100 Nm.

3.7 The Nasmyth Focus

There are two Nasmyth foci at each UT. The corresponding platforms are designated **Platform A** and **Platform B** . For azimuthal angle A = 0 o , Platform A is on the east side of the telescope tube and Platform B on the west side.

3.7.1 Optical Design

Figure 3.16 [GIF: 61k]. Optical design of the Nasmyth focus. The diameters diameters indicated are those of the reflective surfaces.

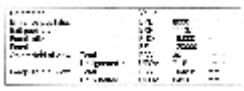

Figure 3.17 [GIF: 39k]. Nominal optical design data at Nasmyth focus.

The nominal **optical design** of the VLT UTs at the Nasmyth focus is shown in Fig. 3.16 and the corresponding, nominal data are given in Fig. 3.17. The diameter of the entrance pupil is nominally 8000 mm.

The tertiary mirror M3 bends the nominal optical axis along the nominal elevation axis. The two Nasmyth foci are fed by a rotation of the tertiary mirror about the telescope axis.

Because of the field curvature, the **image scale** is not constant. Fig. 3.18 gives the distance from the optical axis to the impact of the chief ray on the image surface (curved field) with respect to the sky angle.

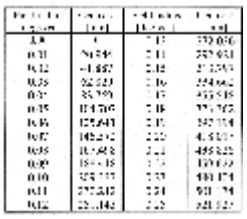

Figure 3.18 [GIF: 62k]. Image scale of the curved image plane at the Nasmyth focus.

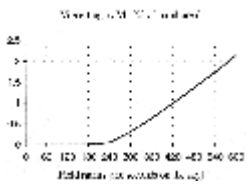

Figure 3.19 [GIF: 19k]. Vignetting by the primary mirror at the Nasmyth focus.

Vignetting by the primary mirror occurs when the aperture beam extends outside the reflective area of the primary mirror M1. With the nominal optical design and nominal M1 bevel size, the unvignetted field of view is 7.15 arcmin in diameter. There is no vignetting by the central hole. The vignetting by M1, in percentage of the area of the entrance pupil (inner diameter 1120 mm, outer diameter 8000 mm) is shown in Fig. 3.19. Vignetting by the tertiary mirror starts with a total field of view of 20 arc minutes.

The only **field aberration** on the curved Nasmyth image is third order astigmatism. The term of astigmatism is increasing linearly like the square of the distance to the optical axis.

3.7.2 Nasmyth Adapter/Rotator

3.7.2.1. General Functions

Figure 3.20 [JPG: 176k]. The Nasmyth Adapter/Rotator, installed at the UT1 (March 1998).

Each Nasmyth Adapter/Rotator comprises two separate functional units: the **Adapter** and the **Rotator** which together form a single sub-assembly. A drawing of the Nasmyth Adapter/Rotator is shown in Figure 3.20.

The **Rotator** forms the mechanical interface beween the Nasmyth instruments and the telescope. It defines the location of the focal plane and allows instruments to be rotated about the telescope optical axis and to follow the rotation of the optical field.

The **Adapter** is used for the following functions:

- field acquisition;
- guiding (auto-guiding mode using the telescope drive alone);
- field stabilisation (auto-guiding mode using the actuation of M2 in addition to the telescope drives for a faster response time);
- wavefront sensing for the Active Optics system;
- deflection of light to coudé, combined and interferometric foci; and
- feeding light from a peripheral reference star into the coudé field for referencing the VLTI.

Figure 3.21 [GIF: 91k]. Plan view of the Nasmyth Adapter/Rotator, seen from the instrument side, showing the Sensor Arm and pick-up mirror.

Each Nasmyth Adapter has a **pick-up mirror** mounted at the end of a **Sensor Arm** which can be rotated in the field of view of the telescope (Fig. 3.21). The centre of the pick-up mirror field of view can be positioned on the optical axis of the telescope. The Sensor Arm, in turn, is mounted on a rotating flange which can be rotated about the optic axis of the telescope (independently of the Rotator) thus permitting the acquisition sensor to explore the entire field of view of the telescope.

Light from the pick-up mirror is split, by means of a dichroic beam-splitter, to feed two separate CCD sensors. One sensor is used for acquisition, guiding and field stabilisation (**AGS**), and the second for wavefront sensing for the Active Optics system (**WFS**). The beam-splitter directs wavelengths in the approximate range 600 - 700 nm towards the AGS; the remaining part of the spectrum is sent to the WFS.

3.7.2.2 Field Acquisition

In acquisition mode the Adapter pick-up mirror is positioned on the telescope axis to relay the central part of the Nasmyth field to the AGS. In this mode, the AGS has the following design performance characteristics:

- *Nominal field of view* : 1 arcmin;
- *Nominal optical bandwidth* : 600 - 700 nm (fixed);
- *Sensor image scale* : 116 µm/arcsec;
- *Sensitivity* : m v = 21 under average conditions and 1 sec integration; and
- *Frame refresh rate* : 2 Hz for full frame, correspondingly faster for partial or binned readout.

3.7.2.3 Guiding and Field Stabilisation

For guiding and field stabilisation modes the Adapter pick-up mirror is centred onto a reference star in the peripheral field of view of the telescope. The star used for guiding is also used simultaneously by the WFS for Active Optics correction in the complementary waveband.

The selection of the most suitable guide star and the positioning of the pick-up mirror is normally done automatically by the telescope control system once the object position and relevant instrument parameters have been defined. The Telescope Control System corrects the guide star reference position during observations for the effects of differential atmospheric refraction between the wavelength used for guiding and the central wavelength used by the instrument, and for non-coincidence of the Adapter axis of rotation and the telescope optical axis.

In guide and field stabilisation modes the AGS has the following performance characteristics:

- *Nominal optical bandwidth:* 600 - 700 nm (fixed)
- *Sensitivity* : In general there will always be a reference star of magnitude m <= 16 suitable for guiding field stabilisation. The sensor limiting magnitude for guiding is m v = 18, and m v = 17 for field stabilisation under average conditions. If the same star is used for image analysis, the limited magnitude is m v = 15.
- *Measurement frequency* : < 70 Hz for field stabilisation, approx. 1 Hz for guiding; and
- *Guiding precision* : The guiding tolerance is included in overall image quality criteria mentioned in Chapter 3.1.1.

3.7.2.4 Wavefront Sensing for Active Optics Correction

The Active Optics system of the VLT will compensate for static or slowly varying optical errors such as those caused by manufacturing errors, gravitational and thermal distortions, the effect of lateral supports which depends on the zenith distance, etc.

During observations, the Adapter WFS will continually provide information on the telescope image quality to the telescope control system for active correction of the primary mirror figure and the position of the secondary, using the same reference star as the AGS. Observers will have no direct control over this function.

3.7.2.5 Shadow from the Sensor Units

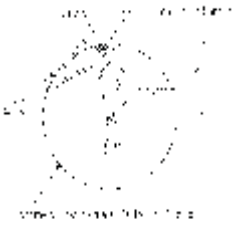

Figure 3.22 [GIF: 37k]. Shadow of the Adapter Sensor Arm in the Nasmyth focal plane.

When the NAOS is not installed, the Adapter Sensor Arm shadows part of the telescope field of view (Fig. 3.22). The exact location of the shadow depends on the position of the reference star in the field. In general, there will be two possible positions of the Sensor Arm for each reference star.

It is possible for the instrument software to specify an area in the telescope focal plane which is to remain unvignetted by the Sensor Arm. If such an area is defined, the telescope control system will preferentially select a guide star which does not cause vignetting of this area. If vignetting of this area is unavoidable, prior authorisation of the observer to proceed will be requested.

3.7.2.6 Compensation of Field Rotation

To compensate for the rotation of the telescope field during observations, the Telescope Control Software continuously controls the position angle of the Rotator and the telescope drives to rotate an instrument attached to the Rotator about the *Telescope Pointing Axis (TPA)* . The TPA, in this context, is an arbitrarily defined point in the telescope field. In instruments such as spectrographs, the TPA will normally be defined by the observer to coincide with the instrument entrance aperture.

The Rotator can rotate without limit in either direction. However, in order to protect cable wrap systems in the instrument, the Rotator electronics is equipped with adjustable range limits which prevent movement beyond preset angles. The Rotator also has an electrical interlock circuit that can be connected to the instrument control electronics to block motion of the Rotator under specific circumstances.

3.7.2.7 Maximum Angular Velocities and Accelerations

The maximum rotational tracking velocity and angular acceleration rates for Nasmyth instruments at a Zenith Distance of 0.5 o , are 26 arcmin/sec and 7.8 arcmin/sec 2 respectively. During telescope slewing, the maximum angular velocity is 8 o /sec and the maximum acceleration is 8 arcsec/sec 2.

3.7.2.8 Focusing

Telescope focusing is achieved by moving the secondary mirror (M2). The optimum focus position is determined by the wavefront sensors in the Adapter and in the NAOS (when used). The allowable range of movement of the focal plane is limited by the range of focus adjustment in the Adapter Sensor Arm, in the case of the normal Nasmyth focal plane, and by the NAOS in the case of the adaptively corrected focal plane.

The telescope control system (and the NAOS, if used) is able to maintain the focus position to within an accuracy of ± 0.25 mm.

3.7.2.9 Calibration Screen

Covers are available to protect the Adapter and instruments against dust, mechanical damage, and strong illumination. On these covers an area larger than the telescope beam has been painted with a white diffusing paint on the side facing the instrument to form a screen that can be illuminated by calibration sources.

For instruments using the NAOS, a calibration source is provided inside the NAOS for recording the instrumental point spread function. In addition, there is a calibration lamp in the centre of M2 (pupil beacon) for calibration and for alignment purposes.

3.7.3 Instrument Interface

Nasmyth instruments with a total mass not exceeding 3000 kg can be attached on the Rotator flange.

The moment applied by the instruments to the Rotator flange with a moment vector perpendicular to the optical axis, must not exceed 30 kNm. Instruments attached to the Rotator flange must not apply a total moment to the Rotator flange due to imbalance and friction, with a moment vector parallel to the optical axis, exceeding 500 Nm in any instrument orientation. The maximum torque component due to friction alone, for example from the instrument cable wrap mechanism, must not exceed 100 Nm.

3.8 The Coudé Focus

Figure 3.23 [GIF: 17k]. The Coudé Optical Train.

The **Coudé Train** (Fig. 3.23) has been modified with respect to the one originally foreseen. Instead of off-axis elliptical mirrors, it is now based on a combination of cylindrical and spherical mirrors.

The new wavelength range of operation (starting from 2.2 μm instead of 0.3 μm) and the reduced field of view (1 instead of 2 arcmin) have relaxed the requirements on the optical train. The performance of the new optical system are somewhat reduced as compared the previous one, but the new concept allows an important cost saving and also suppresses the technological risks induced by the manufacturing of elliptical mirrors at very large off-axis distances.

The beam is sent to the Coudé Train by a concave cylindrical mirror (**M4** , R = 33,100 mm; in front of the the Nasmyth adapter). Relay optics provide an image of the sky at the Coudé focus location with the corect magnification and also an accessible image of the telescope pupil. The relay optics consists of the following mirrors:

- **M5** : concave spherical mirror (R = 8975 mm);
- **M6** : concave cylindrical mirror (R = 290,000 mm) - the cylinder direction is rotated by 90 o with respect to M4;
- **M7** : concave spherical mirror (R = 5176.2mm); and
- **M8** : flat mirror.

The main characteristics of these mirrors are shown in Table 3.6.

Table 3.6: Main Characteristics of Coudé Train Mirrors			
Mirror	**Shape**	**Diameter**	**Incident angle of beam on mirror**
M4	elliptical	115 x 82 mm	45 o
M5	round	580 mm	4.0 o
M6	elliptical	440 x 395 mm	25.0 o
M7	round	275 mm	9.2 o
M8	round	120 mm	11.8 o

The correction of the astigmatism introduced by the spherical mirrors is achieved by the cylindrical ones. Although a cylindrical power on M6 only would have been sufficient, it would have introduced a different magnification factor between the X and Y directions. A second cylindrical power on M4 has been added to compensate for both effects.

An image of the telescope pupil is located near M8 to allow this mirror to be turned into an adaptive mirror.

The main characteristics are: Focal length = 378,400 mm; F/N : 47.3; FOV = 1 arcmin (diameter). The field scale is 1 arcsec = 1.835 mm.

The Strehl ratio of the Coudé image on the optical axis is 0.91 at wavelength 2.25 μm and 1.0 at 10 μm.

3.9 Coating

The **coating unit** for the VLT 8.2-m mirrors has been designed for the deposition of highly reflective, homogeneous aluminium coatings. The **sputter technology** is utilised for the process of the film deposition.

It was built at *Deggendorfer Werft* (Germany) with *Linde A.G.* (Germany) as the main contractor and *BOC-Coating Technology* (U.K.) as the major subcontractor for the vacuum and process technology. The preliminary acceptance test were performed in Germany in 1996 after which the coating plant was dismantled and shipped to Chile. The provisional acceptance tests at Paranal Observatory were done in July/August 1997.

3.9.1 Concept

The **coating unit** includes the following major subsystems: the vacuum vessel and the vacuum generation system, the thin film deposition equipment and the glow discharge cleaning device, the substrate support and rotation system as well as the supporting framework and auxiliary equipment.

The major performance requirements for the coating unit are as follows:

- Coat VLT substrates with pure aluminium thin films (99.995%);
- Allow for single- and multi-pass coating as well as several thin films and multi-layer coatings (at a later stage);
- Utilise high rate magnetron sputtering (min 5 nm/sec);
- Provide high vacuum quality (2 x 10 E -4 Pa);
- Coat with substrate optical surface facing upwards;
- Provide for safe handling, support and treatment of the substrate;
- Provide multiple step, free programmable process sequence control; and
- Coating process down-down time is less than 7 hours.

3.9.2 Implementation

The coating facilities at Paranal are installed in the **Mirror Maintenance Building (MMB)** , located at the Base Camp, i.e. at a distance of about 2 km from the telescopes at the top of Paranal. The MMB comprises two large halls, the assembly hall and the coating hall, arranged in a line.

The **assembly hall** is accessible for the 8.2-m mirror assembly through the 10-m wide entrance door. From this hall the mirrors are transported on an air cushion system into the **coating hall** . The coating hall houses the clean room and the coating unit attached to it. Inside the clean room the mirror washing unit is installed. Next to the coating hall is a machinery room where the auxiliary equipment including power supplies etc. is installed. The clean room provides the adequate environment for the chemical removal of the old coating

and the subsequent cleaning and drying before coating. The clean room is tightly connected to the coating unit in order to assure clean conditions also during opening and closing of the coating chamber.

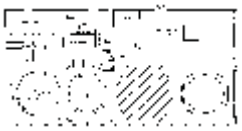

Figure 3.24 [GIF: 95k]. Floor plan of the Mirror Maintenance Building (MMB).

Figure 3.25 [GIF: 48k]. Side view of the Mirror Maintenance Building (MMB).
.

A floor plan of the MMB is shown in Fig. 3.24 and a side view, identifying the main components is shown in Fig. 3.25.

The Coating Unit has the following major subsystems:

- the vacuum vessel upper and lower sections;
- the substrate support system;
- the substrate rotation system;
- the magnetron system with shield and shutter;
- the coating cart with chassis and drive; and
- the equipment.

The **Coating Unit vacuum vessel** is split by the horizontal flange into a lower and upper vessel section. The upper section is fixed to the floor by a support frame that provides free space below the upper vacuum vessel section to allow for the movement of the lower vessel section by means of the Coating Cart. The vaccum vessel has an inner diameter of 9.15 m. The thickness of the shell is 23 mm. The vacuum vessel has a horizontal flange with two O-rings. There are no clamps or bolts between the two halves of the vessel. The lower vessel section contains the mirror support system on its rotation system. The upper vessel section contains the magnetron system and the ports for vacuum system.

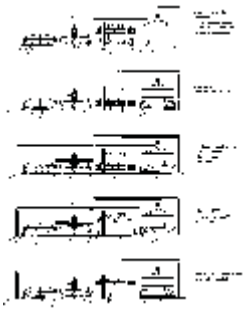

Figure 3.26 [GIF: 83k]. The handling procedure for coating of the VLT M1 mirrors.

Figure 3.27 [GIF: 42k]. Example of the spectral dependance of the reflectivity of test aluminium coatings.

The various stages of the mirror **coating procedure** are shown in Fig. 3.26.

An example of the **spectral dependance of the reflectivity** of some test aluminium coatings is shown in Fig. 3.27.

The first 8.2-m Zerodur mirror was successfully coated on May 20, 1998.

3.10 Polarimetry

The **state of polarisation of incoming stellar light** can be modified when this light is reflected on the mirror coatings. The polarisation effects (phase retardation and di-attenuation) can be particularly important on mirrors working at large incident angles (e.g., M3 and M4 that work at 45 o).

Polarisation effects in the VLT telescopes must be **minimised** for two reasons.

The first is to enable the study of the **polarisation properties of astronomical objects** . For this purpose, the polarisation effects introduced by the telescope optics must be kept at a minimum. The best focus at which to install an instrument intended for astronomical polarimetry is the Cassegrain focus where the number of mirrors is minimised and large incident angles are avoided. This is one of the reason why FORS, which incoporates a polarimetric mode, is installed at this focus.

The second reason to minimise polarisation effects is avaialbility of the interferometric mode (VLTI). Indeed, the fringes observed at the coherent combined focus result from the **superposition of the fringe patterns** formed independently by the two polarisation components. Any differential linear retardation due to polarisation between two interferometer arms would result in a loss of fringe contrast which constitutes the prime observable of the Interferometer.

To limit this effect, the VLTI optical trains (when using UTs, but also ATs) are designed in a **perfectly symmetric way** , ensuring that the light "experiences" the same sequence of reflections in any arm. The only remaining source of differential effects may come from slight differences in the coating characteristics of the individual mirrors. This has been analysed and specified to meet the VLTI performance requirements. Whenever possible, the mirrors will be coated simultaneously in pairs and in the same coating chamber.

VLT Whitebook Chapter 4:M1 Cell and M3 Tower

Figure 4.1 [GIF: 61k]. Location of the M1 Cell and M3 Tower on the main telescope structure.

Figure 4.2 [JPG: 184k]. The M3 Tower protrudes through the central hole in the M1 mirror. Photo obtained on the occasion of the attachment of the M1 Cell to the VLT UT1 structure (March 1998)

The **M1 Cell** and the **M3 Tower** support the main (M1) and tertiary (M3) mirrors. They form a unit which is fixed at the bottom of the telescope structure (Fig. 4.1). They are manufactured by a French Consortium constituted by *GIAT Industries* and *SFIM Industries* .

The four M1 Cells are manufactured at GIAT (St. Chamond) and the M3 Tower at GIAT (Tarbes). The integration of the system, including the active supports of the primary mirror, manufactured by SFIM (Paris), takes place in St. Chamond. The first unit was attached to the UT1 in early March 1998 (Fig. 4.2).

4.1 The Concepts

Figure 4.3 [JPG: 312k]. The M1 active supports, during the installation into the M1 Cell.

The concept of the M1 Cell and of the primary mirror support system of the VLT stems from requirements imposed by the low thickness of the meniscus blank that demands a **very high accuracy of the support system and good structural stiffness** . Despite its moderate thickness, the weight of the primary mirror exceeds 23 tons. To be compatible with the overall VLT telescope design, optimised for a high, first eigenfrequency of the tube, the design work of the M1 Cell had to result in a light and stiff structure and a primary mirror support system able to cope with the inevitable deflection associated to the large dimensions.

Physically the M1 Cell is a **welded space frame metallic structure** that is attached by twelve attachment flanges to the telescope tube. The primary mirror is positioned on its superior side and held in place by 150 axial and 72 lateral supports, cf. Fig. 4.3.

The axial supports are mounted on a lattice structure below the primary mirror, while the lateral supports, distributed at the external rim of the mirror, are mounted on the lateral belt of the M1 Cell. The total weight of the mirror is distributed between the axial and the lateral support systems, depending on the Zenithal Angle (angular distance of the telescope from Zenith).

The **axial supports** of the M1 are constituted by a **passive** and an **active** part. The passive supports consist of hydraulic pads sustaining the weight of the mirror. The pads are connected hydraulically in three 120-degrees sectors of 50 supports each, generating three virtual axial fixed points of the mirror. On each of the hydraulic pads is mounted an active support which is a force actuator able to add a push or pull force to the hydraulic pad in order to change the mirror figure as required by the active optics loop.

Under particular conditions, it is possible to change the connectivity of the axial passive supports so that the mirror behaves as if it is being supported by 6 virtual sectors, for disturbancies above 1 Hz. In this case, the mirror is made more rigid against the wind forces, while still being supported in an isostatic manner.

The **lateral supports** are pure hydraulic pads which are loaded by the weight of the mirror. The pads are connected in two circuits (left and right) in order not to overconstrain the mirror. The lateral supports are connected to the lateral pads of the mirror by means of articulated rods equipped with high precision bearings.

Just below the primary mirror, the M1 Cell contains the **cold plate** , which is used to cool down the M1 by eliminating heat (by radiation and convection) from the back side of the mirror. Coolant is circulated in the system in order to bring the M1 front face to the air temperature during the night. The cold plate is also used to eliminate the heat generated by the 150 active supports so that no heat is dissipated inside the telescope enclosure.

The **M3 Tower** is mounted at the centre of the M1 Cell and extends through the central hole of the primary mirror for support of the elliptical tertiary mirror (M3). It can rotate along its axis, ideally coincident with the azimuth axis of the telescope, in order to point the tertiary mirror towards one or the other Nasmyth focus. The M3 Tower is rotated by means of the M3 Rotating stage located inside the M1 Cell.

The M3 is held in position by three motorised supports, constituting the connection between the M3 cell and the M3 Tower. These supports, known as **attachment and adjustment devices (AAD)** , allow a fine adjustment of the M3 Mirror in order to obtain an accurate pointing recovering possible misalignment and deflection.

The M1 Cell also contains the **primary mirror safety and handling system** . It allows to take over the mirror weight in case of failure of the normal supports, to protect the mirror against earthquakes, and to lift it at the occasion of periodical recoating.

4.2 The M1 Cell

The primary mirror cell (**M1 Cell**) is a three-dimensional structure, located at the bottom of the telescope tube and attached to it by means of 12 pinned flanged connections. It provides the mounting for all "M1 Cell - M3 Tower" equipment, in particular for the M1 axial and lateral supports and the M3 Tower.

The M1 Cell carries the load of the primary mirror and its supporting system, of the Cassegrain instrumentation, of the M3 Tower, of the cold plate and of the control electronics. Central to its performance is a **very high stiffness to mass ratio** . Laser cutting and welding techniques were used for the manufacturing of the M1 Cell. This technology allows the manufacture of complicated structures starting from thin metal sheets. The parts cut from the metal sheets are then welded by laser without fillet material. The minimum amount of heat introduced into the metal guarantees a good dimensional stability.

The M1 Cell resembles a truncated cone with the upper surface having radial dimensions of approximately 10 metres, and a thickness of 2.8 metres. There are **twelve tapered radial rafters** , each one extending from one of the connection flange to the telescope and welded at the centre to three annular belts, two being used for the M3 tower and its rotating stage, and the third holding the Cassegrain instrumentation.

The **top surface** of the M1 Cell is made of 7 concentric rings, and used for mounting the axial and lateral supports. The outermost ring (lateral belt) is used as base for the lateral M1 supports, while the 6 internal rings are used for the M1 axial supports, and for the safety and handling system supports.

The axial supports are positioned in the cut-out of the ladders by interfaces, allowing a fine adjustment of the support position. The position of the cross beams connecting the rafters and contributing to the general stiffness of the M1 Cell is optimised to leave free space for the installation of various electromechanical equipment. These include the electronic cabinets of the M1 Cell-M3 Tower and of the Cassegrain instrumentation, and the various hydraulic components of the M1 hydraulic support system.

A counterweight system for **telescope tube balancing** is used to compensate for instruments of different weights to the M1 Cell. This is achieved by multiple masses secured to the cell structure. The balancing is done manually by adding/removing counterweights.

The M1 Cell is also used to transport cooling fluid, compressed air and electrical connections to the Cassegrain instrument and Adapter/Rotator.

The M1 Cell specifications are given in Table 4.1.

Table 4.1: M1 Cell Specifications	
Dimensions	9.8 x 8.8 x 2.8 m
Mass	10700 kg
Maximum axial deflection at support point	0.75 mm
First eigenfrequency (fully equipped)	14.1 Hz
M1 displacement for Zenithal Angle 0 o - 70 degree o	1 mm

4.2.1 M1 Axial Support System

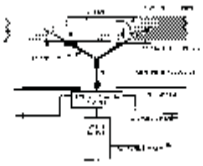

Figure 4.4 [GIF: 10k]. Active axial support system of the M1 Cell.

Figure 4.5 [GIF: 11k]. Passive axial support system of the M1 Cell.

The axial support system makes use of **150 axial support points on 6 concentric rings** , combining a passive (hydraulic) support pad and an electromechanical force actuator or active axial support. The hydraulic pads, connected in three hydraulic sectors, acts like astatic levers, sustaining the mirror weight, while recovering the gravity deflection of the M1 Cell. The force actuators are used for active optics correction by adding or subtracting a force to the fraction of the mirror weight carried by each hydraulic pad (Figs. 4.4 and 4.5).

The axial force (sum of the reaction force of the passive support and of the active force) is applied to load spreaders at the mirror back by means of the axial interface device which is a special flexural joint equipped with a conical interface (push only) to the mirror tripod, allowing differential thermal expansion and protecting furthermore against overload.

The **passive supports** (both the axial and the lateral) make use of two hydraulic chambers, one supporting the weight of the mirror, the other compensating the hydrostatic head generated when the telescope is tilted. The support is largely astatic, to cope with the M1 cell deflection, and it is virtually free from friction and hysteresis. The stiffness of the support is such that the first rigid axial mode of the primary mirror M1 on its supports exceeds 25 Hz, which is important for the dynamics of the telescope and for the resistance to wind buffeting.

By means of the **Volume Adjustment Units (VAU)** which are servo-controlled hydraulic jacks inserted in the M1 passive supports circuits, it is possible to adjust very accurately the position of the primary mirror in piston and tilt.

The topology of the hydraulic circuits of the passive supports can be modified by software to make the system more resistant to wind buffeting, at the expense of a longer settling time of the active force correction. It is therefore possible to shift gradually from a 3 sector whiffle tree to a 6 sector whiffle tree. The principle of a kinematic mount of the M1, however, is always maintained. The shift is done by closing dedicated motorised valves in the pipe networks.

Given the moderate thickness of the blank, the **axial active supports (AAS)** used for active optics must be very accurate. Their accuracy is better than 0.05 N. Their force range, of 500N pull force and 800N push force, depends on various factors, like the final polishing accuracy of the primary mirror, the effort required to bend the primary mirror to Cassegrain shape, and the active optics forces.

Each AAS has its own microcomputer to control its function and to dialogue with the Local Control Unit of the M1 Cell-M3 Tower, by means of a dedicated bus. The individual actuators are composed of an electromechanical part and of an electronic part. The electromechanical part generates a force by the compression of a spring and transmits it to the shaft of the passive hydraulic support through a load cell. The electronic boards, mounted inside a mechanical casing ensuring thermal conduction and electromagnetic protection are cooled by means of heat pipes connected to the cold plate. In this way no heat is dissipated to the surroundings.

A summary of the performance of the axial support system is given in Table 4.2.

Table 4.2: Performance of Axial Support System	
Nominal axial passive force	1500 N
Nominal lateral passive force	3800 N
Axial force accuracy	< 1 N
Lateral force accuracy	< 8 N
Individual Axial Support stiffness	5000 N/mm
Active force range	-500 / + 800 N
Absolute accuracy	0.4 N
Force accuracy resolution	better than 0.05 N
Active force settling time	1 sec (3 sectors) - 5 sec (6 sectors)
Friction in the lateral interface device bearing	< 150 N/mm
Maximum moment in the Axial Interface device	< 2400 N/mm

4.2.2 M1 Lateral Support System

The purpose of the lateral support system is to constrain the rigid body displacements of the M1 mirror in the following three degrees of freedom:

- translation in the direction normal to the tube axis and to the altitude axis;
- translation along the altitude axis; and
- rotation about the telescope tube axis.

The lateral support system is passive and consists of 32 push and 32 pull hydraulic supports distributed around the external edge of M1 mirror, and connecting invar pads bonded to the mirror's edge to the cell structure. The lateral supports are distributed symmetrically with respect to the vertical plane and with respect to the plane containing the optical axis and the altitude axis (Fig. 4.6).

Figure 4.6 [GIF: 27k]. Distribution of lateral support forces.

The 64 supports apply the same nominal force but have different directions of action, which have also the two symmetries described above. Each support produces a force which is described by three components (*axial, radial* and *tangent*).

The resulting force lies for each support in the local plane tangent to the neutral surface of the mirror at that support point.

Upper and lower supports of quadrants located on each side of the vertical plane are hydraulically connected together in two sectors and provide two virtual lateral support points.

Each support includes:

- a **hydraulic piston** connected to a whiffle tree hydraulic network; and
- a later **interface device** connecting each support to the invar pad.

In addition, a **lateral restraining device** constrains the translation along the altitude axis. This device is constituted by 8 additional hydraulic pads connected in an hydraulic circuit to maintain the kinematic mount principle. They are connected to 8 of the 64 invar pads bonded to the mirror edge.

The connection of the lateral supports and of the restraining device to the mirror must be dismounted each time the mirror is taken out from the cell for recoating.

By means of the VAUs, servocontrolled hydraulic jacks inserted in the M1 lateral passive support circuits, it is possible to adjust the mirror position in the direction normal to the tube axis and to the altitude axis. Along the altitude axis the mirror can also be adjusted, although not remotely.

4.3 The M3 Unit

Figure 4.7 [GIF: 31k]. Design of M3 Unit.

The **Tertiary Mirror Assembly (M3 Unit)** is supported by a cylindrical, hollow structure attached to the M1 Cell and passing through the central hole of the M1 mirror. It is located 2.5 metres above the primary mirror. The tertiary tower (the **M3 Tower**) can be rotated by 180 o around the optical axis in order to point the beam reflected on the M3 mirror towards either one of the Nasmyth foci.

The M3 tower is divided in **two parts** . The lower part, containing the rotating stage used to shift the telescope light beam between the Nasmyth foci A and B, is mounted inside the M1 Cell. The upper part, removable, is connected to a flange of the rotating stage. The rotating stage makes use of a pre-stressed bearing and a worm gear drive. A sophisticated control law copes with the friction in the system and ensures a good repeatability of the positioning. Once in the desired position, the tower is locked with a pneumatic brake. This solution, in conjunction with the use of aluminium for the superior part allows to reach a considerable stiffness and stability of the M3 position. The first elastic mode of the tower exceeds 20 Hz.

The M3 mirror/cell consists of a **plane mirror of elliptic shape** and a **mirror cell** . The cell supports physically the mirror, ensures that it keeps the required optical qualities under all telescope attitudes, and constitutes the connection element to the M3 Tower assembly. This assembly supports the interface plate in a kinematic mount, i.e,. without overconstraints and avoiding any thermal deformations. There is also an **alignment target** behind the M3 mirror that is used upon each installation of the M3 Mirror Assembly on top of the M3 Tower.

The **M3 Stowing Mechanism** is used to place and secure the mirror in a vertical position with respect to the tower in order to let the light pass through it when the Cassegrain instrument is used.

The **M3 Mirror/Cell** is attached to the M3 Tower through a device which is also used to provide fine alignment of the mirror (the *M3 adjustment and atachment devices*). The M3 Mirror/Cell is adjustable in orientation (*tilt*) and in translation along the normal to the mirror (*piston*).

Given the large dimensions of the VLT and the obvious difficulty of access to the tertiary mirror, a **motorised support system** for the tertiary mirror has been included to fine tune its position remotely.

In addition, to allow the use of the Cassegrain focus, the M3 is moved outside the beam by a **remotely operated stowing mechanism** , controlled by the Local Control Unit of the M1 Cell-M3 Tower.

The **Cassegrain Beam Shutter** is a movable screen located in the M3 Tower, below the M3 mirror. It is used to protect the Cassegrain instrument from foreign objects, dust and strong light when it is not in use. On the instrument side, the screen is painted white to act as a diffusing screen for instrument calibration.

An **Atmospheric Dispersion Compensator** , when foreseen by the Cassegrain instrumentation, is installed inside the lower part of the rotating stage.

4.4 Control System

The control of the M1 Cell and M3 Tower is essentially performed by a **Local Control Unit (LCU)** and a number of decentralized controllers; see also Chapter 7.

The LCU has the function to control the operation of all the systems inside the "M1 Cell-M3 Tower". It has furthermore the function to interface the "M1 Cell-M3 Tower" to the telescope control system. The communication is established by means of a Local Area Network. The "M1 Cell-M3 Tower" LCU receives commands on the axial and lateral position of the mirror, on the forces to be applied on the mirror and on the position of the M3 mirror. It returns status data to the Telescope Control System (TCS). The LCU furthermore acts in a fully independent way to control the various systems which may have their own local control loop such as the active actuators and the rotation stage of the M3 Tower. It also notifies to the telescope computer a series of status variables and is capable of performing simple failure diagnostics.

The electronics cabinets for the LCU are mounted on the M1 Cell.

4.5 Thermal Control System

A **Thermal Control System** is implemented in the "M1 Cell - M3 Tower" to prevent heat generated by electronics, motors, etc. to deteriorate image quality during observations by inducing air turbulence of deforming the mirrors.

The relevant **heat sources** inside the M1 Cell are the electronic cabinets and the active axial supports. The electronic cabinets are cooled by cooling fluid provided by the telescope structure at the main connection point. The axial supports transfer their heat by means of heat pipes to the radiation cold plate located just below the M1 mirror and mounted on the M1 cell.

The purpose of the **radiation cold plate** is to reduce the mirror seeing by cooling the primary mirror front face. The goal is to bring the temperature of the mirror as close as possible to the temperature of the ambient air at the beginning of the night and to follow its evolution during the night.

The cold plate is realised by means of rolled aluminium plates on which copper tubes are fixed by brazing. The cold plate, located approximately 20 cm away from the rear surface of the mirror, is supported on the M1 cell by elastic dampers to avoid any vibration. The **cold cavity between mirror and cold plate** is closed by a soft rubber seal without contact to the mirror. Small fans in the cavity can be operated to move the air around mylar obstacles to avoid stratification and improving the cooling. Temperature sensors are fixed to the cold plate and to the M1 in order to monitor the cooling process.

Two modes of operation are foreseen, namely the **day and the night modes** . In the day mode the fans are in operation to increase the thermal exchange between cold plate and mirror back, while in night mode they are off to exclude vibration or buffeting. In both modes, the axial active supports are cooled and it is possible to regulate the cooling power according to the temperature needs.

In day mode it is possible to cool the mirror of up to 2 o C/6 hours.

In night mode, it is possible to extract up to 25 W/m 2 from the mirror back.

Given the statistical distribution of the air temperature of the clear nights during the year at Paranal, it is expected that the M1 cooling system, used in conjunction with the air conditioning in the enclosure and temperature prediction models, will allow the temperature of the front mirror surface to be maintained within -1.0 o C/+0.2 o C of the ambient temperature for over 80 % of the total observation time.

VLT Whitebook Chapter 5:The M2 Unit

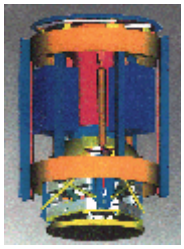

Figure 5.1 [GIF: 112k]. The M2 Unit.

Figure 5.2 [JPG: 504k]. The M2 Unit with the Beryllium mirror at *Dornier* during the Spider tests. The mirror is in front of the granite block used for the testing. The spider structure is anchored to the floor by means of dedicated interfaces, simulating the attachment to the top ring of the telescope. (Photo obtained in November 1997).

The **M2 Unit** is an optomechanical system consisting of a light Beryllium mirror (the **M2 mirror** , cf. Chapter 3.3), the **electro-mechanical device** used to support the mirror and to control its position, and the related **electronics** .

5.1 Main Functions

The M2 Unit performs the following **main functions** :

- sustains the M2 mirror in a stable and safe way in order to reflect the light collected by the primary mirror;
- positions the M2 mirror in order to focus the telescope, inclusive of the focus shift in case of an exchange of focal plane between Cassegrain and Nasmyth;
- centres the M2 mirror with respect to the primary mirror in order to correct the decentring coma;
- modifies, by tilting the M2 mirror, the pointing of the telescope in order to correct image motion generated by wind buffeting or atmospheric disturbances;
- performs a rectangular wave chopping of the M2 mirror between two pre-defined angular positions for background subtraction during infrared range observation;
- baffles the annular region around the M2-Unit to avoid stray light reaching the telescope detector in the focal plane; and
- monitors and transmits information about the temperature of the air surrounding the M2-Unit.

The VLT uses **active optics** . The optical quality of the image is continually monitored by an image analyser using a reference star and the contributions of the various optical aberrations (defocus, astigmatism, coma, etc.) are computed. To achieve the best optical quality, discrete correction commands are given to the primary mirror support system, controlling the shape of the thin flexible M1, and to the M2 Unit, which controls the position of the M2 mirror along 5 degrees of freedom, namely one for focusing, two for centring, and two for pointing.

Focusing of the telescope is affected by disturbances like gravity induced deflections and thermal expansion which cause a modification of the distance between the telescope optical elements. This effect is recovered by the M2 Unit.

Centering is used to laterally align the M2 mirror with respect to the primary mirror. A lateral misalignment of the two mirrors, mainly caused by structural flexibility or by residual optical adjustment errors, produces an optical aberration known as *decentring coma* .

The **pointing** of the telescope is influenced by the tilt of the M2 mirror. This property is used both for correcting the tracking error of the telescope and for chopping during infrared observations.

The **tracking error sources** of the telescope are the control errors of the telescope alt azimuth control system, the deflection of the telescope structure induced by gravity and wind and the atmospheric image motion. All these disturbances do not have a specified direction and vary continuously. A star tracker or autoguider will monitor a reference star and compute the angular error which has to be corrected by the M2-Unit. To correct these fast disturbances the mechanics of the M2 Unit generates moderate magnitude tilt of the M2 mirror.

To observe in the infrared range, the strong background noise of the sky is subtracted from the image to detect otherwise faint sources. This is achieved by a **chopping system** which is located inside the M2 Unit, and which, by a rapid oscillation of the M2 mirror causes a detector in the focal plane to see alternately two different, angularly close regions in the sky, one containing the object and the other not. The signal of the two regions is then subtracted to eliminate the background radiation which may be several orders of magnitude stronger than that of the astronomical object.

5.2 Functional Assemblies

Figure 5.3 [JPG: 51k]. M2 Unit Hardware configuration.

The **M2 mirror assembly** comprises the following functional assemblies, cf. Fig. 5.3:

- the **M2 Mirror** , a lightweight, hyperbolic mirror made of Beryllium in order to minimise its inertia and its mass. The central obstruction area of the mirror (central part which is not optically used) is equipped with an interface used for the mounting of optomechanical auxiliary equipment used for particular observations and for optical alignment.
- the **Mirror Support System** is constituted by three flexural legs fixed at the back of the mirror and mounted on a mirror cell. The flexural legs have the function to accommodate differential thermal expansion between the mirror and the mirror cell. The cell is a ring type (or equivalent) element interfacing the mechanics of the electromechanical assembly. The complete support system has a very low inertia in order not to penalise the performance of the M2-Unit in the fast control of the M2 mirror position.

The **Electromechanical Assembly** of the M2 Unit comprises the following functional assemblies:

- a rigid **Mechanical Structure** connected to the telescope spiders by means of bolted metallic flanges and having the function to physically support
- a **Focusing Stage** , which is used for focusing of the telescope and consisting of a servo controlled motor actuator generating a movement of the M2 mirror along the telescope optical axis. During observation, the M2 mirror is moved stepwise by means of the focusing stage, following the commands issued by the Telescope Control Software (TCS), to minimise the defocus of the telescope to the optimal value computed by the active optics. The focusing system is also operated when changing from the Nasmyth focus to the Cassegrain and vice versa.
- a **Centering Stage** , used to keep the lateral alignment of the M2 mirror with respect to the primary mirror (M1). The stage is designed in such a way that the mirror vertex moves on the surface of an ideal sphere centred on the mirror centre of curvature. During observation, the M2 mirror is moved stepwise by the centring stage to minimise the decentring coma as required by the telescope optical quality, following the commands issued by the TCS.
- a **Tilt/Chopping Stage** . This stage tilts the mirror along an axis contained in the plane perpendicular to the M2 mirror optical axis and ideally positioned at the mirror vertex. This is used to correct errors in telescope tracking and to perform chopping for infrared observation. This stage is equipped with a compensation system, that compensates reaction forces which could cause oscillation of the electromechanical assembly and adversely affect the tracking of the telescope.

- the **Control System** consists of the Local Control Unit (LCU) and of all the electrical and electronic hardware (including power supply) used to control the operation of all the systems inside the M2 Unit. The LCU interacts with the TCS by means of the Local Area Networks. The required positioning parameters are transmitted to the LCU of the M2-Unit for execution through Telescope Control Software. The M2-Unit LCU returns status variables to the TCS and performs internal diagnostics. The LCU, on the other hand, independently controls the function of the auxiliary systems necessary for the proper functioning of the M2-Unit.
- the **Sky Baffle** , which is used to obstruct an annular region of the sky immediately around the M2 Unit for particular observations. The sky baffle is deployed or retracted by means of remote control.
- the **Thermal Control System** , which maintains the external surface temperature within a +/-3 deg C range with respect to ambient temperature. Heat losses outside this limit would cause a deterioration of the telescope optical quality. The M2 Unit is served with a coolant fluid provided through the telescope structure. In addition to monitoring the temperature of internal heat sources the Thermal Control System monitors the temperature of the external housing and of the surrounding air.

5.3 Specifications

Table 5.1 gives the specified values of the main parameters for the M2 Unit.

Table 5.1: M2 Unit Specifications

Parameter	Value	Comment
Focussing:		
Range	-39.0 mm to +8 mm	Nominal Cassegrain position at zero
Velocity	0.5 mm/sec	
Absolute accuracy	± 50e-3 mm	Max.
Differential accuracy	± 1e-3 mm	Max.
Shift of telescope focus due to focusing movement of secondary		
Centering (around center of curvature):		
Range	± 6 arcmin	Max.
Absolute accuracy	± 5 arcsec	Max.
Differential accuracy	± 0.5 arcsec	Max.
Field stabilization:		
Bandwidth	10 Hz	Min.
Angular accuracy	0.05 arcsec rms	0 Hz < f < 6 Hz

	0.1 arcsec rms	0 Hz < f < 10 Hz
Chopping:		
Frequency	0.1 Hz to 5 Hz	Square wave
Duty cycle	0.67 to 1.5	
Amplitude	2 arcmin, peak to peak	Max.
DC Offset	± 1 arcmin	Max.
Settling time	20 ms	Max.
Accuracy	0.1 arcsec rms	Throw < 40 arcsec ptp
Accuracy	0.1 * throw/40	Throw > 40 arcsec ptp
Drift	2 arcsec/h	Max.

VLT Whitebook Chapter 6: Main Structure

Figure 6.1 [GIF: 112k]. The VLT Main Structure with its main subsystems.

The VLT Unit Telescope Main Structure provides a **stable mounting** for the optical components and the focal instruments. It also incorporates the means for accurate alignment of this equipment.

The VLT UT mounting is a **classical alt-az mount** . The overall dimensions are about 22 metres long, 10 metres wide and 20 metres tall. The movable mass is 430 tonnes, including mirror units, adapter/rotators, instrumentation and all subsystems to make the main structure operational.

It allows to **point the optics** to specified celestial objects and to **track** them during the diurnal motion by rotating around two axes. It operates down to about 70 o zenith distance, with a blind spot at zenith of about 1 o in diameter, a consequence of the limited maximum speed and acceleration of the telescope drives. For maintenance purposes, the main structure can be positioned in a horizontal position.

The structure has two main components, the **azimuth structure (the "fork")** and the **altitude structure (the "tube")** .

The azimuth structure is supported by means of **8 thrust hydrostatic pads moving on two concentric tracks** , an inner and an outer, of 9 and 17.2 metres mean diameter. This particular mounting allows a compact and stable arrangement of the telescope structure which is also an advantage during a seismic event. The fork holds the hydrostatic altitude bearings which support and centre the altitude structure, allowing its rotation around the altitude axis (from zenith to horizon).

The **altitude supporting bearings** are placed internally at the telescope centrepiece, almost on the line of the forces transmitted by the serrurier struts of the upper part of the tube and those transmitted by the lower bars holding the M1 Cell. This arrangement has the advantage that the longitudinal dimension of the telescope could be made shorter and the differential tilt deformation of the centrepiece on the hydrostatic altitude bearings at different altitude angles can be kept at an absolute minimum (about 20 arcsec from zenith to horizon).

The structure turns around two axes the **azimuth axis** and the **altitude axis** . The first is aligned towards the true vertical direction (zenith) at the geographical location of the telescope. The latter is perpendicular to the former.

The azimuth rotation is provided by motors driving the fork structure, while the altitude rotation is provided by motors driving the tube structure around two shafts whose centers define the altitude axis.

6.1 Main Components

The VLT Main Structure consists of a large number of subassemblies and items, cf. Fig. 6.1. The following list provides an overview of the main assemblies and their components, with an indication of their interplay.

- The **Tube Structure** with
  - M2 spiders which hold the M2 Unit;
  - a top-ring that connects the serrurier struts and holds the M2 spiders;
  - the serrurier struts that hold the top ring and M2 Unit;
  - a centerpiece that transfers the loads to the altitude shafts;
  - the altitude shafts, the centres of which define the altitude axis, transfer the loads to the fork structure and provide the altitude hydrostatic pads journals; and
  - the flexion bars that provide attachment for the M1/M3 Unit to the centerpiece and transfer of the M1/M3 load to the fork structure.
- The **Fork Structure** with:
  - two Nasmyth adapter flanges that provide the attachment point for the Nasmyth Adapter/Rotator;
  - two Nasmyth platforms that provide access to and support the Nasmyth instruments;
  - two pedestals that transfer the tube structure load to the azimuth tracks and provide attachment points for the coudé tubes;
  - the baseframe, whose floor is part of the azimuth platform, that carries the azimuth hydrostatic pads; and
  - a coudé tube that provides the interface to the coudé mirror units, four maintenance flanges at the four intermediate foci with relative covers and one vacuum pumping system flange.
- **Azimuth Tracks** which support the fork structure providing the azimuth hydrostatic pads journal, including the adjustment system which is used to adjust the tracks during erection, alignment and during operation;
- An **Azimuth Platform** which protects the azimuth tracks and which provides air tight strips for the M1/M3 handling air cushion and access for the Cassegrain instrument carriage. They are made in sectors and provides man holes to access the equipment underneath;
- A **Hydrostatic Bearing System** that provides a proper low friction movement of the telescope without stick-slip effects. It includes the hydrostatic pads, the load carrying pads (axial pads in azimuth, radial pads in altitude), the oil supply unit which provides the oil flow and pressure and distribution pipes, the recovery oil lines, a reservoir to provide oil flow and pressure for emergency smooth stop and the Programmable Logic Control (PLC) which interfaces the Local Control System (LCS);
- **Drive systems** with motors, power amplifiers, transformers, labyrinths to protect the motors from dust without introducing friction, limit switches to limit the rotation range, cooling system to cool the motors, and mechanical contact protection to avoid hard contact between stator and rotor;
- **Encoders** which provide the information about the angular position, including reading heads; mounts to fix and adjust the reading heads, scale tapes, interpolating electronic units and a pre-amplifier;

- **Tachometers** which provide the information about the main structure speed, including the mechanical mounting
- **Cable Wrap Systems** that provide the guidance of the cables and the pipes from the pillar to the fork and from the fork to the tube, and which include drive system to independently drive the cable wraps, position sensors to follow the main structure, the limit switches to limit the rotation range, spare channels for a later installation of pipes and cables;
- **Brake Systems** which provide the braking torque for emergency stop of the main structure;
- **Auxiliary Drives** which allow to move the main structure without using the drive system;
- **Locking Systems** which allow to safely lock the main structure in specified positions;
- **Altitude End Stops** to protect the tube structure in case of emergency;
- Various **Auxiliary Equipment** , including a Temperature Sensing System to map the surface temperature of the main structure and a Cooling System to cool the equipment which produce heat;
- **Cabling and Piping** ; as well as
- **Various Handling Equipment** needed for maintenance, to perform balancing (e.g. dummy modules), protective covers, etc.

6.2 Performance

A primary goal of the VLT is to provide **outstanding image quality** , also under extreme environmental conditions.

The achieved image quality has a **direct implication on the research** that can be done and it depends on the (permanent) optimization of many parameters. These include the optical alignment, the tracking stability of the telescope, the ability of the telescope to avoid perturbations of the incoming light through thermal effects that may degrade the seeing (e.g., hot air columns or static bubbles generated by hot surfaces), as well as mechanical disturbances induced on the structure which may degrade the alignment (e.g., vibrations, shocks).

The **performance parameters** were carefully set to maximise the control bandwidth of the main axes and to minimise possible non-linear effects on the motion, e.g., non-linearities in the drive torque, cogging and ripple; hysteresis in the tachometer when the direction of the rotation is reversed; thermal effects deriving from heat sources placed on the telescope; avoidance and/or suppression of disturbing vibrations from oil and cooling pumps, etc.

These considerations have lead to the following **specifications** of the main design parameters:

- locked rotor eigenfrequency around altitude axis 8 Hz;
- locked rotor eigenfrequency around azimuth axis 10 Hz;
- lowest eigenfrequency of the M2 Dummy along the optical axis 20 Hz;
- lowest rotational eigenfrequency of the M2 Unit Dummy 26 Hz;
- maximum allowable difference of temperature between the surfaces of any heat source;
- cated on the telescope and the surrounding air during observation ± 1 o C;
- maximum cogging torque 2% of maximum torque;
- maximum ripple torque 2% of maximum torque; and
- maximum variation of the hydrostatic bearing oil film over 1 minute is 0.1 mm.

6.2.1 Stiffness and Eigenfrequencies

The mechanical structure was designed at *EIE* (Venice, Italy) for **high, locked rotor eigenfrequencies** . The predicted frequency is calculated by connecting the mechanical structure with the equivalent elastic spring of the motor so that the system is statically defined. The locked rotor eigenfrequency is seen at the motor axis when the telescope is driven and controlled by the drives and defines the behaviour of the telescope in terms of rejection of disturbances.

The higher is the eigenfrequency, the better is the ability of the structure to reject disturbances. In this connection, the **wind** is the most important disturbance acting on the structure and has considerable energy content up to 1 Hz. For this reason, the first locked rotor eigenfrequency around the altitude axis was set to 8 Hz, guaranteeing sufficient control loop bandwidth (about 3 Hz) to ensure good rejection up to 1 Hz.

The components of the **stiffness chain** which define the locked rotor eigenfrequency are (i) the stiffness of the fork and of the tube; (ii) the stiffness of the drive mechanism; and (iii) the stiffness of the hydrostatic bearing system (oil film, oil volume in the oil supply system).

In order to maximise the stiffness of the drive system, it was decided to use **direct drives** . This solution, which also avoids the undesired stick-slip effect, makes it possible to avoid weak points between the point of introduction and the point of use of the drive torque, and does not introduce significant degradation of the overall stiffness of the main structure. The design was performed by *PHASE* (Genova, Italy), and resulted in motors with a mechanical equivalent rotational stiffness of 2 x 10 11 Nm/rad on the altitude axis and of 4 x 10 12 Nm/rad on the azimuth axis.

The **hydrostatic bearing system** , cf. Chapter 6.3 , is also very stiff compared to the mechanical structure to which it is connected. The design of the *Riva Hydroart* (Milan, Italy) resulted in a total mean stiffness of the hydrostatic pads of 6 x 10 9 N/m, including the oil volume of the supply system over the entire operational range.

As expected, the **mechanical structure** turned out to be the weakest component in the chain. It is supported by the thrust bearings on two concentric tracks and is centred by means of four hydrostatic pads on the inner track with a mean diameter of 9 metres. On the one hand, this design has allowed savings in dimensions while increasing the overall stiffness of the main structure. On the other hand, it has lead to certain problems in connection with the stiffnes of the lowest frame of the fork.

The final design of the VLT Main Structure meets the locked rotor specification, but has decreased the **lowest telescope frequency to about 7.2 Hz** (oscillation of the fork along the altitude axis).

Figure 6.2 [GIF: 38k]. The structural response of the Top Unit of the VLT tube, as predicted and measured during test assembly at the factory. There is good, overall agreement.

It is important to assess also the **dynamic performance of the Top Unit** - defined as ensemble of the M2 Unit, spiders and top ring - under a number of perturbances, in particular wind buffeting and the inertial forces due to the movement of the M2 mirror while chopping or tip-tilting to perform field stabilization (Fig. 6.2). The aerodynamic forces due to wind applied at the M2 level will cause variation of the Optical Path and therefore disturbances to the obseravtions in interferometric mode.

Initial calculations led to an optimized design, with **rounded cross section of the top-ring and spiders** that minimises wind drag forces, and a pyramidal mounting of the M2 unit to increase the axial stiffness and to decrease the disturbance torque on the altitude axis due to wind buffeting action on the top ring. A dynamic test was that showed the structural damping to be somewhat lower than the one assumed (0.75% instead of 1%).

6.3 Bearings

The **hydrostatic bearing system** of the VLT main structure has been designed at *Riva Hydroart* (Milano, Italy). It has five components:

- altitude thrust cylindrical bearing pads;
- altitude centring flat pads;
- azimuth thrust flat bearing pads;
- azimuth centring cylindrical pads; and
- azimuth platform thrust flat bearing pads.

The pads are **self-adjusting** to adapt to the journal imperfections. This is done by means of an oil-filled backchamber that allows the pad to rotate around any axis. The backchamber is also used in the adjustment of the pads height during mounting.

The **altitude axis** is equipped with two pairs of thrust pads per shaft and with two counteracting axial centring pads per part that overconstrain the tube on the fork. This solution was adopted to make full use of the stiffness of the fork to increase the lateral eigenfrequency of the telescope. The centring pads are designed to accommodate the possible small differential expansion of centrepiece and fork pedestals.

The **azimuth thrust bearing system** is made of 8 pairs of equal pads with 4 on the inner and 4 on the outer track. The azimuth centring pads system is composed of 4 pairs of pads.

This system, by maintaining a constant pressure, also helps in keeping accurately centred the azimuth axis of the telescope at a much better degree of precision than that provided by the track itself.

6.4 Drives

The **drive system** has been conceived by *PHASE* (Genova, Italy). The use of motors of large diameters poses several technical problems, also to the design of the mechanical structure, e.g.:

- high stability of the relative movement of the mechanical attachment areas must be ensured, due the small air gap between magnets and windings;
- mechanical design of the structure must absorb the magnetic forces acting between magnets and windings;
- ripple torque and cogging torque must be reduced to a level that is compatible with the main structure control requirements; and
- the cooling of the motors is difficult because of their size and the large material thickness may result in a non-uniform temperature distribution.

Consequently, the drive system was specified with the following key parameters:

- Full scale torque: 72 kNm (altitude) and 125 kNm (azimuth);
- ripple torque: 2% peak to peak of average (momentary) torque;
- cogging torque: 2% peak to peak of full scale torque;
- full power bandwidth: 30 Hz (-3 dB); and
- small signal bandwidth: 500 Hz (-3 dB).

The adopted solution is to use **segmented motors** with a "sandwich-like" design of the windings around the rare-earth permanent magnets. This has solved three of the problems listed above. The magnetic forces are always balanced, the scale dependent effect of the cooling problems has been reduced, and the ripple and cogging torque have been diminished, also by using a skewed arrangement for the magnets. The air gap is 1.5 mm on both side of the magnets and has required a careful design of the telescope structure to ensure that no interference between magnets and windings is encountered in the entire operational rotation range, i.e., 90 o in altitude and ± 270 o in azimuth.

The drives are brushless. The two altitude motors are composed of 6 winding segments fixed on the fork arm and of 10 permanent magnet segments; each develop a maximum continuous torque of 36 kNm. The azimuth motor is divided in 4 sectors, each composed of 4 winding segments, 16 in total, mounted on the telescope fork and 44 permanent magnets segments mounted on the inner track, it develops 125 kNm maximum continuous torque.

The ripple and cogging torque have been measured on a prototype of the motors and the values are twice better than what was specified.

The **drive tachometers** use one winding segment per motor in altitude and one segment per sector in azimuth. This solution has allowed to avoid friction-coupled tachometers and thus all the inherent problems of mechanical slip. The problems of the ripple and the hysteresis were solved by prudent choice of materials and design.

6.5 Encoders

6.5.1 Design Goals

Based on earlier experience at ESO, it appeared from the outset that the demanding angular resolution (0.01 arcsec), accuracy (0.1 arcsec), and repeatability (0.05 arsec over 1 hour) needed to meet the pointing and tracking requirements of the VLT could best be achieved by using a **directly coupled encoder** . This avoids the problem of non-monotonic readings due to the mechanical slip usually present in a friction coupled encoder.

The main problem for the VLT encoders was linked to the large diameter of the axes to be equipped, introducing a problem of both high- and low-frequency errors into the readings as well as stability problems in the shape of the mounting rings.

A solution was proposed, based on a special application of an already existing and thoroughly tested Laser Doppler Distance Meter, used to measure linear distances by means of the Doppler effect. The arrangement studied for the VLT application was based on double reading heads at an interval of 25 mm that emit two laser beams reflected by mirrors. The angle is calculated trigonometrically. A test programme was performed to qualify the system.

6.5.2 Implementation

Nevertheless, in spite of the good results obtained during the qualification programme, this encoder has experienced certain problems during the implementation on the telescope, mainly due to difficult calibration and signals' handling. Since a correct implementation would have required a long time and thus a certain risk of delaying for an unknown period the commissioning of the telescope, it was decided to switch to a classical optical encoder produced by *Heidenhain* (Traunreut, Germany). That solution could not be implemented at the beginning of the project for technological reasons.

However, during the past years the supplier has made considerable progress with this type of encoder and especially in the way of mounting the scale tape on a circular trunnion without strain to the scale, i.e. without introducing errors into the readings. The encoder change required to machine on-site for the azimuth axis of UT1, using the telescope as tool machine, a 7.5-m diameter grove for installation of the tape on which the angles are read and to build mechanical parts to adapt the new encoder to the actual telescope lay-out.

The machining was performed to the required tolerances by the *Atelier de la Meuse* (Belgium) in three days. The encoder was mounted and put in operation by ESO within 15 days. The software used to operate the encoder had already been developed for the NTT and was adapted to the actual configuration of the VLT encoder (8 reading heads instead of 4). The azimuth encoder grove was machined with a 54 micron run-out with respect to the inner track centering surface, allowing *Heidenhain* to guarantee an accuracy better than 0.1 arcsec RMS. The subsequent operation of the encoder has shown that it fulfills the required specifications, thanks to the high stability of the mounting.

The altitude encoder was installed directly on the supporting ring directly at the Heidenhain factory and was calibrated to an absolute accuracy of 0.025 arcsec RMS.

6.6 Pointing and Tracking

6.6.1 Design Goals

The following design goals were adopted:

The **absolute pointing accuracy** of the telescope after correction with the pointing model and resetting on one point on the sky shall be better than 1 arcsec RMS.

The **final guiding accuracy** of the telescope in closed loop with active tracking on a guide star and active correction with the secondary mirror shall be better than 0.05 arcsec RMS.

6.6.2 Implementation

The assembly of UT1 has contributed to the identification of a number of critical areas. As a consequence, some modifications will be made to take full advantage of the capabilities of the telescope. They include:

1. The filling of the hydrostatic bearing system with oil must be done with extreme care. The presence of air must absolutely be avoided, in particular in those components whose stiffness is of primary importance for the dynamic behaviour of the main structure.

   At this moment, the lowest eigenfrequency of the telescope is 5.5 Hz, instead of 6.5 - 7 Hz, while the lowest eigenfrequency of the main structure itself, with the M1/M3 and M2 dummies and hydrostatic pads off, is 8.4 Hz instead of 7.5 Hz, as expected on the Paranal soil. This appears to indicate the presence of some air in the pad pockets that will have to be eliminated. A technical solution that guarantees automatic elimination of air from the hydraulic circuit and from the pad pockets will be implemented;

2. The drives have shown disturbance effects (cogging and ripple) that are smaller than specified; still the values measured at the factory in Milan were better than those in Paranal. This is due to a lesss optimal alignment of the motor segments with respect to the magnet segments. Thus, the assembly of the altitude drives must be done carefully so that the air gap is symmetrical over the entire rotation range; and
3. The design of the encoder mechanics will later be modified in order to allow easier alignment of the reading heads with respect the scale tape.

6.7 The Nasmyth Platforms

Figure 6.3 [GIF: 30k]. Lay-out of the Nasmyth platform.

The two Nasmyth platforms (Fig. 6.3) provide access, support, handling and alignment device interfaces for the Nasmyth instruments. The platform dimensions are 4.1 x 6.0 metres.

The maximum vertical, distributed load on the Nasmyth platform is 6000 N/m 2. The maximum concentrated load on the Nasmyth platform floor is 25000 N.

VLT Whitebook Chapter 7: Control Software

The entire **VLT Control Software** is based on a **distributed computer architecture** . The final layout of the computers (workstations and microprocessors), networking devices and underlying concepts have been tested, both during real observations with the NTT and on the socalled VLT Computer Control Model in Garching, a very useful off-line subset of the computer equipment that is used in the VLT control room and the telescope area of a Unit Telescope.

The VLT **common software** , including a real-time database, is the stable core of the entire VLT control software. This comprises also high level applications, like the Real-Time Display (RTD), the Panel Editor and the CCD software to be used for technical CCDs. It is distributed under a policy of regular releases, subject to automatic regression tests and is also used by VLT Consortia and Contractors.

There are also modules added to insert the VLT control software into the **Data Flow** context, interfacing it in particular to Scheduler and Archive.

7.1 Distributed Architecture - Networks

7.1.1 Logical Lay-out

Figure 7.1 [GIF: 36k]. Logical lay-out of the VLT LANs. The label on the top of each shaded block indicates how many times it needs to be reproduced in order to complete the VLT.

The logical lay-out of the **Paranal Telescope Area LANs and computer equipment** is illustrated in Fig. 7.1. Note that for reasons of simplicity, only the LANs of one Unit Telescope and one instrument are shown in this figure. It clearly illustrates the distributed nature of the VLT computer architecture.

Experience about this particular architecture has been collected with the NTT. In addition, the existence of several Unit Telescopes introduces the need for an ATM backbone at the VLT observatory. This means that additional testing has been required to try out the technology implied in the concept of Fig. 7.1, i.e., including the associated ATM switches, routers and related performances.

It should be noted that the NTT network deviates from the design shown in Fig. 7.1 by its lack of a User Station LAN. At the VLT, a **User Station LAN** is needed to make instrument switch-overs as simple and transparent as possible, also from the point of view of the screens and keyboards that are used. This leads to the requirement that for each UT there must be a separate User Workstation (WS), with X-terminals, on which the operator works, connecting to the instrument that actually receives the light beam. For the networks, this translates into a User Station LAN. The NTT, as a single telescope, does not need such a separate LAN, and can have the necessary workstations/peripherals directly on the General Services LAN.

7.1.2 LAN Requirements

The data that will be transferred over the Paranal Telescope Area (TA) LANs are basically of four types (for references to LAN-names, see Fig. 7.1):

1. **Control Information** goes over all LANs. It consists of control commands and corresponding replies going to or coming from any WS involved in the control chain. This type of traffic requires a bandwidth of about 1 Mbit/s on the backbone, and much less on the Instrument and Telescope LANs. This requirement can easily be met by standard *Ethernet* (10 Mbit/s). The requirement for determinism (maximum 200 ms delay for a reply to a command) does not cause difficulties due to the architecture of the SW, with well localized server processes for each specific subsystem and the nature of the traffic - in general, LCUs do not take initiative to communicate, and send short replies to the commands they receive.

2. **Data from technical CCDs** (slit viewing cameras, guide cameras, wavefront sensors) require up to ~5 Mbit/s per camera for shorter periods, i.e., these data do not have to be sent continuously to a WS or over the backbone. Again, standard Ethernet can handle this traffic. All LANs are involved.
3. **Astronomical data from scientific CCDs or IR detectors** . These data travel over the Instrument LAN, and via the Backbone LAN also to the User Station LAN and General Services LAN (e.g., for Archiving). Although the requirements for or expected performances of several of the instruments to be installed are not yet very specific, ISAAC, CONICA and the FIERA CCD controller are considered as worst cases for these purposes; they are able to produce 30-40 Mbit/s on their instrument LAN. The combined throughput over the backbone has to be multiplied with the appropriate factor (number of detectors that are expected to transfer data simultaneously over the backbone).
4. **Data for field stabilization and rapid guiding** . A small amount of data, transferred between two particular hosts. For these data, determinism is very important and is obtained over Ethernet by dedicating a private LAN to this purpose. This is limited to the Guide/ Acquisition LAN.

7.1.3 Test Camera on UT1

Figure 7.2 [GIF: 59k]. Lay-out of the VLT LANs needed for the operation of the Test Camera.

In order to illustrate the above described architecture, the complete lay-out of the Control LANs around the first instrument to be mounted at the VLT, i.e., the **Test Camera** at the UT1 Cassegrain focus, is shown as an example in Fig. 7.2. It specifies the hostnames, but leaves out reference to equipment which is not directly related to this set-up (e.g., the Coude Control LCU in the Telescope Control LAN).

Note that the Ethernet/LANE switches in the Control Building (*sta2, su11, sgs1*) are physically a single device (e.g. a CISCO Catalyst 5000 switch, which has up to 48 fibre ports). Also, the backbone which is here shown to it full size, can be kept to a more modest size (one ATM switches only) during this operation, as few ports are required.

Note also that this Figure illustrates the separation of the subnets, and to which subnet each node belongs. In other words, it gives information about the Network Interface Cards of hosts, but not about the physical location of the screen(s) attached to any of these hosts. Thus, although the Telescope Control WS is on the Telescope Control LAN, its screen is an integral part of the User Station, as are the screens of all devices on the User Station LAN.

7.2 The VLT Common Software (VCS)

The basic body for the VLT Control Software is the **VLT common software (VCS)** . It consists of a layer of software over the Unix operating system, in the case of workstations and on top of the VxWorks operating system, for the Local Control Unit (LCU) microprocessors. It mainly provides common services, like an architecture-independent message system, a real-time database for all telescope and instrument parameters, error and logging systems and a large number of utilities and tools. The inner mechanisms of the common software on the workstation side are provided by a commercial software product from *Hewlett-Packard* , called **RTAP** .

The original idea of a thin layer of software common to all Observatory application software, has evolved in the course of time. It has progressed to include more and more high-level applications, like the entire CCD control software used both for scientific and technical CCDs (e.g., guide cameras) and other general purpose software used by the instrumentation (e.g., Real-Time Display software and INS common software). There are now structures, guidelines and recipes to write control software as well as examples including the so-called **standard commands** , within the scope of the VLT common software.

The VLT common software is used across all on-line computers at the VLT Observatory (telescopes and instruments) and is designed, implemented and maintained by the **VLT software group** . This group is also responsible for monitoring software developed outside ESO and for its subsequent integration into the VLT control software at the VLT Observatory.

7.3 Hardware

The VLT control system is based on a distributed architecture. Workstations provide the user level interaction and coordination but all actions are taken by the **Local Control Units (LCUs)** .

The telescope is controlled by a set of LCUs, including those for the altitude axis, azimuth axis, telescope enclosure, adapters, hydrostatic bearings, combined M1, M2 and M3 subsystems. These LCUs live off (boot from) their respective Telescope Co-ordination Software (TCS) workstation.

Each adapter is equipped with two Technical CCD Cameras, the Guide Camera and the Image Analysis Camera, each with its own LCU.

Each of the scientific instruments have one or more LCUs for function control and an LCU for each scientific detector. These LCUs all hang off their respective Instrument Workstation.

7.4 Time Keeping

The control system relies on a dedicated **GPS receiver** for UT time. The receiver electronics has a backup clock, should no satellites be available.

The time is distributed to the workstations and the LCUs via *ntp* , with the exception of the some LCUs which have a TIM board that receives the signal from the GPS directly. The TIM board provides the absolute time, e.g., for tracking axes, and has a further backup-battery backed clock on-board for cases of complete GPS failure.

7.5 Central Control Software

The VLT control system is built on a large layer of common software, refered to as the **Central Control Software (CCS)** which in turn lives on top of the HP RTAP software. RTAP is a commercial real time system, which includes a real-time database and messaging system. Another common module is provided by LCC, the CCS equivalent running on the LCUs.

Communication between the LCUs and the workstations is done either via messages or via database reads and writes. To this purpose, the database on the LCUs (or parts thereof) is SCANned into the RTAP database on the workstation.

Scans can be triggered on change or by polling at a fixed frequency.

RTAP : The control system relies heavily on Rtap, a commercial real time system (HP). RTAP provides the workstation database and messaging systems for the control system.

CCS : The Central Control Software provides the basic interface between the various processes and for all the error logging etc.

LCC : The version of CCS/RTAP that runs under VxWorks on the LCUs.

seqWish : This is the main command language for the control system. A derivative of the TCL wish allows a single process to issue commands to any subsystem of the telescope.

7.6 Telescope Coordination Software

The Telescope Coordination Software (TCS) is composed of many **software modules** , each of which consists of one or more processes. To unify and simplify the access from users to the TCS functions the TCS Interface was developed, represented by an interface module (*tif*).

The TCS-interface module is responsible for providing the **central and only command interface** between external users and the TCS. The users are typically higher-level applications, such as instrumentation High-level Operations Software, or interactive user interfaces related to these applications. The user processes communicate with the TCS by sending commands to and receiving replies from the tif. The TCS-interface internally dispatches the commands to the responsible TCS processes, receives their replies and passes them back to the originator.

The overall TCS design foresees to run **one TCS-interface instance per telescope focus station** . Each TCS-interface instance has access to all TCS processes involved in controlling the corresponding focus, but only one instance at a time is connected to the telescope, due to the fact that only one focus at a time has the light-beam.

At any one time, only **ONE** external user can have command access to a given TCS Interface, this is guaranteed by the booking system. The TCS Interface itself provides no access control functionality.

There are three operational configurations for a user (instrument):

- access to the telescope and indirectly to the adapter;
- access to the adapter only; and
- access to the data query library only (the data query library is based on a database with public attributes) depending on which focus it has booked and on what the booking master has configured to be available for that focus.

Figure 7.3 [GIF: 10k]. User access to the Test Camera (TC).

Fig. 7.3 shows as an example a configuration where instrument INS 3, connected to Cassegrain focus has the light beam. The arrows in the figure represent permitted command/reply paths. There are three User <---> TCS-Interface <---> TCS chains, one per focus. Every attempt of a user to send a command to another chain, to another TCS-interface or directly to a TCS module is rejected by the booking system. Moreover, only public commands are allowed.

The TCS operator (a user with operator level), however, can access all tif instances and all TCS modules and can also use maintenance commands.

7.7 Instrument Processes

7.7.1 Observation Software

The instrumentation software on the VLT is built around some very basic principles. The **Observation Software (OS)** only knows about the current single exposure being executed. The next or previous exposure are meaningless concepts to OS. All parallelism possible within the instrument control is handled by the OS.

The OS also handles all communications between the three subsystems involved in the observation namely (ICS - Instrument Control Software, DCS - Detector Control Software and TCS - Telescope Coordination Software). The OS is built up from a number of sub-modules described below.

7.7.2 Detector Control Software

The **Detector Control Software (DCS)** , either controlling Scientific CCDs or Infrared Detectors, has a workstation part and an LCU part that actually does most of the work. Additional software runs inside the detector controllers but this is extremely well shielded from the control system. The main interface to the CCD software is located on some Instrument Workstations, but the same basic tasks may be differently organised for each CCD being controlled.

The *ip (Image Processing)* and *it (Image Transfer)* tasks also run on the LCU. The CCD software transfers the image from the LCU to the workstation when the image processing is finished. Because the image must always be presented to the user in a fixed orientation in the case of a scientific CCD where the readout port maybe on the opposite side to the pixel nominated as (1,1), the entire image may be readout into the LCU before it is transferred to the workstation. In this case the CCD software in the LCU flips the image in the memory so as to present it to the user with pixel (1,1) at the bottom left.

Image Processing includes CCD provided functions such as centroiding (used by the autoguiding) or minimum, maximum calculation. When these are enabled, the image has to be completely within the LCU memory before transfer.

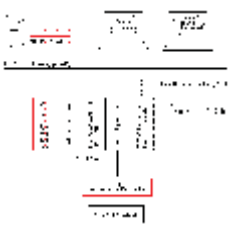

Figure 7.4 [GIF: 13k]. CCD stand-alone system hardware architecture.

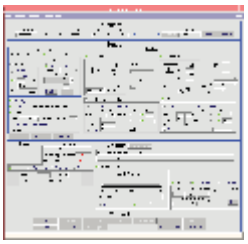

Figure 7.5 [GIF: 49k]. Control panel for stand-alone system.

The lay-out of the stand-alone TCCD control software is shown in Fig. 7.4., indicating that the software is distributed over three hardware platforms: the WS, the LCU and the ACE transputer network. The control panel corresponding to this stand-alone set-up is shown in Fig. 7.5.

7.7.3 Real Time Display

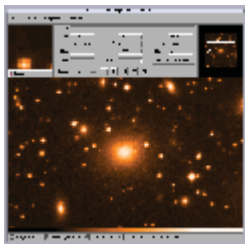

Figure 7.6 [GIF: 96k]. Example of screen dump of the Real Time Display.

The **Real Time Display (RTD)** facility is used for the readout of all detectors. This is a very versatile tool for the provision of very fast displays of images as they are transmitted, according to the needs of real-time operation at the telescope of infrared detectors and technical CCDs. In addition to using the RTD to view the data as taken by the detectors, it is also possible to use it to open any FITS file, display its header and print it. An example of a screen-dump of the RTD is shown in Fig. 7.6.

Using the attach/detach camera commands it is also possible to choose to look at the readout from the selected camera. The data are transferred to the workstation memory and are scaled and displayed by the RTD. The widget provides a large number of scaling and colour options as well as real-time updates on the real pixel values and cuts across the image.

7.8 Integration of the VLT Control and Data Flow Software

A feature of the VLT software is the **high level of integration** achieved between the VLT control software and the Data Flow software, providing an end-to-end concept to the observing process, from proposal preparation to data archiving and data reduction. This integration was planned and first implemented at the NTT. The VLT Data Flow System and the associated software is described in Chapter 10.

7.8.1 Requirements for the VLT Control Software

When the VLT Instrumentation Software concepts were conceived as part of the VLT control software, it was stipulated that the Instrument Software engines should basically deal with a single exposure only, one at a time. The parameters needed to define any such exposure are stored in **set-up files** , which constitute the most direct interface for the operation of the VLT. Consequently, the control software for all instruments must include graphical user interfaces to edit, display and save these set-up parameters. It must also have a set of standard commands, for instance to execute set-ups and to start an exposure.

With the addition of the **VLT Sequencer** , as an external process on top of this, sequences of commands can be collected into Sequencer scripts; this scheme can be used to obtain more complex scenarios than just a single exposure, as mentioned above.

7.8.2 The High Level View: Observation Blocks

Observation Blocks (OBs) play an essential role in the Data Flow. An Observation Block constitutes the smallest observational unit for the VLT. It is a rather complex entity, containing all information necessary to execute sequentially and without interruption a set of correlated exposures, involving a single target, i.e. a single telescope preset.

Each Observation Block contains one or more **templates** . A template is a script, dealing with the set-up and execution of one or more exposures of a particular kind, e.g. calibration or dark current exposures; as seen from the VLT control software, this is just a Sequencer script. The exact parameters for a template, e.g., the exposure time, is part of the information contained in the Observation Block, as are additional requirements for scheduling and data reduction. These parameters are defined by the astronomers during Phase II Proposal Preparation (P2PP), while building their Observation Blocks with the software tools provided for that purpose.

7.8.3 Templates

The templates themselves are sequencer scripts with commands to a single subsystem of the instrument control OS. The OS then communicates the instructions to the instrument, the detectors or the telescope. Although in theory it is possible to allow direct communication to any subsystem, this is actively discouraged since the supervisory role of OS ensures that the activities can be coordinated and there is not too much intelligence in the templates.

A typical template may provide for imaging with a certain instrument, combined with a number of offsets. The parameters to the templates are defined in a **Template Signature File (.tsf)** which is exported by the control system to the Phase 2 Proposal Preparation (P2PP) system, cf. Chapter 10.

Once P2PP has been used to generate the parameters for the specific TSF, their combination is stored in the container, the OB.

7.8.4 Broker for Observation Blocks

The control software for several instruments was in different stages of development when the Data Flow concept of Observation Blocks was finalized. A new interface layer between the Data Flow software and the VLT control software was therefore developed as part of the VLT common software. On the side of the VLT Control Software, it mainly consists of a single process, called **Broker for Observation Blocks** (or short - and affectionately - **BOB**).

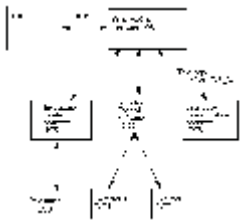

Figure 7.7 [GIF: 8k]. Illustration of the *Broker for Observation (BOB)* process.

This process requests and receives from the short-term scheduler the Observation Block to execute next. It then breaks down this Observation Block into its constituent templates, and tries to execute them one by one. The templates being nothing else than a particular kind of Sequencer scripts with accompanying parameters, the VLT Control Software knows how to handle it from there on. The process on the VLT Control Software side is graphically presented in Fig. 7.7.

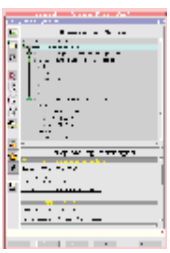

Figure 7.8 [GIF: 29k]. Partial screen dump of the *Broker for Observation (BOB)* .

BOB has been implemented using the Sequencer (or Tcl/Tk) scripting language, partially with the help of the Panel Editor. It constitutes one of the main graphical user interfaces of the instrument operators at the telescope, showing the high level view of operation. With the help of this user interface, Observation Blocks can be loaded, executed, skipped, paused, aborted, etc. During execution, the status of the individual templates is graphically indicated, and a log of their communication with the low level control software can be displayed. A partial screen dump of BOB can be seen in Fig. 7.8.

Much effort and emphasis goes into the development of templates for every instrument. These templates belong to the instrument just like any other piece of its control software. Although the astronomers cannot edit these templates themselves, they can of course set the related parameters while they are building the relevant Observation Blocks.

One of BOB's tasks is to return the status of the currently executing Observation Block. It does so at the level of the individual templates: it will inform the Data Flow world if a template was started, paused, aborted or finished, etc. This way, the data reduction pipeline and quality control processes do not have to wait until the entire Observation Block has been finished before starting their analysis on the astronomical data, while the scheduler can monitor the progress of an Observation Block and estimate when the next one will be requested.

Trivial type and range checks on template parameters can be exercised as soon as they are entered during the preparation of Observation Blocks. However, it is also necessary to have a more complete check that involves the combinations of parameters and the instrument software and database, thus increasing the confidence in the correctness of individual Observation Blocks. For that purpose, BOB can also run in non-graphical mode. Together with the instrument software in simulation mode, this is the best verification that can be performed without actually executing the Observation Blocks at the VLT itself.

Although BOB was initially designed to cooperate with the short-term scheduler, it can in the meantime also read in Observation Block descriptions from files, without having to communicate with the Data Flow world. This has been particularly useful for the engineers, who during the later phases of the development process needed a high-level tool to exercise their software. This off-line mode of operation is of course also very practical during the implementation and testing of templates.

VLT Whitebook Chapter 8: 8. Instrumentation

8.1 Overall Concepts

A large number of advanced instruments are being built for the VLT and are now in different stages of completion. Most of these are constructed in collaborations between ESO and consortia of astronomical institutes in the ESO member states.

An overview of the instruments and their locations at the VLT foci is given in Table 8.1.

Table 8.1: First-Generation VLT Instruments

Telescope	Instrument		
	Cassegrain Focus	Nasmyth A	Nasmyth B
UT1	FORS1	ISAAC	CONICA
	SINFONI		NAOS
	Laser Guide Star		
UT2	FORS2	FLAMES	UVES
UT3	VISIR	VISITOR	VIMOS
UT4	*FORS1*	*CRIRES*	NIRMOS

These instruments will be capable of performing a large variety of observations, in many different modes. Together, they cover the current scientific desiderata and goals, as established for the VLT. The scientific drivers for each of the instruments are elaborated below

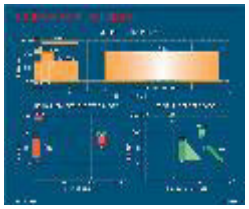

Figure 8.1 [JPG: 408k]. The domains of the first-generation instruments in terms of spectral region, spectral resolution and number of objects that can be observed simultaneously.

Fig. 8.1 gives an overview of VLT instruments, by spectral resolution, spectral region and number of simultaneously observable objects.

This chapter provides information about the individual instruments and their main scientific drivers. Since the projects are at different stages of completion, the level of detail varies and is dependent on the current degree of definition.

8.2 Optical region (300 - 1000 nm)

There will be five major instruments in the optical region, **FORS** (in two copies), **UVES** , **FLAMES** and **VIMOS** . They will operate in different modes, including direct imaging, low- and high-resolution spectroscopy and multiple-object spectroscopy.

8.2.1 FORS (FOcal Reducer/low dispersion Spectrograph)

8.2.1.1 Instrument Concepts

Figure 8.2 [GIF: 28k]. Design of FORS.

Figure 8.3 [GIF: 118k]. View of FORS1 during laboratory tests.

The VLT FORS instrument is designed as **all-dioptric focal reducers** (Fig. 8.2). Two copies are being built (Fig. 8.3). They will be capable of doing:

- direct imaging;
- long slit grism spectroscopy;
- multi object grism spectroscopy;
- polarimetry (FORS1);
- medium dispersion echelle grism spectroscopy (FORS2)

and all sensible combinations of these modes (e.g. imaging- or spectropolarimetry) in the wavelength range from 330 nm to 1100 nm.

Two angular resolutions and hence field sizes can be selected by a remotely controlled exchange of the **collimator** . The resulting fields of view will be 6.8 x 6.8 arcmin in the standard resolution mode and 3.4 x 3.4 arcmin in the high resolution mode. The **scientific grade detector** is a 2048 x 2048 pixel CCD with 24 µm pixels, thinned and anti-reflection coated. The complete detector system is provided by ESO's Optical Detector Team.

A large selection of **filters and grisms** is available: three wheels in the parallel beam can accommodate up to 21 filters, grisms and polarization optics. Two additional wheels in the converging beam of the camera in front of the camera field lens can together take up to 8 interference filters. One position always remains free. The **retarder plate mosaics for linear and circular polarization measurements** are mounted separately and can be rotated for the determination of the position angle.

Standard spectroscopic resolution is up to R = 1700 with a 1 arcsec slit width. For **long slit spectroscopy** , a number of slits will be available with fixed widths (0.4 to 1.9 arcsec), spanning the full 6.8 arcmin field and selected by a movable decker. **Multi object spectroscopy** of up to 19 objects can be performed. The slits (each 22 arcsec long) are formed by 19 pairs of slitlets. These slitlets are moved independently of each other to allow extremely versatile observational scenarios.

The two copies of FORS are basically identical, however, with the following diffences:

- polarization optics will only be installed in FORS1
- a set of echelle grisms will be available for higher spectral resolution (up to spectral resolutions of about 2700) in FORS2
- a mask exchange unit (MXU) will be installed in FORS2 for extended multiobject spectroscopy on up to 100 objects simultaneously.

A novel kind of atmospheric dispersion corrector has been developed for both FORS instruments.

8.2.1.2 Science Objectives

These are the main science objectives of FORS:

- redshifts of distant galaxy clusters ($z > 0.5$, $V \sim 25$)
- galaxy counts, colours and morphology down to $V \sim 27 - 28$;
- quasar - galaxy associations, fuzz around quasars;
- gravitational lenses: arcs, multiply lensed quasars, lensing galaxy;
- spectropolarimetry: white dwarfs, active galactic nuclei (AGNs), jets, broad absorption line quasars, BL Lacertae objects, optically violent variables (OVVs);
- chemical abundances in extragalactic stars and emission line nebulae.

8.2.1.3 Observational Capabilities

The following tables summarize the **design benchmarks** of the FORS Instrument for **direct imaging** , **spectroscopy** and **polarimetry** (FORS1 only), respectively.

Table 8.2: FORS - Direct Imaging

Mode	Standard Resolution (SR)	High Resolution (HR)
Field of view	6.8 arcmin x 6.8 arcmin	3.4 arcmin x 3.4 arcmin
Scale	0.2 arcsec/pixel	0.1 arcsec/pixel
Image quality	80% in 0.2 arcsec within 4.0 arcmin	80% in 0.1 arcsec within 2.0 arcmin
	from the optical axis	
Transmission	>50% (>355 nm)	>50% (>355 nm)
	>62% (>360 nm)	>65% (>365 nm)
	peak 75% at 450 nm	

Table 8.3: FORS - Spectroscopy

Disperser	grisms
Standard dispersion	~45 - 170 Å/mm
High dispersion	~15 - 41 Å/mm
Long slit spectroscopy	9 slits, 0.4 arcsec - 1.9 arcsec x 6.8 arcmin
Multi object spectroscopy (FORS1 and FORS2)	slitlet type
	individually configurable

	19 slits
	22 arcsec slit length
	field of view 6.8 arcmin x ~4 armin (SR)
	field of view 3.4 armin x ~2 arcmin (HR)
Extended MOS (FORS2 only)	slit mask type
	max. 10 fields per night
	field of view
	minimum slit width 0.6 arcsec
	curved slits possible

Table 8.4: FORS - Polarimetry (FORS1 only)

Possible observations	- linear polarization - circular polarization - imaging and spectroscopy
Technical realization	- stripmask in focal plane - rotatable superachromatic retarder plate mosaics in parallel beam - Wollaston prism in parallel beam
Obtainable precision	- position angle: 0.1 o ; - degree of polarization: < 1% - limiting magnitudes (B): ~24m (imaging) ~20m (spectropolarimetry)

Limiting magnitudes of point sources have been calculated for a detector read-out noise of 5 electrons RMS and a calibration accuracy of 5% in direct imaging, spectroscopy, and polarimetry.

Direct imaging : limiting magnitudes for point sources calculated for S/N = 5, detector read-out noise 5 electrons RMS and a calibration accuracy of 5%:

Table 8.5: FORS - Limiting Magnitudes (Direct Imaging)

Filter	Seeing (arcsec)	Integration Time		
		60 sec	600 sec	1800 sec
U	0.5 1.0	25.0 24.2	26.5 25.5	27.0 25.9
B	0.5 1.0	26.3 25.5	27.5 26.5	27.9 26.8
V	0.5 1.0	25.8 24.9	26.8 25.7	27.2 26.0
R	0.5 1.0	25.3 24.4	26.3 25.1	26.6 25.3

Spectroscopy : limiting magnitudes in spectroscopy calculated for S/N = 10, a seeing of 1 arcsec and a grism with a reciprocal dispersion of 130 Å/mm. Detector properties as for the imaging modes:

Table 8.6: FORS - Limiting Magnitudes (Spectroscopy)

Wavelength (nm)	Dispersion (Å/mm)	Integration Time		
		60 sec	600 sec	1800 sec
360	150 50	18.3 17.2	20.7 19.7	21.9 20.9
440	150 50	19.8 18.8	22.3 21.3	23.4 22.4
550	150 50	19.7 18.6	22.1 21.1	23.2 22.3
650	150	19.4	21.8	22.8

	50	18.3	20.8	21.9

Limiting magnitudes calculated for **imaging and spectropolarimetry** for point sources (FORS1 only). Exposure time 1 hour, seeing and slit width 1 arcsec, dispersion of 1.25 Å/pixel for spectropolarimetry. The S/N was adjusted to give a 1% accuracy in the degree of linear and circular polarization. Detector properties as for the imaging modes:

Table 8.7: FORS - Limiting Magnitudes (Imaging and Spectropolarimetry)

Filter	Mode	Linear	Circular
U	photometry spectroscopy	22.1 15.9	22.8 17.9
B	photometry spectroscopy	23.3 17.4	23.6 19.5
V	photometry spectroscopy	22.6 17.3	22.8 19.3
R	photometry spectroscopy	22.1 17.0	22.1 19.0

8.2.1.4 Instrument Status

Two copies of FORS are being built: **FORS1** will go to Unit Telescope 1 in 1998, **FORS2** will go to UT2 in 1999. It is foreseen to move FORS1 from UT1 to UT4 in 2001.

The project management and history are outlined in the following table:

Table 8.8: Status of FORS

Built by	Consortium of *Landessternwarte Heidelberg* , *University Observatory Göttingen* and *University Observatory Munich* (Germany) (under ESO contract)
Location	UT1 (Cassegrain); UT2 (Cassegrain)
No. of	60N:40N (FORS1); 20N (FORS2)

guaranteed nights	
History	Approved: May 1991 Preliminary Design Review: April 1992 Final Design Review (Optics): Feb. 1993 Final Design Review (Mechanics, Electronics, Maintenance, Handling, etc.): Feb. 1994 Final Design Review (software): Sep. 1994
Present status	FORS1: Preliminary Acceptance Europe (15 May 1998) FORS2: End of Manufacturing Phase

8.2.2 UVES (UV-Visual Echelle Spectrograph)

8.2.2.1 Instrument Concepts

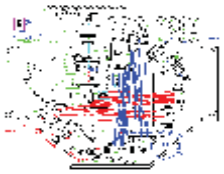

Figure 8.4 [GIF: 37k]. UVES detailed design plan showing table layout.

Figure 8.5 [GIF: 176k]. The red echelle under test in the ESO optical laboratory on the "TNO" efficiency measuring machine. The blue and red UVES echelles are among the world's largest monolithic gratings. Each echelle is a mosaic consisting of two grating replicas on the same blank.

UVES is a two-arm crossdispersed echelle spectrograph covering the wavelength range 300 - 500 nm (blue) and 420 - 1100 nm (red),with possibility to use dichroics (Fig. 8.4). The spectral resolution for a 1 arcsec slit is about 40 000. The maximum resolution that can be attained with still adequate sampling, using a narrow slit, is about 110 000 in the red and 80 000 in the blue.

The dioptric cameras offer fields with a diameter of 43.5 mm (blue) and 87 mm (red) and have external focal planes for easy detector interfacing and upgrading during the life of the instrument. The baseline CCD detector is a 2k x 4k, 15 µm pixel size thinned, back-illuminated EEV chip. For the red arm, the possibility of using an MIT/Lincoln labs high-resistivity chip to boost NIR QE and reduce fringing is being investigated.

Each arm has two crossdisperser gratings (Fig. 8.5) working in first order; the order separation is 12 arcsec minimum. The spectrum can be scanned on the CCDs in both directions.

Figure 8.6 [GIF: 160k]. UVES: A view with the top of the enclosure removed to better view the functions on the table. The blue and red ray paths have been drawn in.

Figure 8.7 [GIF: 176k]. View of UVES on Nasmyth B platform of UT2, with the enclosure in the upper position.

Auxiliary devices include the usual calibration lamps, an iodine absorption cell for high precision radial velocity studies, image slicers, depolarizer, image derotator, ADC and filter wheels. On-line information on the object position and the energy passed by the slits is provided by technical CCD slit viewers and exposure meters.

A recent addition is a fiber port for 8 fibers (e.g. 6 objects, 2 sky) feeding the red arm. With fibers of 1 arcsec diameter, this facility will provide the possibility to perform multi-object cross-dispersed echelle spectroscopy with R ~ 40 000 in the spectral range 420 - 1100 nm. The fiber inputs are located on the multifiber positioner at the other Nasmyth focus of UT2.

The instrument components are placed inside a passive enclosure (Fig. 8.6) which provides thermal isolation from the environment. The control and CCD electronics are located in temperature controlled cabinets outside the enclosure. All functions (image slicers, filters, ADC etc.) are permanently on-board and remotely selectable without manual intervention. A continuous flow of LN2 coolant for the CCD's is supplied by an external vessel with an autonomy of at least 2 weeks. These measures are expected to lead to high stability and repeatibility of calibrations both over short and extended periods of time.

UVES will be located on the Nasmyth platform B of UT2 (Fig. 8.7).

8.2.2.2 Science Objectives

The main science objectives of UVES are:

- Structure, physical conditions and abundances of interstellar and intergalactic gas at early epochs from the absorption spectra of high redshift QSO's;
- Kinematics of gas and stars in galactic nuclei;
- Kinematics and mass distributions of star clusters;
- Composition, kinematics and physical conditions of the interstellar medium in the galaxy and in nearby systems;
- Chemical composition and atmospheric models of galactic and extragalactic stars;
- Substellar companions of nearby stars (high-precision radial velocity studies over long timescales);
- Stellar oscillations.

8.2.2.3 Observational Capabilities

Table 8.9 lists the main observational capabilities. More details will be found in the Operating Manual (available in May 1998):

Table 8.9: UVES Observational Capabilities

Parameter	Blue	Red
Wavelength range	300 - 500 nm	420 - 1100 nm
Resolution-slit product	41,400 arcsec	38,700 arcsec
Max. resolution	~80,000	~110,000
Limiting magnitude (3hr, S/N~10, median seeing)	18.7 at R = 55,000 in U	20.3 at R = 55,000 in V 18.7 at R = 90 000 in V
Overall detective quantum efficiency (DQE) (from top of the telescope, wide slit)	6 % at 320 nm 15 % at 470 nm	18 % at 500 nm 9 % at 900 nm (with EEV chip)
Camera	dioptric F/1.8, 70 µm/arcsec field 43.5 mm diam.	dioptric F/2.5, 97 µm/arcsec field 87 mm diam.
CCDs and pixel scale	2K x 4K, EEV 15 µm pixels (0.22 arcsec/pix)	mosaic of two 2K x 4K, EEV 15 µm pixels (0.16 arcsec/pix)
Echelle	41.59 g/mm, R4 mosaic	31.6 g/mm, R4 mosaic
Crossdispersers (g/mm and blaze)	#1: 1200 g/mm, 330 nm #2: 660 g/mm, 420 nm	#3: 600 g/mm, 510 nm #4: 316 g/mm, 770 nm
Typical wavelength range/frame	80 nm in 30	200 nm in 45 orders

	orders	
Order separation (minimum)	12 arcsec or 50 pixels	12 arcsec or 75 pixels

8.2.2.4 Instrument Status

The system integration of UVES is planned to start in May 1998 at ESO's Garching facilities and first (solar) spectra will be produced soon thereafter. Commissioning on Unit Telescope 2 will start in August 1999. The instrument is planned to be released for general use in January 2000.

Table 8.10: Status of UVES

Built by	ESO
Location	UT2 (Nasmyth)
No. of guaranteed nights	None
Present status	Delivery of all major parts in progress, system integration to start May 1998

8.2.3 FLAMES (Fibre Large Area Multi-Element Spectrograph)

This is a multi-object facility at the UT2 Nasmyth Focus A, with access over the full useful field (25 arcmin diameter).

8.2.3.1 Instrument Concepts

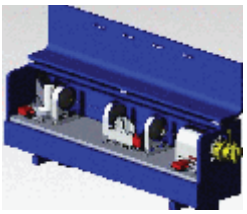

Figure 8.8 [GIF: 76k]. Design of the GIRAFFE spectrograph.

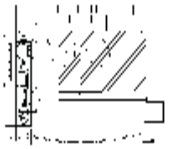

Figure 8.9 [GIF: 15k]. Schematic view of FLAMES.

The **FLAMES** concept stands for **F** ibre **L** arge **A** rea **M** ulti- **E** lement **S** pectrograph (a former, similar project was known as **FUEGOS**). At its heart is a rotating fibre-optic positioner, built by an Australian consortium and put on the Nasmyth A focus of UT2. This positioner will be able

- to feed UVES with 8 individual fibres, giving a spectral resolution of 40,000 on 8 different stars;
- to feed the R = 15,000 spectral resolution GIRAFFE optical spectrograph (Fig. 8.8) with either single fibres, small packs of fibres, or a single large pack;
- to feed a similar near-IR spectrograph (AUSTRALIS) in the 1 - 1.8 μm region, at a spectral resolution of about 12,000.

8.2.3.2 Science Objectives

The main science objectives of GIRAFFE are:

- Large Scale Structure through Red Shift Surveys;
- Dynamics of Clusters of Galaxies;
- Abundance of Stars in Clusters and Selected Regions Stellar Populations in nearby Galaxies;
- Stellar Kinematics in Clusters and Galaxies;
- Gravitational Lenses;
- AGNs, QSOs;
- Dynamics of Dwarf Spheroidal Galaxies;
- Outflows in Young Stellar Objects;
- Kinematical Structures in the Central Parts of Galaxies;
- Substellar Companions in Low Main Sequence Stars.

8.2.3.3 Observational Capabilities

The **Oz-Poz positioner** is a tumbling system analogue to the 2DF positioner at the Anglo-Australian Telescope. The fibres are put in position, while the system is observing on the sky, resulting in little time loss for observational set-up.

The **GIRAFFE spectrograph** has three modes:

- **MEDUSA** , with 130 single fibres, with an aperture of 1.2 arcsec on the sky (plus 5 fibres used for simultaneous wavelength calibration). With these fibres, two spectral resolutions of 15,000 and 7,500, respectively, will be attained;
- **Mini-ARGUS** , with 21 octogonal mosaics of 21 fibres, each with a square 0.6 arcsec aperture on the sky. The spectral resolutions will be 25,000 and 12,500. Each mini-ARGUS will be individually positioned;
- **ARGUS** , with a fixed simple pack of 30 x 15 fibres and spatial samplings of 0.6 and 0.3 arcsec. Spectral resolutions are as above.

The spectrograph uses one 2k x 4k CCD detector, with 15 μm pixels, illuminated at F/2. It has an 180 mm beam, and uses an R2 echelle (316 g/mm) or an R1 echelle for the lowest resolution. Wavelength coverage is respectively lambda/19 and lambda/9.5. Order selection is made through filters and the gratings have a prefixed set of angular positions, in order to cover any desirable wavelength.

8.2.3.4 Instrument Status

This programme is currently under discussion with the Australian partners (for the positioner), the Observatoire de Geneve, Observatoire de Meudon and Observatoire de Toulouse (for GIRAFFE). ESO will issue an Announcement of Opportunity for the procurement of the multi-object near-IR spectrograph.

A decision is expected in June 1998. ESO will be in charge of the connection to UVES and of the "Super"-Observing System which will orchestrate this multi-instrument system.

Table 8.11: Status of FLAMES	
Built by	ESO, Observatoire de Geneve, Observatoire de Meudon and Observatoire de Toulouse
Location	UT2 (Nasmyth)
No. of guaranteed nights	TBD
Present status	Under consideration

8.2.4 VIMOS - VIsible MultiObject Spectrograph

8.2.1.1 Instrument Concepts

VIMOS, and its clone for the near-infrared (1 - 1.8 μm) NIRMOS, are multi-slit spectro-imagers for the Nasmyth focii of UT3 and UT4, respectively. Both cover four adjacent fields of about 7 arcmin x 7 arcmin each; as such they offer the widest field accessible for imagery at the VLT, as well as the largest multi-object spectrographic capability, with up to 750 object spectra obtained in a single exposure by VIMOS.

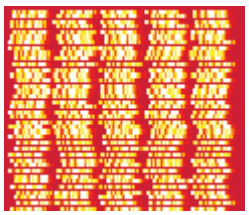

Figure 8.10 [GIF: 184k]. Multi-object spectra. Display of one VIMOS quadrant (low spectral resolution).

Figure 8.11 [GIF: 48k]. Schematic view of VIMOS.

8.2.4.2 Science Objectives

The main objective of VIMOS is to study of the early Universe through massive deep surveys, typically reaching back to an epoch when it was 10 to 20% of its current age. To this aim, VIMOS is complemented by the near-IR instrument **NIRMOS** . While VIMOS will basically observe objects of redshifts below 1 and above about 3 (i.e., when the Lyman discontinuity is redshifted into the B band), NIRMOS will observe objects in the intermediate range of redshifts (for which there is virtually no spectral signature in the visible).

VIMOS and NIRMOS with their large field (14 x 14 arcmin) will reach unprecedented high multiplex gains and be the workhorses of the VLT for large-field imaging and spectroscopic surveys. For both instruments together, the main scientific objectives are:

- Primary Objectives:
  -
  - Evolution of field galaxies;
  - Evolution of large scale structure;
  - Evolution of galaxies in clusters;
  - Search for distant QSOs.
- Secondary Objectives:
  - Gravitational lensing and distribution of dark matter;
  - Study of the environment of AGN's, quasars and radio galaxies;
  - Search for sub-stellar objects (brown dwarfs);
  - Abundances and ages of stars clusters and obscured regions.

8.2.4.3 Observational Capabilities

The field of view is split in four identical channels. Field lenses provide a corrected telescope focal plane where flat masks are inserted in spectroscopic mode (with grisms).

- imaging and multi-object spectroscopy in 4 x 7 arcmin x 7 arcmin
- spectral coverage: 0.36 - 1.0 μm
- spectral resolution: ~ 300 and ~ 2000
- ~ 150 slits @ R = 2000, ~ 750 slits @ R = 300
- 4 x 2k x 4k CCD detectors, 15 μm pixels
- Detection limit range in spectroscopy: V = 24-25

In addition, a 1 x 1 arcmin integral field capability is offered.

8.2.4.4 Instrument Status

The VIRMOS consortium presented the result of the Phase A study to ESO in September 1996. The ESO Scientific and Technical Committee (STC), during its November 1996 meeting, recommended to proceed with the realization of VIMOS and NIRMOS, with the aim to have VIMOS installed on the VLT by Q/1 in 2000 and NIRMOS by Q/3 in 2001.

Table 8.12: Status of VIRMOS

Built by	The VIRMOS Consortium: *Laboratoire d'Astronomie Spatiale* (LAS, Marseille), *Observatoire Midi-Pyrénée* (OMP, Toulouse) and *Observatoire de Haute-Provence (OHP)* in France; *Istituto di Fisica Cosmica del CNR and Osservatorio Astronomico di Brera* (IFCTR-OARr, Milano), *Osservatorio Astronomico di Capodimonte* (Napoli) and *Istituto di Radioastronomia CNR ed Osservatorio Astronomico di Bologna* (IRA-OABo, Bologna) in Italy; under ESO contract
Location	UT3 (Nasmyth)
No. of guaranteed nights	TBD
History	Approved: Dec. 1996 Preliminary Design Review: TBD Final Design Review : TBD
Present status	Design study

8.3 Near-IR Region (1 - 5 μm)

8.3.1. ISAAC - Infrared Spectrometer And Array Camera

8.3.1.1 Instrument Concept

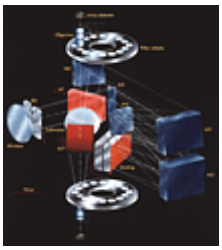

Figure 8.12 [GIF: 184k]. ISAAC optical layout. The two cameras at the top and bottom are optimized for the 1-2.5 μm and 2-5 μm regions and used to re-image the telescope focal plane or the intermediate spectrum formed by the grating spectrometer unit.

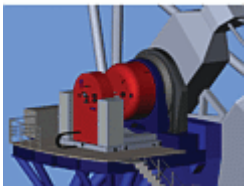

Figure 8.13 [GIF: 144k]. CAD view of ISAAC together with its cable co-rotator installed at a VLT Nasmyth focus.

ISAAC covers the wavelength range 1-5 μm and is designed primarily for:

- "wide" (2.5 x 2.5 arcmin) field imaging;
- long slit low and medium resolution spectroscopy

Fig. 8.12 shows the optical layout of ISAAC. At the top and bottom are two cameras which are optimized for the 1-2.5 μm and 2-5μm ranges and used to either re-image the telescope focal plane or the intermediate spectrum produced by the grating spectrometer. Light enters via the window on the left; passes through either a field mask or slit; is directed to the cameras or spectrometer by the selector mirror M1 and then to the short or long wave camera via the collimator lens and mirror M7. Imaging through the slit is also possible e.g to check object centering. The pupil image produced by the lens collimator has a diameter of 25 mm and each of the cameras comprises two filter wheels (28 positions) and an objective wheel providing various magnifications at the detector and a maximum field of 2.5 x 2.5 arcmin.

ISAAC is currently equipped with a short wavelength Rockwell 1024 x 1024 pixel Hg:Cd:Te array and a long wavelength SBRC 256 x 256 pixel InSb array. It is planned to retrofit it soon with a 1024 x 1024 SBRC ALADDIN array.

The spectrometer module is based on a system of three hyperbolic mirrors (M3-5) which produces a 10 cm diameter collimated beam and is re-fed, after diffraction at one of the back to back Littrow mounted gratings, to produce the intermediate spectrum close to M6.

The optical assembly is cooled to 77 K and housed in a ~ 1.5-m diameter vacuum vessel attached to the Nasmyth adapter flange. Some key features of the cryomechanical design are the use of:

1. diamond turned, post polished, metal mirrors;
2. cryogenic stepper motor (5 phase) driven worm gears for the 11 cold functions;
3. two closed cycle coolers for maintaining the optics at 77 K and the detectors at 30-60 K;
4. a liquid nitrogen pre-cooling circuit to accelerate cooldown;
5. a magnetic bearing turbomolecular pump flanged directly to the vacuum vessel to maximize the pumping speed;
6. a cable rotator to carry cables, closed cycle cooler hoses and cooling fluid to the Nasmyth mounted electronics;
7. a track mounted maintenance carriage for easy installation and removal of the instrument.

Fig. 8.13 shows a CAD view of ISAAC and its support equipment installed at one of the Nasmyth foci of the VLT. Figs. 8.14 - 8.17 provide various views from the integration in the Garching laboratory.

Figure 8.14 [GIF: 144k]. ISAAC, almost completely assembled with the large slit/mask wheel clearly visible at the front.

Figure 8.15 [GIF: 144k]. Front view of ISAAC partially assembled. Visible on the sides of the instrument (in orange) are the lifting devices for mounting the instrument on the adapter/rotator flange on the Nasmyth platform.

Figure 8.16 [GIF: 120k]. One ISAAC camera. Visible are the objective wheel, and two filter wheels. The detector is not shown.

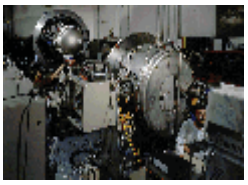

Figure 8.17 [JPG: 160k]. ISAAC undergoing final integration and testing at the Assembly Laboratory at Garching, prior to being shipped to the ESO observatories in Chile. (Its smaller brother, SOFI, is seen in the background; it was mounted on the NTT at the end of 1997). The complete optical system is housed in the vacuum vessel with diameter of 1.7 metres and cooled to a temperature of -200 o C.

8.3.1.2 Science Objectives

Some of the broad scientific themes which ISAAC is expected to address are listed below. Most take advantage of its relatively large imaging field and capability for immediate spectroscopic follow-up of objects detected.

Extragalactic

- Deep (K > 23) surveys;
  - Galaxy counts
  - Extension K-z Hubble diagram (q0 /evolution)
- Survey and study of high z galaxies (field, QSO absorption line systems, radio galaxies);
- Search for high-z clusters;
- Fundamental plane of high z cluster ellipticals;
- Starburst galaxies;
- Physical conditions/abundances in SN;
- Distance scale (cepheids, red s/giants, type1SN);
- Physical conditions/abundances in high z quasars;
- Nature of AGN central sources and their interaction with circumnuclear gas;
- Stellar populations in galaxies via IR spectroscopy;
- AGB stars in LMC, SMC and GC

Galactic

- Deep surveys for low mass stars;
- Survey and nature of IR objects embedded in molecular clouds;
- Stellar cluster abundances/ages.

8.3.1.3 Observational Capabilities

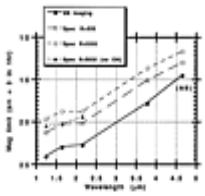

Figure 8.18 [GIF: 21k]. ISAAC limiting magnitudes for point sources (S/N = 3 in 1 hr) with FWHM = 0.6 arcsec seeing. Pixel scales down to 0.15 arcsec (0.07 arcsec) are available to exploit the improved magnitude limits and spatial resolution possible with better seeing.

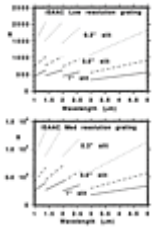

Figure 8.19 [GIF: 31k]. ISAAC spectral resolving powers with the low and medium resolution gratings and two pixel matching to 3 different slit widths.

Details of the **observational modes** are given in Tables 8.13 and 8.14 and performance estimates are presented in Fig. 8.18 and Fig. 8.19.

Table 8.13: ISAAC (Imaging)					
	1 - 2.5 µm		**2 - 5 µm**		
Scale [arcsec/pix]	0.15	0.27	0.07	0.15	0.5
Field [arcsec]	150x150	150x150	17x17	42x42	128x128
Filters	J, H, K', K, 1.06, HeI 1.083, 1.187, cont. 1.215, [FeII]1.26, Pbeta 1.282, [FeII] 1.64, 1.71, HeI 2.058, 2.09, H2 2.12, Br gam 2.166, 2.195, 2.28, H2 2.248, CO 2.336. Wollaston prism, 3 grating order isolation S1, S2, S3		L, M, M nb, cont. 3.2, 3.28, cont. 3.8, Br alpha, 4.05, Wollaston prism, 2 grating order isolation S3, S4		

Table 8.14: ISAAC (Spectroscopy)			
	1-5µm		
Low Resolution Rs	~500		
Medium Resolution Rs	~3000		
Slit width [arcsec]	1	0.6	0.3

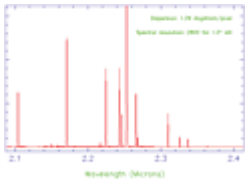

Figure 8.20 [GIF: 8k]. ISAAC Neon spectrum in the K band.

As an example, a Neon spectrum in the K band obtained during the laboratory tests in Garching is shown in Fig. 8.20. The measured spectral resolution is 2800 and is within specifications.

8.3.1.4 Instrument Status

ISAAC is now in the final system test phase at ESO in Garching. It will be shipped to Paranal in June 1998. Installation on UT1 is planned in November 1998.

A calibration plan has been defined and the Observation Blocks for more modes plus an imaging pipeline have been successfully tested with SOFI at the NTT.

A preliminary version of the user manual has been produced.

Table 8.15: Status of ISAAC

Built by	ESO
Location	UT1 (Nasmyth)
No. of guaranteed nights	None
Present status	System tests

8.3.2 CONICA - High-Resolution Near-Infrared Camera

8.3.2.1 Instrument Concepts

The high-resolution, near-IR camera **CONICA** covers the infrared wavelength range from 1 - 5 μm and is designed primarily for:

- infrared imaging with the highest possible spatial resolution;
- low- resolution spectroscopy with high spatial resolution;
- moderate - precision polarimetry.

The camera will be installed at the Nasmyth B focus of the VLT Unit Telescope 1 to operate in conjunction with the Nasmyth Adaptive Optics System (NAOS). CONICA is designed to exploit the adaptively corrected telescope image at wavelengths longwards of 2 μm. Speckle interferometry can be performed, primarily at the shorter wavelengths.

The telescope (AO) image is projected onto the camera's entrance focal plane inside the cryogenic instrument. An achromatic BaF 2 /LiF lens doublet collimates the F/15 beam and forms a pupil image at a cold stop. Analyzing optics residing in three large wheels are inserted into the beam here. One of the mirror/lens camera objectives forms the final image on the detector.

Figure 8.21 [GIF: 28k]. Design of CONICA.

Figure 8.22 [GIF: 14k]. CAD view of CONICA.

The detector is a 1024 x 1024 InSb ALADDIN array with 27 μm pixels.

Four different camera magnifications are provided for:

- diffraction-limited imaging with over-critical sampling of the Airy disk (> 2 pixels) at all wavelengths. The usable field is limited only by the size of the detector;
- a "large field" of 73 arcsec diameter.

A number of optical elements can be inserted into the optical beam near the pupil plane to provide analyzing capabilities:

- two-dimensional spectroscopic imaging
  is possible with wideband and narrowband filters covering the entire 1 - 5 μm wavelength range, and with a tunable Fabry-Perot (R = 1800) for the K-band;
- low-resolution grism spectroscopy can be performed in all wavelength bands;
- polarization analyzing capabilities with Wollaston prisms are available, as well as
- wiregrid analyzers and
- coronographic masks in the focal plane.

All optical stops and analyzing elements are mounted interchangeably on wheels inside the cryogenic environment. The camera is housed in a cryogenic dewar. The operating temperatures of ~ 80 K for the optical system and 20-70 K for the detector are produced by a closed-cycle cooler.

A tunable atmospheric dispersion compensator (TADC) is employed for broadband imaging at short wavelengths. The TADC and an optical calibration unit for flux, flatfield and wavelengths are located outside the cryogenic environment.

The entire instrument will be attached rigidly to NAOS and the Nasmyth adapter/rotator to compensate for the apparent sky rotation.

8.3.2.2 Science Objectives

The development of CONICA has been based on the following scientific objectives:

Galactic Astronomy:

- Outflows and disks of young stellar objects
- Search for low-mass/ substellar companions of nearby stars
- Structure of young embedded objects
- Ionization fronts in HII regions
- Galactic center
- Close companions and circumstellar material around T-Tauri stars
- Structure of Red Giant envelopes

Extragalactic Astronomy:

- Quasars and host galaxies
- Emission line imaging of super-luminous IRAS galaxies
- Search for Black Holes in centers of galaxies
- Power station of Seyfert galaxies and quasars
- Resolved images of radio jets and hot spots
- Obscured quasars
- The cosmic distance scale

8.3.2.3 Observational Capabilities

The observational capabilities of CONICA may be summarized as follows:

Table 8.16: CONICA (Imaging)				
Camera	f/51	f25.5	f/12.75	f/6.37
Scale [mas/pix]	13.6	27.3	54.6	109.2
Field [arcsec]	14 x 14	28 x 28	56 x 56	73 Ø

BB Filters : J, H, K, K', L, M, Continuum 1.04 μm

NB Filters : Ice 2.90, 3.07, 3.30, 3.60, HeI 1.08, P gamma 1.094, OII 1.237, FeII 1.257, P beta 1.282, FeII 1.644, H 2 (1-0) S(7) 1.748, H 2 (1-0) S(1) 2.121, Pf gamma 3.74, Br alpha 4.051, Pf beta 4.653

Polarization : 4 wiregrid, 2 Wollaston prisms

Spectroscopy : tunable cryogenic Fabry-Perot (K-band), R~1800
Grisms covering J, H, K, L, M bands

The following performance limits are expected:

Table 8.17: Performance Limits of CONICA					
Band	**J (1.25)**	**H (1.65)**	**K (2.2)**	**L (3.8)**	**M (4.8)**
wavelength/D [mas]	33	43	57	99	125
scale [mas/px]	13.6	13.6	27.3	54.6	27.3/54.6
BB imaging	26.9	26.3	25.4	19.1	17.1
R=50	25.8	25.1	24.6	18.0	16.1
R=500	24.0	23.5	22.6	16.7	14.5
R=1800 (FP)			21.8		

speckle	16-18	16-18	15-17		
Limiting Magnitudes (3 sigma, T int = 1hr).					

8.3.2.4 Instrument Status

Table 8.18: Status of CONICA

Built by	*Max-Planck-Institute for Astronomy* (Heidelberg) *Max-Planck-Institute for Extraterrestrial Physics* (Garching) in Germany (under ESO contract)
Location	UT1 (Nasmyth), coupled to NAOS
No. of guaranteed nights	45
History	Contract Contract Signature: 1991 Preliminary Design Review: 1993 Final Design Review : 1997
Present status	Instrument in the construction phase. Preliminary Acceptance in Europe in Q/4 1998

8.3.3 CRIRES - VLT High-Resolution IR Echelle Spectrometer

8.3.3.1 Instrument Concepts

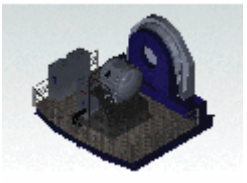

Figure 8.23 [GIF: 176k]. CAD view of CRIRES.

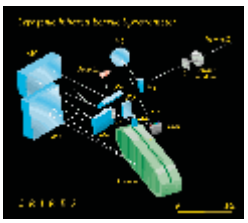

Figure 8.24 [GIF: 31k]. Design of CRIRES.

This cryogenic high-resolution IR spectrograph (Fig. 8.23) has been conceived for the VLT in order to exploit the enormously *enhanced sensitivity* provided by a dispersive instrument with a large detector array at an 8 m telescope. The gain (up to 8 mag. compared to previously available facilities) entails a quantitative and *qualitative* improvement of the observational capabilities. It can boost all scientific applications aiming at *fainter objects, higher spatial* (extended sources), *spectral* and *temporal resolution.*

An Adaptive Optics clone of ESOs MACAO system (cf. Chapter 8.6) has been foreseen, to feed CRIRES.

The design is shown in Fig. 8.24.

8.3.3.2 Science Objectives

The IR spectrograph will make previously inaccessible phenomena and objects available for spectroscopic studies. The detailed science objectives are identified in Table 8.19.

Table 8.19: CRIRES Scientifix Objectives
Extra-Solar Planets
Radial velocities studies
Direct spectroscopic detection and characterization: CO, CH4.
Solar System
Chemistry/phys. conditions/velocity fields/structure

Giant planets/Titan	H3+, CH4, NH3, CH3D, AsH3, H2O,C2H2,C2H6, PH3, CH3, NH3, HCN, C2H2, C2H6, PH3, CH3, NH3, HCN
Terrestrial planets	CO, HCL, HF, HDO, H2O, OCS Mars imaging (0.1 arcsec - 40 km) spectr. of CO depletion.
Io	spatial/time mapping of volcanic activity (SO2)
Pluto/Charon/Triton	search tenous CO, CH4 atmos.
Comets	(resolve nuclei), H2O abundance, temperature, velocities, minor species.
Stars	
Stellar evolution/nucleosynthesis (OB, AGB stars, cluster red giants, cool MS, C & S stars in galaxy, S/LMC, nearby glaxies), CNO isotopic abundances unique in IR.	
Stellar mass:atom/mol. lines from secondaries	
Stellar winds/mass loss, OB, WR, AGB stars in galaxy and S/LMC, CO,SiO,C2H2, HCN	
Atmospheric structure & oscillations in cool stars	
Magnetic fields	
Star Formation Regions/ISM	
Accretion/Outflow from embedded YSOs	
ISM chemistry/ cloud structure, H3+, H2O, CH4, C2H2, NH3	
Extragalactic	
AGN	Velocity structure of BLR, NLR, CLR & molecular clouds, H recombination, [FeII], [SiIV], H2 lines suffering low dust extinction

Quasars	Chemical/physical state of gas in early universe through absorption lines, Ly_alpha, CII, OI, CIV, MgII, Fe.

8.3.3.3 Observational Capabilities

The cryogenic echelle will provide for **high-resolution spectroscopy in the 1 - 5 μm range** the VLT. This instrument employs the largest available grating for a **spectral resolving power of 100,000** with a 0.2 arcsec slit. Simultaneous spectral coverage is maximized through one or several large (1024 x 1024 pixel) detector arrays in the focal plane. In the single order mode, the second array dimension is exploited for **1-dimensional spectral imaging** along the ~ 50 arcsec slit. In addition, a **crossdispersed mode** with ~ 10 arcsec slit length is foreseen to further increase the instantaneously covered spectral range.

Functionally, the instrument can be divided into three units. The fore-optics section provides for field de-rotation and low-order adaptive optics correction for point source light concentration on the narrow predisperser entrance slit. The prism predisperser isolates one echelle order and minimizes the total amount of light entering into the high-resolution section. A camera in the predisperser can record the low-resolution spectrum reflected off the echelle entrance slit. The high-resolution section comprises the collimator, the echelle which is tilt-tuned for wavelength selection, the camera providing the 0.1 arcsec/pixel plate scale, and the detector(s). The calibration unit outside the cryogenic environment contains light sources for flux/wavelength calibration and detector flatfielding. The instrument will be coupled to an external curvature-sensing AO System.

Observational capabilities and predicted performance are given in Tables 8.20 and 8.21

Table 8.20: CRIRES Cryogenic Echelle Main Characteristics	
Parameter	**Value**
Focus	Nasmyth
Configuration	stationary
Wavelength range	1 - 5 μm
Slit width-res. power product	20,000
Echelle	40 cm length, 31.6 lines/mm
Optics	reflective
Detector	1024 x 1024 x 3
Pixel size	0.1 arcsec
Spectral format	single order or crossdispersed
Slit length	~ 50 arcsec
Operating temperature	60-80 °K
Detector temperature	~30 °K
background subtraction	on-chip
Instantaneous wavelength coverage	1200 A (single 1024 detector)

Table 8.21: CRIRES Performance Limits						
Limiting magnitudes (for S/N = 3 in 1 hr)						
Wavelength (μm)	1.2	1.6	2.2	3.3	4.2	4.7
mag	18	17.5	17	15	13.5	12.5
Integration times (required for S/N = 100 on a 5th and a 10th mag star)						
Wavelength (μm)	1.2	1.6	2.2	3.3	4.2	4.7
T [sec], mag=5	< 1	1	2	2	3	5
T [sec], mag=10	50	100	160	350	6,000	15,000

8.3.3.4 Instrument Status

This instrument is now in the design phase. The Final Design Review is planned for 2000.

Table 8.22: Status of CRIRES	
Built by	TBD
Location	UT4 (Nasmyth) in 2002
No. of guaranteed nights	TBD
History	Approved: Nov. 1997 Preliminary Design Review: 1998
Present status	Design phase

8.3.4 NIRMOS - Near InfraRed MultiObject Spectrograph

8.3.4.1 Instrument Concepts

NIRMOS, and its clone for the optical region VIMOS, are multi-slit spectro-imagers for the Nasmyth focii of UT4 and UT3, respectively. Both cover four adjacent fields of 7 arcmin x 7 arcmin each; as such they offer the widest field accessible for imagery at the VLT, as well as the largest multi-object spectrographic capability, with up to 750 object spectra obtained in a single exposure for VIMOS. As an example, Fig. 8.25 show the multi-object spectral display in one NIRMOS quadrant at high spectral resolution.

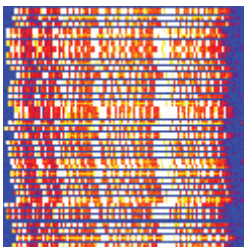

Figure 8.25 [GIF: 168k]. Multi-object spectral display in one NIRMOS quadrant (high spectral resolution).

Figure 8.26 [JPG: 48k]. Design of NIRMOS.

Fig. 8.26 shows the design of NIRMOS. The field of view is split in four identical channels. Field lenses provide a corrected telescope focal plane where flat masks are inserted in spectroscopic mode (with grisms).

8.3.4.2 Science Objectives

The main objective of this instrument is to study of the early universe, through massive deep surveys, typically when it was 10 to 20% of its current age. To this aim, NIRMOS is complemented by **VIMOS** which will basically observe objects of redshifts below 1 and above ~ 3 (when the Lyman discontinuity is redshifted into the B band), whereas NIRMOS will observe objects in the intermediate range of redshifts (for which there is virtually no spectral signature in the visible).

VIMOS and NIRMOS will reach unprecedented high multiplex gains and be the worhorses of the VLT for large field imaging and spectroscopic surveys.

For these instruments, the main objectives are:

- Primary Objectives
    - Evolution of field galaxies;
    - Evolution of large scale structure;
    - Evolution of galaxies in clusters;
    - Search for distant QSOs
- Secondary Objectives
    - Gravitational lensing and distribution of dark matter;
    - Study of the environment of AGN's, quasars and radio galaxies;
    - Search for sub-stellar objects (brown dwarfs);
    - Abundances and ages of stars clusters and obscured regions

8.3.4.3 Observational Capabilities

- imaging and multi-object spectroscopy in 4 x 6 arcmin x 8 arcmin
- integral field spectroscopy in 1 x 1 armin area
- spectral coverage: 1.0 - 1.8 μm
- spectral resolution: ~ 2000
- ~ 180 slits @ R = 2000
- 4 x 2k x 2k IR detectors, 18.5 μm pixels
- Detection limit range in spectroscopy: V = 22-23

Fig. 8.26 shows a schematical image display of one NIRMOS quadrant, in spectroscopic mode at high spectral resolution.

8.3.4.4 Instrument Status

The VIRMOS consortium presented the result of the Phase A study to ESO in September 96. The ESO Scientific and Technical Committee (STC), during its November 1996 meeting, recommended to proceed with the realization of VIMOS and NIRMOS, with the aim to have VIMOS installed on the VLT by Q/1 2000 and VIRMOS by Q/3 2001.

Table 8.23: Status of NIRMOS

Built by	The VIRMOS Consortium: *Laboratoire d'Astronomie Spatiale* (LAS, Marseille), *Observatoire Midi-Pyrénée* (OMP, Toulouse) and *Observatoire de Haute-Provence (OHP)* in France; *Istituto di Fisica Cosmica del CNR and Osservatorio Astronomico di Brera* (IFCTR-OARr, Milano), *Osservatorio Astronomico di Capodimonte* (Napoli) and *Istituto di Radioastronomia CNR ed Osservatorio Astronomico di Bologna* (IRA-OABo, Bologna) in Italy; under ESO contract
Location	UT4 (Nasmyth)
No. of guaranteed nights	TBD
History	Approved: Dec. 96 Preliminary Design Review: TBD Final Design Review : TBD
Present status	Design study

8.3.5 SINFONI - SINgle Far Object Near-ir Investigation

8.3.5.1 Instrument Concepts

Figure 8.27 [JPG: 46k]. Design of SINFONI.

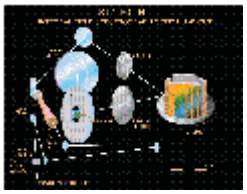

Figure 8.28 [GIF:41k]. Design of SINFONI Integral Field Spectrograph.

SINFONI is the result of the coupling of two sub-modules, already at the design phase, the *Max-Planck-Institut für Extraterrestische Physik* 's integral field spectrograph **SPIFFI** , and ESO's medium-order Laser Guide Star curvature Adaptive Optics system, **MACAO** . MACAO is designed to work both with Laser and Natural Guide Stars, and it is the first curvature AO system designed for such a hybrid operation; cf. Chapter 8.6.

The specifications are as follows:

- 32 x 32 spatial pixels;
- multiplied by 1024 spectral pix;
- spatial sampling variable from 0.35 arcsec to 0.05 arcsec;
- 1.0 - 2.4 µm range;
- spectral resolution 6,000 and 10,000.

A 35-element curvature Adaptive Optics system (built by ESO) feeds the instrument (built by MPIE Garching) with a small corrected field. A set of enlargers transfers this field to an image slicer which maps the roughly square field onto a long-slit. A "conventional" spectrographic assembly then delivers a spectrum for each individual spatial "pixel" on an 1k x 1k infrared array. The spectrographic part, including the image slicer, is cooled. The baseline spectral resolution (6,000) has been chosen for maximum detectivity after night-sky rejection.

8.3.5.2 Science Objectives

SINFONI will be particularly suited for the following types of observations:

- Detection/Study of quasar fuzz, distant ellipticals, primeval galaxies;
- Detailed analysis of distant radio/interacting galaxies;
- Central regions of moderate z galaxies;
- Regions of stellar formation;
- Galactic Center;
- Surfaces of planets/satellites.

8.3.5.3 Observational Capabilities

Limiting magnitudes will be comparable to those of ISAAC for a stellar (point) source). Depending on the atmospheric (seeing) conditions, data cubes up to the diffraction limit of the telescope will be obtained, albeit wthin a very small field (~ 1.6 x 1.6 arcsec).

8.3.5.4 Instrument Status

Table 8.24: Status of SINFONI

Built by	*Max-Planck-Institut für Extraterrestische Physik* and *ESO*
Location	UT1 (Cassegrain)
No. of guaranteed nights	TBD
History	STC Approval: May 1998 Preliminary Design Review: November 1998 Final Design Review : July 1999 Commissioning: June 2001
Present status	Preliminary design study of MACAO and SPIFFI sub-units in progress

8.4 Mid-IR Region (8 - 25 μm)

8.4.1 VISIR - VLT Mid Infrared Imager Spectrometer

8.4.1.1 Instrument Concepts

It was early concluded that it is desirable to have at the VLT a sophisticated multimode instrument built for the thermal mid-infrared regions and similar to the VLT near infrared instrument ISAAC.

This instrument, **VISIR** is expected to optimally exploit the VLT and its site while being fully complementary to spacebased infrared astronomy.

VISIR will be an instrument which is currently not available at any other observatory. In order to gain experience how to operate and use such an instrument, ESO is operating **TIMMI** , a substantially smaller but still quite powerful multimode thermal infrared instrument at its 3.6-m telescope on La Silla. This instrument is available to all interested scientists as a common user facility.

TIMMI is now more than four years in operation. To bridge the gap between TIMMI and VISIR - especially in the view of the success of ESA's ISO mission, a second generation instrument, **TIMMI2** , is presently under construction for the 3.6-m telescope on La Silla. It will benefit from all improvements of the 3.6m upgrade project and feature a state-of-the-art detector as well as many more observing modes when compared to TIMMI. Most notable it will have a polarimetric option and full access to the atmospheric Q-band (17-24 μm).

8.4.1.2 Science Objectives

The mid-IR region is optimal for the study of "warm" dust (140 - 400 K) and of the gaseous component through a large number of ionic, atomic and molecular lines. Astrophysical applications are numerous and varied, e.g. planetology, planet formation, stellar formation, checmistry of the interstellar medium and galaxy evolution. For many of the domains, the negligible absorption by dust in this spectral region is a big advantage, e.g. for witnessing the birth of stars or peering deep inside the nucleus of an active galaxy.

8.4.1.3 Observational Capabilities

VISIR will provide for the following observing modes:

- *base line:*
  - diffraction limited imaging with variable magnification utilizing broad and narrow-band filters up to a maximum field of 80 x 80 arcsec ² between 8-13 µm and 16.5 - 24.0 µm
  - long-slit spectroscopy between 7.9-14 µm with R ~250 and > = 30,000

Figure 8.29 [GIF: 33k]. The VISIR cryostat.

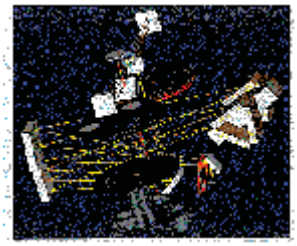

Figure 8.30 [GIF: 18k]. Design of the VISIR spectrograph.

Fig. 8.29 shows a CAD representation of the VISIR cryostat. Fig. 8.30 shows the design of the spectrograph.

VISIR includes the following additional modes which allow to even better utilize the VLT while not contributing significantly to complexity, price or technical risk:

- long-slit spectroscopy between 7.9 -14 µm with R ~ 10,000;
- long-slit spectroscopy between 16 - 24 µm with R ~ 3,500 and > = 15,000.

Note that the value for the spectral resolving power here given corresponds to the diffraction limit.

It should be noted that the final sensitivity achieved with VISIR will be largely independent of the exact technical details and will be determined by the quality of the site and the telescope. This is one of the consequences of operation in the background-noise limit. The sensitivity expected for VISIR (10 sigma in one hour) for spatially unresolved sources (i.e. <= 0.3 arcsec at a wavelength ~10 µm) is given in Table 8.25.

Table 8.25: VISIR Sensitivity				
Mode	**Wavelength Range [µm]**	**Limiting Mag/Flux mag/Jy - W/m²**		**Comments**
N-band imaging	8-13	12.1/5.4 E-4	8 E-17	
Q-band imaging	16.5-24.0	7/13 E-3	3.3 E-16	details will depend strongly on filter characteristics and atmospheric conditions
10 µm spectroscopy R~300-500	7.9-14	9.0/8.7 E-3	6.5 E-18	
10 µm spectroscopy R~7,000	7.9 - 14	7.0/60 E-3	2.5 E-18	
10 µm spectroscopy R~30-50,000	7.9-14	4.6/0.5	3.8 E-18	will depend somewhat on exact embodiment, detector, etc.
20 µm spectroscopy R~3,000	16.5-24.0	5.0/90 E-3	4.0 E-18	sensitivity is a strong function of wavelength strong because of atmosphere

8.4.1.4 Instrument Status

VISIR is now in the preliminary design phase where the findings of the phase-A-study will be developed intoa more detailed design, including prototyping of critical items.

Table 8.26: Status of VISIR

Built by	*Service d'Astrophysique CEA/DAPNIA* (Saclay, France) with *NFRA* (Dwingeloo, The Netherlands) (under ESO contract)
Location	UT3 (Cassegrain) in 2001
No. of guaranteed nights	TBD
History	Preliminary Design Review: Oct. 1997 Final Design Review : TBD
Present status	Design study

8.5 NAOS - Nasmyth Adaptive Optics System

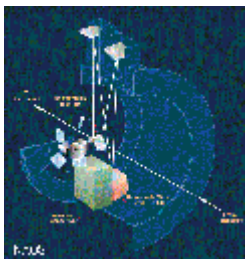

Figure 8.31 [GIF: 63k]. The Nasmyth Adaptive Optics System (NAOS).

The NAOS (Nasmyth Adaptive Optics System, cf. Fig. 8.31) is attached to the Adapter-Rotator.

Optimised for full correction at 2.2 µm, the sub-aperture size at location of the primary mirror is of the order of the Fried diameter at this wavelength. This corresponds to about 250-300 sub-apertures and actuators which, with currently available technology corresponds to a pupil diameter of about 110 mm at the location of the deformable mirror. The position of the Adaptive Optics output focal plane is determined by the position of the AO WFS. The AO WFS can accommodate distances in the range 140-160 mm from the flange.

The optical layout has been designed to minimise the number of reflecting surfaces and deliver an F/15 output beam to the instrument with an image scale of 582 µm/arcsec. The system keeps the image of the telescope pupil at 16 m as it is at the normal Nasmyth focus. The only remaining aberration is the field curvature which has a radius of 1110 mm.

The available Field of View at the Nasmyth corrected focus is 2 arcminutes which corresponds to the maximum isoplanatic patch expected at an observing wavelength of 5 µm.

The second flat mirror, which is either a dichroic or a beam splitter, is mounted on a wheel with five positions. This reflects the infrared light towards the instrument and transmits the visible light (or light in the 1-2.5 µm range in the case of IR wavefront sensor) towards the wavefront sensor unit. The characteristics of the dichroic or beam splitter elements were defined according to the instrument observing requirements.

8.5.1 NAOS Concept and Scientific Drivers

The basic purpose of NAOS is to provide atmospheric correction to and optimise the scientific output of CONICA. Therefore, NAOS will provide corrected scientific images in the 1-5 µm range, by using a visible or infrared reference star for wavefront sensing.

The scientific drivers of NAOS can be summarised in two wavelength domains, the *non-thermal domain (1-2.5 µm)* and the *thermal domain (3-5 µm)* .

8.5.1.1 Non-thermal Domain (1-2.5 μm)

Compared with its main competitor, the Hubble Space Telescope (HST) and its Near Infrared Camera, CONICA with NAOS can compete in that domain only by providing better final images, that is close to the diffraction limit of an 8 m telescope, but obviously then only on a limited sample of objects. The scanning Fabry-Perot offers a spectro-imaging capability unique when compared with the HST.

1. When a bright reference star is available close to the science object, it shall be possible to reach directly a near diffraction-limited image (Strehl ratio > 0.7) even if the target is very faint.
2. When the science object is relatively bright, and the reference star reasonably bright/close, a goal moderate > 0.2 Strehl will allow to reach finally near diffraction limited imaging through post-exposure deconvolution.
3. The scanning Fabry Perot capability in the K band offers a mode not in competition with the HST. Hence, even very partial correction images at 2.2 μm (FWHM = 0.2 arcsec) will be still competitive.

Obviously, in all cases we expect these performance to be achieved with the faintest possible reference stars. In term of Adaptive Optics, requirements 1, 2 and 3 can be translated respectively into:

1. getting a minimum Strehl ratio of 0.7 at 2.2 μm for median seeing conditions, when a suitable reference star is available;
2. getting the maximum possible sky coverage compatible with achieving a 0.2 arcsec FWHM images at 2.2 μm, again for median seeing conditions. The Adaptive Optics sky coverage is here defined as the percentage of the sky than can be reached, while keeping the required performance.

Regime 2 will be completed by a comprehensive (off-line) data reduction package, reconstructing the PSF from the Adaptive Optics data in order to derive deconvolved images or by blind deconvolution techniques. In addition and especially in the J and H bands, such low mode Adaptive Optics corrections will be used to boost the limiting magnitude of the CONICA speckle mode and therefore ultimately reach the diffraction limit of the 8 m telescope.

8.5.1.2 Thermal domain (3-5 µm)

The previous requirements will in principle essentially optimise the work at 3 and 5 µm. However, since a large fraction of science targets lies in obscured regions of the Galactic plane and/or are internally obscured themselves, one needs an additional near infrared (1-2.5 µm: TBC) wavefront sensor which will also be needed for shorter wavelength work on these objects. A longer wavelength sensor will add most post AGB stars envelopes as possible targets, but would probably limit too much the sky coverage (TBC).

In addition, two special requirements come from the high thermal background in that domain:

- getting the lowest possible thermal emissivity from NAOS;
- providing a thermal emission subtraction technique, with the goal of non compromising the S/N ratio by more than 20 % by using for instance a low frequency chopping technique which may lead to severe constrains on the NAOS operation. The procedure to achieve this last requirement is the responsibility of CONICA although advises from the NAOS team will be welcome.

8.5.2 NAOS Preliminary Performance

The basic parameter used for the image quality performance evaluation of NAOS is the long-term Strehl ratio at a given wavelength defined as the ratio between the peak intensity of a point source to the one that would be achieved with a prefect diffraction-limited system.

In what follows, the expected performance of NAOS in the visible and in the IR is characterized.

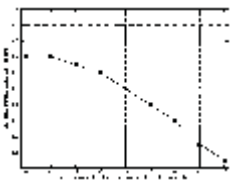

Figure 8.32 [GIF: 10k]. NAOS Strehl ratio in the visible.

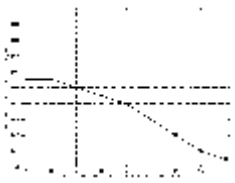

Figure 8.33 [GIF: 10k]. NAOS Strehl ratio in the IR.

8.5.2.1 NAOS Image Quality Performance with the Visible WFS

NAOS, when using either the visible or the IR wavefront sensor (WFS), will provide an on-axis Strehl ratio at 2.2 μm at least equal to the requirements shown in Fig. 8.32, under the conditions specified in Table 8.27 and 8.28:

Table 8.27: NAOS Visible WFS Performance Requirements

Seeing (0.5 μm):	between 0.25 and 0.85 arcsec
Adaptive optics correlation time (@ 0.5 μm):	> 3 ms
Performance stability over:	> 20 minutes
Large scale of turbulence:	infinite
Telescope altitude angle:	< 30 o ; (0 o ; zenith)
Reference source apparent diameter:	from point like up to 2 arcsecs
Reference source spectrum:	G0
Reference source position:	on axis
WFS bandpass:	450-900 nm
Telescope residual image motion with a ground wind speed of v <10 m/s and integration time of 10 ms.	

The number of corrected modes and reconfiguration of NAOS will be optimised according to working conditions (magnitude and contrast of the reference object, seeing conditions, angular distance between the object and the reference star).

Strehl ratio requirements in the 1-5 μm range can be calculated accordingly.

8.5.2.2 NAOS Image Quality Performance with the IR WFS

NAOS, when using the IR wavefront sensor, will provide an on-axis Strehl ratio at 2.2 μm at least equal to the requirements shown in Fig. 8.33 under the following conditions:

Table 8.28: NAOS IR WFS Performance Requirements

M seeing (@ 0.5 μm):	between 0.25 and 0.85 arcsec
Adaptive optics correlation time (0.5 μm):	> 3 ms
Performance stability over:	> 20 minutes
Large scale of turbulence:	infinite

8.5.2.3 NAOS Limiting Conditions for Visible and IR WFSs

Under the following limiting conditions, all functional requirements will be met but with degradation of performance TBD at a later stage:

1. The wavefront sensor design will allow the use of astronomical objects (as reference star) with an apparent diameter up to 4 arcsec (not including the seeing effect). This may lead to have several WFS optical sets in order to provide the best possible correction when sensing with point-like reference sources.
2. NAOS will operate under atmospheric correlation time as low as 1 ms (@0.5 μm).
3. NAOS will operate under seeing conditions as high as 2 arcsec. Above this value, the correction can be stopped after sending an exposure stop request to the instrument.
4. NAOS will be able to use a reference star up to 1 arcmin off-axis (2 arcmin diameter).
5. NAOS will be able to provide image correction for the science path in the bandpass 1-5 μm.
6. Accuracy of the wavefront sensing on extended object with 50 % of the energy in the core will be investigated (in particular with respect to the threshold determination in the centroiding calculation).

The scientific interest and possibility to use asteroids or small planets as reference stars will be investigated.

8.5.3 Status

NAOS is now in the final design phase.

Table 8.29: Status of NAOS	
Built by	*ONERA, Observatoire de Paris* and *Observatoire de Grenoble (France)* (under ESO contract)
Location	UT1 (Nasmyth), with the Infrared Camera CONICA in 2000
No. of guaranteed nights	TBD
History	Approved: Nov. 1996 Preliminary Design Review: Dec. 1997/May 1998 Final Design Review : end of 1998
Present status	Design study

8.6 MACAO - Multiple Application Curvature Adaptive Optics

Figure 8.34 [JPG: 42k]. Schematic representation of the optical design of MACAO.

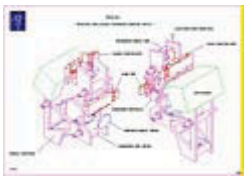

Figure 8.35 [JPG: 56k]. CAD drawing of MACAO.

MACAO is an adaptive optics system based on wavefront curvature sensing. It is built by the ESO Adaptive Optics Group. It is designed to operate at the Cassegrain focus of UT1, with a faint star (*Natural Guide Star*) as well as with an artificial star (*Laser Guide Star* , cf. Chapter 8.7). MACAO will be one of the two subsystems of *SINFONI* (Chapter 8.3.5). A clone of MACAO is also foreseen for *CRIRES* (Chapter 8.3.3), at a second stage.

8.6.1 The MACAO Concept

MACAO is a 35-element curvature system, capable of **correcting up to 28 modes of the optical wavefront** . The choice of the number of actuators and of the curvature wavefront sensor, is optimized for use with imaging spectrographs in the 1 - 2.5 µm wavelength range, with faint guide stars and extragalactic targets.

MACAO will deliver diffraction-limited images in the 1 - 2.5 µm range and will be able to suppress the seeing-induced image effects to a level **below 0.1 arcsec FWHM** . If necessary, the data obtained by SINFONI may be deconvolved post-facto, using the wavefront sensor and mirror commands data, to recover the Point Spread Function (PSF) during the science exposure. The 0.1 arcsec spatial resolution goal is crucial for front-line investigations, e.g. for spectroscopy of high red-shift (z > 2) objects.

8.6.2 Technical Description

A customized, integrated **Avalanche PhotoDiode (APD) wavefront sensor** is being developed to optimize the performance of MACAO. The wavefront sensor geometry shown in the color picture has been chosen to minimize the noise propagation. The APDs allow photon counting with 73% peak QE at 680 nm, and are read-noise free. The choice of APDs for the wavefront sensor allows to run the AO system at high, closed-loop bandwidths (150 Hz at 0 dB).

When the Laser Guide Star is used, tip-tilt (or image motion) will be sensed on a separate Natural Guide Star. A system for **Tip-tilt Removal with Avalanche Photodiodes (STRAP)** has been previously developed at ESO and will be implemented in MACAO. It is optimized for Natural Guide Star tip-tilt sensing.

The tip-tilt Natural Guide Star may be selected in a 2 x 3 arcmin field around the scientific target. The tip-tilt signal is downloaded on the curvature mirror for the low-stroke, high-frequency components, and to the VLT M2 Steering Unit, for the high-stroke, low-frequencies. This avoids the need to implement a fast steering mirror in the MACAO optical relay.

For servicing and maintainance, MACAO will be pulled in and out of SINFONI on its handling tool, with high precision repositioning. MACAO is enclosed in a light-tight cover, so that stand-alone operation is possible even during daytime, for calibration, testing or operator training. The includes calibration and self-test units.

The number of warm mirrors for the optical relay from the Cassegrain f/13.4 to the f/17 input focus of SPIFFI has been minimized to four, all with enhanced silver coated. One of them is the 35-actuator, curvature-deformable mirror (DM). The dichroic mirror that separates Visible and Near-IR wavelengths (i.e. the wavefront sensor and the spectrograph feeds), forms the entrance window of the dewar.

These features impose careful mechanical design and flexure control of the SINFONI structure. The structural flexure is taken care of by the AO system, except for the differential flexure between the wavefront sensor and the IR detector. The science requirements impose a maximum of 15 milliarsec of angular field differential flexure, over 2 hours operation.

8.6.3 Performance Simulations

Numerical and analytical simulations have been performed for MACAO. The *Paranal Model Atmosphere* is used, with 0.65 arcsec median seeing, and a coherence time of 6 msec at 550 nm. The performance of MACAO with Natural and Laser Guide Stars has been computed, including figuring and sensor noise effects, time-delay and anisoplanatism effects. The predicted performance is given in terms of Strehl Ratio and long-exposure Point Spread Function (FWHM). For the Laser Guide Star simulations, the cone effect and the field anisoplanatism of the tip-tilt reference star are taken into account as well.

Results of some of the simulations are shown in Figs. 8.36 - 8.39.

Figure 8.36 [JPG: 37k]. Numerical simulation of Natural Guide Star (NGS) performance of MACAO. Long exposure H-band Strehl ratio on-axis.

Figure 8.37 [JPG: 37k]. Numerical simulation of Natural Guide Star performance of MACAO. Long exposure K-band Strehl ratio on-axis.

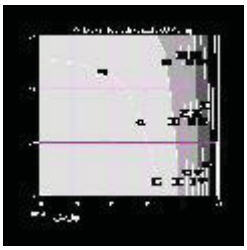

Figure 8.38 [JPG: 18k]. Laser Guide Star (LGS) performance of MACAO. Analytical simulation with a 5W LGS and a tip-tilt NGS. Iso-FWHM curves in the K-band are labelled in arcsec. The X- and Y-axes indicate the tip-tilt NGS V-magnitude and elongation in arcsec, respectively.

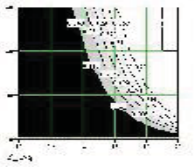

Figure 8.39 [JPG: 30k]. Mean sky coverage in terms of the probability to find a NGS of a given V-magnitude (X-axis) and at a given distance in arcsec from the science target (Y-axis).

8.7 Laser Guide Star

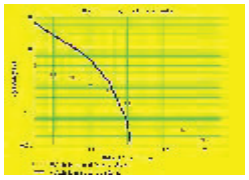

Figure 8.40 [JPG: 28k]. This plot shows the probability to obtain a given K-band Strehl Ratio for the average sky density, using Laser and Natural Guide Stars. It corresponds to a system that corrects 100 Karhunen-Loewe atmospheric modes, under average Paranal atmospheric conditions.

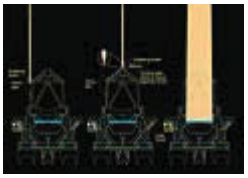

Figure 8.41 [JPG: 52k]. The three different laser propagation methods that are being explored; the baseline solution is the one in the middle.

Although the VLT **Laser Guide Star Facility (LGSF)** , technically speaking, forms part of the UT1, it is described here, because of its close interaction with the AO instruments.

Several simulations (Fig. 8.40) have shown that the use of an artificial source as reference star for Adaptive Optics (AO) will greatly increase the scientific return of the high spatial resolution instruments using AO. In particular, extragalactic studies of objects that are mostly out of the galactic plane will benefit from this.

The Laser Guide Star (LGS) is an artificial source for the AO servo loop reference. For this will be used a 4W CW Sodium Laser (589 nm), which is focussed at 90 km altitude in the mesosphere via a dedicated 50 cm diameter launch telescope. An atomic sodium layer is present at that height, which backscatters the spot image and produces a m V = 10 artificial star to guide the AO servo-loop.

It is proposed to equip UT1, i.e. UT with AO instruments, with a Laser Guide Star Facility (LGSF), with a high-power laser and dedicated Hard- and Software. This facility is considered as a telescope facility by the instruments and by the AO systems. The LGSF has the tasks to maintain a steady, projected laser beam quality, to point the artificial star, to correct the upgoing atmospherically induced jitter, and to enforce the appropriate safety measures. Three laser propagation methods are being explored, cf. Fig. 8.41. The baseline solution is to input the light from the back of the secondary mirror.

It is proposed to **host the laser in a dedicated room** , under the Nasmyth platform. 10 KW of plug power and power dissipation are necessary, as well as good mechanical stability and vibrational isolation. The beam is then propagated to the launch telescope via a set of relay mirrors, or preferably via a single mode fibre carrying high laser power. Experiments with the MPI-ALFA system at Calar Alto (Spain) are progressing, to validate the latter solution.

ESO is studying innovative technologies for the LGSF in collaboration with the MPI-E in Garching and industry. This work has high technological content. Two crucial areas are explored: innovative, high-efficiency lasers, and high laser power fibre propagation. The experience already available in the ESO member countries is fully exploited to build a state-of-the-art LGSF for the VLT.

The work on the LGSF has been approved and is now in the feasibility study phase, until November 1998. According to the proposed planning, the Preliminary Design Review and Final Design Review will be done in 1999. It is expected that the LGSF will be commissioned on the UT1 towards the end of 2001. The AO systems on that telescope, NAOS and MACAO, and the sofisticated instruments attached to them, will then be ready to make full use of it.

8.8 Visitor Focus

A **Visitor Focus** is being reserved at one of the Nasmyth foci of UT3.

The main purpose is to permit **innovative observations** by small teams' stand-alone instruments, not burdened by the requirements for fully automated VLT general use instruments. In addition, this will provide a powerful scientific/technical test bench for new instrumental concepts, eventually to be incorporated later in standard VLT instruments.

A set of **guidelines** will be produced in late 1998 on how to propose and carry out this type of observation. It will in particular encompass a formal request to the OPC and, when warranted, a prior technical feasibility check at one VLT Nasmyth fully functional mock-up (like the one at ESO-Garching

VLT Whitebook Chapter 9: 9. Interferometry

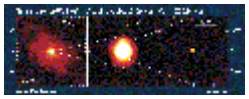

Figure 9.1 [GIF: 136k]. Simulated 2.2 μm images of an active galaxy at a distance of 5 Mpc, when observed at three different spatial resolutions. Left: 0.5 arcsec resolution (adapted from a SHARP/NTT image of NGC 1068). Middle: 0.06 arcsec resolution (adaptive optics on a UT). Right: 0.003 arcsec resolution (VLTI). The galaxy is assumed to contain a point-like AGN surrounded by a star cluster, cf. Chapter 9.2.8. From Genzel et al. (1995).

It has always been ESO's aim to operate the VLT in an interferometric mode (the Very Large Telescope Interferometer - VLTI) which allows the coherent combination of stellar light beams collected by the four 8-m Unit Telescopes (UTs) and by several smaller Auxiliary Telescopes (ATs).

A revised VLTI implementation plan was approved by the ESO Council in 1996 to provide the **VLT interferometric array** , consisting of two UTs and two ATs by the year 2002 and, if financially feasible, integration of the full array of three ATs and four UTs by 2006.

The desirability of carrying out the full VLTI programme as originally envisaged at the earliest possible moment remains, however, especially in view of the of **VLTI's exceptional capabilities** and resulting potential for new and exciting discoveries. In recent years, interferometric projects have begun to play a central role in ground-based high-resolution astronomy, and numerous instruments have been completed or are in the process of construction. The impending presence of these new instruments represents an important incentive both for clarifying the scientific cases for various VLTI implementation phases and for ensuring VLTI's competitiveness in the international context over the next 10-20 years.

In order to study these issues and to establish a clear set of guiding principles for the development of the VLTI, an **Interferometry Science Advisory Committee (ISAC)** was established in April 1995. This Committee has reviewed the scientific rationale and the corresponding technical requirements of the VLTI.

The following overview of the VLTI is based on the conclusions of the Committee and the resulting implementation plan.

9.1 Concepts and Implementation Plan

Based on the scientific goals (cf. Chapter 9.2), ISAC has identified a set of **top level technical requirements** which are feasible within the current project framework:

- There shall be a phased approach to the implementation of the VLTI. The first phase shall include the 8.2-m Unit Telescopes (UTs) from the start, and shall focus on spectral regimes where telescopes can perform near the diffraction limit with a minimum of adaptive control. The capability, within the budget, to open the spectral ranges towards shorter wavelengths for all telescopes, in particular to the near-infrared regime with UTs using higher order adaptive optics systems, shall be investigated.
- The VLTI shall acquire first fringes around the turn of the century in order to ensure competitiveness with other interferometry programmes.
- Auxiliary Telescopes (ATs) should have a diameter of the order of 1.8-m as a compromise between cost and sensitivity.
- A field of view (FOV) for the science target of 2 arcsec ("primary beam") is sufficient. In order to enable phase referencing as well as narrow-angle astrometry, the capability to do interferometry at a second field position ("secondary beam") within 1 arcmin radius from the science beam shall be included.
- The VLTI shall have the capability to simultaneously combine four telescopes, including at least two 8.2-m UTs and up to three ATs.
- Beam combination instruments shall operate in "single mode" (fringe detection on fields of the size of the Airy disk) in the red, near-infrared, and in the mid-infrared.
- The VLTI shall have narrow-angle astrometric capability with a precision comparable to the atmospheric limit.
-

9.1.1 VLTI Development

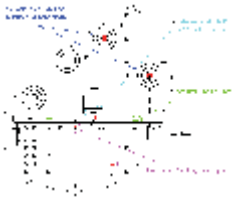

Figure 9.2 [GIF: 16k]. General layout of the VLTI and its major components for Phase A (for Phase B in parentheses).

The present budget limitations require an **implementation of the VLTI in two phases (A and B)** . The first and most expensive Phase A is covered by ESO's financial projections. Since ATs make up a large part of the cost, it has been decided to build two of them in Phase A and to defer the third to Phase B. Because of the long lead times for the ATs, fringes will be observed first with UTs. To be able to exercise and test the interferometry subsystems with little impact on other programmes at the higly demanded UTs, it is the intention to use simple siderostats at the AT stations observing bright stars until the ATs become available.

The **Array Configuration** is discussed in Chapter 2.4. The array consisting of solely the UTs is referred to as the **VLT Interferometer Main Array (VIMA)** . The interferometric array consisting solely of the ATs is called the **VLT Interferometer Sub-Array (VISA)** .

At the completion of Phase A, the VLTI will consist of the following subsystems:

1. Coudé optical trains on two UTs;
2. Two delay lines;
3. Two test siderostats, to be replaced by the ATs;
4. Two ATs, relocatable between 30 stations, cf. Fig. 9.2;
5. Control system; and
6. Beam combination instruments.

The following subsystems will be added during Phase B:

1. Third AT;
2. Optical trains on remaining UTs; and
3. Two additional delay lines.

Phase A is underway and is expected to last until the end of 2002 when regular science observations will begin. "First fringes" by the coherent combination of two UTs will be observed early 2000, if the Phase A coudé trains are installed on UT1 and UT2, the delay lines are in place, and the first instrument is completed. First fringes with ATs are expected in early 2002 after installation of AT1 and AT2.

The kick-off of Phase B, which represents about 25% of the total cost, depends on the availability of additional funds. If started mid-2000, interferometry with all four UTs and three ATs may begin in 2003.

9.1.2 Implications

In what follows some consequences of this concept, especially in terms of limitations on wavelength coverage and FOV, are discussed.

9.1.2.1 Wavelength Range

Figure 9.3 [GIF: 8k - 9k]. Resolution of an 8-m UT (left) and a 1.8-m telescope (right) at the seeing characteristics of Paranal. Median seeing refers to r 0,550 = 15.6 cm, best 10% of seeing to r 0,550 = 22.4 cm, and worst 10% seeing to r 0,550 = 9.8 cm.

ISAC recommended to focus for the earliest operational phases on the **near and thermal IR spectral** regions where Unit and Auxiliary Telescopes would be diffraction limited with tip-tilt compensation. Fig. 9.3 shows the resolution attained by 8-m UTs and 1.8-m ATs on Paranal without and with fast tip-tilt only compensation.

An 8-m UT achieves the best resolution for wavelengths above 5 μm under median seeing conditions without any compensation, and is close to the diffraction limit for these wavelengths when image motion is controlled. A 1.8-m AT operates at the diffraction limit for wavelengths above 2 μm. Thus **operation without higher-order adaptive optics** will be optimum in the thermal IR (5 μm and longer) with the UTs and in the near-IR (1 - 2.4 μm) with the ATs.

Without adaptive optics beyond tip-tilt compensation, the UTs would not be significantly more sensitive in the near-IR than the ATs. ESO therefore currently pursues the development of low-cost adaptive optics systems specifically tailored for interferometry with the UTs in the near infrared.

Diffraction within the collimated beams inside the delay line tunnel limits the suitability of the ATs for use in the N and Q bands. The implications of doing interferometry with UTs in the thermal IR need further detailed investigations considering that beam combination occurs after more than 20 reflections at room temperature. However, fringes appear at precisely known frequencies and their position can be modulated in time by small variations of optical delay. This should substantially facilitate their detection against the sky background.

9.1.2.2 Field of View

The **reduction of the available FOV to 2 arcsec** makes a substantial reduction of the optics in the delay lines possible. The beam diameter which the delay line primary optics must accommodate is now at most 15 cm. The dimensions of the cat's eye primary mirror is reduced from a size of about 1 m to 60 cm. Another consequence of the field reduction is that severe requirements on the lateral stability of the delay line carriage motion can be relaxed substantially, making simpler drive concepts viable.

A reconstructed image of an object with the VLTI is most likely limited by **incomplete UV coverage** , in particular when the number of baselines is initially small. The imaging beamcombiner in the laboratory which was originally conceived for a co-phased FOV of 8 arcsec will therefore not be part of the early VLTI. Phase referencing, for which the field is larger than 8 arcsec, is better implemented with a dual feed (see below). Beam combination will occur in the first phases within the instruments.

9.1.2.3 Dual Feed

The desire for including **narrow-angle astrometric capability** into the VLTI has lead to a decision to replace the original 8 arcsec continuous field with dual feeds. These allow selecting two positions at the coudé focus to be directed towards the delay lines and the laboratory. One beam will propagate the light from the science target, the other one will propagate the beam of a near-by phase reference (UTs and ATs) or an astrometric reference (ATs only). The concept behind the phase reference is similar to a reference star for adaptive optics; it serves for image and fringe tracking if the science target is too faint. There are limits to the field angle which come from atmospheric anisoplanatism.

The coudé foci of both UTs and ATs will be equipped with dual feeds. One position will be on the optical axis. The other position will be within a range of 5 - 60 arcsec from the axis anywhere within the coudé foci. The **two beam lines** will share the delay lines for any given telescope, making differential delay lines necessary. Although designs for dual feeds exist elsewhere, they are not easily adapted to VLTI because the requirement on spectral coverage and astrometric precision essentially exclude transmissive optics.

The requirements and engineering implications of narrow-angle astrometry are very severe and need thorough studies. The atmospheric limits to astrometric precision depend linearly on field angle and amount to about 10 μarcsec with a 100 m baseline and 30 min of integration. Achieving this precision in practice requires knowledge of the instrumental differential delay between the primary and secondary beam to 5 nm accuracy.

9.2 Scientific Goals

The ambitious scope of VLTI remains unchanged, despite the limitations imposed by current financial constraints. The great complexity of this unique facility implies that it is difficult to specify fully its astrophysical repercussions in advance of operation. However, the **primary scientific issues** that it seeks to address are quite well defined.

In what follows, short summaries are given of some of these research goals, as identified by the Interferometry Science Advisory Committee (ISAC). This list impressively illustrates the great width of science programmes that will become possible with the VLTI. It is at this moment obviously neither frozen nor complete, and it will be further developed after community reflection and comment.

9.2.1 Extrasolar Planets

Searches for extrasolar planets have gained importance, both in the professional arena and in the public perception of astronomy. The recent detections of several Jupiter-mass planets has generated much interest, and it is widely believed that more giant gaseous planets around solar-type stars can be found by **precise radial-velocity and astrometric surveys** . Both of these methods are indirect, in that they measure the motion of the star around the barycenter of the star-planet system. While radial velocity searches may soon become a very efficient method to detect exoplanets, they cannot determine separately the planetary mass and its orbital inclination. In contrast, astrometric observations give the mass directly. In planetary systems which are viewed ``pole-on'' astrometry provides the only way to detect reflex motion.

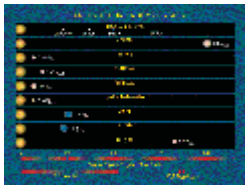

Figure 9.4 [GIF: 48k]. Schematic representation of the known exoplanets and their distances from the central star. The corresponding linear resolutions of one VLT UT and the VLTI are indicated.

The VLTI may become an extremely powerful instrument for **precise narrow-angle astrometry** . For instance, the atmospheric limit for determining the separation vector between two stars which are 10 arcsec apart is about 10 μarcsec for a 30 min integration. This is a challenging but solvable task that requires monitoring the baseline vector inside the interferometer with superior precision and measuring the differential delay between the two stars at the ~ 0.005 μm level. The implementation of an astrometric mode in VLTI with these capabilities would allow the detection of Sun-Jupiter systems out to a distance of 1 kpc and smaller planets (10 Earth masses) around the closest stars.

A possible strategy for a VLTI astrometry program would be to observe about **200 target stars in near infrared with VISA** . They must be bright enough for fringe tracking (K < 12), which will allow the astrometric reference sources to be relatively faint (K < 17) and ensure that phasing references can be found for almost any object of interest. The integration time would be half an hour per star per night. With thirty observations of each target star over ten years, this would require a total commitment of 300 nights on VISA over a decade. The data for each star would be used to solve for relative parallax and proper motion, with any residuals indicating the presence of planets. Motion ambiguities would be resolved by the use of two or three different astrometric reference stars for each target.

9.2.2 Low Mass Stars and Brown Dwarfs

90% of all stars in the Galaxy are less massive than the Sun. Still, the properties of stars with low or very low masses are much less known than those of the more massive ones. Establishing an **observational mass-luminosity relationship** for stars with very small masses is a very active field of research, but current observations are not able to significantly constrain the lower end of the mass spectrum produced by the star formation process.

Sub-stellar objects - **Brown Dwarfs** - are even less well understood. After a long and eventful search, the question of their existence has recently been settled unambiguously by some clear detections. This has opened a new field of study of these interesting objects which will allow theory to be related to observations. However, this relation is rather indirect, because the classical observables of a brown dwarf (broad-band photometry and spectrum) are determined by its very thin atmosphere, while its physical status depends mostly on the age and mass.

Progress in understanding low-mass stars and brown dwarfs thus requires a method for determining masses. A first step is to perform radial velocity surveys of large samples of low-mass stars in search of spectroscopic binaries. However, while these surveys provide fundamental statistical results, they can only yield masses for each component when combined with direct imaging measurements. The combination of high precision (about 15 m/s) radial velocity data with Hipparcos parallaxes and **accurate angular separations from VISA** will allow the determination of masses of very low mass stars to precisions at the percent level. Even the mass of a suspected 0.03 solar mass brown dwarf companion could be estimated with ~ 5% accuracy, firmly establishing its sub-stellar nature and allow to test evolution scenarios for such objects.

9.2.3 Star Formation and Early Stellar Evolution

Young stellar objects (YSOs) exhibit a large variety of different phenomena, such as infrared excesses, luminosity variations and highly collimated jets with velocities of several hundred km/s. These phenomena suggest the presence of a circumstellar accretion disk and strong magnetic fields. Understanding the inner regions of YSOs is an important area of current research and is related to the question of the formation of the solar system. The similarity of some YSOs to AGNs, in particular the classical T Tauri stars, implies that progress in understanding the physics of star formation may have important implications for extragalactic astronomy as well.

A major program for the VLTI is the systematical study of the **rich circumstellar environments of YSOs** at a resolution of about 2 milliarsec, corresponding to 0.3 AU (20 - 30 solar radii) for the nearest star-forming regions at a distance of 150 pc. The angular resolution of the VLTI will give access to the phenomena in the inner regions around YSOs and will provide important input to the theoretical models. Although the VLTI will still not be able to resolve the innermost parts of the accretion disk - where material is presumably funnelled via magnetic fields onto the stellar surface and where other parts of the rotating magnetosphere accelerate and collimate the outflowing matter - observations just outside these regions should allow meaningful extrapolations.

The key capabilities of VLTI in this field are its **high angular resolution, sensitivity and infrared response** . Important parameters to be determined include the morphology of circumstellar disks, the temperature distribution, the relative contributions from scattered stellar light and thermal disk emission, the disk chemical composition and the properties of dust grains. The question of how YSO jets are accelerated and collimated may also be addressed as well as possible connections between variations of the central star and the formation of new knots in the jets. For instance, in a jet moving at 300 km/s, a new knot resulting from an outburst would be detectable after a few days, allowing its proper motion to be accurately measured (similar to VLBI observations of QSO jets).

Another possible programme is the measurement of **orbits of very close binaries** . High angular resolution is needed to produce accurate masses for lunar-occultation and spectroscopic binaries within a reasonable time: an orbit of 4 AU will be completed in 8 years. Masses from such orbits will finally provide urgently needed empirical checks on the evolutionary tracks used in interpreting the observations of young stars.

9.2.4 Stellar Surface Structures

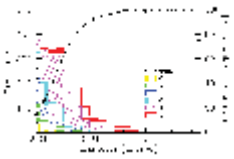

Figure 9.5 [GIF: 13k]. Histogram of CADARS (Catalogue of Apparent Diameters and Absolute Radii of Stars; Fracassini et al., 1988) stars with apparent diameters above 1 mas and declinations south of +40 o. The solid line represents the cumulative frequency.

A recent survey indicates that about 2000 stars with declinations less than +40 o have apparent diameters of one milliarcsec and more and therefore are resolved to VLTI baselines in the NIR (Fig. 9.5). Most of these are late type giants. Half of them have apparent diameters of 2.5 milliarcsec or more and will permit **detailed studies of their surfaces** with the superior imaging capability of VLTI. This will make possible the study of physical characteristics of surface phenomena and their variation with time.

Important surface phenomena are due to hydrodynamic and magneto-hydrodynamic effects and result in large scale convection cells in the outer convection zones and concentrations of magnetic fields. The study of **convection** through surface temperature and line-of-sight velocity variations provides clues to the fundamental properties of the convection zone. The temporal variation of active regions gives insight into the underlying dynamo processes which generate **magnetic fields** in stars.

The detection of surface features on cool giants and supergiants using large single telescopes has been one of the most important successes of interferometric imaging - the best studied example is **Betelgeuse** , the disk of which displays a small number of **bright, unresolved features** . The relationship, if any, between these features and the well documented mass loss and variability of Betelgeuse is at present unclear. These appear as bright ``hotspots'' of emission and are probably the result of large-scale convective upwellings of material from hotter regions of the stellar interior.

The observed number, evolution timescale and brightness are all consistent with such an hypothesis, but their detection has raised a number of further questions that will likely be amenable to large interferometers like the VLTI. Possible **science goals** for such observations are frequency of occurrence, evolutionary timescale, multiplicity, location and mass loss.

Other problems that may be addressed by the VLTI include **accurate angular diameter measurements** , which lead to effective temperature, and studies of the **atmospheric structure** , best addressed by a combination of programmes: (i) detailed studies of selected sources; (ii) monitoring of selected sources every month; and (iii) a survey of the local neighbourhood.

9.2.5 Be Stars

Be stars show H-emission that is strongly variable and usually double-peaked. They are also known to be rapid rotators, which led Struve in 1931 to suggest that the emission arises in a **circumstellar disk of ejected matter** . This model has not been universally accepted, but optical interferometry has now confirmed that Be star envelopes are indeed flattened.

Ad-hoc models based on a disk geometry have been successful in describing the **winds** of Be stars. The currently assumed mechanism for **disk formation** involves Coriolis forces in the radiation-driven wind of a rapidly rotating star that force the flow of gas towards the equatorial plane and create a very thin, dense disk, but many questions still remain unsolved. In particular, this model significantly underestimates the actual amount of matter in the disk and it predicts a disk opening angle which is much smaller than that derived from the statistics of shell stars. Also, the important **variable character of Be stars** (short-, middle- and long-term) is not understood. Indeed, different mechanisms could reproduce the classical measurements.

The analysis of the interferometic data through the different variation cycles will greatly facilitate the determination of the correct processes. The VLTI at optical and infrared wavelengths is very well suited to **resolving the disk structure of Be stars and monitoring time variability** . There are more than 100 Be stars brighter than 6th magnitude and they have already been well studied by classical techniques (spectroscopy, photometry, polarimetry). Interferometry brings new constraints on the **size and morphology of the disk** (including velocity and density fields), on the **central star** itself (radius, ellipticity, surface activity and limb-darkening) and on the effects of a **binary companion** .

Be stars are excellent targets for long-baseline interferometers, due to the simultaneous presence of a point-like continuum source (the central star) and a resolved structure (the emitting envelope). The program demands a good spectral resolution (R = 10,000 in the visible and R = 100-1000 in the Near-IR). Moderate (u , v) coverage is sufficient because the geometry is simple, and strong constraints can be placed on the physical processes involved in the Be phenomenon. The large apertures of the VLTI will allow to achieve high spectral resolution maps in a few nights.

9.2.6 AGB stars

All stars with initial masses less than 8 solar masses end their lives on the **Asymptotic Giant Branch** . An AGB star has a degenerate C/O core surrounded by a very extended convective atmosphere from which mass is lost via a dense and dusty outflow at rates of 10 -8 to 10 -4 solar masses per year with expansion velocities of 5 - 30 km/s.

The **mass-loss mechanism** in AGB stars is poorly understood. It is believed to be related to the slow pulsations and the formation of dust, which is subsequently pushed out by radiation pressure. Improving our understanding of the physical mechanisms that drive this process is important because mass loss dominates AGB evolution and also because AGB stars play an important role in the chemical evolution of galaxies by returning gas and dust to the ISM.

Main questions to be addressed are: (i) Where does the dust form in the extended atmosphere? (ii) What is the role of the pulsations in the mass loss process? (iii) Which molecules are depleted in the dust formation region? (iv) How does dust formation depend on the phase of the pulsation and on the chemical composition of the star?

The mid-infrared region is ideal for studying **dust formation** near AGB stars and the accompanying depletion of atoms and molecules. Pilot observations at 10 μm and baselines up to 13 metres, have allowed a detailed study of the inner radii for some of the brightest late-type stars. The VLTI is uniquely suited to extending this work to fainter and more distant objects and with higher spectral resolution. For example, the location and properties of the silicate dust can be studied by measuring the change in size of the object as a function of wavelength through the silicate features at 9.7 and 18 μm. The layers above the photosphere in which dust forms may extend to about 10 stellar radii, i.e. several tens of milliarcsec at distances of 500 - 1000 pc and thus easily accessible to VLTI. Direct imaging of the stellar disk will also be possible, so limb darkening and **distortions from sphericity** can be measured. If an AGB star is imaged throughout a pulsation cycle and if simultaneous radial velocity data are taken, its **distance** can be directly measured.

Many post-AGB candidates were discovered in the IRAS point source catalogue to show warm dust (500 K) and turn out to be **binaries** , e.g., the ``Red Rectangle''. It appears that mass loss on the AGB can be affected by the presence of an unseen companion, with mass being stored in a circum-binary disk. It is currently unclear whether these disks are stable and how they affect the further evolution of the object and the formation of a planetary nebula. The **sizes of the disks** should be from a few to several tens of AU, which means they can be resolved by the VLTI at distances up to 500 pc.

9.2.7 The Galactic Centre

The **central 0.1 pc** of the Galaxy will be an important target for VLTI at wavelengths from 2 to 10 µm. The resolution of the VLTI at 2 µm is about 2 milliarcsec, which at the Galactic Centre corresponds to 15 AU or about 1500 times the Schwarzschild radius of a 10 6 solar mass black hole.

The primary goal will be to look for the presence of a **central massive black hole** by measuring the three-dimensional velocity field of the star cluster centered on IRS16. The current astrometric program at the NTT will be continued with higher precision and radial velocities may be determined at very small distances from the center of the star cluster, where observations with single telescopes are limited by field crowding.

Another very important goal for the VLTI will be detailed observations of the **infrared sources** close to the position of SgrA*. It is presently unclear whether any of the objects found at 2.2 µm the true counterpart of the compact radio source. The study of a potential IR counterpart of SgrA* would give completely new insights into the vicinity of the central object of our Galaxy, and could perhaps give us a direct view of the putative accretion disk.

In addition, the high angular resolution of the VLTI will permit to obtain infrared spectra of individual stars in this very crowded region. It will thus be possible to make a census of the **stellar population** in this area, to check whether there is ongoing star formation in the vicinity of the Galactic Centre, and to search for ``peculiar'' stars, which may be the remnants of stellar collisions. Observations at 10 µm would also reveal the distribution of warm dust associated with SgrA*.

Observing the Galactic Centre is quite a challenging task for the VLTI because of the **high density of sources** . Hybrid configurations formed by combining the UTs with the ATs will give good coverage of the (u , v) plane, in particular when the technique of multi-frequency synthesis is employed.

The **focal plane instruments** needed for observations of the Galactic Centre are (i) an instrument for the mid-infrared with spectral resolution R ~ 200, and (ii) a near-infrared instrument with R ~ 2000. For the investigation of SgrA*, polarimetric capabilities would be very valuable. See also Chapter 9.7.

9.2.8 Active Galactic Nuclei (AGNs)

AGNs are thought to be powered by **accretion onto a massive black hole** . For reasons that are not understood, but are probably related to the way galaxies form, there are many more AGN at high redshifts than locally, e.g., the space density of high-luminosity AGNs at z ~ 2 is 100 - 1000 times greater than at the present epoch.

Although our understanding of the AGN phenomenon has increased dramatically, major fundamental issues remain unsettled. These include the precise mechanisms involved in feeding the central black hole, the relationship between AGN activity and ultraluminous starbursts, and the reason why some AGNs in elliptical galaxies are radio loud (but not those in spirals). The relationship between members of the AGN zoo, ranging from the brightest quasars to barely-active Seyfert galaxies, is not understood.

Infrared imaging of the central regions is clearly important in order to understand the underlying phenomena. Dust near the nucleus will be heated by the UV flux from the central engine and there is good evidence that most, if not all, the infrared emission from AGN comes from heated dust. The size of the emitting region is quite small, about 5 pc or 0.16 arcsec in NGC 4151 at 10 μm.

Figure 9.6 [GIF: 7k]. Angular extension as a function of redshift for regions with linear sizes of 1 pc (open squares), 10 pc (open triangles), 100 pc (filled squares) and 1 kpc (open circles). The calculations assumed H 0 = 75 km/s/Mpc and q o = 0.5. The difference in look-back time between adjacent symbols is constant and equal to about 0.5 Gyr.

About 20 - 30 nearby Seyfert galaxies are bright enough to be used as references for fringe tracking. For these, the **central parsec** can be probed in the optical and infrared. It is also useful to probe larger scales in more distant objects, to trace any cosmological evolution. Fig. 9.1 shows simulated images of a typical AGN observed at different angular resolutions and Fig. 9.6 shows how the angular sizes of the relevant regions scale with redshift.

The overall impact of VLTI in extra-galactic astronomy will depend on the **sky coverage** . If fringe tracking cannot be done on the object itself, a nearby reference star can be used. It is thus important to search for new objects (radio selected or by-products of planned surveys) located near bright stars. The situation will improve when the Laser Guide Star (cf. Chapter 8.6) becomes available.

9.3 UT Coudé Trains

The early use of 8.2-m UTs with VLTI requires coudé optical trains, cf. Chapter 3.8. Since the use of UTs from the H-band towards longer wavelengths is emphasised, a simpler and cheaper optical design has been introduced in a change from the original concept. It is based on the replacement of large off-axis elliptical mirrors by spherical mirrors. The astigmatism and field scale anisotropy resulting from this change are compensated on-axis by replacing two flats with weak cylindrical mirrors. Fig. 9.7 shows the on-axis Strehl ratio as a function of wavelength. The main contributing aberration is astigmatism.

Figure 9.7 [JPG: 6k]. On-axis Strehl ratio as a function of wavelength for the new UT coudé trains.

The on-axis performance of the modified coudé optics is very satisfactory over a large spectral regime, including the visible, when atmospheric distortions are taken into account. The Strehl ratio degrades with increasing field angle but the resulting fringe contrast loss will always be small compared to the loss due to atmospheric piston anisoplanatism.

Two out of the four UTs will be equipped with coudé trains during the first phase. The decision which telescopes to equip will be influenced by scientific, schedule, and technical considerations.

9.4 Auxiliary Telescopes and Stations

The conceptual design of the **Auxiliary Telescope System (ATS)** features 1.8-m telescopes in alt-az mount with mechanical bearings. The axes are controlled through optical encoders and friction coupled or direct drives. The optical layout is similar to that of the VLT UTs. It includes a coudé train with an intermediate pupil image to enable fast tip-tilt compensation (and possibly later adaptive optics).

The **coudé beam** is collimated and sent horizontally to the Delay Line Tunnel through underground light ducts. The ATs are self-protected against wind and adverse weather conditions by built-in wind shield protective cover.

The ATs are movable on a rail network and can be located on any of the 30 observing stations through a kinematic interface. Each telescope is equipped with a transporter which handles the telescope for the relocation and houses a number of auxiliary equipment. During observation, the transporter is anchored on separate foundations isolated from the ground to avoid transmission of vibrations from the wind shield and auxiliary equipment.

ESO will contract to industry the final design, manufacturing and testing of the ATs, including optics, mechanics and control for the telescope and its transporter. Integration and testing of the ATs at the observatory will be performed by ESO staff.

9.5 Delay Lines

The Delay Lines equalise **optical path length differences (OPD)** and **transfer a pupil at a fixed location inside the interferometry laboratory** .

The optical path length differences are caused by the geometric path length difference between telescopes (in any given configuration), due to the diurnal motion of the astronomical source during observation (sidereal motion), and the rapid fluctuations due to atmospheric disturbances and/or mechanical vibrations.

To perform the compensation of the OPD, the delay lines include an **optical retroreflector (Cat's Eye)** which moves during observation. The range required for OPD equalisation is 120 m which implies a mechanical stroke of up to 60 m for each delay line. This motion must be very accurate and smooth in order not to distort the interference fringe pattern formed at the interferometry focus. The longitudinal position of the Cat's Eye must be continuously monitored and controlled by a fast metrology system; high dynamic stability and adequate drives and bearings are required to avoid vibrations.

The second purpose of the delay lines is to image the pupil of the telescope at a fixed position inside the interferometry laboratory for beam management. A **mirror with a variable curvature** is used at the focus of the Cat's Eye. This mirror has been developed especially for this purpose by the *Laboratoire d'Optique de l'Observatoire de Marseille* .

Figure 9.8 [JPG: 112k]. Schematic representation of the VLTI Delay Line, showing the retro-reflector on its moving base.

Fig. 9.8 shows a design concept which has been established by ESO to study the technical feasibility within the interface, environment, and operational constraints.

A contract for the VLTI Delay Lines was let with *Fokker Space* (The Netherlands) in early 1998. According to the present design, the rapid path length variations are corrected by the **fine positioning loop** where a Piezo actuator mounted on the backside of the VCM (Variable Curvature Mirror - M3) is used to correct the fast OPD variations as measured by the Fringe Sensing Unit (FSU). The latter provides a signal to the Delay Line system via a fast link to the Delay Line Local Control Unit. An optical datalink to the Cat's Eye on the carriage ensures the transfer of data to the Piezo controller.

The carriage is driven by a **Linear Induction Motor** . The coils for the motor are mounted on the floor and the magnets are mounted on the bottom of the carriage. A Metrology System consisting of a laser-interferometer. Main characteristics include:

- **OPD range:** > 120 meters;
- **OPD resolution:** < 20 nm;
- **OPD stability:** < 14 nm over any 0.01 sec (Visible); < 50 nm over any 0.05 sec (Near-IR); < 225 nm over any 0.3 sec (Thermal IR);
- **Absolute position repeatability:** 50 μm (over total stroke length) and 1 μm (over 3 metres of observation stroke length)
- **Maximum velocity:** 0.5 m/sec;
- **Velocity accuracy:** 1 μm/sec; and
- **Minimum observation time:** > 600 sec.

As for the ATs, integration and testing of the delay lines at the observatory will be performed by ESO staff.

9.6 Beam Combination and Fringe Detection

The **Beam Combination Laboratory Area** provides the following functions during Phases A and B: beam alignment (image and pupil position alignment), calibration, fringe tracking, beam combination and fringe detection.

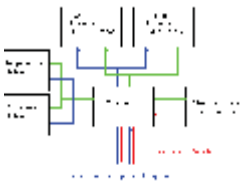

Figure 9.9 [GIF: 128k]. General interferometry laboratory layout.

Fig. 9.9 shows an overview of the layout for Phase A. Stellar light beams enter the laboratory from below. A switchyard which consists of dichroic and reflective mirrors direct the light towards the instruments and to the image and pupil alignment and fringe sensor systems. A calibration unit which provides a number of sources in the visible and infra-red feeds the alignment units and the beamcombiner/fringe detector instruments and assures their intercalibration. Wide-band visible and laser light will be available for this purpose, as well as for the alignment of the beam combination/fringe detection instruments. Laser metrology beams feed the fringe tracking sensor for internal calibration. Another metrology beam travels back to the telescopes and determines the delay line zero position for the internal path during a set-up phase.

A prototype of the fringe sensor is under development at the *Observatoire de Côte d'Azur* (Nice, France). It uses a long stroke synchronous demodulation technique to detect both the presence and the position of stellar fringes in the H band. The error signal is fed back to the delay line control system to provide real time fringe stabilization.

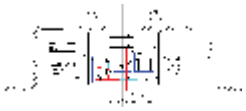

Figure 9.10 [GIF: 11k]. Preliminary configuration of the Interferometric Laboratory.

Fig. 9.10 shows the central part of the tunnel and the laboratory. Primary and secondary beams emerging from the delay line cat's eyes are directed towards the laboratory in the upper half. The switchyard is near the centre of the layout. Instruments are on the top and right. Fringe and image sensors are to the left. The structure to the lower right is the metrology beam launching system.

ESO's partners to the agreement on the enhancement of the VLTI, the CNRS (France) and the MPG (Germany), will contribute to the beam combination and fringe sensing instruments in the form of equipment and manpower.

9.7 VLTI Instruments

The focus of the VLTI will be equipped with three instruments:

- **AMBER** (**A** stronomical **M** ultiple **BE** am **R** ecombiner): The near-infrared/red VLTI imaging and spectroscopic instrument using phase closure and operating first in the near infrared, then down to H-alpha;
- **MIDI** : The **MID** - **I** nfrared instrument operating at 10 μm; and
- **PRIMA** : The **I** nstrument for **P** hase- **R** eferenced **I** maging and **M** icroarcsecond **A** strometry.

In what follows, details are given about these instruments, as they have now been defined or envisaged.

9.7.1 AMBER

The **A** stronomical **M** ultiple **BE** am **R** ecombiner (**AMBER**) instrument is in the study phase. Two working groups have worked on the concept for the imaging and spectroscopic instrument. This instrument complies with the ISAC recommendations and the revised ESO implementation plan.

The identified **primary science objectives** are:

- study of the inner 1 pc of active galactic nuclei;
- direct detection of massive extrasolar planets;
- study of the circumstellar environment in star forming regions; and
- multiple objects, fundamental stellar astrophysics.

The **main characteristics** of this instrument are:

- design of a 3-way beam combiner;
- spatial filtering and accurate visibility calibration;
- high optical throughput thanks to adaptive optics;
- early operation with 2 UTs in 2000 in the near-infrared (1 - 2.5 μm);
- spectral resolution up to 10,000; and
- spectral extension toward the red when ATs will be available (0.6 - 2.5 μm).

9.7.1.1. Instrument modes

Three instrument modes have been identified:

Imaging Mode (IM) . It will be dedicated to the study of relatively complex spatial structures with a visibility accuracy of about 1%. Recombination of several beams is desirable in order to increase the (u, v) coverage. This mode should also allow us to push the performance of the instrument in sensitivity.

High Precision Visibility Mode (HPVM) . It is foreseen for high dynamic range study of relatively simple objects, like multiple systems or massive hot Jupiters around stars. The goal is to have the most accurate calibration procedure possible.

High Spectral Resolution Mode (HSRM) . This mode is recommended for the study of stellar lines. The spectral resolution is emphasized even if the accuracies in visibilities or the sensitivity performance are not extreme.

9.7.1.2 Extension capabilities

The imaging and spectroscopic instrument should develop in different progressive stages. Even if it offers a 3-way beam combiner, the AMBER instrument will start by combining only two beams. However, it may be desirable to extend the capability of the instrument in the future:

- **Wavelength coverage** . Extension to shorter wavelengths is foreseen when ATs will be operational. Adaptive optics will allow extension downward 0.6 μm with ATs. Extension to longer wavelengths (up to 5 μm) is also possible.
- **4-way beam combiner** . With 2 UTs, 2 ATs, 3 active delay lines and a passive one, one can combine 4 beams. This will increase the number of baselines for which it is possible to measure visibilities simultaneously.
- **Dual feed** . Telescopes will be equipped with dual star feed for the astrometric instrument. Tracking the fringes and correcting the wavefronts on a separate reference star will improve the sensitivity of the instrument.
- **Extended adaptive optics** . The sensitivity of the instrument is driven by the AO correction. Therefore increase of the degree of AO correction is desirable as a long term goal.
- **Coupling with other instruments** . The interface with other instruments is desirable. For example, the imaging instrument can provide fringe sensing in the NIR domain for the 10 μm instrument.

9.7.1.3 VLTI interface

Interfacing with the VLTI can be done in two different ways. The proposed scheme of the VLTI Control Software (VLTICS; cf. Chapter 9.8) shows a general VLTI user interface, which receives high level commands from the VLTI Instrument. Therefore AMBER will behave as the master, requesting services to the VLTI Control Software.

9.7.1.4 Spectrograph

The maximum spectral resolution desired in K is 10,000. The maximum number of lines per mm usable in K is about 500 l/mm and a 40 mm grating is needed for a 10,000 resolution, considering an equivalent width of 2/D for the spatial filter in the dispersion direction. This sets the beam diameter. Combining the dispersion of the grating and the size of the detector pixels 40 μm gives a chamber focal length of 800 mm. To decrease the size of the spectrograph, the chamber contains two off-axis mirrors whose combination has an equivalent focal length of 800 mm. It is then possible to include the spectrograph inside a cryostat with interior diameter 200 mm and length 400 mm.

The resolutions will be 10,000, 2000, 50 and 0. The first two will be obtained with 500 l/mm and 100 l/mm gratings, the third with the prism and the last with a flat mirror.

9.7.1.5 Detector

Because of the many different approaches to fringe detection required by the several observing modes, the control of the detector is best seen as an independent subsystem.

The detector itself will be of the **PICNIC type** , sensitive in the range 1 to 2.5 um, with 256 x 256 pix of 40 μm and RON 20 e -. The main feature of this detector is the ability to perform fast readout of selected rows and columns, which is a necessary requirement when dealing with fast data flows. The peak data rate in the most demanding mode (fast acquisitions of dispersed spectra along several lines of pixels) is estimated to be 0.6-1.0 Mb/s. Such data rates can be effectively dealt with in subarray mode, as has been shown by an application implemented on a NICMOS array and under further development at the Arcetri Observatory.

Due to the high data rate, the **raw data storage** should be implemented in the most direct way, from the detector electronics directly to the disks and tapes that form the acquisition subsystem. Those subsystems that will also need access to the raw data (such as the so-called quick look monitor, the VLTI database, etc.) can do so at lower priority through the LAN.

9.7.1.6 Instrument control

The control of the instrument is a subsystem by itself. The user must be able to control directly some subsystems (such as the FSU, the AO, etc.). Observing procedures are defined as sequences of commands to the different subsystems. Subsystems dialog via on-line database.

The actual data acquisition will represent a critical task for this software, due to the **large volume of data** that may be expected, at least under some observing modes. The data flow from the detector (PICNIC module) to the data storage devices (disks and DATs or equivalent) should be as fast as possible. These devices should be accessible also by a powerful workstation that will enable the user to analyze the data almost in real-time, by running a subset of the actual data reduction package on the data being acquired.

This preliminary reduction is essential, in order to give the user a feeling of the progress of the observation and choose the next moves. A **quick-look programme** should run automatically on a separate WS monitor, where the user can observe the progress of a number of selected quantities (such as for instance seeing, visibility, fringe tracking error, etc.).

9.7.2 MIDI

9.7.2.1 Priorities

MIDI stands for the **MID - I** nfrared instrument operating at 10 µm. The following priorities guide the current development work:

- The main emphasis is on developing an instrument working in the **10 µm window with one baseline, measuring visibilities** . The measuring modes include one aiming at good sensitivity, sacrificing accuracy; one aiming at good accuracy at the expense of reduced sensitivity; and at least one intermediate arrangement;
- A natural enhancement of the capabilities of the instrument would be the extension to the **20 µm range and to higher spectral resolution** ; and
- For a second phase of the instrument development, it is considered necessary to provide **phase measurements** : either by phase closure measurements with at least three input telescope beams or by tying the 10 µm instrument to the external phase-referencing instrument, or by both methods. At this stage also the simultaneous use of four telescopes will be considered. External fringe tracking is highly desired. For all sources with suitable spectrum and geometry it should provide substantial gains in sensitivity.

9.7.2.2 Optical design

In general, the MIDI optical design has to provide the following **functions** :

- to accept beams of 80 mm diameter;
- an image plane on the detector;
- the beam combination not too far from the pupil plane;
- very good suppression of thermal emission from the surroundings in laboratory, delay lines, and telescopes;
- an image sharpness which puts most of the light on one pixel (to reduce readout noise);
- the possibility to introduce monomode fibres for beam cleaning;
- the possibility to extract photometric signals before beam combination;
- light inputs for verifying the interferometric operation of the instrument at 10 μm;
- acceptable complexity and preferable compact design; and
- to allow - in principle - the inclusion of a third and forth beam for phase closure measurements.

The studies performed so far have shown that satisfying solutions can be found, both with reflective and with transmissive optics. The present design in addition keeps the option to use most of the optical train, both for 10 μm and for 20 μm observations, and it therefore mostly uses reflective optics. The pros and contras of making simultaneous 10 μm and 20 μm observations possible are still being discussed. In any case, a dedicated, sensitive 10 μm channel will be available in the instrument.

For **phase closure measurements with three or four beams** , the optics used for beam combination and imaging onto the detector will have to undergo profound changes.

The **main characteristics** of MIDI are indicated in the table.

Table 9.1: MIDI Main Characteristics

Parameter	Specification	Value
Wavelength coverage		10 μm band (8 μm - 13 μm)
	expandable to	20 μm band (17 μm - 26 μm)
Field of view		± 1 arcsec (for object acquisition)
Airy disk (UTs)	at 10 μm	0.26 arcsec (for measuring)
Airy disk (ATs)	at 10 μm	1.14 arcsec (for measuring)
Coherence time	at 10 μm	100 ms (for fringe measurement,
Atmospheric OPD jitter	rms	22 μm
	p-p	66 μm
Differential dispersion	in 100 m of air	0.9 μm (10 μm to 20 μm)
		46 μm (1.6 μm to 10 μm)
Atmospheric	for chopping	200 ms
Input beam diameter	from UTs	80 mm
	from ATs	18 mm
Pixel size	of detector	50 μm
Limiting Magnitude	at 10 μm	5.0 mag (low accuracy mode)
Limiting Magnitude	at 10 μm	1.8 mag (low accuracy mode)

9.7.2.3 Detector

Array Detectors of the needed dimensions of a few hundred pixels are available. Somewhat surprisingly, readout noise is not necessarily negligible, even in the high-background environment of the VLTI in the thermal infrared. This results from the limited well capacity of 10 7 electrons for the available detector chips. It is the intention to acquire the "science grade" detector late in the project in order to profit from expected improvements in well capacity and readout noise. Until then, "engineering type" detectors of lower quality will be used for the development of the instrument.

9.7.2.4 Observing Modes

There will be several methods to determine the **fringe contrast** :

- **"shift and add" mode** : a fringe measurement is possible within the coherence time of 100 ms. In this bright source mode, the instrument could in principle track the fringes by its own;
- **"speckle" mode** : power spectrum averaging over many individual short (100 ms) exposures should recover a range of fringe signals which are too weak to be found in the "shift and add" method; and
- **"blind integration" or "fringe stabilised" mode** : for this faint source mode the fringes have to be stabilised externally (by a fringe tracker or by one of the other instruments), and it has to be assured that the fringes will be stabilised also inside the instrument. Then the individual short exposures can be averaged coherently by stacking the exposures. This is the most sensitive mode of the instrument. Internally in the instrument, if simultaneous 10 μm and 20 μm measurements are possible, then e.g. the 10 um channel could be used to stabilise the fringes for the 20 μm measurement. The atmospheric dispersion is small enough (0.9 um over 100 m of air between 10 μm and 20 μm) to allow simultaneous measurements in these wavelength bands.

9.7.2.5 Measuring Modes

This refers to calibrating the fringe amplitudes in terms of visibilities, and it requires to measure the total flux of the source (as opposed to the correlated flux giving the fringe amplitude). The total flux measurement requires the usual infrared techniques of chopping and nodding with the telescopes. This helps to overcome the difficulties that the mid-infrared detector array flat fields are non-linear, load dependent and variable with time. Three modes are possible:

- **"unfiltered" mode** : the measurement of fringe amplitude is continued for a while (a few minutes), then the next few minutes are used for a determination of the flux of the source. This sequence is repeated as necessary. No spatial filtering is applied to the beams before beam combination. In this mode, fringe recovery is necessary only once every 10 min or so. Visibilities are calculated from the averages on correlated and uncorrelated flux. The resulting accuracy in visibility is estimated to be 5% - 10%;
- **"filtered" mode** : to reduce the phase fluctuations in the beams, a spatial filter is introduced into each beam before beam combination. The fringe signal is measured for one coherence time only. Chopping allows to measure the background flux during the following coherence time, and this sequence is repeated many times. It may be necessary to recover or even find the fringes again after each chopping. In this mode, it is again the combined flux of the two beams which is measured. Visibility is calculated by applying a correction for the varying flux entering through the spatial filters on the basis of this combined flux. The resulting accuracy is estimated to be a few percent; and
- **"filtered and referenced" mode** : similar to the "filtered" mode, but after the spatial filter and before beam combination part of the light in each beam is extracted for separate photometry. The visibility measurements then are corrected for the varying flux through the spatial filters on the basis of the individual flux measurements per beam. This allows to evaluate the geometrical mean of the individual fluxes, which is needed for the true correction. The resulting accuracy in visibility is estimated to be 1%. (At 2 μm, with the corresponding mode at the IOTA interferometer, even 0.3% have been reached occasionally).

9.7.3 PRIMA

PRIMA stands for **I** nstrument for **P** hase- **R** eferenced **I** maging and **M** icroarcsecond **A** strometry. This instrument is still being discussed and the specifications below are provisional.

PRIMA will be able to perform excellent and unique science, also of comparatively faint objects, by making use of the large collecting area of the four 8.2-m VLT UTs. The development of this instrument will become a technology driver, also for space interferometry.

It will operate according to the following **principles** :

- dual-field single-baseline instrument;
- usable for narrow-angle astrometry and also phase-referenced imaging; and
- two possible setups: multiplexed coincident beams or separate beams with metrology.

The **overall requirements** for PRIMA are:

- Astrometric accuracy 50 μarcsec initially, 10 μarcsec finally;
- 5 nm differential metrology, 50 μarcsec baseline vector calibration (for 10 μarcsec precision);
- Operation in K, L and M band for imaging, and in the K band only for astrometry;
- Fringe tracking sensitivity K = 11 for ATs; and
- Spectral resolution (in science channel) variable, up to R = 3000

The following key science topics have been identified for **Phase-Referenced Imaging** :

- Active galactic nuclei, radio galaxies and quasars;
- High-redshift galaxies;
- Stellar population in the Galactic Center cluster;
- In general: faint science close to guide stars; and
- Observing and fringe tracking at different wavelengths.

In addition, the key science topics for **Microarcsecond Astrometry** are:

- Detection and orbits of extrasolar planets
- Orbits of wide binaries and brown dwarf companions
- Component masses in hierarchical triple systems
- Parallaxes of Cepheids, AGB stars etc.
- Proper motions and orbits in the Galactic Center cluster
- Proper motions in clusters and dwarf spheroidals

The instrumental concept is based on certain **field-of-view requirements** :

- Astrometric search for exoplanets needs dual "zero" field;
- Astrometry in Galactic Center is more efficient with 1 or 2 arcsec field; and
- Some imaging applications also require non-zero field.

However, field distortions are important and a non-zero field poses substantial technical challenges.

9.8 VLTI Control System

During an interferometric observation, the successful **coordination of all the complex and heterogeneous devices** of the VLT Interferometer (VLTI) depends on the effectiveness and reliability of the control system, which carries out the ultimate system integration.

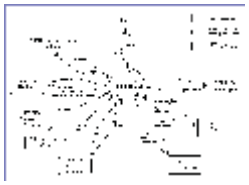

Figure 9.11 [GIF: 10k]. The VLTICS in its operational environment.

The **VLTI Control System (VLTICS)** (Fig. 9.11) is designed to satisfy both specific technical requirements and general operational constraints. It will profit by the valuable experience gained during the development of the control system for the VLT UTs (TCS), inheriting the same principles and standards. Since the VLTICS is a direct client of the TCS, the uniform architecture simplifies the interface definition and the data communication protocol.

9.8.1 Control Hardware

Because of the number, the heterogeneity and the locations of the Interferometer components, the VLTICS is based on a **distributed, multi-platform, network-based architecture** . Local Control Units (LCUs), composed by a VME backplane equipped with CPU boards and interface cards, perform real-time control of VLTI subsystems. Multi-user multi-tasking workstations (WSs) run high-level coordinating tasks and the graphical user interface software. Network links will provide the communication layer among all the computing nodes and a dedicated Time Bus will convey the time synchronization signal.

The VLTI Control Hardware has an interface to the VLTI Instrumentation Control Hardware through the **VLTI Backbone Network** , and to the VLT Telescope Control System through a router connecting the VLTI and the VLT Backbone Networks.

The system is designed to be **highly modular** , in the sense that the hardware and the software devoted to control a subsystem must have complete functionality by themselves, without any knowledge about other subsystems. Therefore direct links between LCUs are avoided, unless very special high bandwidth requirements necessitate dedicated point-to-point communication channels.

The VLTICS uses **VLT standard electronics** . The workstations are equipped with X11 graphical terminals. The local area network employs Ethernet and ATM technology, using optical fibers.

9.8.2 Control Software

The **VLTI Control Software** is essentially constituted by a set of running programs (processes), distributed on LCUs and WSs. They cooperate exchanging messages and sharing a common on-line database. The real-time control software of a subsystem run entirely at LCU level, while software of coordinating is implemented at the WS level. The software is built in functional layers; each layer provides all the required services to the next upper layer and hides the details of the lower layers.

The VLTI Control Software is entirely based on the VLT Common Software (CCS/LCC), cf. Chapter 7.2. It is composed by a set of software packages and modules. Three main packages are:

- The **Interferometer Supervisor Software (ISS)** provides the functions to operate the entire VLTI, including system start-up and shut-down, array configuration setting, observation preparation and run. It coordinates the high level tasks of all the main VLTI components.
- The **Auxiliary Telescope Control Software (ATCS)** provides the functions to operate each AT, both at subsystem level (low level control of each device) and at coordination level (e.g., during presetting, tracking, relocating to another station), and to command a group of ATs as a single entity.
- The **Delay Line Control Software (DLCS)** provides the functions to operate the array of all DLs. It coordinates the operation of the DLs and provides control of each DL, both at subsystem level (low level control of each device) and at coordination level (e.g. during presetting, searching for fringes, blind tracking, fringe tracking).

The rest of the VLTI Control Software is arranged into the **VLTI Subsystem Software** , which refers to the programmes needed to control those VLTI subsystems that are not already part of the Auxiliary Telescope System and of the Delay Line System. These control programmes are, as usual, organized in modules. The following subsystems are available:

- VLTI UT Coudé (COU);
- Transfer Optics (TO);
- Internal Alignment Units (IAU);
- Fringe Sensor Unit (FSU);
- Image Alignment Unit;
- Pupil Alignment Unit; and
- Fringe Phase Alignment Unit.

VLT Whitebook Chapter 10: Science Operations

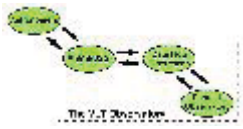

Figure 10.1 [JPG: 208k]. Top-level of the VLT operations model.

The VLT must be operated in a manner that will result in the **greatest scientific return.** To that end, ESO has undertaken the study and development of operational strategies for the VLT. Several key requirements emerged from this study, e.g.:

- The VLT must maximally utilize the available observing time by flexibly adjusting to changing observing conditions, instrument availability and scientific priorities;
- VLT instruments should be continuously calibrated and monitored to ensure the accuracy of calibration and the long term performance of the instruments; and
- Data from the VLT should be delivered to astronomers in raw and processed forms so that data analysis overheads are diminished and scientific assessment of data is accelerated.

To fulfill these requirements, ESO has undertaken the design and development of an end-to-end system for the flow of science data through the VLT Observatory. The **VLT Data Flow System (DFS)** is a set of software systems which follow the observing process from proposal entry to archival research. These software systems will be operated by various groups within ESO at different stages in the observation cycle. The interaction of the science operations groups (Fig. 10.1) within the VLT Observatory are described in detail in the **VLT Science Operations Plan** .

This chapter outlines the VLT Data Flow System, its interaction with users and the operational tasks performed by each subsystem.

10.1 Concepts

10.1.1 High-Level Requirements

The **VLT Science Operations Plan** addresses the basic flow of science data through the VLT, the ESO organizational and operational structures necessary to facilitate that data flow and the specific operational procedures and manpower involved.

The global requirement is to **maximize the scientific return of the VLT** . In this context, the **most efficient use of the VLT** is a prime concern. To this end, new operation modes have been implemented so that the telescopes, the astronomical instruments, and data flow can work together in a fully coordinated fashion and are able to adapt quickly to the prevailing observing conditions.

By 2001, the data flow from Paranal is expected to exceed 30 Tbytes/year, or ~100 times the 1998 data flow from the La Silla Observatory.

This has resulted in the adoption of the following high-level requirements:

- A considerable fraction of the observations are carried out in **service mode** , i.e. by ESO staff according to the specifications of the proposers;
- Service observations are done by **selection of alternatives from a prepared medium-term schedule** in flexible response to changing observing conditions;
- **Operation of telescopes and instruments will be carried out by ESO personnel** at the direction of ESO staff astronomers and visiting astronomers;
- For all supported instrument modes, an associated **calibration plan** will be developed. This plan will be executed automatically and produce calibration data that will ensure the long term usefulness of the raw science data. Calibration plan data will enable ESO to monitor instrument performance and long term trends in instrument and telescope behaviour; and
- VLT operations will produce **quality-controlled science data** that combines raw and calibration frames into final data products that contain physical as well as instrumental units.

10.1.2 Services and Products

The astronomical community will receive the following **set of services and products** :

1. User Support for
    - preparation of proposals,
    - preparation of observations,
    - execution of observing programs,
    - calibration and analysis of data,
    - archival research;
2. On-line and off-line data reduction and calibration software;
3. Calibration data;
4. Data products in instrumental and physical units;
5. Flexible short, medium and long term observation semester scheduling tools;
6. Quality control of data products and performance monitoring of instruments; and
7. Comprehensive archive of all scientific, technical and ancillary data.

These services and products represent the functions and outputs of the various component systems in the VLT Data Flow System (DFS) and are described in more detail below. The operation of the DFS is refered to as **Data Flow Operations (DFO)** .

10.1.3 Operation Modes

The VLT will be operated in two fundamental modes, **visitor** and **service** . In both modes, astronomical programmes will be executed by ESO telescope and instrument operators under the direction of ESO staff astronomers or visiting astronomers.

10.1.3.1 Visitor Observing

Visitor Observing is the mode of choice for programmes requiring intimate familiarity with the scientific programme, e.g., when major decisions need to be taken in direct response to the observations obtained. Visitor observing is also necessary when the requested scientific program requires an instrument mode that is not supported by service observing or when it involves a visitor instrument.

Visiting Astronomers (VAs) carry out their own observations on dates fixed in the semester schedule. **Utilities for planning** of observing runs are provided by ESO. They include selection of guide stars, estimation of exposure times, off-line training sessions with the on-line data reduction software, access to archival and catalogue resources as well as short-term scheduling tools.

Standard calibration observations are performed in order to ensure a minimum data quality, and all information needed for later archival research is supplied. ESO will automatically perform those observations mandated by the calibration plan for a given instrument.

Remote Observing is not considered an observing mode in its own right but is equivalent to Visitor Observing, however, with the difference that the astronomer interacts with the ESO staff at Paranal and supervises the observations remotely from Garching. Remote observing may not be suitable and offered for all instruments or instrument modes.

The **data link between Garching and Paranal** will support fast transfer of the observational data, real-time transmission of video images for target acquisition, and effective means of communication with the on-site staff. Support by VLT scientists is available in Garching. Remote astronomers have access to all computer-based utilities in Garching in just the same way as astronomers visiting Paranal.

10.1.3.2 Service Observing

Service Observing is the operating mode of the VLT whereby the astronomers specify observations and ESO performs these observations for them.

This mode ensures that programmes of the highest scientific importance get the best chance to be executed. Within any given programme, applicants can focus on the scientifically most important targets rather than on filling nights.

A significant fraction of the VLT observations will be carried out in Service Mode. This does not mean that this kind of observing is the primary driver for VLT Science Operations. In order to maximize **quality and quantity of the VLT observations** , most of the tools described below support the needs of visiting astronomers as well as those of service mode programmes.

As a rule, programmes with special requirements on observing conditions will be conducted in service mode.

10.1.3.3 Choice of Operation Mode

Applicants are requested to specify whether they prefer service or visitor mode observations. The ESO Directorate decides upon this request based on recommendations by the Observing Programmes Committee (OPC) and existing constraints.

Programs that can proceed only on the basis of extensive real-time decisions by the astronomers are usually not suitable for service observing. However, the threshold depends on the time interval between different phases of the execution, the predictability of the schedule, the means of communication between Observatory and astronomers and the experience of the Observatory staff.

For a small number of programmes with the highest scientific priority assigned by the OPC, ESO undertakes all possible effort to execute these programs.

For all other programmes, the probability of execution or complete execution will depend on the scientific grading and scheduling possibilities. In any case, ESO attempts to avoid that adopted programmes are left incomplete at a level where the data are insufficient to achieve the scientific goals. Likewise, ESO will guarantee that the exposures obtained in service mode will be executed to within the stated uncertainties and tolerances of the observational conditions.

10.2 Data Flow Overview

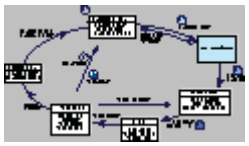

Figure 10.2 [GIF: 14k]. Schematic representation of the VLT Data Flow System.

This chapter outlines the **structure and function of the VLT Data Flow System (DFS)** . The subsystems are described in detail in Chapters 10.3 - 10.7.

The VLT DFS is a **closed-loop software system** and is shown in Fig. 10.2.

The DFS identifies systems that track the flow of data from proposal entry to storage of data products in the VLT Science Archive Facility. The **DFS main component systems** are: Program Handling, Observation Handling, VLT Control System (VCS; cf. Chapter 7), Science Archive, Pipeline and Quality Control. Each of these are discussed in more detail in the following subchapters.

The processes defined by the DFS are the basic components of VLT science operations. Astronomers and observatory operations staff interact with, and operate these components.

10.2.1 Programme Handling

Scientific proposals to use the VLT are made in a **two-step process** , similar to that employed for some other telescopes, e.g., the HST.

During **Phase 1** , astronomers specify the scientific justification for their proposal and indicate the type and amount of telescope resources they require.

These proposals are judged by the Observatory Programs Committee (OPC) and time is awarded. These awards, together with instrument availability and technical constrains form the input data of the **Long Term Schedule** for a semester on the VLT.

10.2.2 Observation Handling

During **Phase 2** of the proposal preparation process, successful programmes convert their observing programs into structures which are schedulable and executable by the VLT. These files are called **Observation Blocks (OBs)** and combine together target and instrument data for one or more exposures on typically a single astronomical object.

The description of an instrument within an OB is called a **Template** . A subset of instrument modes and functions supported by ESO is presented as a template whose input values are set by the astronomer during OB creation.

Observation blocks are the quantum of data that flows within the DFS, collecting **data and status information** as they flow. Observation Blocks are submitted to an **OB Repository** from which a medium-term and short-term schedule can be constructed for service mode observations or from which a visiting astronomer can schedule his/her nights' observations.

Observation handling also receives information from the **Astronomical Site Monitor (ASM)** to assist the observers to choose the most appropriate observing strategy.

10.2.3 OB Execution

OBs contain instructions and data that are executed by the **VLT Control System (VCS)** , for a detailed description, cf. Chapter 7. This results in telescope movement, instrument control and data being taken by VLT instruments.

Completion status on this execution is signaled to the DFS and data is stored on the on-line archive system.

10.2.4 Archiving

Data from VLT instruments are initially stored on the **Online Archive System (OLAS)** . From there, they are copied to permanent media and shipped to Garching for ingestion into the **VLT Science Archive Facility** .

Data is bundled for individual visitor observing programs and distributed.

10.2.5 Pipeline

Some instrument modes will be supported by data reduction pipelines that remove instrumental signatures and apply physical unit calibrations. The **Data Organizer** assembles calibration and raw data to be processed by the pipeline following analysis recipes specified in a **Reduction Block (RB)** .

10.2.6 Quality Control

Every VLT instrument will have a **calibration plan** that specifies a series of data-taking actions necessary to properly calibrate raw data and monitor instrument performance.

OBs corresponding to the calibration observations are created by the **Quality Control System** . The resulting raw data are processed by Quality Control and used to repopulate the calibration data base, track instrument performance in the short and long term and maintain the accuracy of instrument simulators. Quality Control will also define new technical programs for instruments and submit them for telescope time approval. Quality Control will also provide online systems at the telescope to help data flow operations staff assess whether service mode data has been taken under the conditions specified by the astronomer.

10.2.7 Data Format and Units

The only supported format for the exchange of observation data between ESO and astronomers is **FITS** . However, ESO maintains the right to use ESO-defined extensions of the FITS standard. ESO provides translation facilities so that ESO FITs files are digestible by IRAF and IDL, as well as MIDAS.

All physical units used conform to the SI conventions as laid down in the IAU Style Book.

10.3 Programme Handling (Phase 1)

During Phase 1, proposers must prepare all information required to **assess the scientific merits and the feasibility** of their programme. The applications are submitted electronically to ESO. After subsequent processing, they are evaluated and the successful ones will later be stored in the Science Archive so that the resulting scientific data in the Archive become more meaningful for future users. They remain confidential until all data have been released.

10.3.1 Proposal Preparation

Applications for observing time are invited twice a year for one semester each. Deadlines for the submission of VLT proposals are **April 1 and October 1** . The semesters last from April 1 to September 30, and October 1 until March 31.

All major **user documents** are available in printed and electronic form. The electronic versions are available from ESOs WWW site (HTML, PDF or PS), also by anonymous FTP. ESO maintains WWW pages specifically to assist with proposal preparation and contain pointers to all relevant documents and up-to-date information on instrument, telescope and site status. New editions of user documentation are made available as the need arises and are announced in the Messenger or on the ESO WWW homepage.

There is one general **VLT User Guide** which gives an overview of the primary capabilities of the VLT and its instruments, other on-site facilities, pointers to more detailed information, procedures for applications for observing time, and VLT operating procedures. This document enable proposers to assess the best ways to use the VLT facilities to perform a given observion. This includes comparisons of instruments with similar or overlapping capabilities.

Each instrument is described in a separate **Instrument Manual** . They serve to provide all information about an instrument so that a proposer can decide whether the instrument is appropriate to reach the intended scientific goal and can write a proposal and also describe the operations, required calibrations, and data reductions. They normally include typical operational overheads, typical exposure times and S/N ratios, standard calibration observations, scope and limitations of routine calibrations, a list of recent publications based on observations obtained with the instrument, pointers to sources of more detailed information, and a subject index.

Web pages are used as the fastest means of **informing the user community** of recent changes not covered by instrument and operating manuals and other major user documents. A news section and an archive are maintained with information about recent changes. In addition, the current observing schedule is posted. In the case of programmes to be carried out in service mode, astronomers can also obtain information of the degree of their completion. Information will also be provided via the ESO Messenger.

Software simulators exist for some instruments to generate synthetic data. Simulation software will not be exported to ensure that it is up-to-date. Access is provided via the WWW or directly in Garching and on Paranal. **Exposure time calculators (ETCs)** which compute the S/N as a function of exposure time and target brightness are supported for the widest possible range of instrument modes.

For all frequently used instrument modes, complete and fully documented sets of **representative observations** (sample data) are offered.

Guide stars must be selected for approved observing programmes. However, for programmes requiring adaptive optics, availability of a suitable reference star is a prime feasibility criterion and for every object to be observed with adaptive optics a reference star must be identified by the applicants and included in the application form. A Guide Star Selection System is made accessible via computer networks.

10.3.2 Proposal Processing

Receipt of proposals, checking for technical completeness, scientific and technical evaluation, and the archiving of the successful programmes is supported by a computer-based **Proposal Entry System** . Thus, all proposals must be submitted in a fixed machine-readable format. The system rejects proposals, which are not received in the proper form or lack required information. Meaningful diagnostics of the processing errors are supplied, enabling the applicants to incorporate the necessary corrections.

Receipt of valid proposals is acknowledged, and a unique **Proposal Identification Number (PIN)** is assigned. Proposals retain this number throughout their life cycle.

Proposals, which after the passing of the deadline, do not conform to the requirements are rejected and the applicants informed. All information relating to such applications is deleted after 2 years.

In addition to the scientific justification and a description of the purpose of the observations, proposals must provide at least the following information: a target list (coordinates, magnitudes, etc.) with information about the type of objects, technical information (instrument modes and setups, accuracies needed, calibration requirements, prefered observing mode, etc.) and information about the proposers, including a list of publications related to the proposal, and an account of previous VLT programmes.

The database created by the Proposal Entry System is used as the only source of information for proposal processing. The submitted information about the combination of targets and instrument modes is automatically **cross-correlated with the Science Archive** . If a duplication of existing data results, the OPC is informed.

Every proposal undergoes a **technical feasibility check** by Science Operations staff, but in view of the large number of proposals, this step can only aim at identifying obvious problems. Special requirements for Phase 2 proposal preparation are identified. Science Operations staff analyzes whether proposals are suitable for service observing. Corresponding reports are also submitted to the OPC and the ESO Directorate.

All applications received by the deadline are examined by the OPC. The **OPC panels** provides recommendations for each proposal on the the scientific priority, the amount of observing time (with an estimate of the minimum time needed to achieve meaningful results), scheduling constraints, a recommendation for observing mode (service or visitor), a justification of the recommendations and comments to the proposers. Final approval of all observing and test programs and the conditions of their execution is given by the ESO Directorate, who prepares the semester schedule based on the recommendations by the OPC.

VLT programmes approved for service observing will be split into the three categories:

- **Category A (highly ranked by the OPC).** All possible effort will be made to execute all the OBs corresponding to these programmes in the requested observing period. Programmes will be placed in this group primarily because of their high OPC ranking but also to fill some undersubscribed set of observing conditions (e.g. poor seeing during bright-time);
- **Category B (well-ranked by the OPC).** Programmes in this category will only be executed if no Category A programme can be executed; and
- **Category C (ranked at the cut-off line by the OPC).** These programmes will be executed only if no Category A or B Programmes can be executed.

ESO makes every possible effort to perform **very-high priority service-mode observations** . High-priority observations, which for some reason could not be completed, may be carried over to the following period; the status of such programs is reported to the OPC which may update its recommendations. The astronomers are informed as well. ESO reserves the right to declare a program substantially complete. If an observing program carried out in visitor mode fails or cannot be completed, it has to be re-submitted.

The decision about **lower-priority service-observing programs** is taken during medium- and short-term scheduling and depends on weather, instrument availability, and the possibility to build an efficient schedule.

The OB database is updated as observations are accumulated, and the medium-term schedule for service observations is adapted accordingly.

10.4 Observation Handling (Phase 2)

Following the evaluation outlined above, proposers are informed about the result of their application. Short summaries of the scientific and feasibility assessments are provided. In the same communication, successful applicants are asked to prepare **Phase 2** of their proposals.

In the case of **service mode observations** , proposers will be asked to prepare OBs with the **P2PP Tools** made available by ESO approximately two months before the observations will be scheduled. A detailed **User Manual for the P2PP System** is provided (26).

Astronomers going to Paranal (**visitors' mode**) will also be asked to prepare OBs in advance, but can produce OBs at the observatory.

10.4.1 Proposal Preparation

In order to make VLT operations transparent and to facilitate the following procedures, a **contact scientist** is assigned to each successful application. They advise the astronomers on all matters concerning Phase 2 of the proposal preparation and the scheduling and execution of service observations. They can later also be consulted in connection with the reductions and calibration of the observations and archival research issues. Contact scientists are backed up by the operations team of specialists. This team comprises people in Garching as well as at Paranal.

An **Observation Block (OB)** contains two types of information; one describes the astronomical target and the other the instrument setup. Target descriptions and instrument templates can be flexibly coupled within OBs to observe multiple objects with the same instrument setup or the same target with a number of instrument modes.

The instrument setup is prespecified by the corresponding **Templates** . Proposers fill in fields associated with a given template (e.g. CCD window size) to specify the complete instrument setup for a given target. Not all modes of an instrument will be accessible via templates (requests for access to instrument modes outside what is available within ESO supplied templates have to be submitted in Phase 1).

Each instrument is described in a comprehensive **Operating Manual** . The manuals explain what information has to be provided during Phase 2 of the proposal preparation in order for service observations to achieve the best return. Items usually to be covered by the manuals include, among others,

- a statement of the user's and ESO's responsibilities, respectively;
- a detailed outline of capabilities and limitations of available templates
- outlines of strategies for optimal instrument settings for given scientific purposes and observing conditions;
- a description of a sample session and a summary of standard observing OBs; as well as
- a check list and a calibration plan.

Among the various information to be provided, especially in connection with observations in service mode are (the same information are also needed for most observations in visitor mode):

- **Final coordinates (possibly with an error estimate)** : For position sensitive observations, an offset relative to a star with known absolute coordinates is desirable. Alternately, a statement clearly identifying the object must be given. A **finding chart** considerably facilitates target acquisition. The correctness of the information provided is the exclusive responsibility of the
- **Guide Star Selection** : At least one guide star has to be selected for each OB. More than one guide star may be required, especially for moving targets. Several stars can be attached to any target in order to reduce the impact of unknown problems. The availability of suitable guide stars is important because part of their light has to be used for image analysis and the setting of the active optics system;
- **Calibration needs** : A calibration plan which describes the instrument calibration maintained by the Observatory and the minimal calibrations is provided by ESO. The calibration principles generally depend on the type of data rather than the nature of the observing program. Instrument calibrations are prepared by ESO, especially for the standard templates and Observation Blocks. Additional calibrations must not jeopardize quality of the scientific data to be obtained or interfere with observations. Astronomers are encouraged to perform or request additional calibrations needed to achieve their scientific goal. The time needed for additional calibration observations made during the night will be subsumed under the allocated observing time of the program. ESO maintains a list of suitable calibration sources and procedures for all observing modes. Routine standard calibrations are performed for the most frequently used modes.
- **User Requirements** : VLT service mode users will be able to specify conditions under which OBs are to be executed. They include airmass, Moon phase and elongation, seeing and sky transparency as well as IR Emissivity. These conditions will be checked by the service mode observer using Quality Control Tools.

10.4.2 OB Processing

Once OBs are prepared by the PI, they are submitted to ESO. All submitted OBs reside in the **Observation Block Repository (OBR)** . From here, OBs can be checked-out, edited and resubmitted.

A programme can only be executed when its OBs are submitted. Submitted OBs are subjected to **validation** and the PI is informed of any errors. OBs with errors can be checked-out by the PI, edited and resubmitted for further validation. The validation process checks the requested instrument and target parameters against scheduling constraints and any instrument availability or template issues.

The final product of Phase 2 of proposal processing is the populated OBR. For each OB, the following information must be available:

- target-specific information: name, coordinates, proper motion, magnitudes and colors or fluxes (if available);
- guide stars and/or reference star(s) for observations with adaptive optics;
- one or more templates with associated parameters;
- scheduling constraints (e.g., time or weather);
- observation constraints (e.g. seeing, airmass, sky emmisivity, etc);
- the priority assigned by the astronomers;
- the unique proposal identification number;
- the priority assigned to the program by the OPC; and
- any comments by the OPC or ESO staff.

In additional the following optional information may be present:

- an pointer to the location of a digitized finding chart; and
- one or more links to other observations of the same program so that logical sets of observations (e.g., using to the standard observation blocks) can be defined.

10.5 Scheduling and Execution of Observing Blocks

The efficient scheduling and execution of Observing Blocks (OBs) is a crucial element of the DFS and has been given special attention. Real-time tests with the NTT have been very useful in this respect and have demonstrated the overall advantages of this system.

10.5.1 Scheduling Considerations

The OBR will be filtered by the **Medium-Term Scheduler (MTS)** to produce a pool of OBs that can potentially be observed in a 1-2 week period. The resulting list is used as the input to the **Short-Term Scheduler (STS)** which acts during one observing night. It is based on scientific priorities, weather predictions and instrument availability. The STS can be recomputed at short notice to take account of changing conditions and priorities.

The MTS will support an accounting system which flags all exposures that have been successfully carried out. Updates are made at the end of each night on the basis of the reports provided by the service observers. The report states for each Observation Block whether the quality requirements are fulfilled. The degree of completion of service observing programs and other statistical information needed by the MTS is computed.

All components of P2PP are able to satisfy the **special requirements** of a number of less-frequent observing modes, e.g. moving targets, time-critical observations, non-standard calibrations, OBs which can be fully defined only after other VLT observations have been inspected.

The application and proposal preparation and processing procedures for **Targets Of Opportunity (TOOs)** is essentially the same as outlined above. When a target of an approved program becomes known, the PI informs ESO. Observation Blocks must then be specified. The observations are executed in service mode. If an instrument change is required or a visitor mode program needs to be interrupted, the scientific priority of the program(s) concerned will be taken as the primary criterion according to a policy to be established by the OPC.

In exceptional, not predictable cases, ESO may be contacted with a request for observations of targets of opportunity. There may also be other special circumstances which necessitate deviations from the regular procedures followed for the allocation of observing time. A small fraction of the observing time will be set aside for this purpose (**Director's Discretionary Time**). The Director General specifies the decision-taking mechanisms and also the criteria for interrupting ongoing programs or equipment changes. Such observations are carried out in service mode and, if necessary, the corresponding OBs may be prepared by ESO staff.

10.5.2 Execution of Observing Blocks

The execution of OBs is done from the VLT Control Room, where ESO and Visiting Astronomers interact with the DFS and the VLT Control System (VCS) through a number of tools.

The VCS contains those systems responsible for the control of the telescope and its instruments, cf. Chapter 7. The DFS interacts with VCS via a **carriage return paradigm** in which executable information (OBs) is passed from DFS to VCS and raw data frames are returned. The VCS signals the OB completion status (complete, aborted, failed) to the DFS. The VCS requests the next OB to be executed from DFS and as such DFS is the server to a VCS client.

A variety of **software tools** are provided for astronomers at the telescope to choose OBs and submit them to be executed by the VCS.

The **Short Term Scheduler (STS)** produces a potential list of OBs for execution according to selection functions involving science priority, observing conditions and instrument availability.

The Observing Tool (OT) allows this list and the OBR on Paranal to be browser for the next OB to be executed.

The **VCS Broker of Observation Blocks (BOB)** (cf. Chapter 7.8.4) accepts the incoming OB on the VCS side and begins execution.

OBs may also be created and edited at the telescope. For this purpose a real-time version of the P2PP tool (**P2PP-VM**) allows OBs to be submitted directly to BOB from the P2PP system. BOB signals the completion status of the OB to the astronomer.

All instruments for the VLT can be accessed directly from their individual control interfaces. Should the DFS fail to produce an OB for BOB, **direct instrument control** is possible by ESO staff.

Data is displayed via Quick-Look tools such as the **Real Time Display (RTD)** directly from the Instrument Control Systems. The DFS provides **Quality Control Tools** at the telescope to assess the extent to which the data comply with the conditions specified in the OB. Data are also available at an off-line workstation in one of three FITS formats appropriate to ESO MIDAS, IDL or IRAF. Astronomers can run these environment at the off-line workstation to assess data quality.

Data resulting for all OBs is sent to the **On-Line Archive System (OLAS)** for the particular Unit Telescope.

The observational process - the execution of the OBs - is supported by data from an **Astronomical Site Monitor (ASM)** that continually logs the ambient conditions, including the air temperature, pressure and humidity, the wind speed and direction, the seeing, the sky brightness/emissivityand transparency, the precipitable water vapor content and the dust content of ambient air. In addition, the temperature and wind flow parameters are measured inside the domes. The ASM operates and delivers the measurements automatically. A graphical representation of any of the measurements collected in the previous 48 hours is available on all VLT control terminals. Five-minute averages of the measurements obtained are logged and periodically transferred to the Science Archive.

10.6 Pipeline Processing and Quality Control

Pipelines controlling the **data gathering, calibration and archiving processes** at a telescope like the VLT must continuously adapt to changing conditions. First, the four VLT UTs will be equipped with a number of instruments at any time, offering a large number of observation modes that are activated according to programmes and the observing conditions, e.g., changes in the recorded Point Spread Function (PSF). Progress in instrumentation and even modifications in instrument operation modes must also be handled by the data pipelines.

This calls for a constant adaptation of the calibration strategies, and may even involve a complete paradigm shift, for instance to **model-based calibration** , cf. Chapter 10.6.3.

The loop is ultimately closed by a **quality control** (Chapter 10.6.2) process that transforms modern observatories into production plants reliably delivering calibrated scientific data to the PIs. This control itself requires an in-depth understanding of the instrumental characteristics and the calibration process, achieved by reference to instrument models.

10.6.1 Calibration

The VLT DFS pipeline is designed on a number of general principles including **independence** from the data reduction system, events and context driven actions, and **support** of calibration strategies and reduction levels.

The goal of the reduction is to process the observation in order to measure **physical quantities** such as flux, position, time, wavelength or polarization, with the best possible accuracy. For non-trivial observation modes, there might be several ways to back-project the observation equation, yielding to different calibration strategies.

The flexibility necessary to evaluate alternative calibration strategies is built in the pipeline by means of pipeline configuration files, a macro language describing the classification, reduction and product handling rules.

The events received by the pipeline identify new frames, start and end of templates and OBs. On each event, a sequence of actions is executed by the pipeline, including classification, data reduction, and product handling actions allowing to store, copy, or distribute the products of the pipeline. The data reduction actions are defined by the pipeline independently of any data reduction system by means of **Reduction Blocks** . A mapping is invoked at execution time to translate the Reduction Blocks for processing by the data reduction system.

The **observation equation** describes the convolved effects of the atmosphere, optical, and detector components on the physical signal of the astronomical target. The observation equation is based on a model view of the instrument and on simplifying assumptions (e.g. linearity of the detector, independence on the polarization). The **model of the instrument** is characterized by the optical path and the state of the optical components along the optical path, corresponding respectively to the observing mode and instrument configuration. The selection of calibration solutions is therefore based on the optical path and the configuration of the instrument.

The **configuration information** is necessary to select the calibration solutions but not sufficient to decide which reduction recipe must be applied to specific data. A context information is also required, defining the scope of the observation program, such as maintenance, technical, or scientific purpose. All three information of events, frame classification, and context is derived from the FITS header of the frames.

The calibration procedure of astronomical data usually involves **intermediate reduction levels** before the analysis step. Once the integrity of the FITS files reaching the pipeline has been verified, the pipeline will process and deliver data to different reduction levels. The detector level includes the determination of the zero-point of the measurements (bias, dark-current), pixel-to-pixel sensitivity and detector non-linearities. The geometry level includes optical instrument distortions and projections (spectrographs, interferometer or Fabry-Perot projections), including if necessary the astrometry calibration. The photometry level includes corrections for sky background, atmospheric extinction and absolute flux calibrations. The VLT pipeline will correct the data up to the photometry level. The analysis level is the measurement of those physical parameters relevant to the scientific program,and usually involves assumption on the characteristics of the astronomical target.

10.6.2 Quality Control

The main activity of **Quality Control (QC)** is to assess the quality of the raw data generated by the instruments and the pipeline products. Controlling a quantity involves a measurement procedure and the comparison of the measure to a pre-determined target value. The elements of control consist of a quality parameter, a measurement procedure, a target value, a decision logic, and an action.

Depending on the parameters being controlled, there are several levels of control. The first will verify that the observation conditions requested by the user have been fulfilled (**QC level 0 - QC0**). At the next level, is is ascertained that the data can be calibrated by providing the adequate reference calibration solutions (**QC level 1 - QC1**).

A further step verifies that the observation equipment is performing as expected by comparing its actual performance by means of instrument models (**Short Term Trend Analysis - STTA**). Finally one will make sure the evolution of the characteristics of the observation process are properly understood and taken into account in the calibration plan (**Long Term Trend Analysis - LTTA**). Each of these activities is performed on a different time scale.

Figure 10.3 [JPG: 136k]. The **VLT Data Quality Control system** . The QC0 and QC1 levels (upper line) are applied to service-mode and visitor-mode data. The dashed line shows short-term and long-term trend analysis (STTA and LTTA), primarily based on technical programs and service-mode data. The preparation of reference calibration data involves stages of pre-processing and certification. The dotted line shows the distribution from a central calibration database to the local copies used by the pipelines.

The proper flow of information (cf. Fig. 10.3) must be established to support the QC decision making process consisting of the approval of Observation Blocks, the certification of reference calibration data, and the release of reduced data.

10.6.2.1 Quality Control Level 0

QC0 is to verify that the **user requested parameters** , evaluated by the scheduler to trigger an observation, have been all respected during the observation.

This post-observation verification is performed independently and will catch variations of the observation conditions that might have occured after the schedule evaluation. QC0 involves only access to the raw frames or the FITS header. It can therefore be applied to all frames produced by the instrument.

10.6.2.2 Quality Control Level 1

QC1 is the verification of the data by measuring parameters on reduced frames. It involves the association of calibration data and pipeline processing. Depending on the parameter controlled the processing is performed directly at the instrument pipeline after the observation or in prior to the release of the user data package.

It involves two stages, corresponding to the preparation of reference calibration solutions using technical program data, and the control and application of the calibration solutions using scientific program data.

Applied to user data, QC1 includes the stage of data reduction and the measurement of quality parameters (e.g., image quality) on the reduced data. This stage of control is applied to service-mode observation data and, to the extent that the observation mode is supported by the pipeline, to visitor-mode programs. Reduced data, QC report, calibration solutions and reduction logs constitute the reduction data products.

10.6.2.3 Trend Analyses

In **Short-Term Trend Analysis** , the calibration data produced by technical programs, service observing, and when applicable visitor programs, are compared to the previous reference calibration data. Statistical results are stored until the creation of new reference calibration data. The results are stored on a central QC machine remotely accessed by Data Flow Operations. Variations of the instrument performance are studied and compared to the predicted results given by instrument models.

In **Long-Term Trend Analysis** , the characteristics of reference calibration data are compared over extended periods of time by retrieving historical records from the complete calibration database, part of the Science Archive.

10.6.3 Instrument Models for Calibration and Quality Control

Efforts are currently underway to implement a new concept of data reduction at the VLT, based on **Instrument Models** . The essential ideas are explained below.

With ever more complex instruments entering service, an increasingly high importance is assigned to **calibration tasks** . Most of the current calibration concepts are based on the principle of comparison with empirical readings from so-called *standards* . Although computational tools have become much more elaborate, at the very basis are empirical relations obtained from data containing noise. The calibration strategies currently adopted in most of optical astronomy are empirical methods aimed at ``cleaning'' data from instrumental and environmental effects by a sequential application of instrumental corrections. Usually the transformation of detector based units into astrophysical units is done as a separate last step at the boundary between calibration and data analysis. The whole sequence makes it hard to arrive at a physical understanding of variations in instrumental characteristics which ought to drive maintenance measures or algorithmic solutions.

The gap between the calibration of individual observations and the monitoring of instrument performance can been closed by new operational concepts, such as the one designed for the VLT DFS, supplemented with the development of a **physical calibration concept** . In this context, **instrument models** that provide the means to simulate the observational data gathering process from first principles form the basis for instrument configuration control, predictive calibration, and forward analysis.

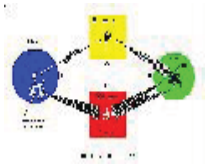

Figure 10.4 [JPG: 136k]. The generic data gathering and analysis scheme in astronomy.

Fig. 10.4 depicts the **generic information flow** in observational astronomy. An observation operator (the telescope-instrument combination) projects a sub-volume of the Universe's parameter space into the raw data domain. In the classical approach to interpret these raw observational data astronomers attempt to apply another operator - the **calibration** - in order to project back into the physical parameter space (eg. flux scales), with the intent to obtain the ``true'' spectral energy distribution of a source or its ``true'' morphology and surface brightness distribution. If it were not for photon shot noise and detector noise, we could in principle find an inverse of the ``observation'' operator performing an exact re-projection. Radio interferometry and high energy experiments often come very close to achieving exactly that. At optical wavelengths, however, direct inversion is out of question because of noise.

Fig. 10.4 shows another route to arrive at statistically more sound estimates for the targets properties - the **forward analysis** . It rests on the ability to simulate the observational process in all its (relevant) detail on noise free models of targets. The range of model targets that can have possibly led to the raw data actually acquired might then be explored for example by Monte-Carlo optimization procedures. If ``standard'' sources are simulated by this process, one arrives at **predictive calibration** , supporting the classical schemes in instrumental modes not properly covered by empirical data.

Using the contemporary and the long term trended data base of engineering parameters for such models, a **predictive calibration** scenario becomes feasible. The models then provide very educated guesses of calibration relations, which need to be adjusted only in low order terms, e.g., linear offsets determined from actual short exposure calibration data.

Until now, a main objection to this approach has been the lack of control of the setup of ground-based astronomical instruments. However, much more **rigid configuration control** is being implemented at the VLT (and at other observatories), and is a vital component of the VLT operations concept. Data analysis methods based on physical models of such controlled configurations enjoy a large gain over purely empirical methods. Furthermore, a physical model based approach removes the non-uniqueness of the relation between engineering parameters and coefficients in empirical relations. This offers operational advantages such as methods for automatic configuration control and instrument check-out.

With experience from some actual case studies at hand, and recognizing that there is a large overlap in requirements for the operation of the pipeline calibration between HST and VLT instrumentation, the ST/ECF at the ESO HQ has started a study, aiming at the **future implementation of predictive calibration** at the VLT.

10.7 Archiving and Distribution

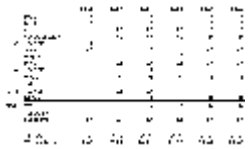

Figure 10.5 [GIF: 4k]. The data volume expected from the VLT instruments, expressed in gigabytes for a typical night during steady state operations. The estimated total rates per night are derived by making assumptions on a mixture of instrument usage for a typical night.

The VLT will deliver a **Science Archive** of astronomical observations approaching the 100 Terabytes mark already within its first six years of operations. The data volume expected from the different instruments over the next years is shown in some detail in Fig. 10.5.

10.7.1 Basic Considerations

ESO is undertaking the design and development of both **On-Line and Off-Line Archive Facilities** . The VLT Archive System goals may be summarized as follows:

- to **record the history of VLT observations** in the long term and provide the memory of observatory operations;
- to provide a **research tool** , i.e., make the Science Archive another VLT instrument;
- to help VLT operations to be predictable by providing **traceability of instrument performance** ; and
- to support **observation preparation and analysis** .

They are based on some fundamental policy considerations about the extraordinary research potential of the VLT, and the desire to make the results from this new facility available to the broadest possible community in an expedient and reliable way.

The VLT Observatory, with its wide-spread instrumental capabilities and unique data assurance tools will generate a large reservoir of science data with well understood instrument performance and stable calibration. An archive of these observations will allow astronomers to re-analyze the data from different perspectives. Such systems have shown in the past to develop enormous scientific value. Best known examples are the science archives of the IUE satellite and of the Hubble Space Telescope. In both cases, the data archives have delivered to the community many times more data than the telescope themselves.

The experience of building and operating a science archive for the ESO New Technology Telescope (NTT at La Silla) has allowed to understand and master the issues involved in dealing with weather dependency and evolving instrument configuration of a ground-based telescope.

Due to the very large data volume expected from the VLT, handling of data for research projects with archive data becomes a task manageable only through large facilities (e.g., disk farms, cpu processing power, etc.) and a corresponding data handling environment (common algorithms, databases, catalog correlation tools, etc). In order to support the maximum scientific exploitation of the archive, ESO is planning and developing a **Science Archive Research Environment** that will support the massive processing of archive data for selected Archive Research Programmes.

The assessment of instrument and telescope performance relies heavily in resorting to the memory of the system. Monitoring the engineering and scientific throughput requires access to a large database of runtime parameters, physical characteristics and configuration data. **The VLT Engineering Archive** will cover these needs and include tools to analyze and correlate this large data warehouse.

The VLT Science Archive system will **provide tools and interfaces to astronomers** that will enable them to access survey data, common astronomical catalogs, archive data, publications, observatory ambient condition measurements and other information sources. Such tools will be geared to support the preparation of observation projects but also support the post-observation analysis phase.

10.7.2 System Components

Figure 10.6 [GIF: 7k]. Overview of the VLT Archive System Architecture with the main components, the On-Line Archive Facility (OLAF) and the off-line Science Archive Facility (SAF).

The main components of the VLT Archive System are the **On-Line Archive Facility (OLAF)** and the off-line **Science Archive Facility (SAF)** .

The **On-Line Archive System (OLAS)** takes care of receiving the data and creates the Observations Catalog while the **Archive Storage system (ASTO)** saves the data products onto safe, long-term archive media.

The **SAF** includes a copy of ASTO used for retrieval and user request handling, the **Science Archive System (SAS)** and the **Science Archive Research Environment (SARE)** .

All the data is described in an **observations catalog** which typically describes the instrument setup that was used for the exposure. Weather and seeing information is recorded in an ambient conditions database. Engineering data, instrument configurations and the operations logs are stored in the **Engineering Archive** databases.

In addition to the raw science data, all calibration files will be available from the calibration database. The calibration database includes the best suitable data for calibrating an observation at any given time.

The archive system includes a number of innovative features both in technology as well as from the point of view of information handling, e.g. **Replication, Safe Store and Data Volume** , and **Distributed Modularity** .

Data storage for on-line use (at Paranal) must be able to hold 1 - 2 weeks of data (approximately 0.5 Tbyte) to support single service mode runs, short-term trending on the mountain and loss of links to Garching. The total storage environment must be able to store approximately six months of VLT data to cover semester access from Chile.

For convenient trend and efficiency analyses, the on-line (fast) storage capacity is sufficient for three months' accumulation of data (1 - 10 Tbyte). In addition, the calibration data base is kept on-line for at least one year.

The main archive is maintained at Garching. The baseline option for the **transfer of the data from Paranal** is initially removable media. The processing capacity must be allow to handle all VLT observations corresponding to an average 24-hour period within 8 hours. Data enter the main archive within 10 days of the observations.

10.7.3 The Science Archive Research Environment

Observation data will be stored within the VLT Science Archive Facility and will be available to Science Archive Research programmes one year after the observation was made. However, in face of the very large data amounts, the selection of data for a particular archive research project quickly becomes an unmanageable task. This is due to the fact that even though the observations catalog gives a precise description of the conditions under which the observation was made, it does not specify the scientific contents of the data.

Hence, archive researchers have to first do a pre-selection of the possibly interesting data sets on the basis of the catalog, then assess each observation by possibly looking at it (preview) and/or by running some automated task to determine its suitability.

Already during the first year of operations, the VLT will be delivering data quantities that make it not feasible to follow the same procedure for archive research. New tools and data management facilities are required. The **ESO/CDS Data Mining Tools** project aims at closing the gap and develop methods and techniques that will allow a thorough exploitation of the VLT Science Archive.

Archive Research Programmes are user-defined processing chains that are applied to the raw data. Each of the processing steps is called a Reduction Block (RB) that consist of one or more processes which are treated by the system as 'black boxes', i.e. without any knowledge of its implementation. However, the reduction block interface (input and output data) do comply to a well defined specification. This feature allows any reduction module to become part of the chain. In fact, this flexible architecture also allows the research programme to analyze different kinds of data from images and spectra to catalogs and tables of physical quantities.

The output of an archive research programme will be derived parameters that are fed into the Data Mining Database. From there on, the archive research programme will be able to use cross-correlation tools to sort and analyze object parameters for a large sample.

Several external users will be able to use the browsing facility of the on-line catalog simultaneously. Retrieval requests are supported at a level of up to 100 per year initially; later growth may be by more than an order of magnitude so that the data output of the Archive might exceed the input by a factor 2-5.

Data dissemination is by means of removable media. Distribution via electronic networks is being considered for small data sets.

10.7.4 Access to Catalogs and Survey Data

An essential service offered by the VLT Archive System is the on-line **access to survey data** such as the Digitized Sky Surveys I and II and to very large astrometric catalogs. Such services are used by the Telescope Control System for telescope guiding, by astronomers when preparing observations and by survey projects to quality check processing results.

The development of search engines for large catalogs is an ongoing activity that has already shown a high level of acceptance by the community. ESO is now capitalizing upon this expertise and will develop the search engine for the GSC-II export catalog that is expected to include more than 2 10 9 objects with positions and colors.

The work is supported by the ESO-developed SkyCat , a widely used tool that combines visualization of images and access to catalogs and archive data for astronomy.

Appendix:

Figure 1.1.:

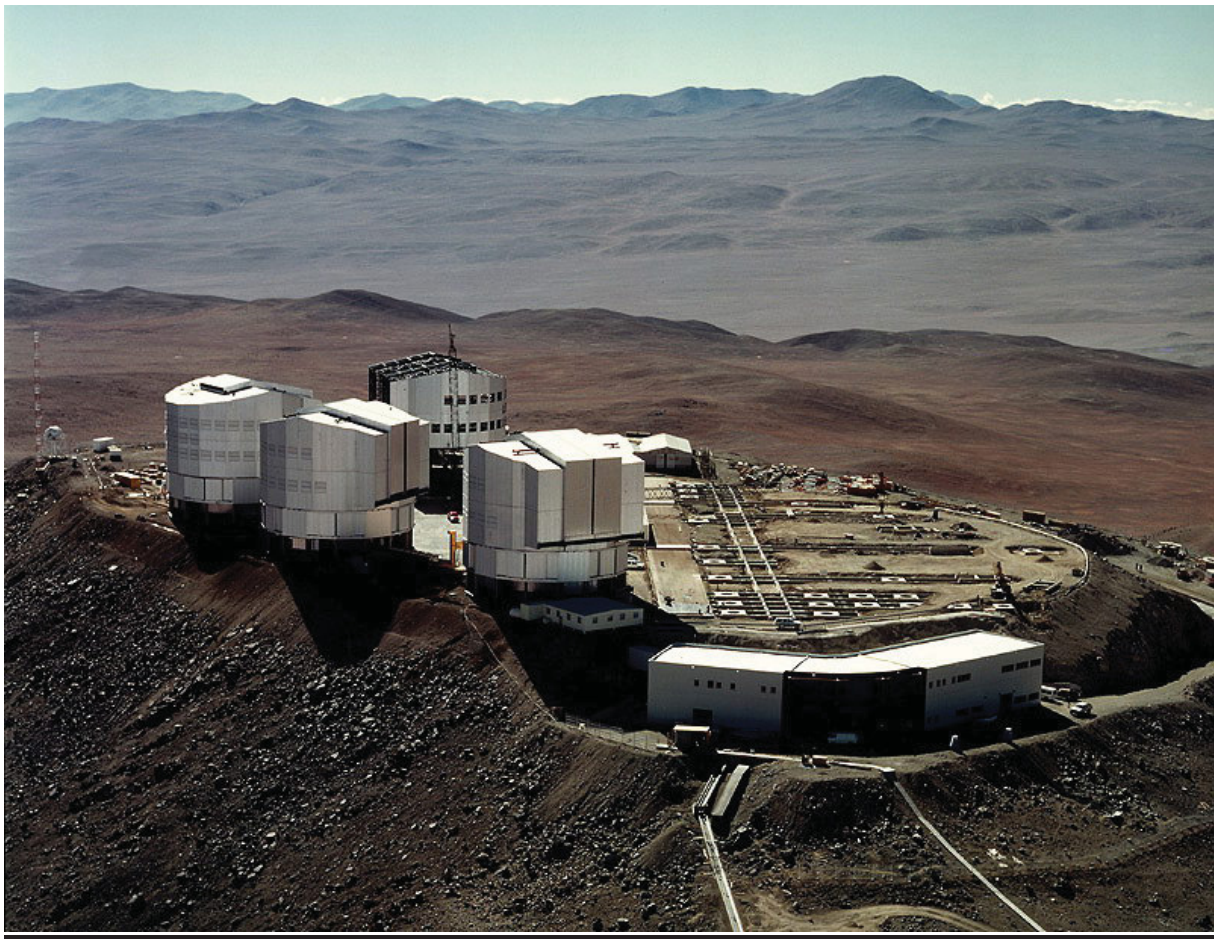

Figure 1.2.:

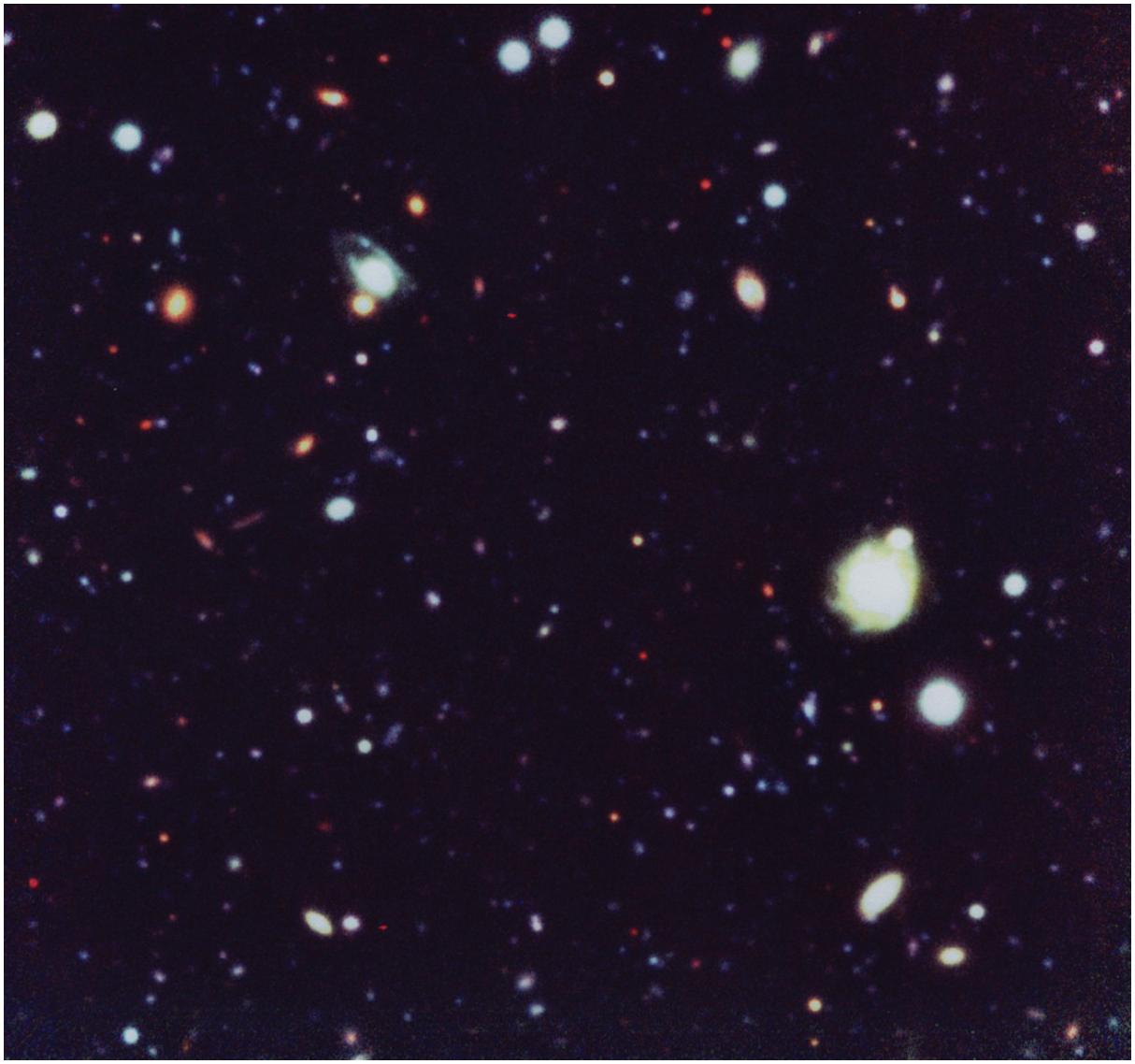

Figure 1.3.:

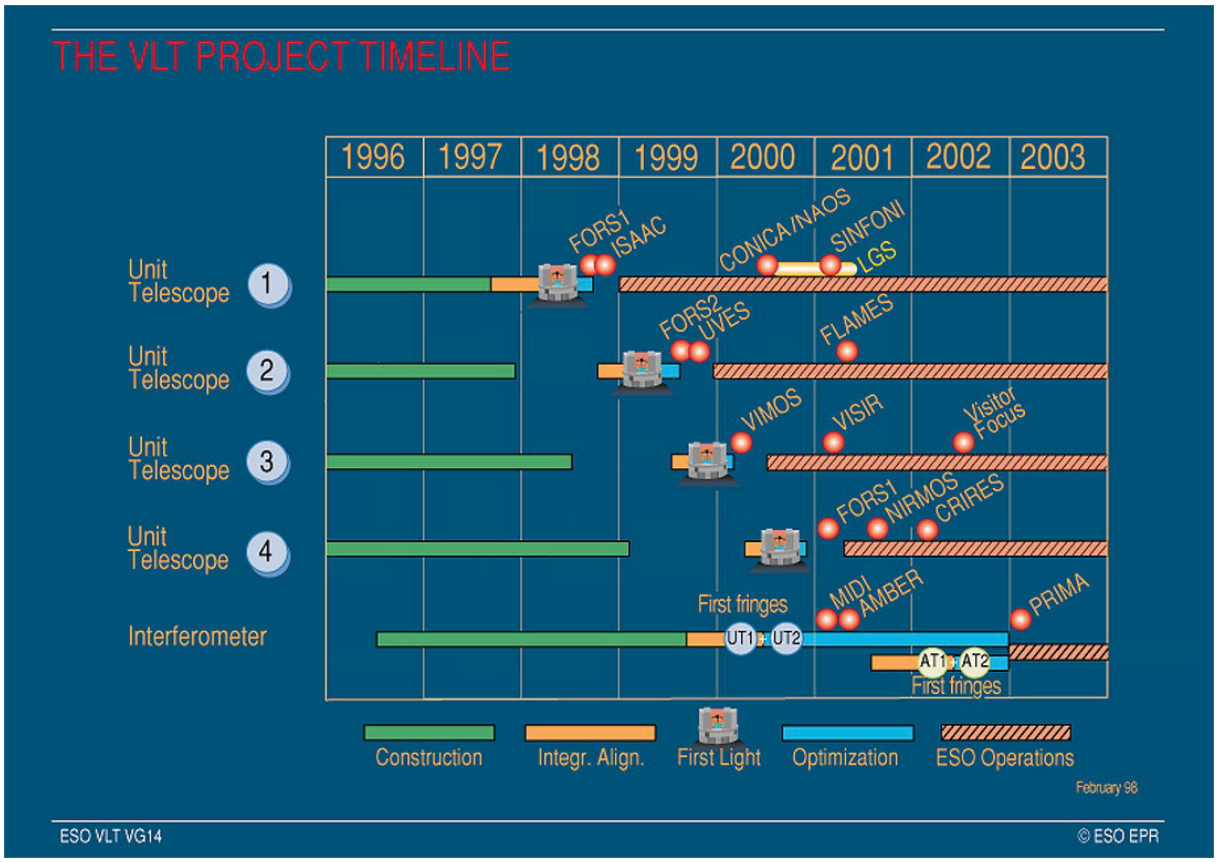

Figure 1.4.:

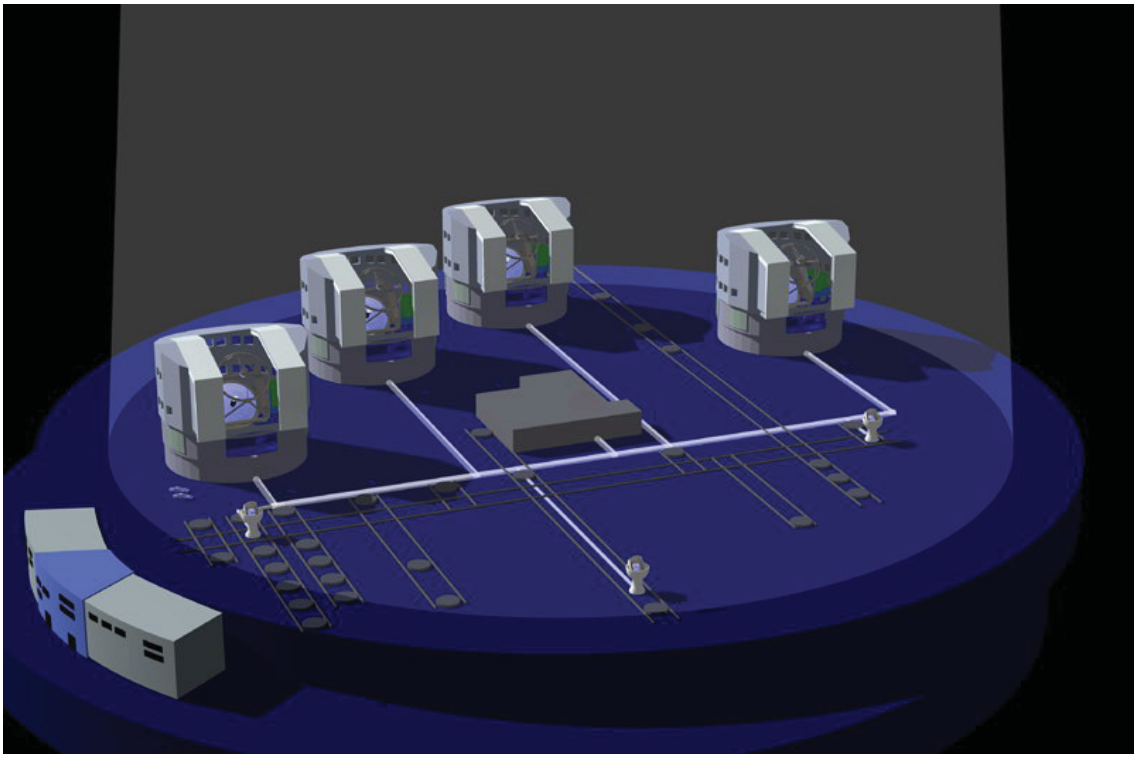

Figure 1.5.:

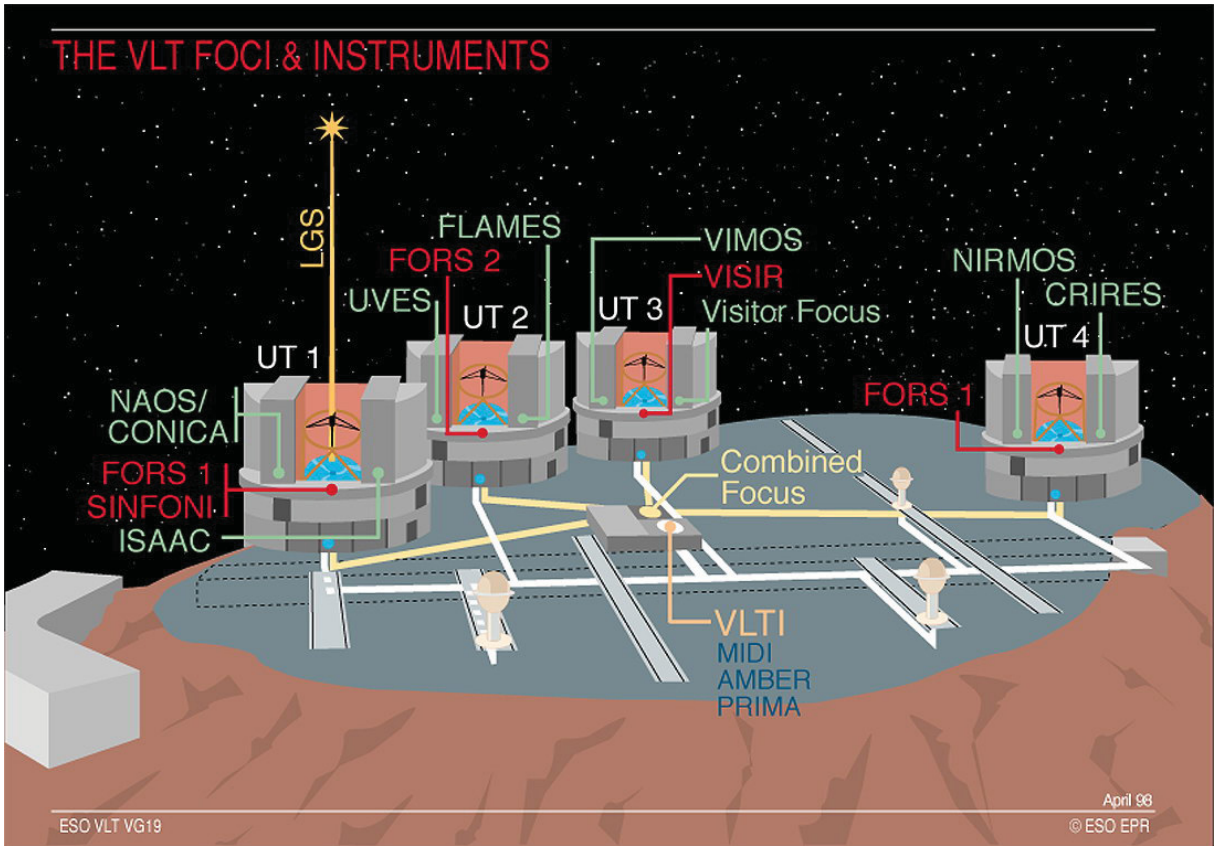
THE VLT FOCI & INSTRUMENTS
LGS
FLAMES
FORS 2
UVES
UT 2
VIMOS
VISIR
UT 3
Visitor Focus
NIRMOS
CRIRES
UT 4
UT 1
NAOS/
CONICA
FORS 1
SINFONI
ISAAC
FORS 1
Combined
Focus
VLTI
MIDI
AMBER
PRIMA
April 98
ESO VLT VG19
© ESO EPR

Figure 2.1.:

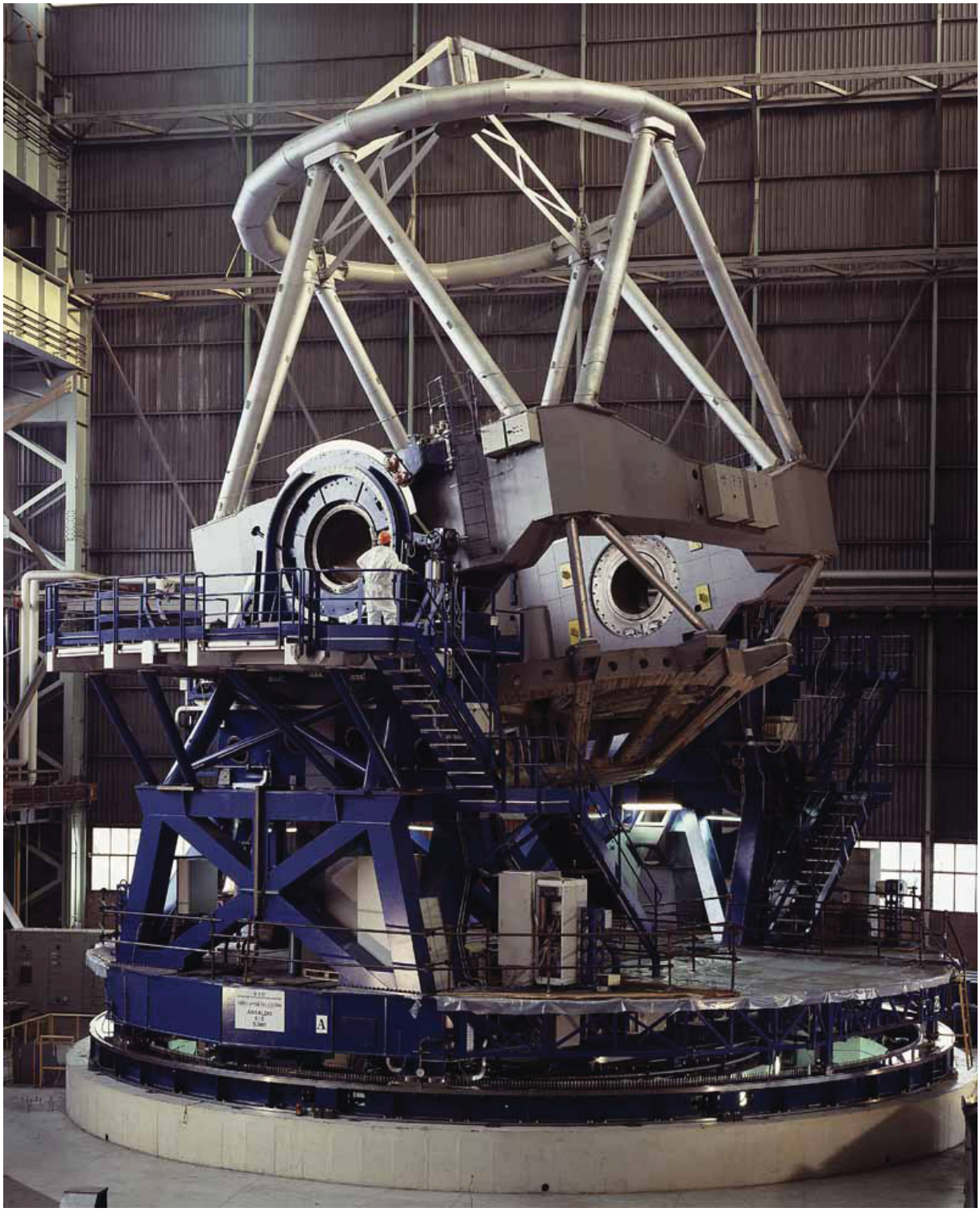

Figure 2.2.:

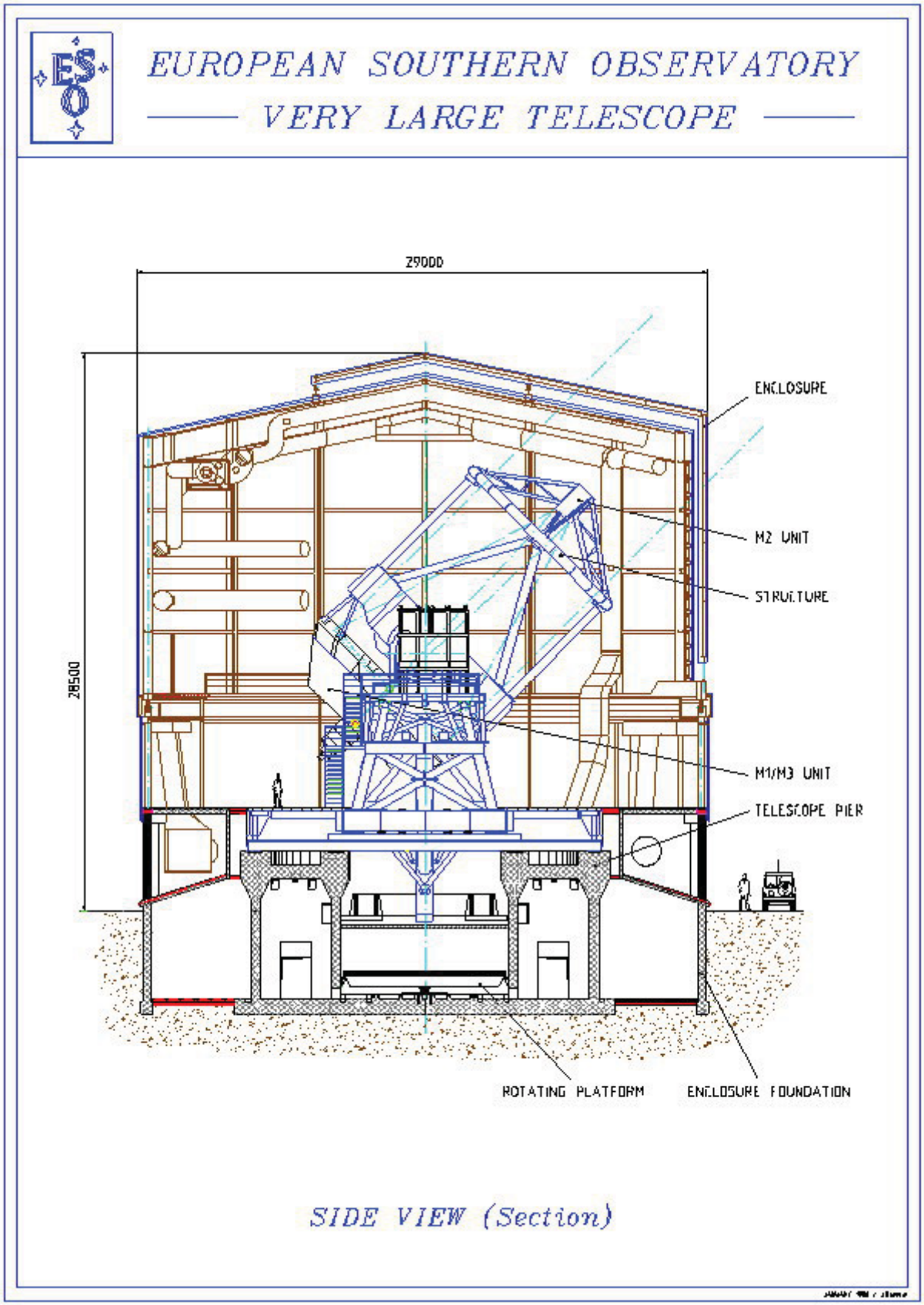
EUROPEAN SOUTHERN OBSERVATORY
VERY LARGE TELESCOPE
29000
28500
ENCLOSURE
M2 UNIT
STRUCTURE
M1/M3 UNIT
TELESCOPE PIER
ROTATING PLATFORM
ENCLOSURE FOUNDATION
SIDE VIEW (Section)

Figure 2.3.:

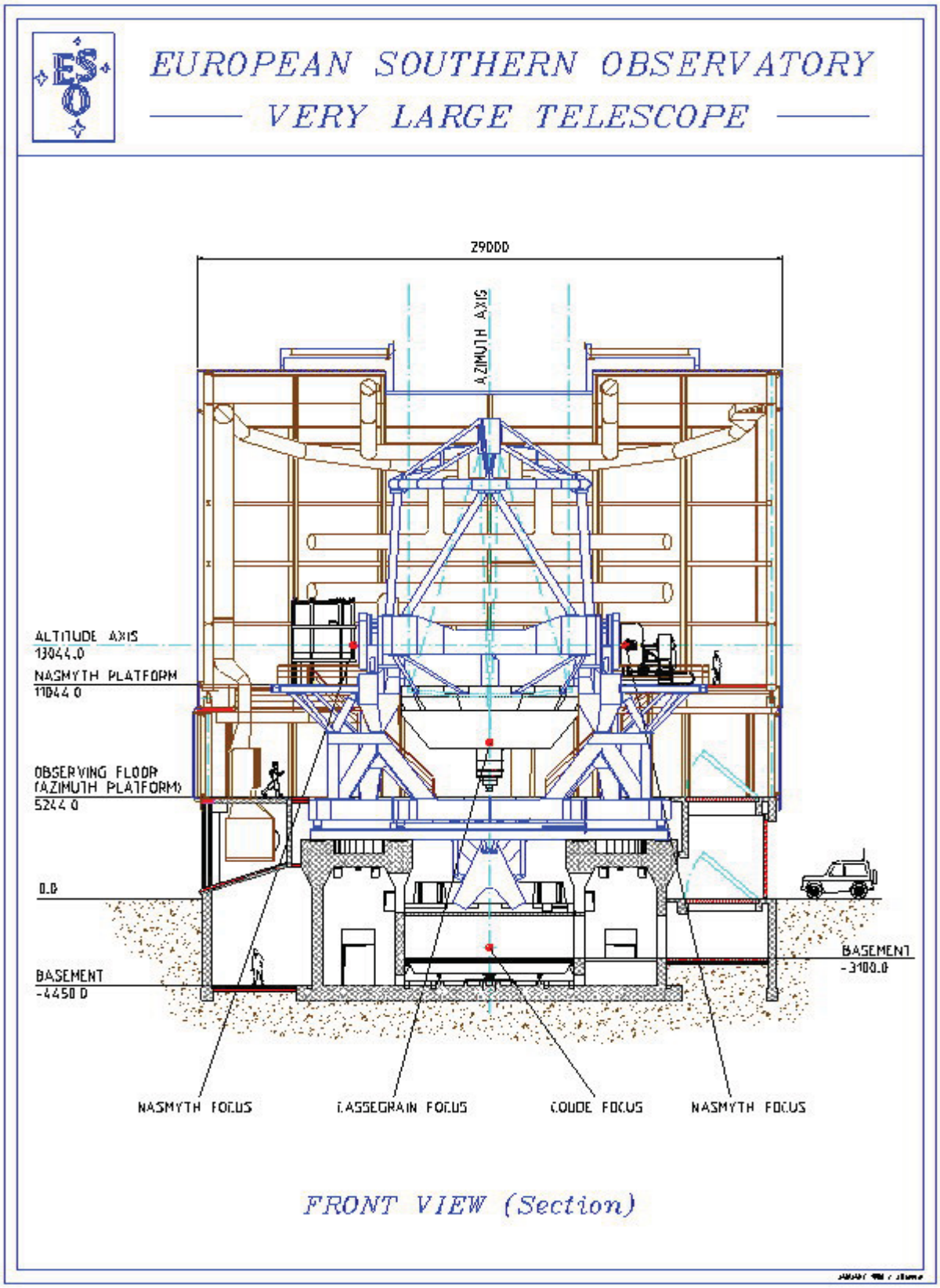
EUROPEAN SOUTHERN OBSERVATORY
VERY LARGE TELESCOPE
29000
AZIMUTH AXIS
ALTITUDE AXIS
13044.0
NASMYTH PLATFORM
11044.0
OBSERVING FLOOR
(AZIMUTH PLATFORM)
5244.0
0.0
BASEMENT
-4450.0
BASEMENT
-3100.0
NASMYTH FOCUS
CASSEGRAIN FOCUS
COUDE FOCUS
NASMYTH FOCUS
FRONT VIEW (Section)

Figure 2.4.:

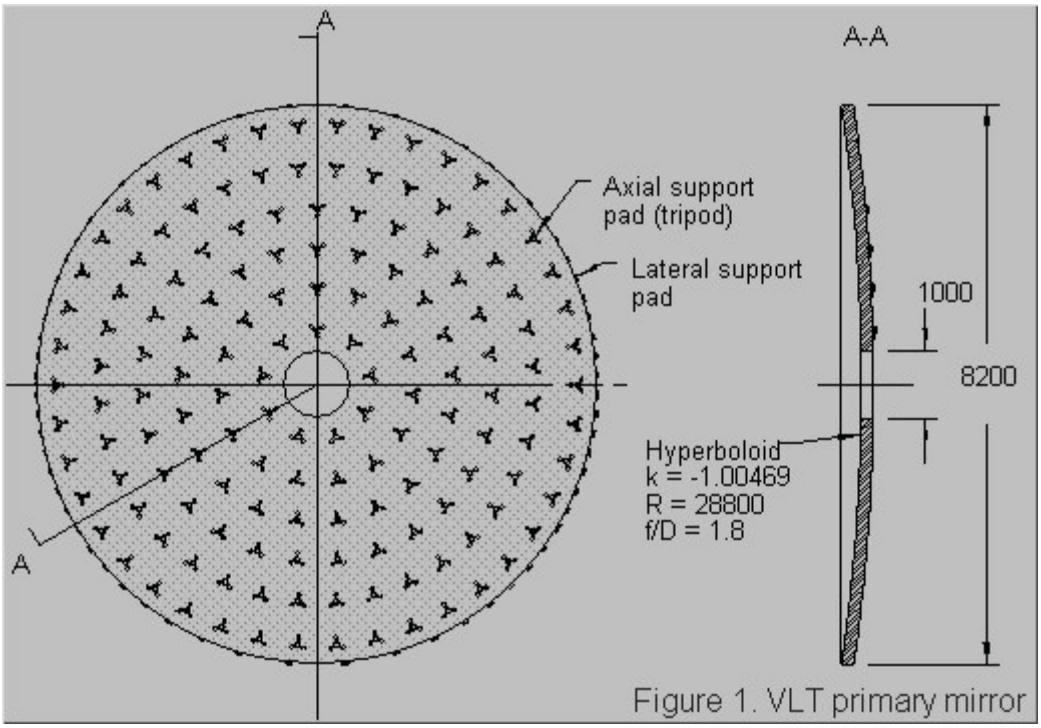

Figure 2.5.:

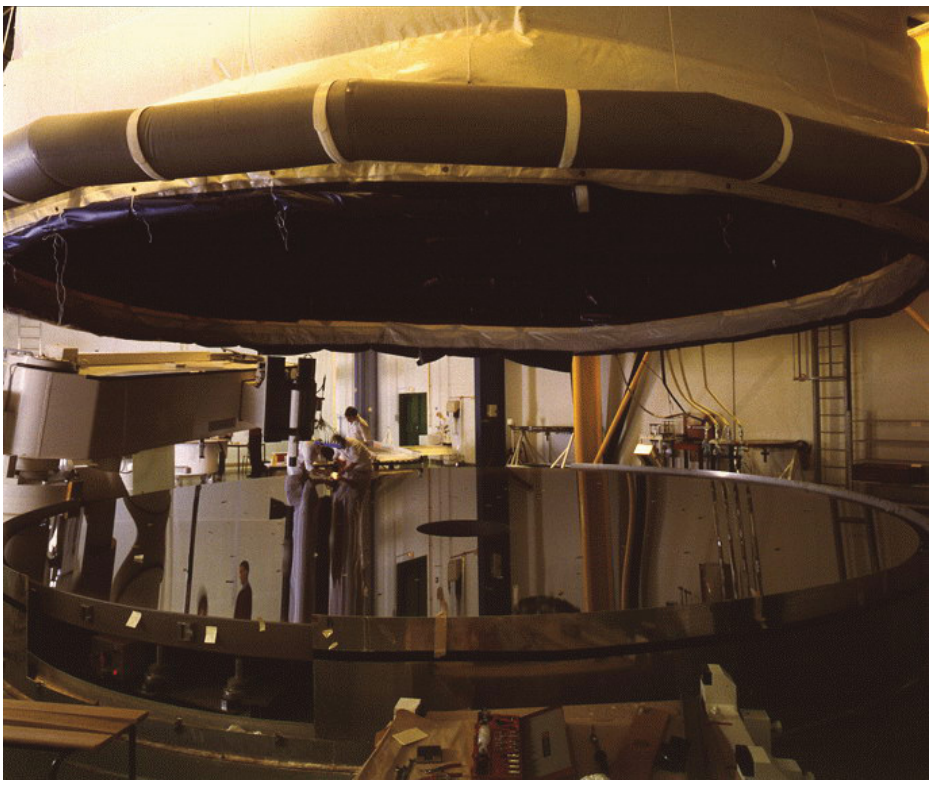

Figure 2.6.:

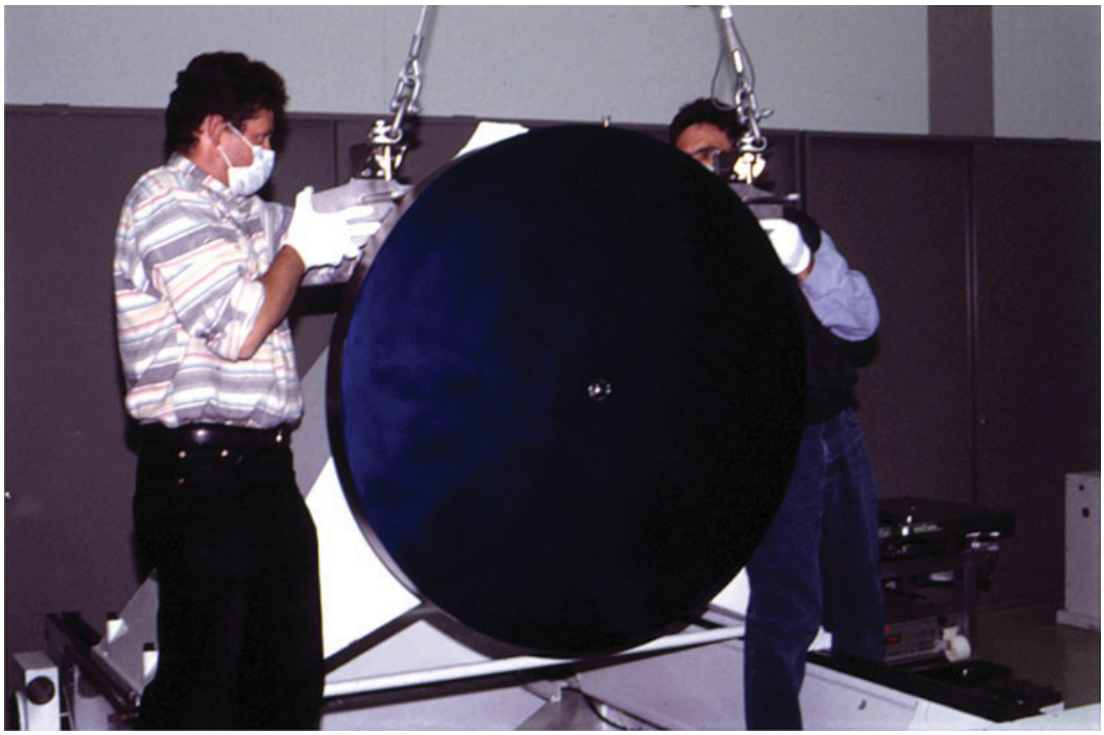

Figure 2.7.:

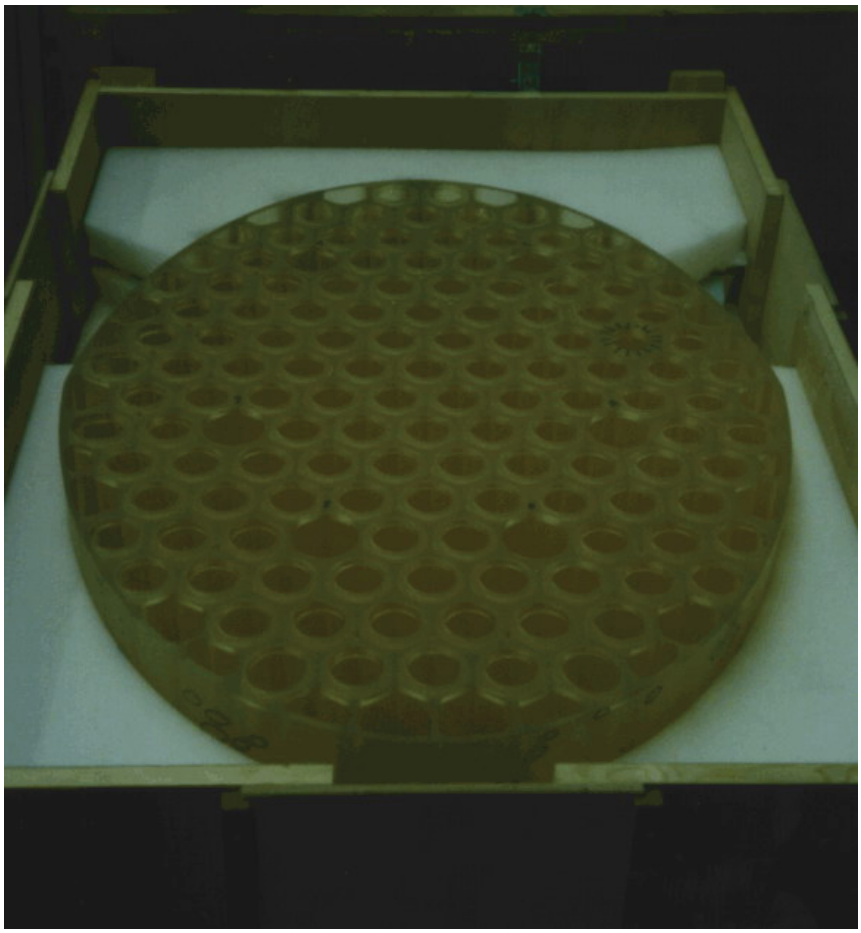

Figure 2.8.:

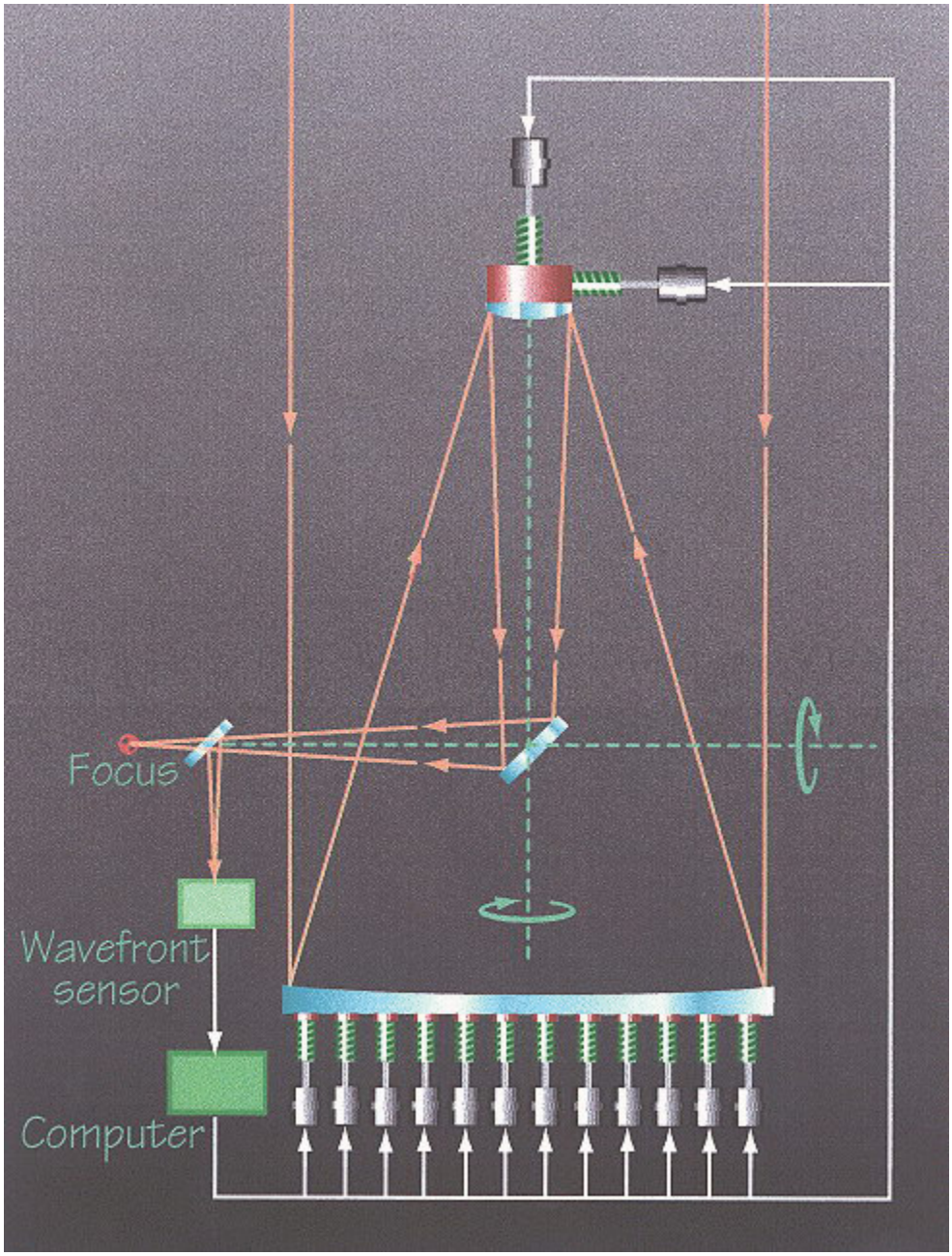

Figure 2.9.:

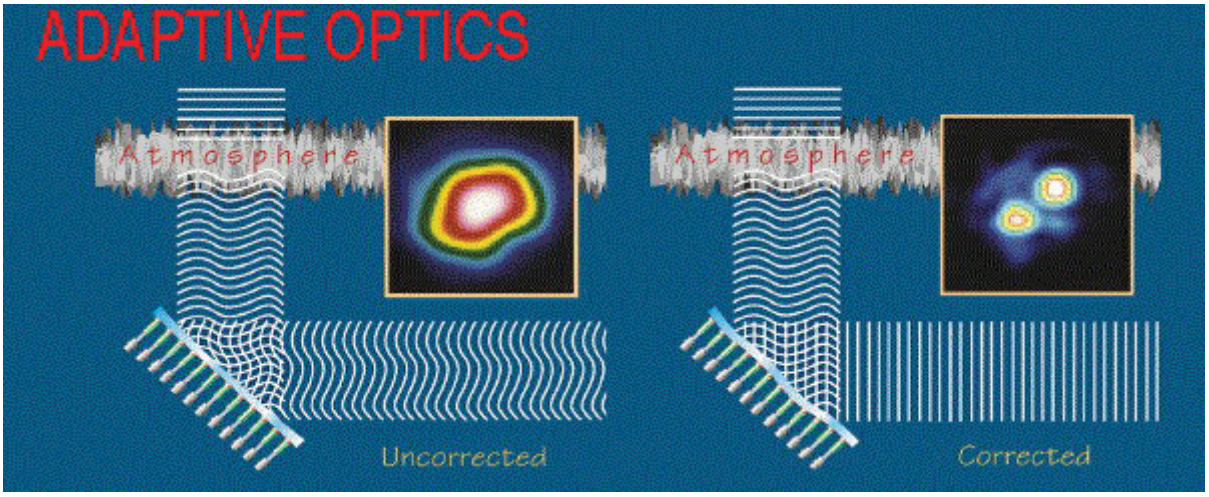

Figure 2.10.:

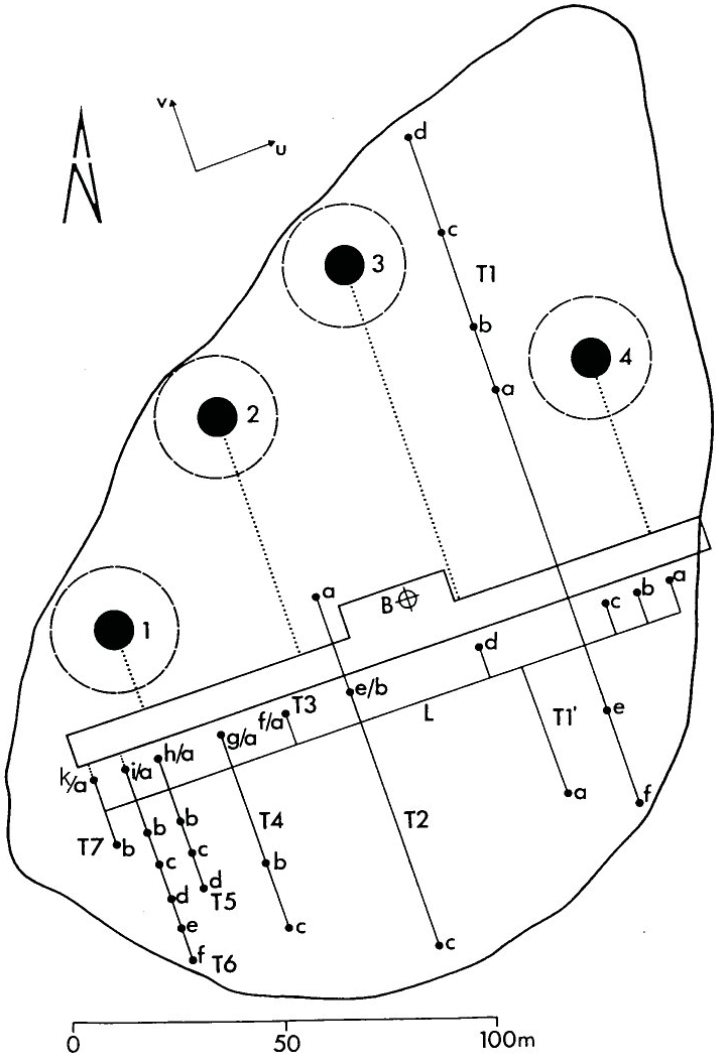

Figure 2.11.:

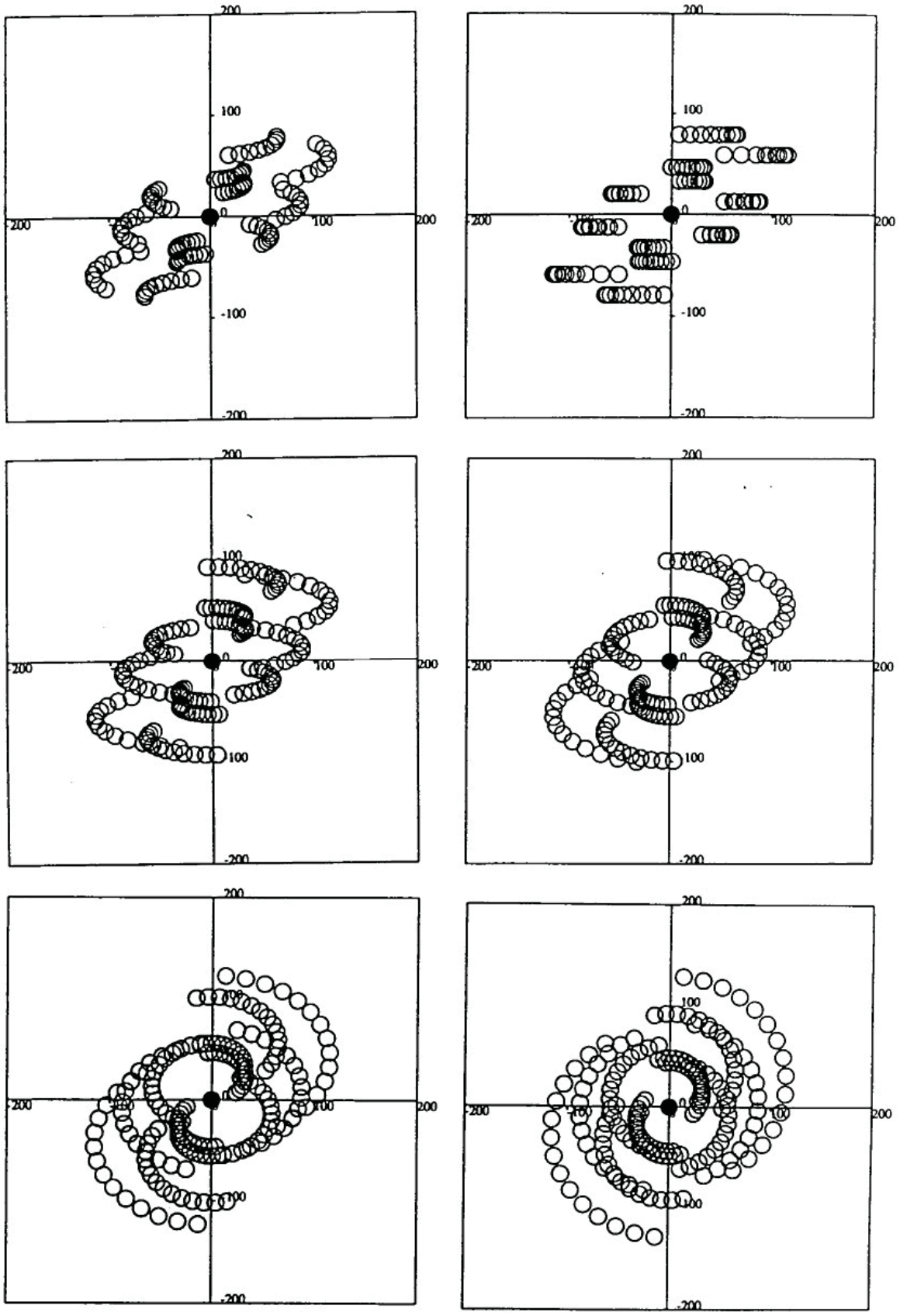

Figure 2.12.:

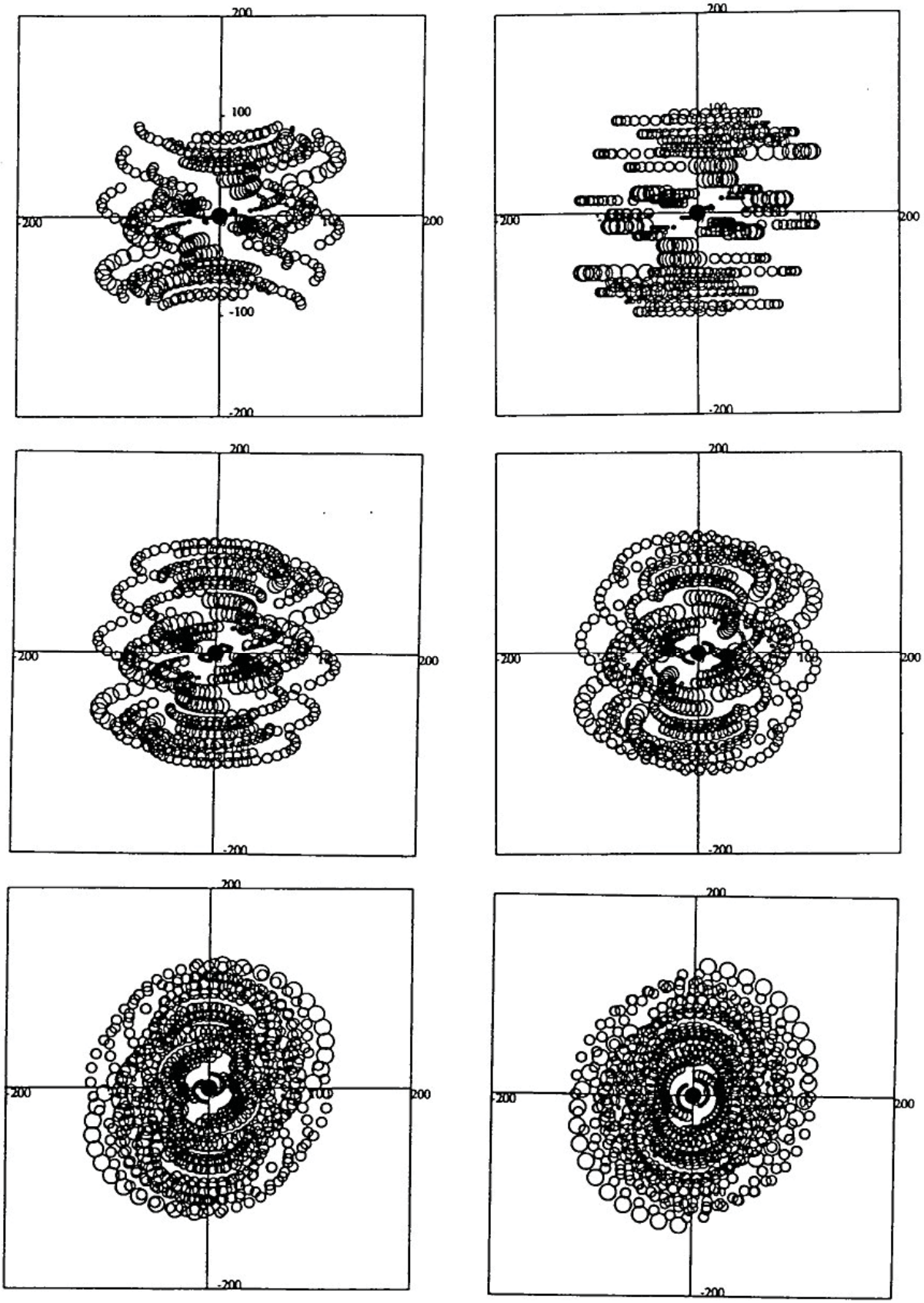
200
100
-100
-200
200
200
200
100
-200
200
200
200
100
-200
200
200
200
100
-200
200
200
200
100
-200

Figure 2.13.:

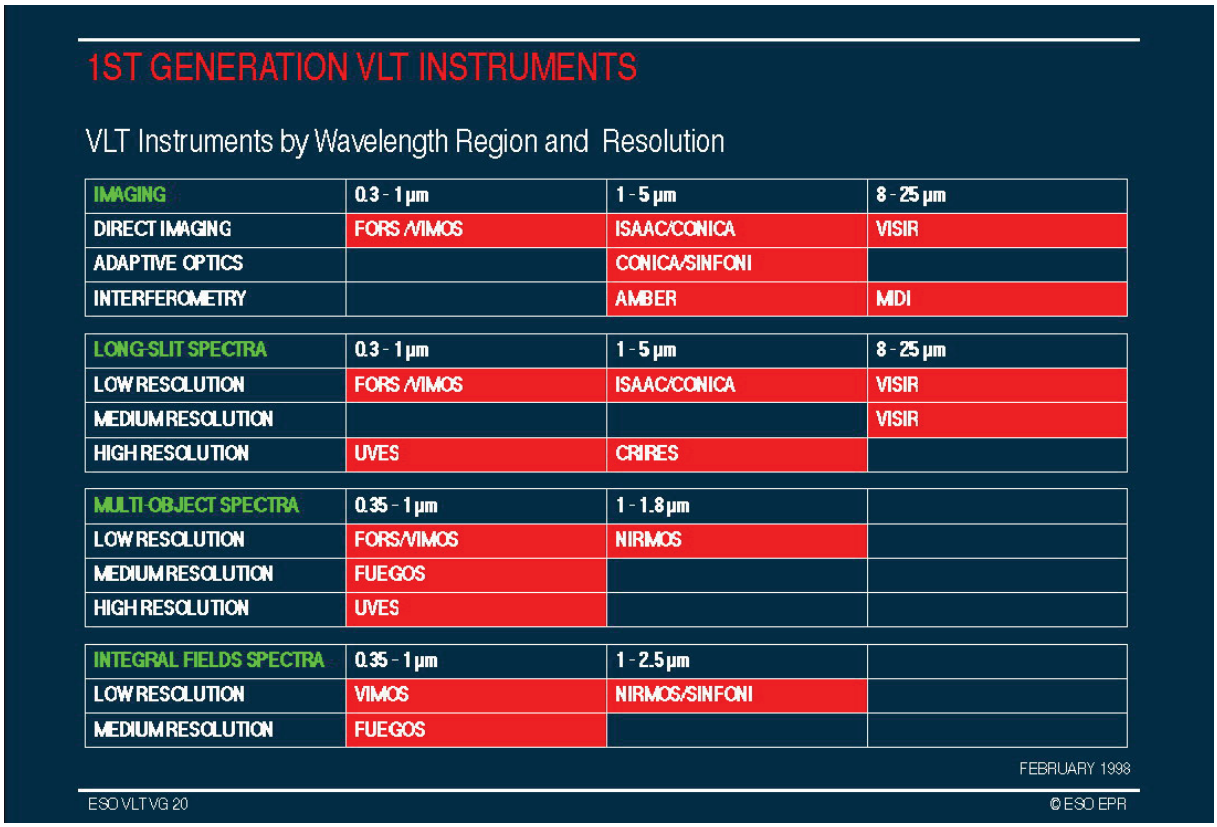

1ST GENERATION VLT INSTRUMENTS

VLT Instruments by Wavelength Region and Resolution

IMAGING	0.3 - 1 µm	1 - 5 µm	8 - 25 µm
DIRECT IMAGING	FORS /VIMOS	ISAAC/CONICA	VISIR
ADAPTIVE OPTICS		CONICA/SINFONI	
INTERFEROMETRY		AMBER	MIDI

LONG-SLIT SPECTRA	0.3 - 1 µm	1 - 5 µm	8 - 25 µm
LOW RESOLUTION	FORS /VIMOS	ISAAC/CONICA	VISIR
MEDIUM RESOLUTION			VISIR
HIGH RESOLUTION	UVES	CRIRES	

MULTI-OBJECT SPECTRA	0.35 - 1 µm	1 - 1.8 µm	
LOW RESOLUTION	FORS/VIMOS	NIRMOS	
MEDIUM RESOLUTION	FUEGOS		
HIGH RESOLUTION	UVES		

INTEGRAL FIELDS SPECTRA	0.35 - 1 µm	1 - 2.5 µm	
LOW RESOLUTION	VIMOS	NIRMOS/SINFONI	
MEDIUM RESOLUTION	FUEGOS		

FEBRUARY 1998

ESO VLT VG 20

© ESO EPR

Figure 2.14.:

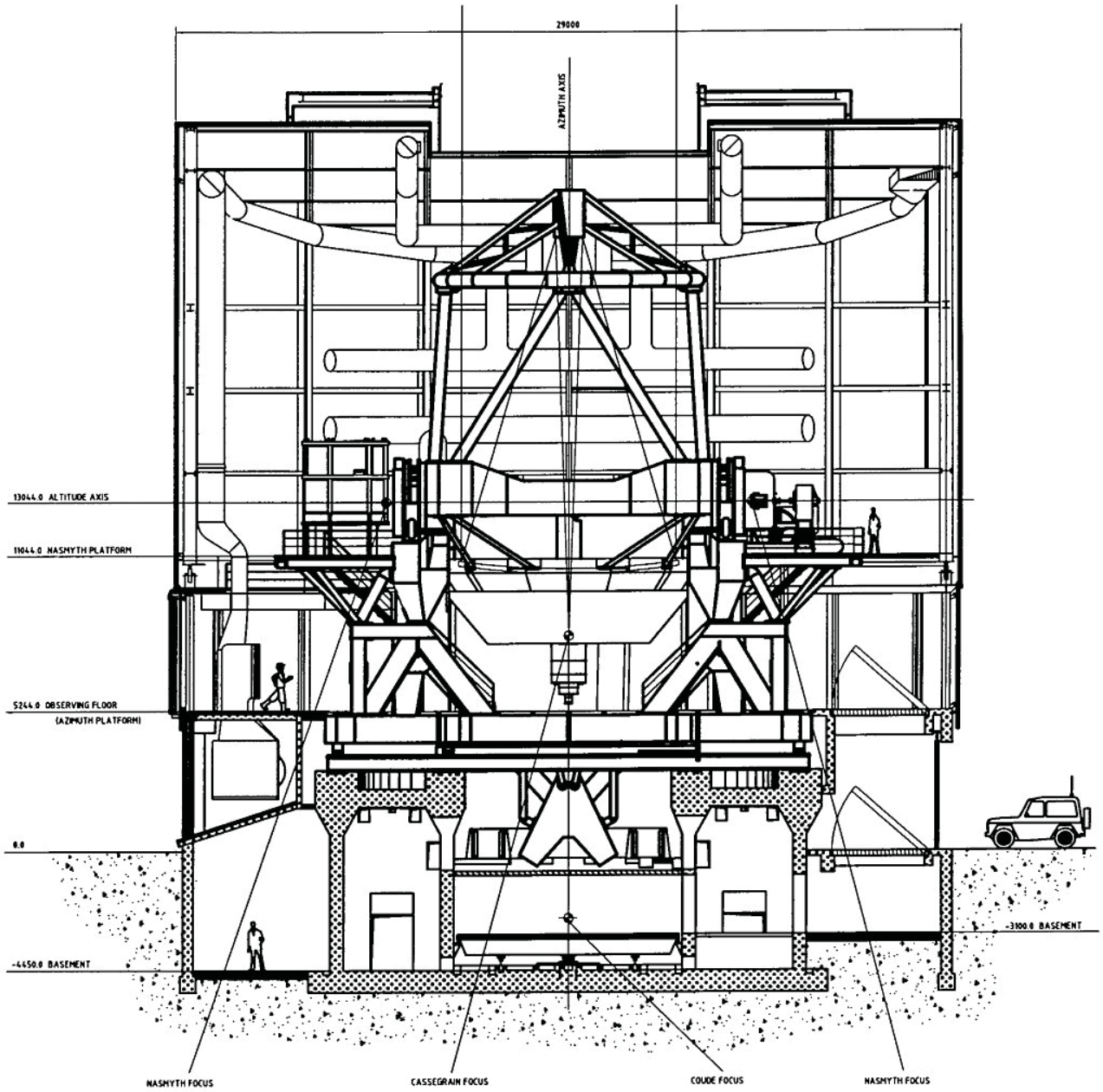
29000
AZIMUTH AXIS
13044.0 ALTITUDE AXIS
11044.0 NASMYTH PLATFORM
5244.0 OBSERVING FLOOR
(AZIMUTH PLATFORM)
0.0
-4450.0 BASEMENT
-3100.0 BASEMENT
NASMYTH FOCUS
CASSEGRAIN FOCUS
COUDE FOCUS
NASMYTH FOCUS

Figure 2.15.:

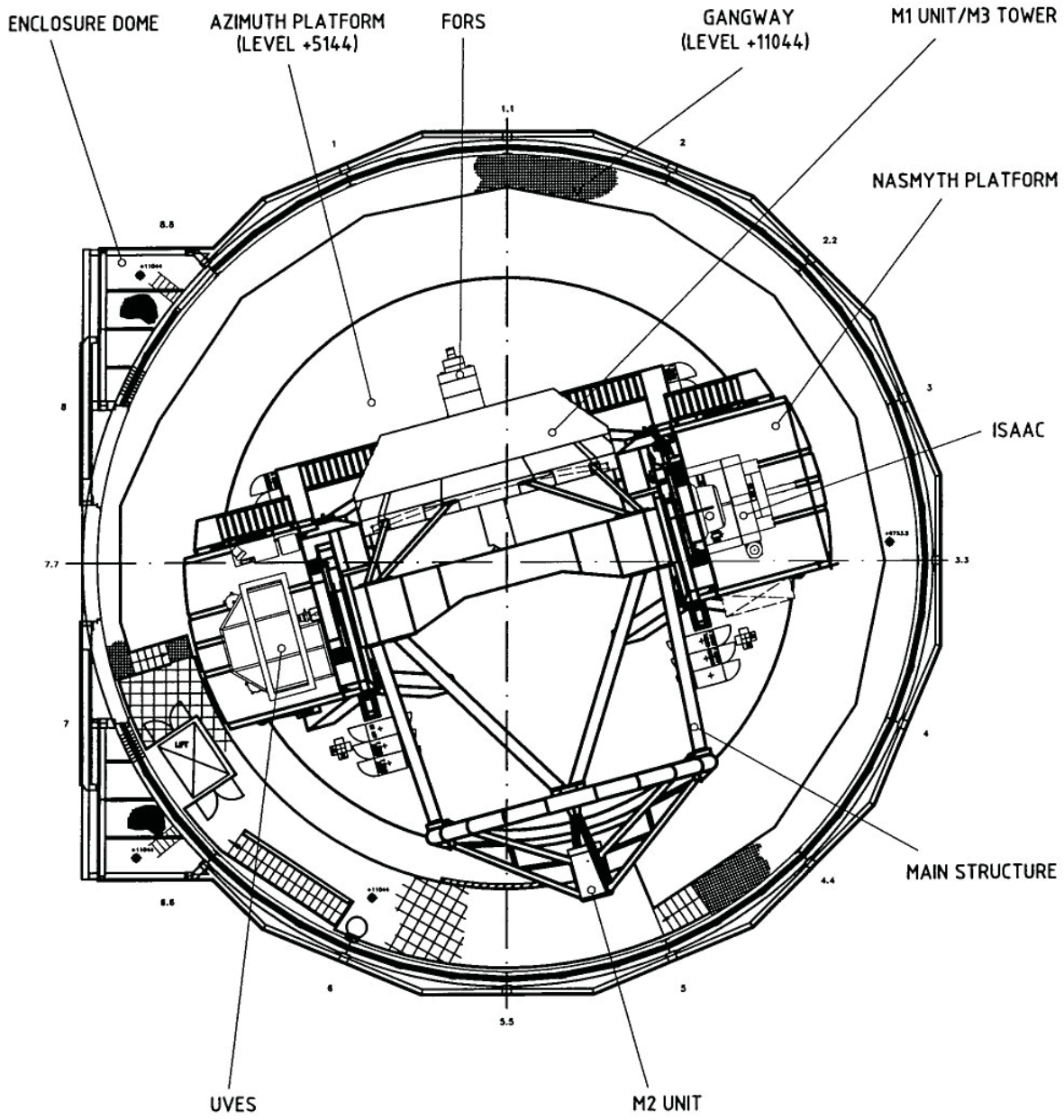
ENCLOSURE DOME
AZIMUTH PLATFORM
(LEVEL +5144)
FORS
GANGWAY
(LEVEL +11044)
M1 UNIT/M3 TOWER
NASMYTH PLATFORM
ISAAC
MAIN STRUCTURE
UVES
M2 UNIT

Figure 2.16.:


Pacific Ocean
Antofagasta
la Negra
Caleta
del Cobre
Hotel
area
2635
CERRO
PARANAL
Cerro
Armazones
3064
B70 Old Panamerican Highway
Paposo
Taltal
Panamerican Highway
0
50 km
Pacific Ocean
Antofagasta
La Silla
La Serena
Santiago
CHILE
0
200km

Figure 2.17.:

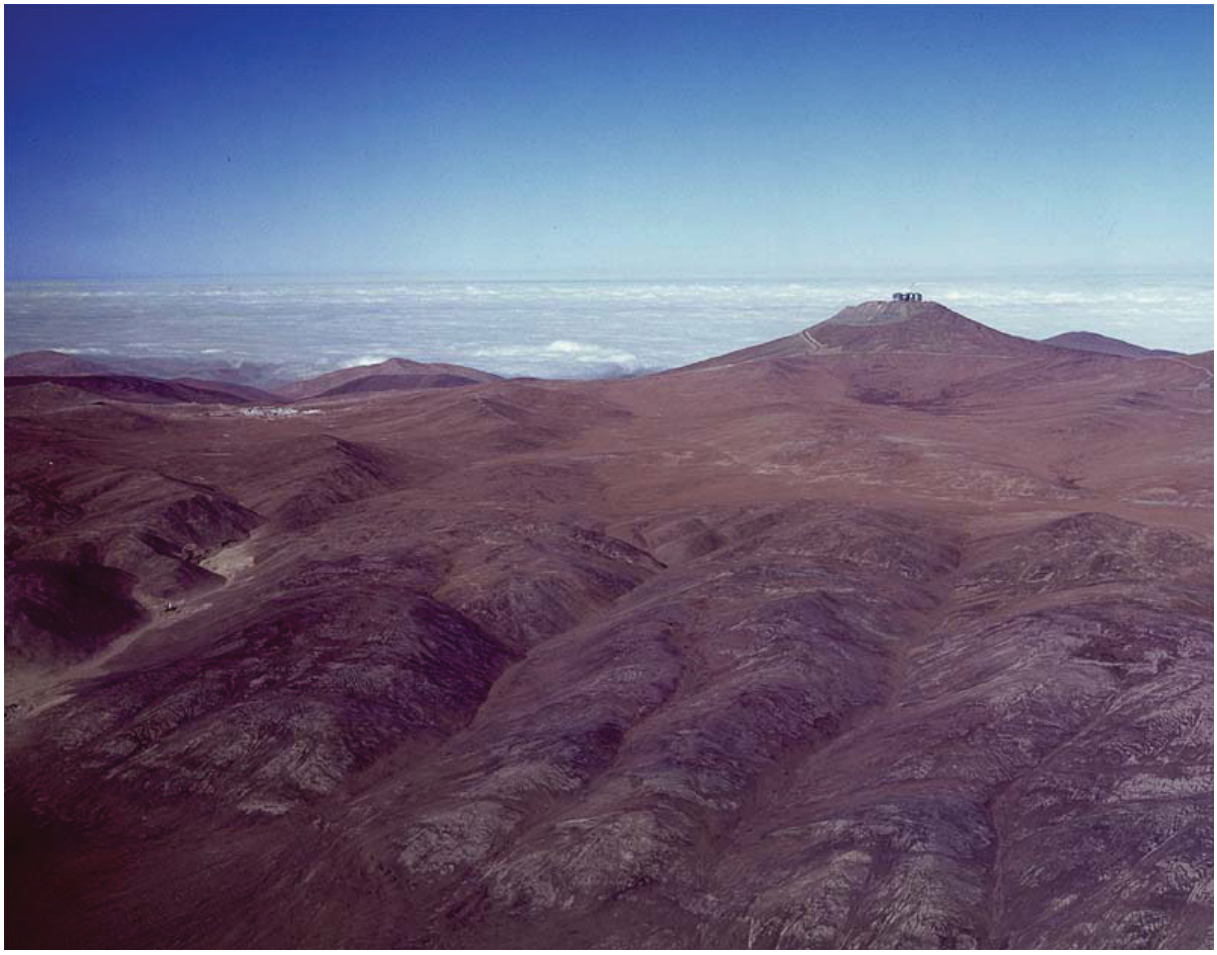

Figure 2.18.:

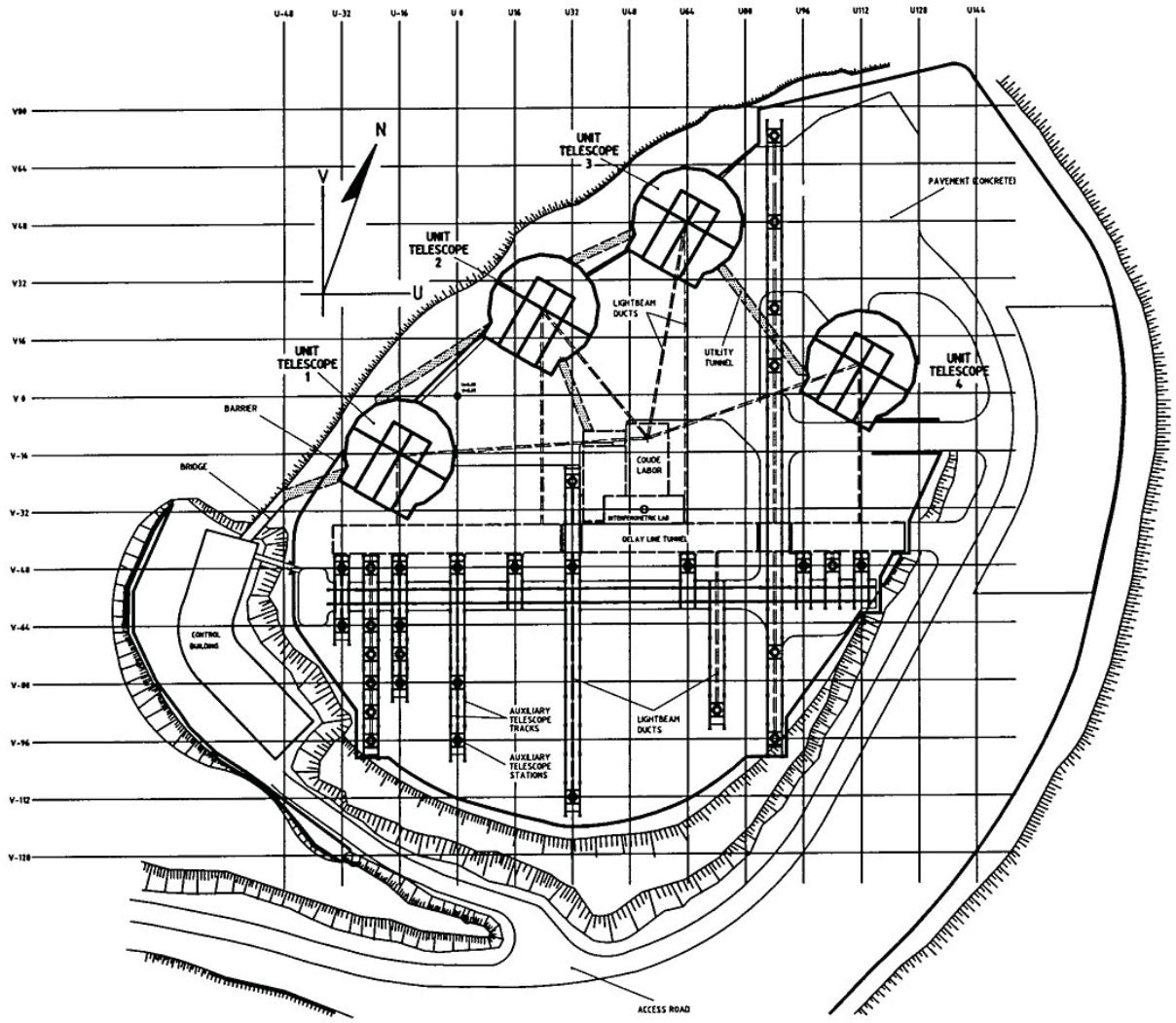
N
V
U
UNIT TELESCOPE 1
UNIT TELESCOPE 2
UNIT TELESCOPE 3
UNIT TELESCOPE 4
PAVEMENT (CONCRETE)
LIGHTBEAM DUCTS
UTILITY TUNNEL
BARRIER
BRIDGE
COUDE LABOR
INTERFEROMETRIC LAB
DELAY LINE TUNNEL
CONTROL BUILDING
AUXILIARY TELESCOPE TRACKS
AUXILIARY TELESCOPE STATIONS
LIGHTBEAM DUCTS
ACCESS ROAD

Figure 2.19.:

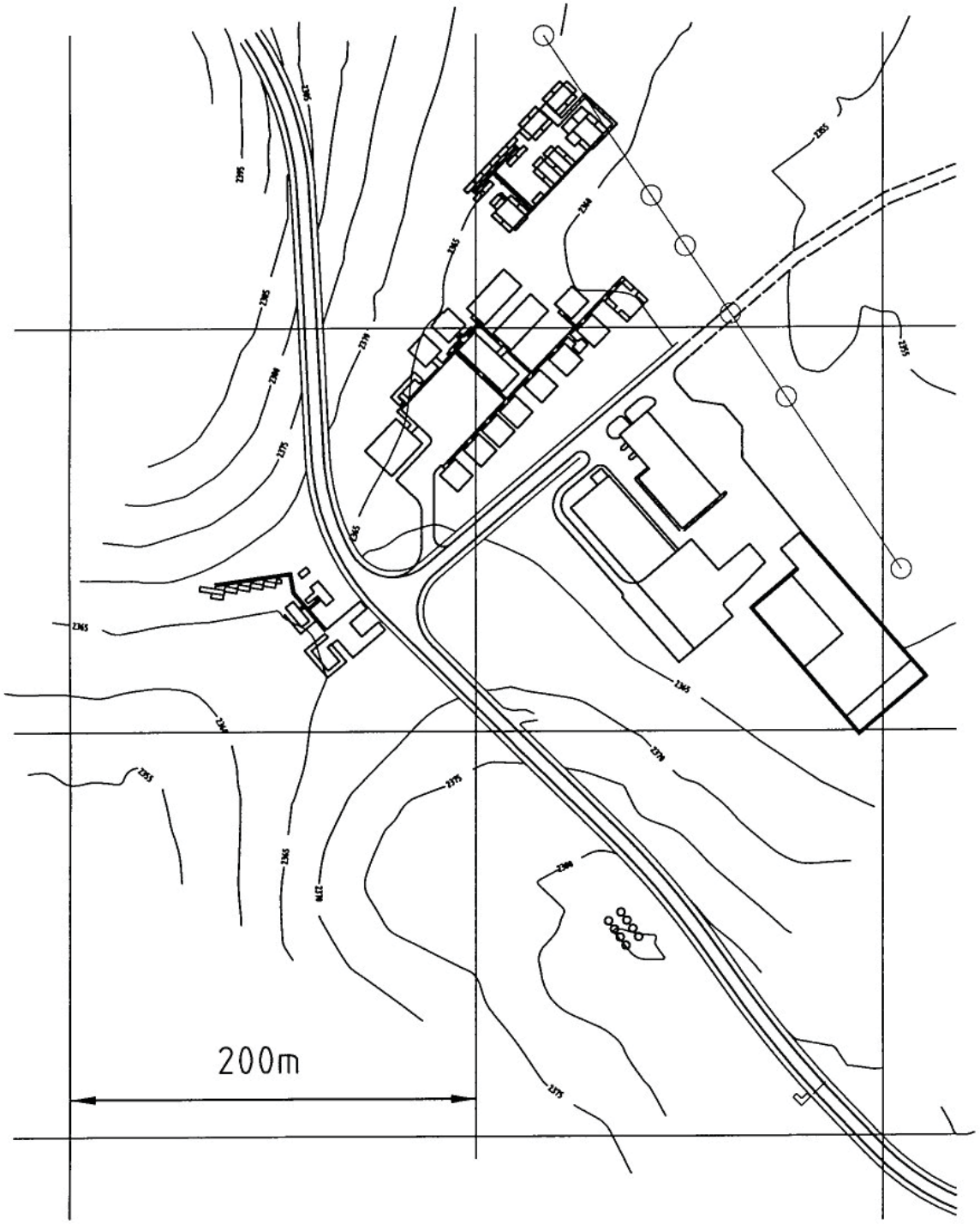

Figure 2.20.:

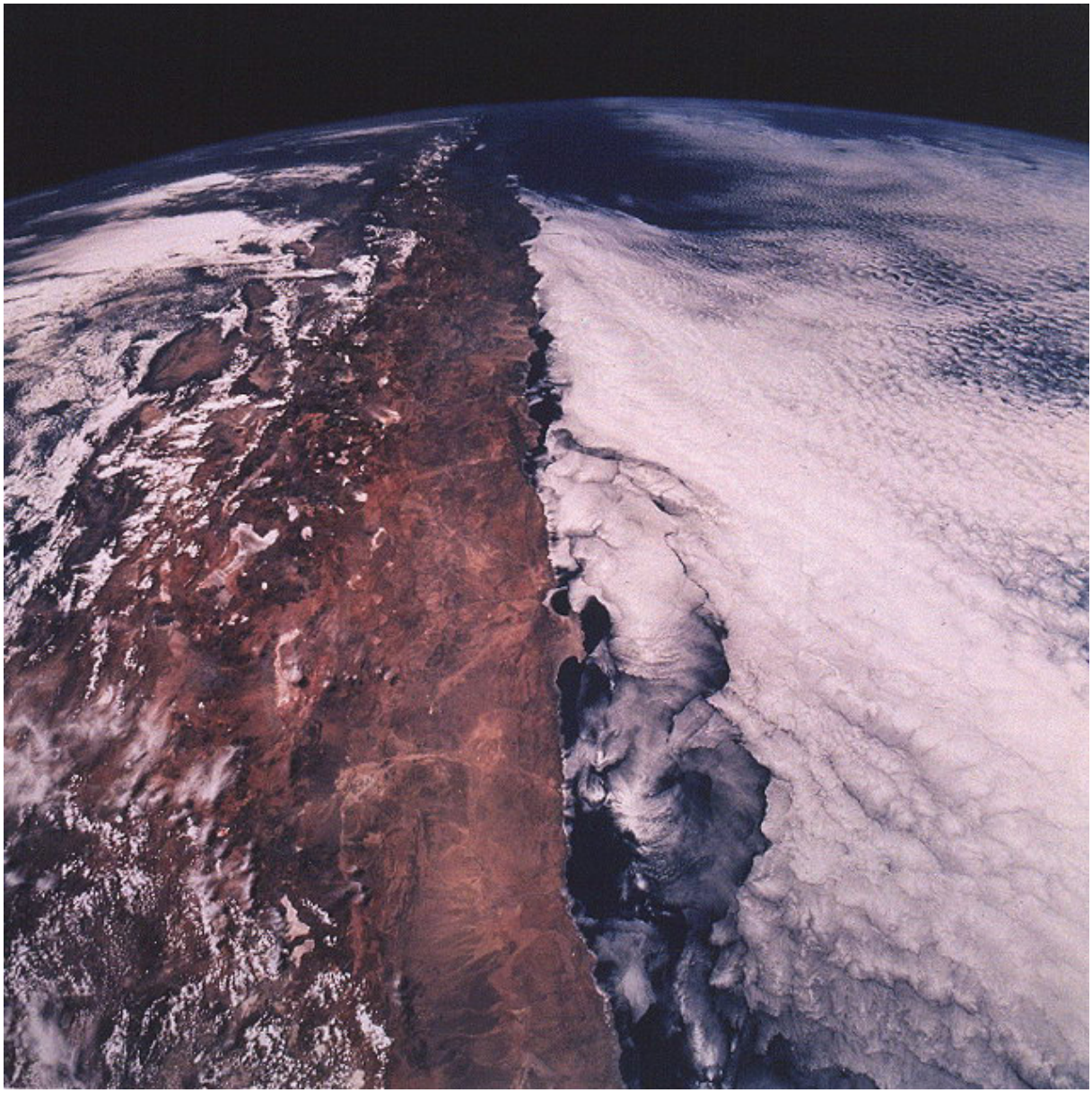

Figure 2.21.:

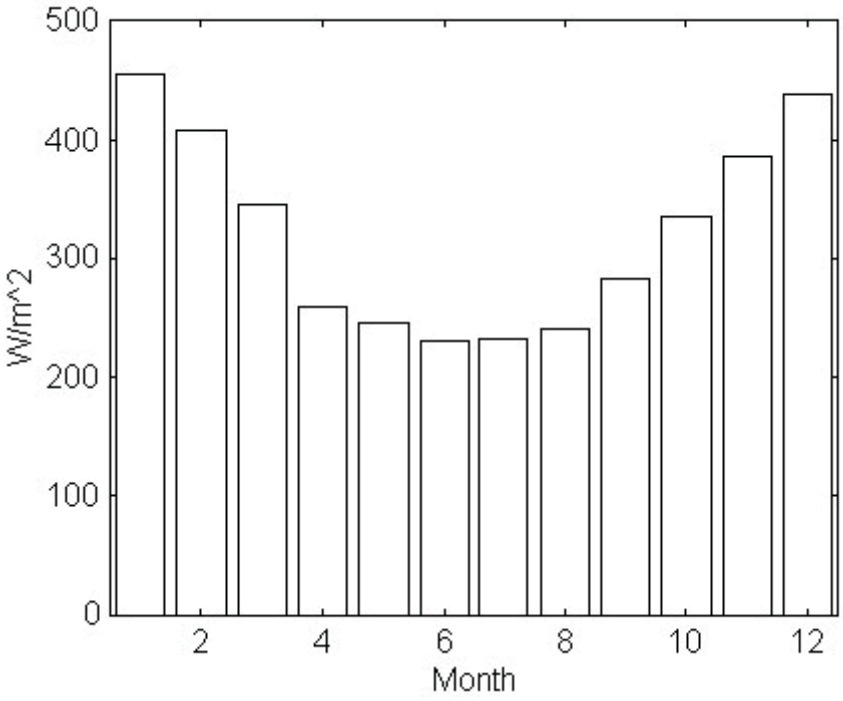

Figure 2.22.:

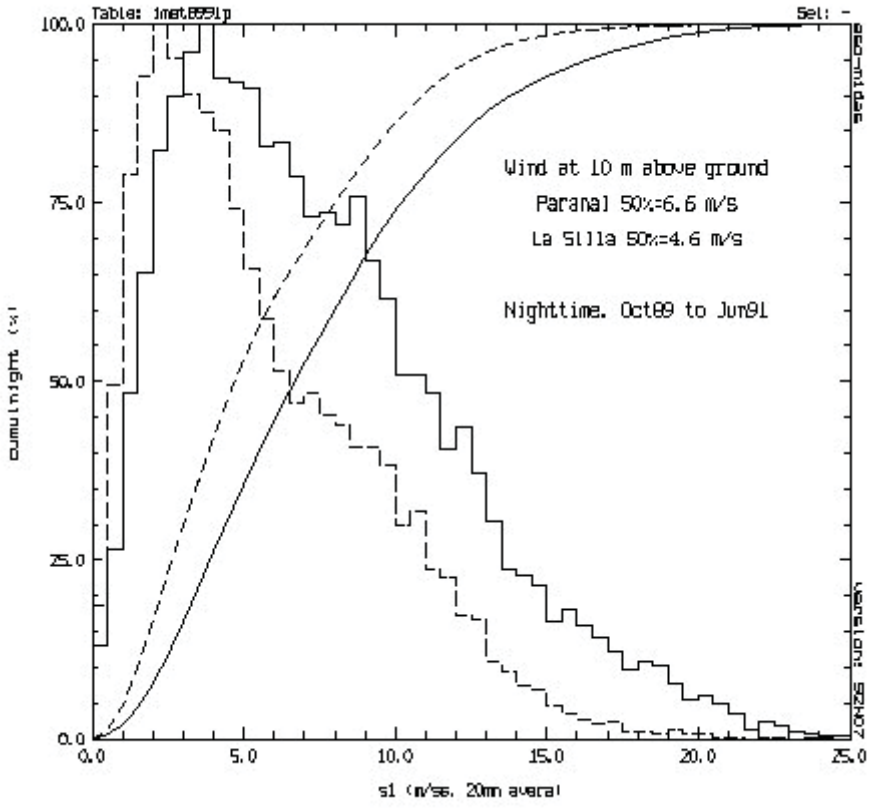

Figure 2.23.:

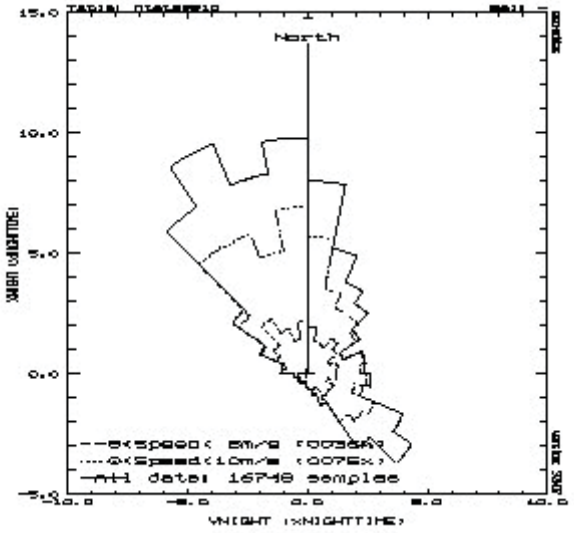

Figure 2.24.:

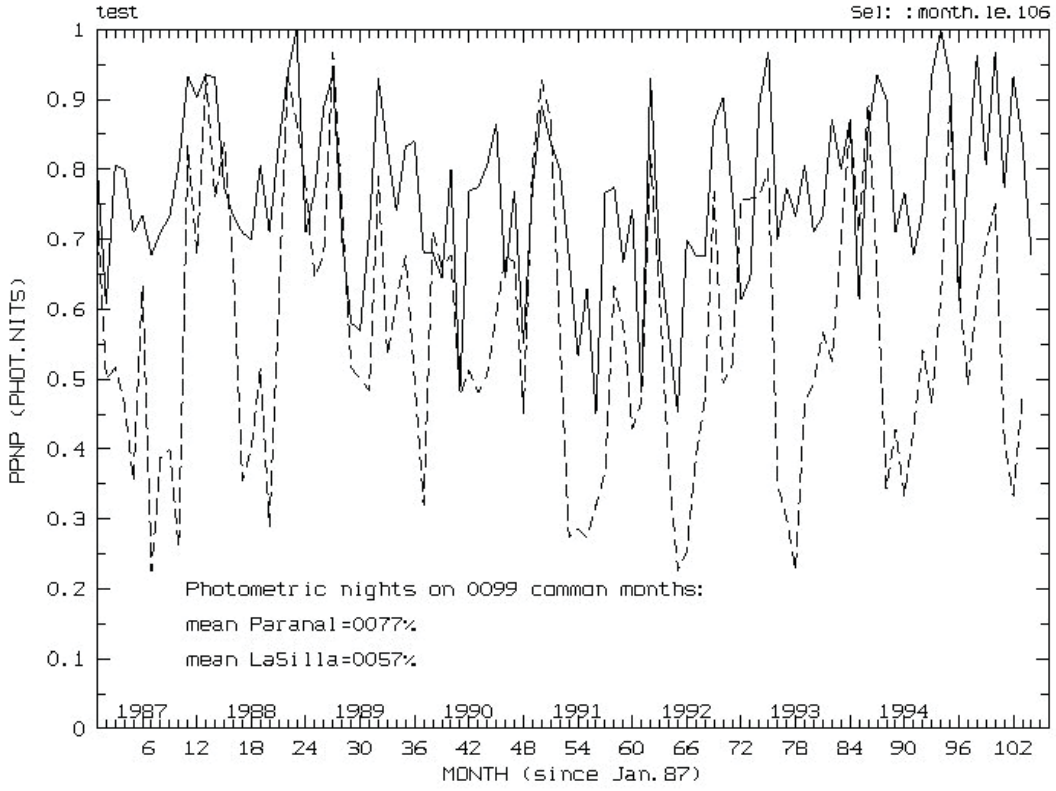

Figure 2.25.:

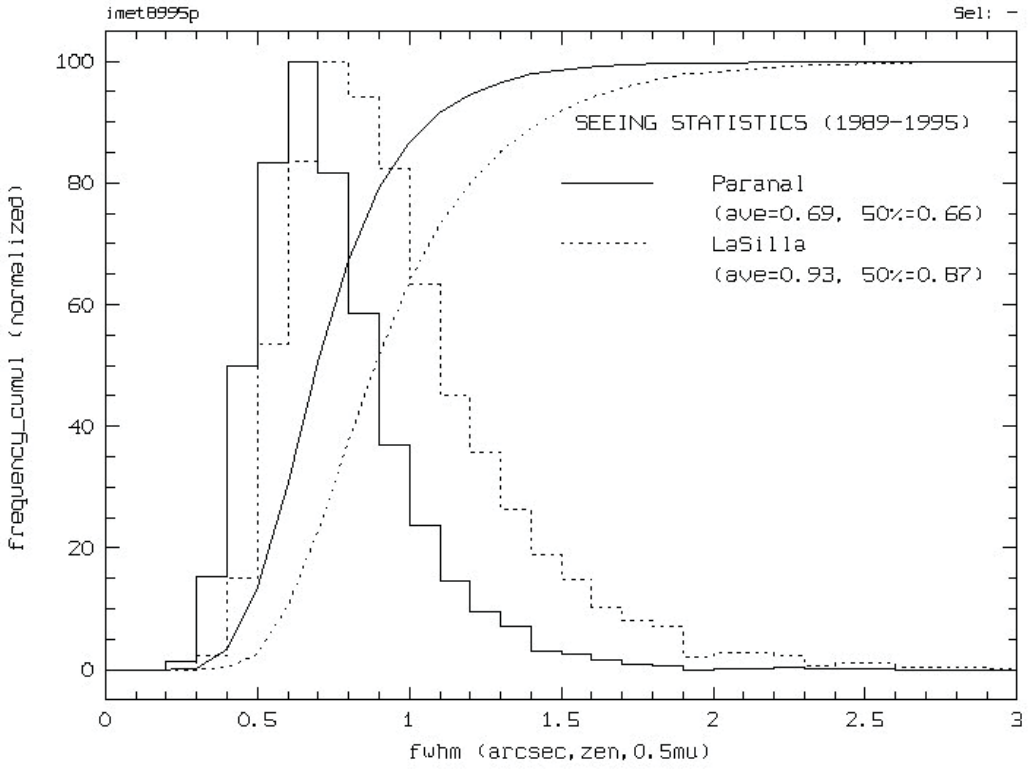

Figure 2.26.:

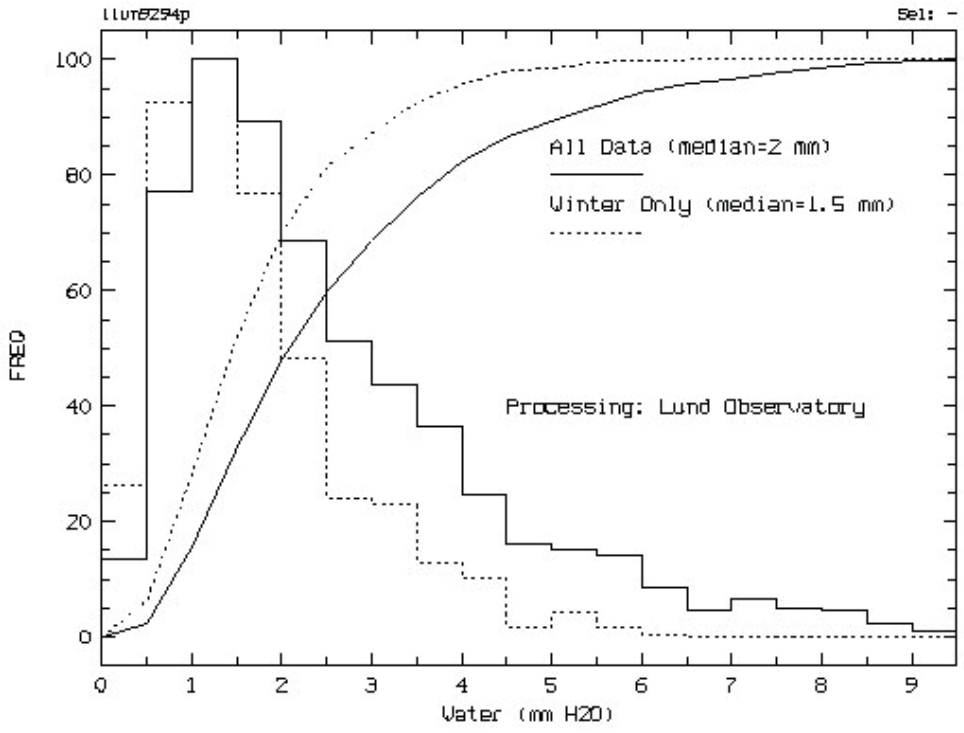

Figure 2.27.:

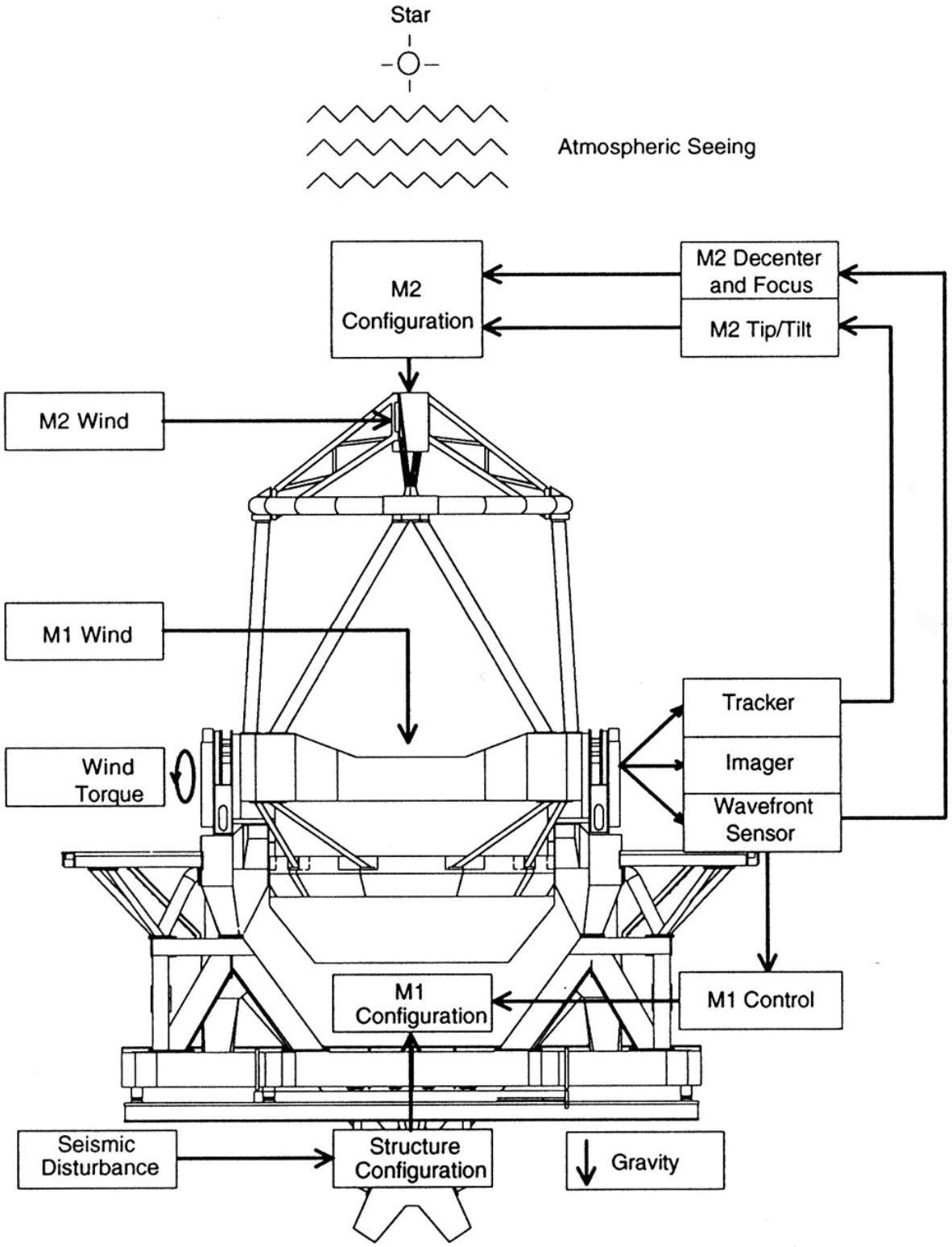
Star
Atmospheric Seeing
M2 Configuration
M2 Decenter and Focus
M2 Tip/Tilt
M2 Wind
M1 Wind
Wind Torque
Tracker
Imager
Wavefront Sensor
M1 Configuration
M1 Control
Seismic Disturbance
Structure Configuration
Gravity

Figure 2.28.:

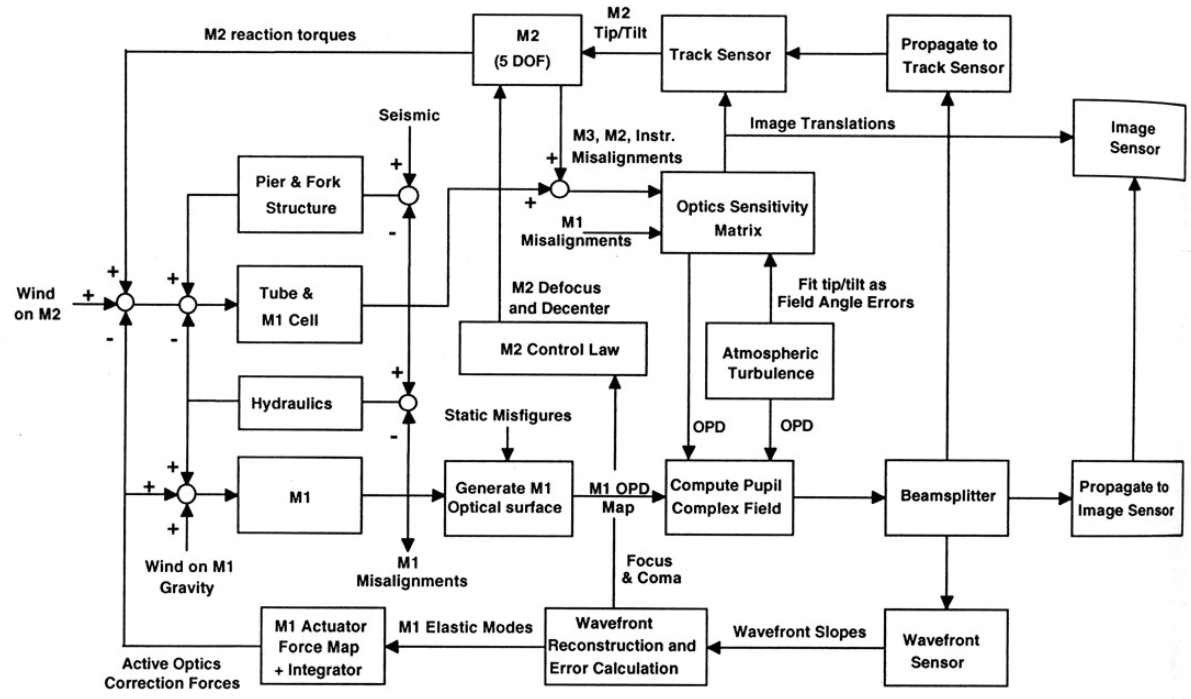
M2 reaction torques
M2
(5 DOF)
M2
Tip/Tilt
Track Sensor
Propagate to
Track Sensor
Image Translations
Image
Sensor
Seismic
M3, M2, Instr.
Misalignments
Pier & Fork
Structure
Optics Sensitivity
Matrix
M1
Misalignments
Wind
on M2
Tube &
M1 Cell
M2 Defocus
and Decenter
Fit tip/tilt as
Field Angle Errors
M2 Control Law
Atmospheric
Turbulence
Hydraulics
Static Misfigures
OPD
OPD
M1
Generate M1
Optical surface
M1 OPD
Map
Compute Pupil
Complex Field
Beamsplitter
Propagate to
Image Sensor
Wind on M1
Gravity
M1
Misalignments
Focus
& Coma
M1 Actuator
Force Map
+ Integrator
M1 Elastic Modes
Wavefront
Reconstruction and
Error Calculation
Wavefront Slopes
Wavefront
Sensor
Active Optics
Correction Forces

Figure 3.1.:

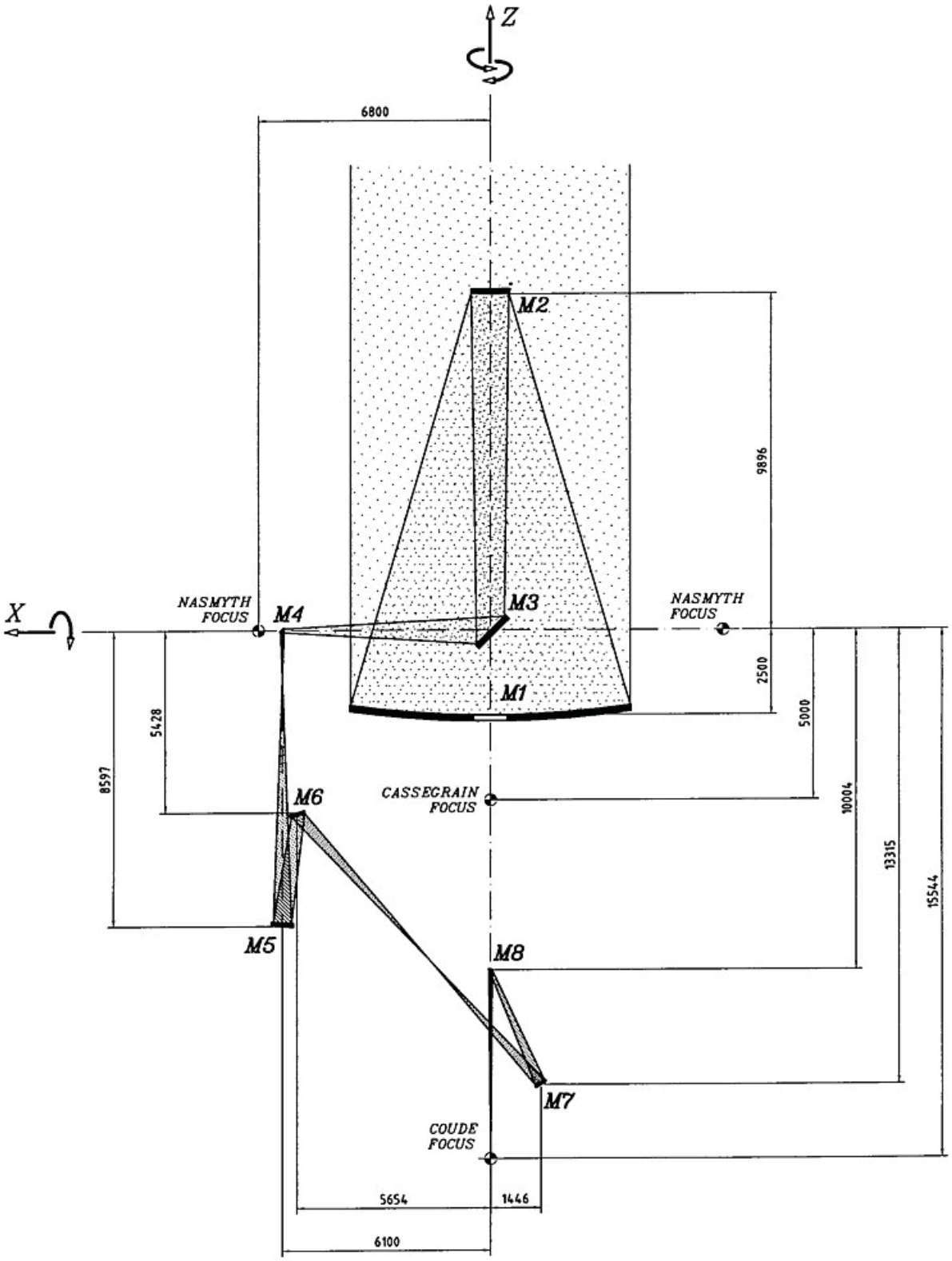
Z
X
6800
M1
M2
M3
M4
M5
M6
M7
M8
NASMYTH FOCUS
NASMYTH FOCUS
CASSEGRAIN FOCUS
COUDE FOCUS
9896
2500
5000
10004
13315
15544
8597
5428
5654
1446
6100

Figure 3.2.:

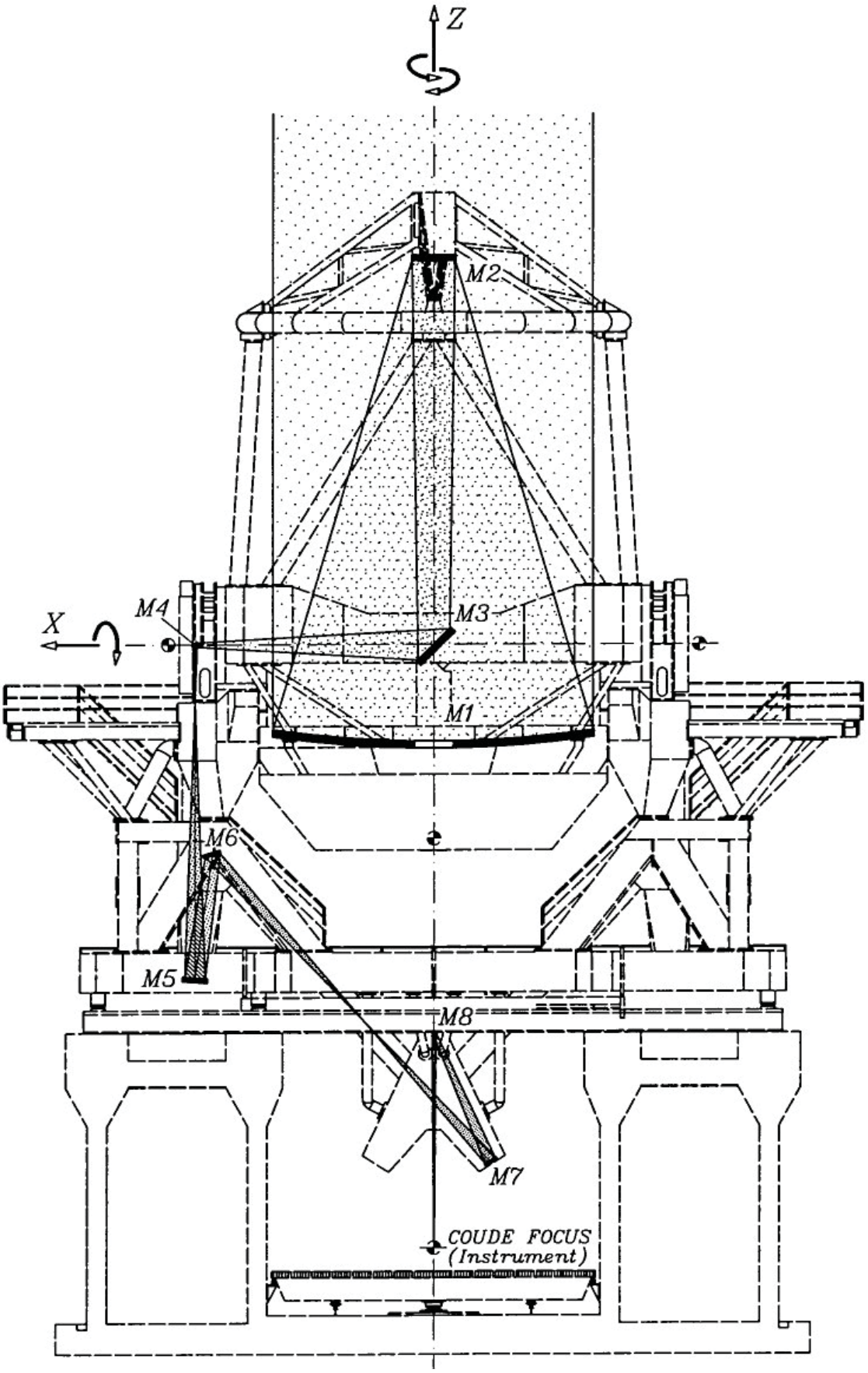

Figure 3.3.:

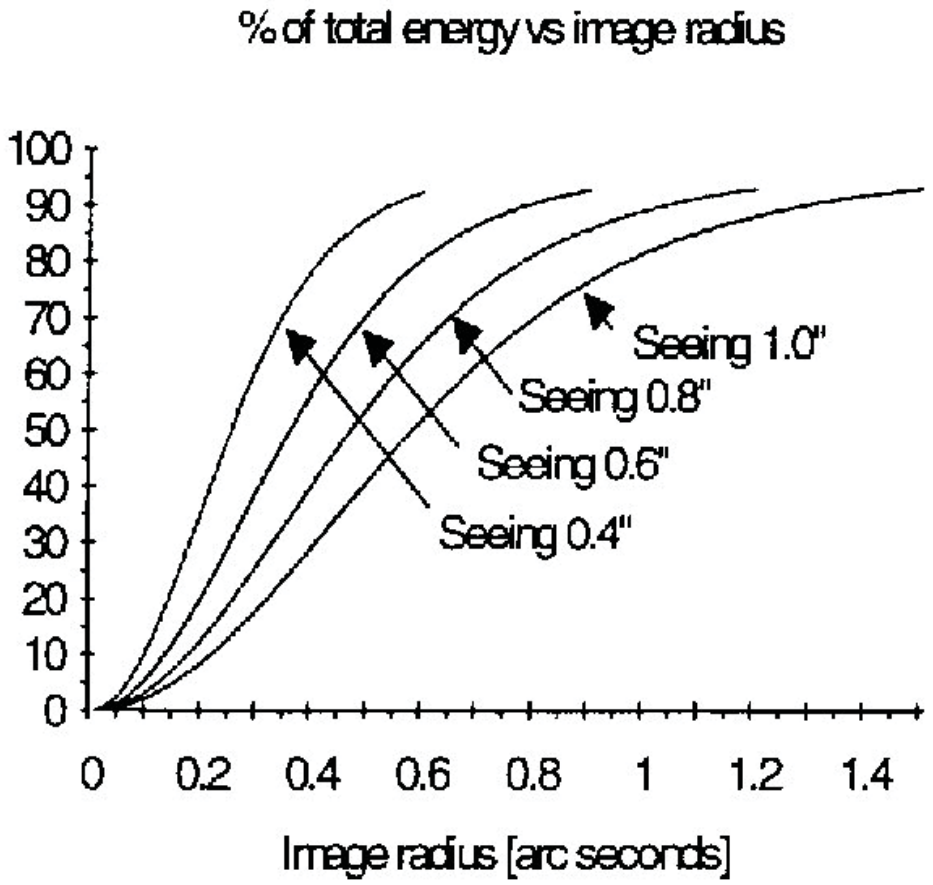

Figure 3.4.:

Figure 3.5.:

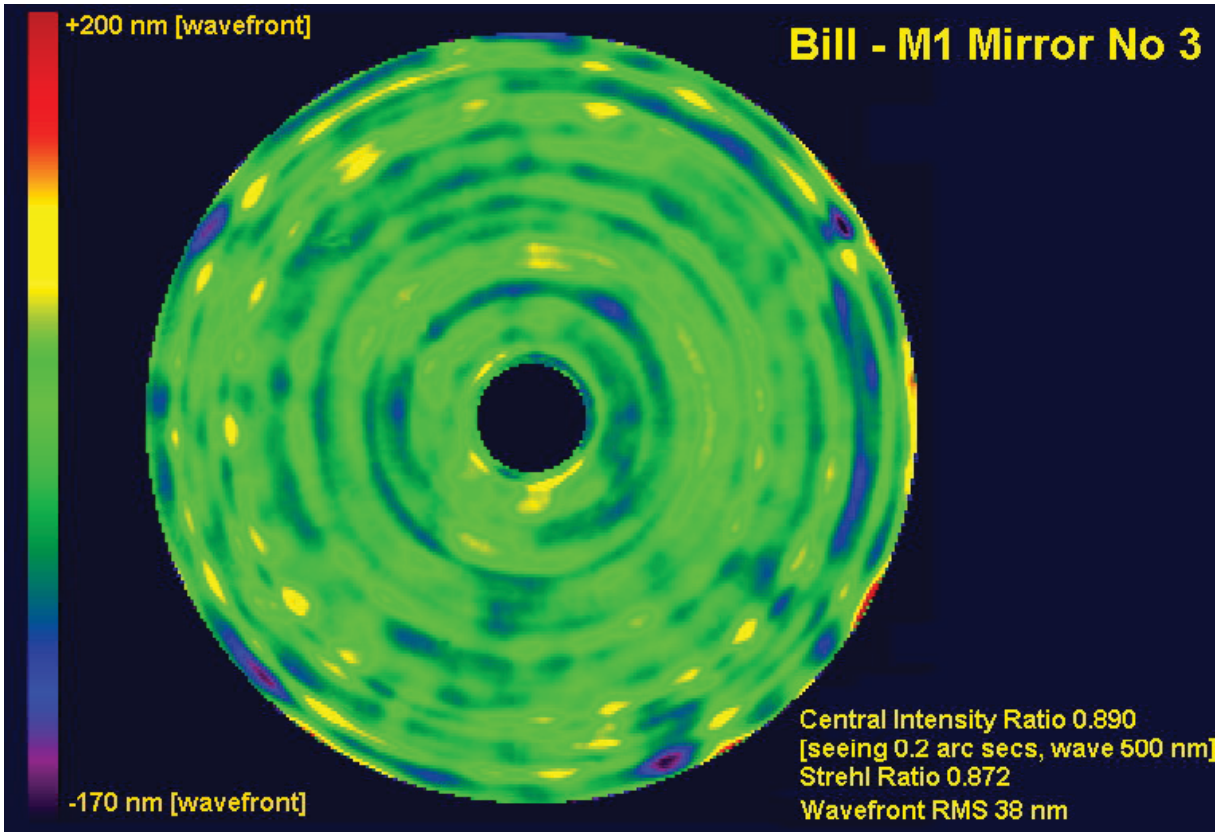

Figure 3.6.:

Figure 3.7.:

Figure 3.8.:

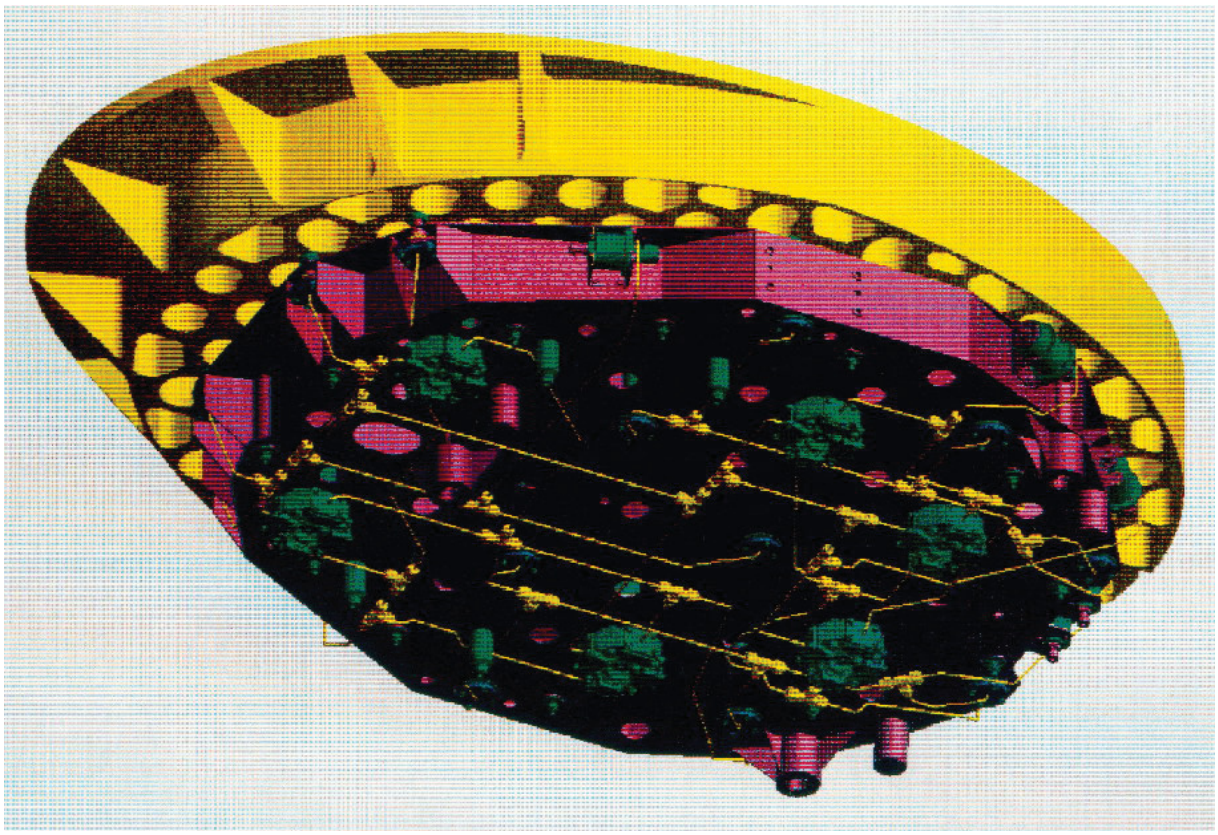

Figure 3.9.:

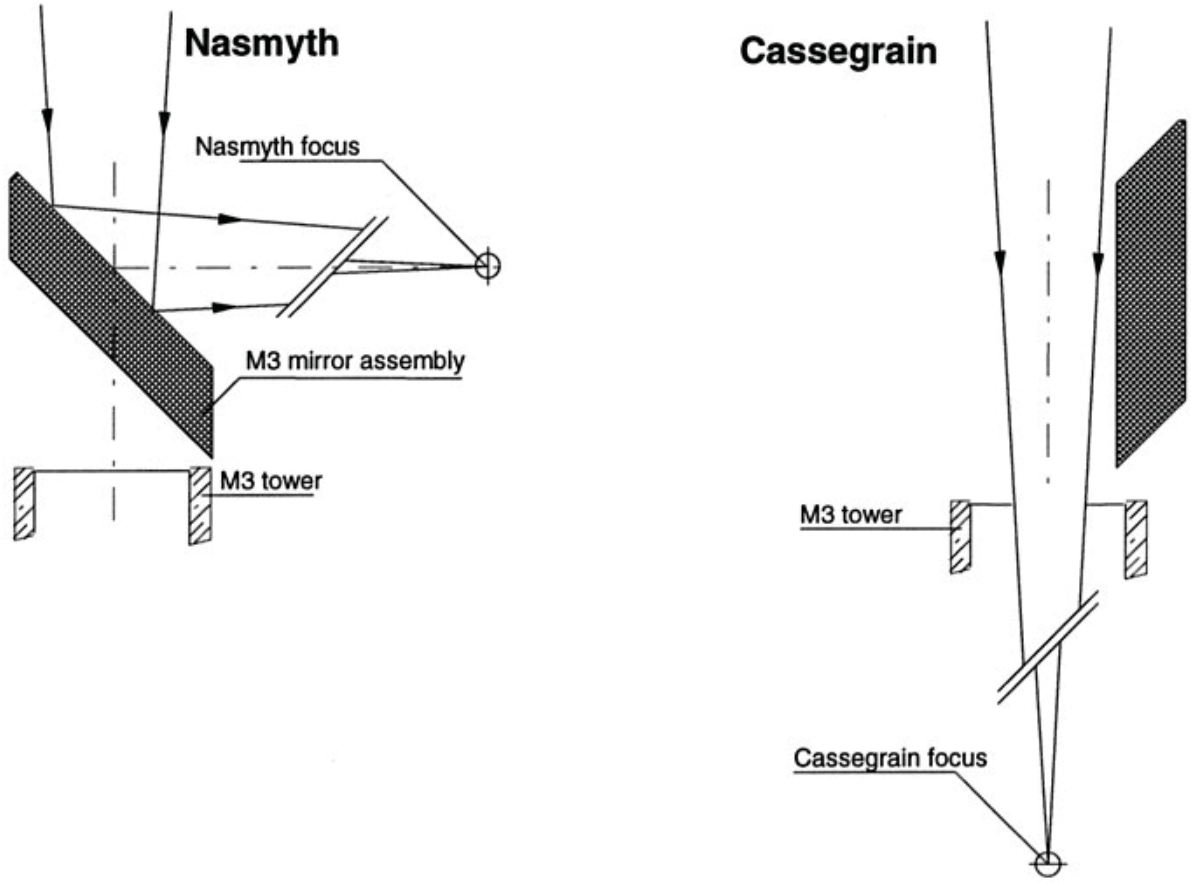
Nasmyth
Nasmyth focus
M3 mirror assembly
M3 tower
Cassegrain
M3 tower
Cassegrain focus

Figure 3.10.:

Figure 3.11.:

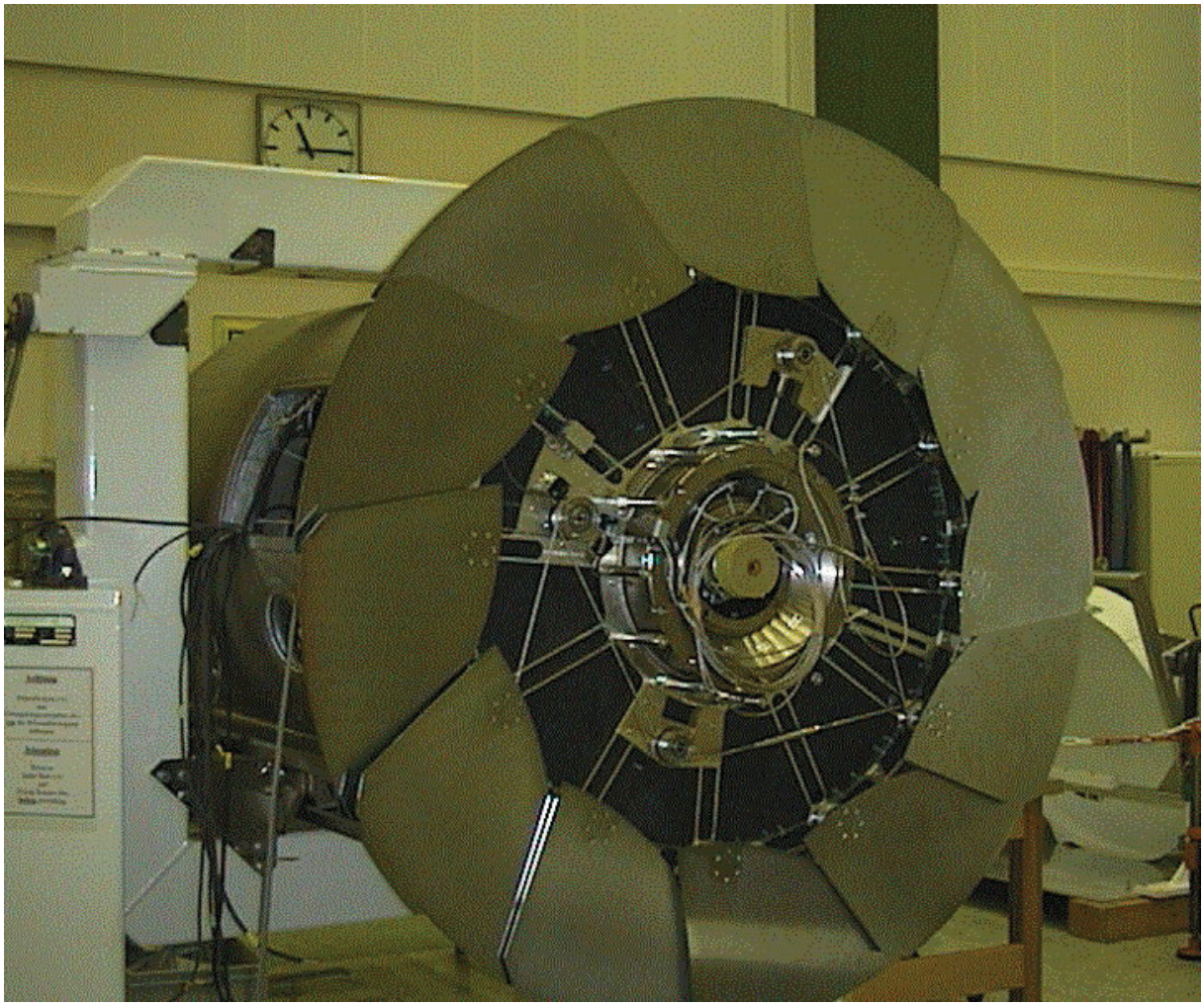

Figure 3.12.:

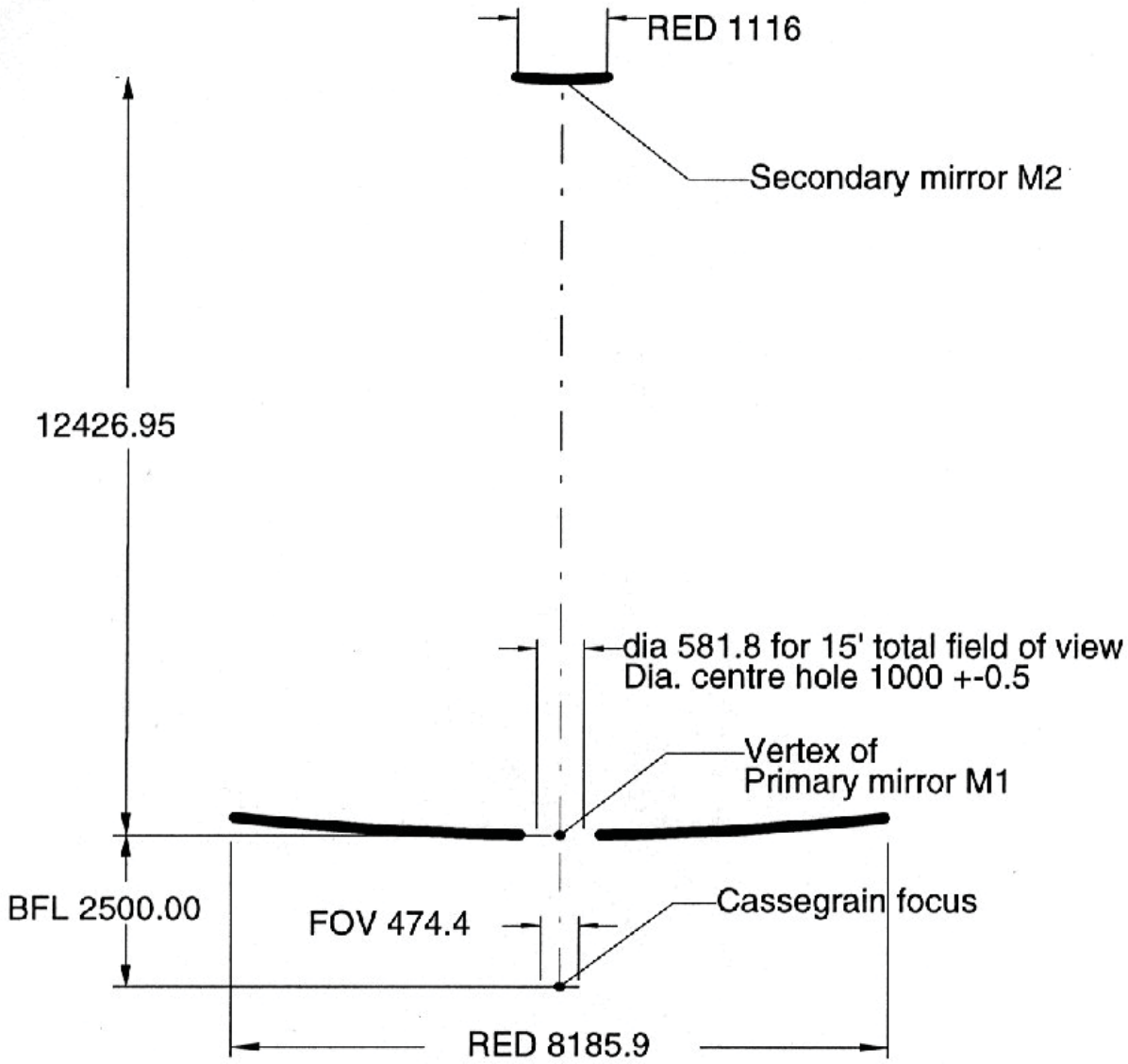

Figure 3.13.:

Parameter		Value		
Entrance pupil dia.		EPD	8115.0	mm
Exit pupil dia.		EXP	1113.1	mm
Focal ratio		FNO	13.4106	-
Focal length		EFL	108827	mm
Object field of view	Total	FOV	15	arc min
	Unvignetted	UFOV	2.68	arc min
Image field of view	Total[4]	FOV	474.4	mm
	Unvignetted[5]	UFOV	85.0	mm

Figure 3.14.:

Field radius [Degrees]	Centroid [mm]
0.00	0.000
0.01	19.006
0.02	38.011
0.03	57.015
0.04	76.017
0.05	95.017
0.06	114.014
0.07	133.008
0.08	151.998
0.09	170.984
0.10	189.964
0.11	208.938
0.12	227.906

Figure 3.15.:

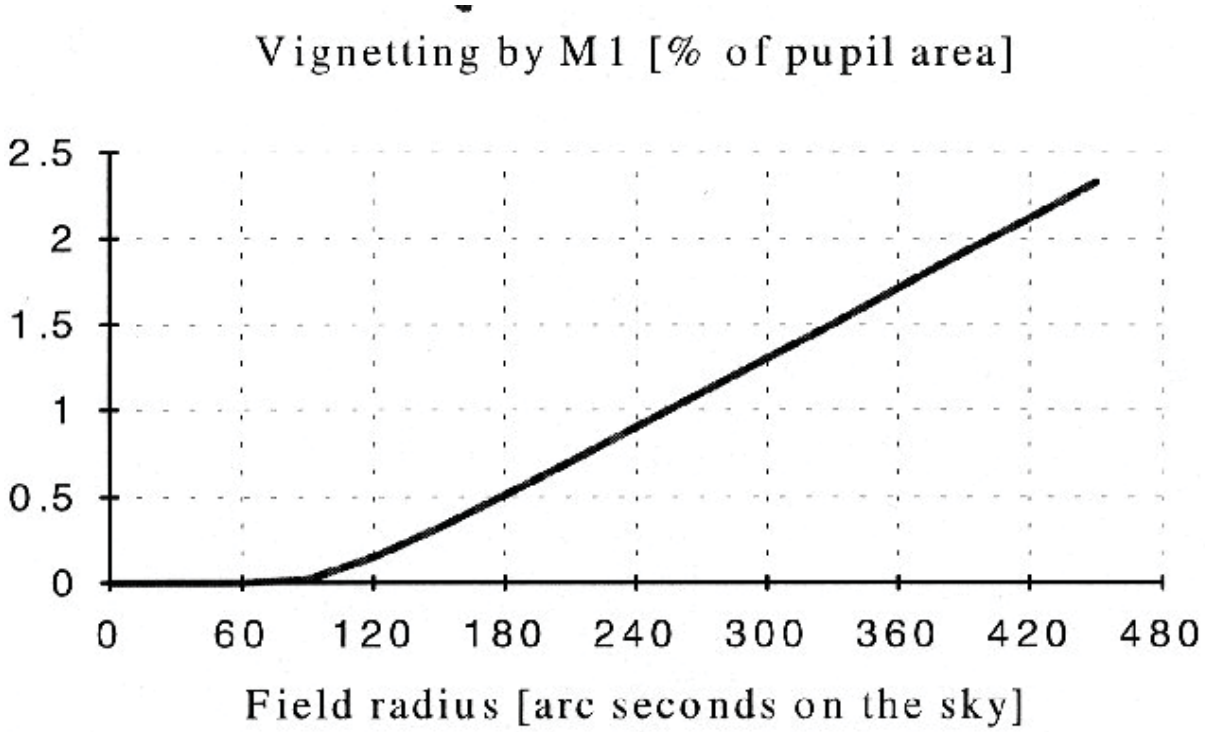

Figure 3.16.:

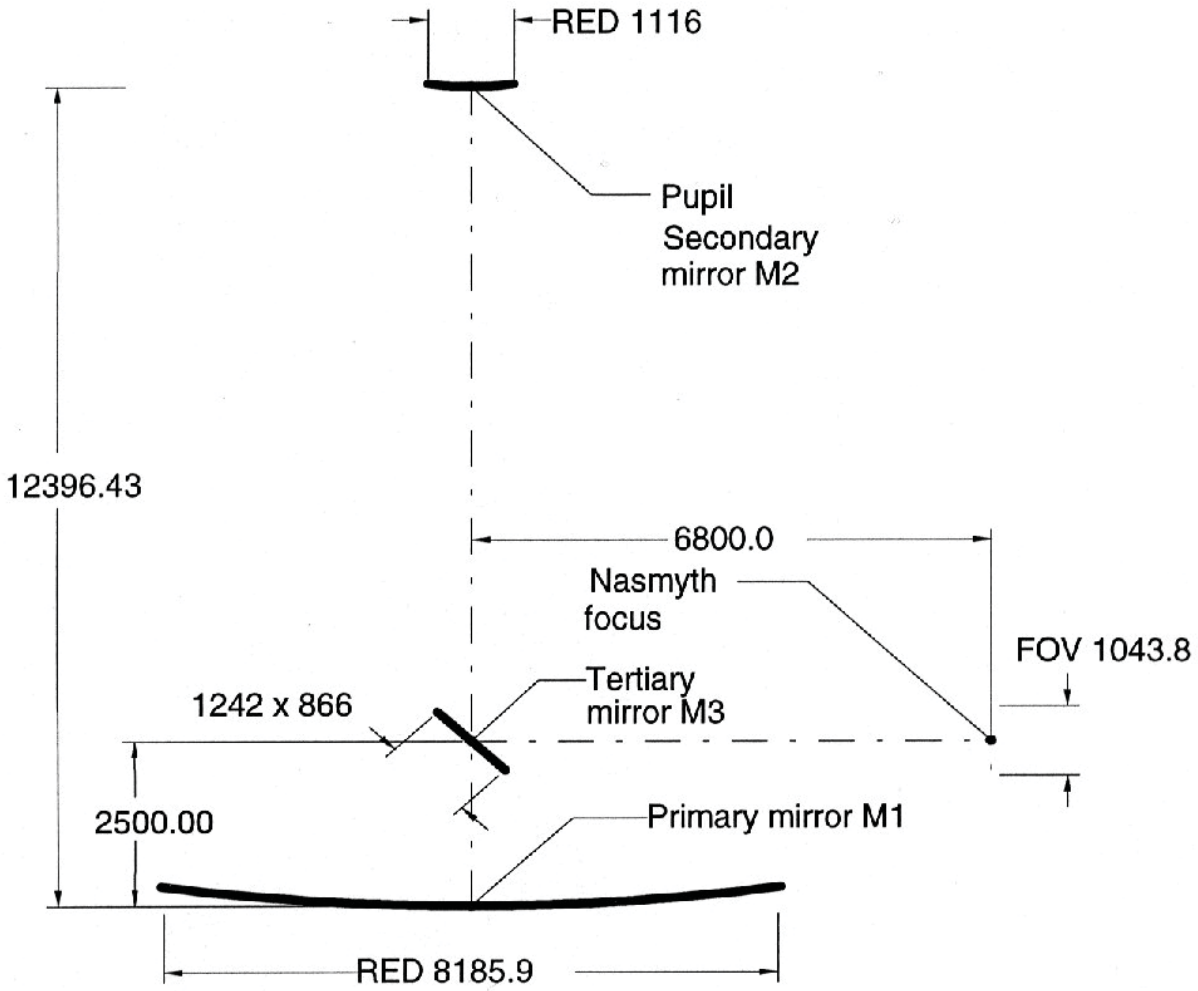

Figure 3.17.:

Parameter		Value		
Entrance pupil dia.		EPD	8000	mm
Exit pupil dia.		EXP	1113.1	mm
Focal ratio		FNO	15.000	-
Focal length		EFL	120000	mm
Object field of view	Total	FOV	30	arc min
	Unvignetted[17]	UFOV	7.15	arc min
Image field of view	Total	FOV	1043.8	mm
	Unvignetted[18]	UFOV	249.6	mm

Figure 3.18.:

Field radius [degrees]	Centroid [mm]	Field radius [degrees]	Centroid [mm]
0.00	0	0.13	272.036
0.01	20.944	0.14	292.921
0.02	41.887	0.15	313.797
0.03	62.829	0.16	334.662
0.04	83.769	0.17	355.518
0.05	104.707	0.18	376.362
0.06	125.641	0.19	397.194
0.07	146.572	0.20	418.017
0.08	167.498	0.21	438.826
0.09	188.418	0.22	459.622
0.10	209.333	0.23	480.404
0.11	230.242	0.24	501.174
0.12	251.143	0.25	521.927

Figure 3.19.:

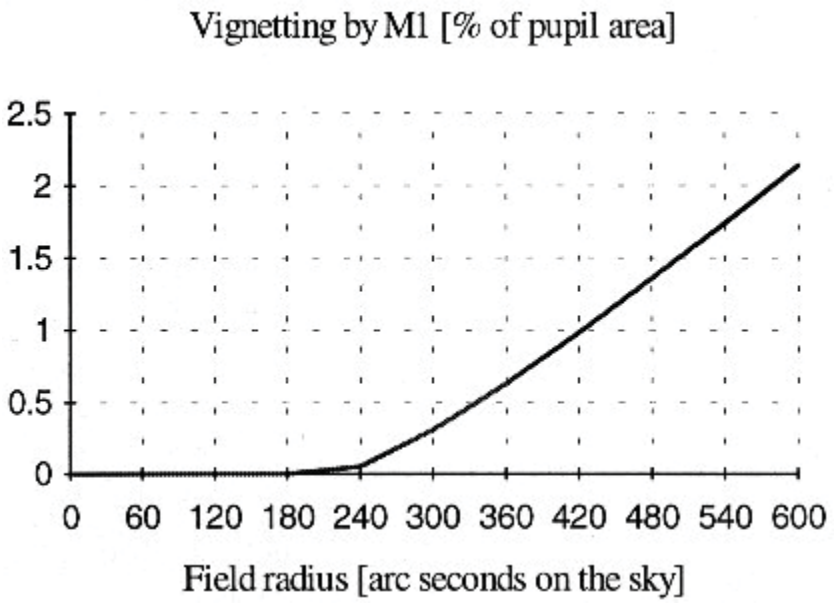

Figure 3.20.:

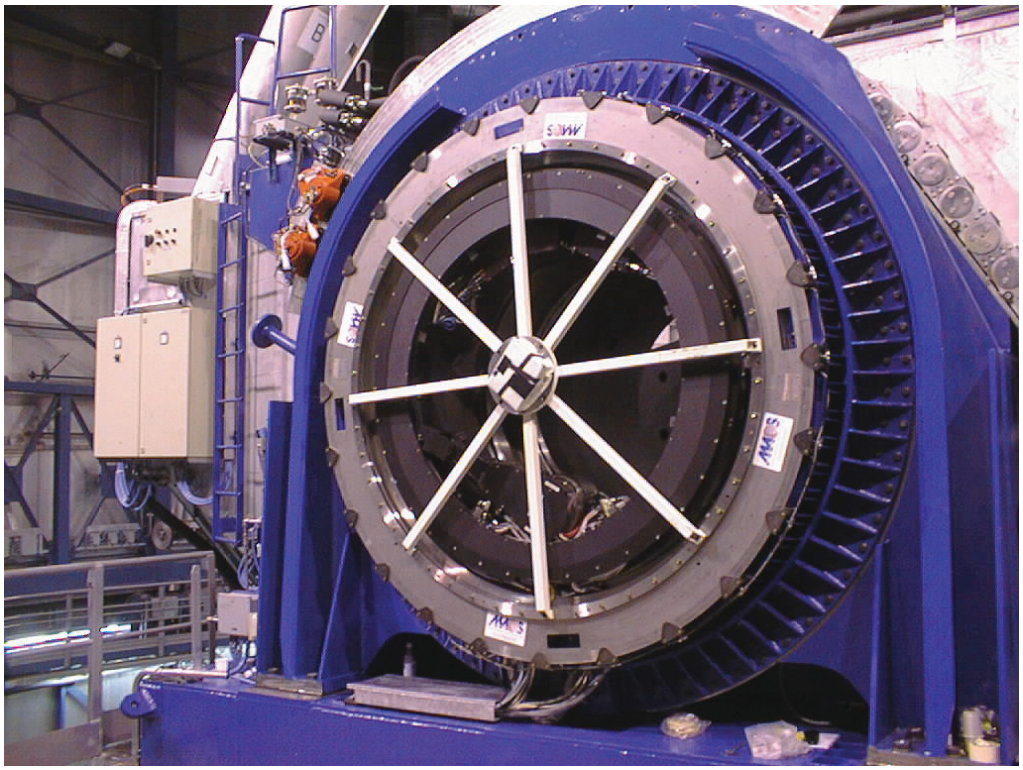

Figure 3.21.:

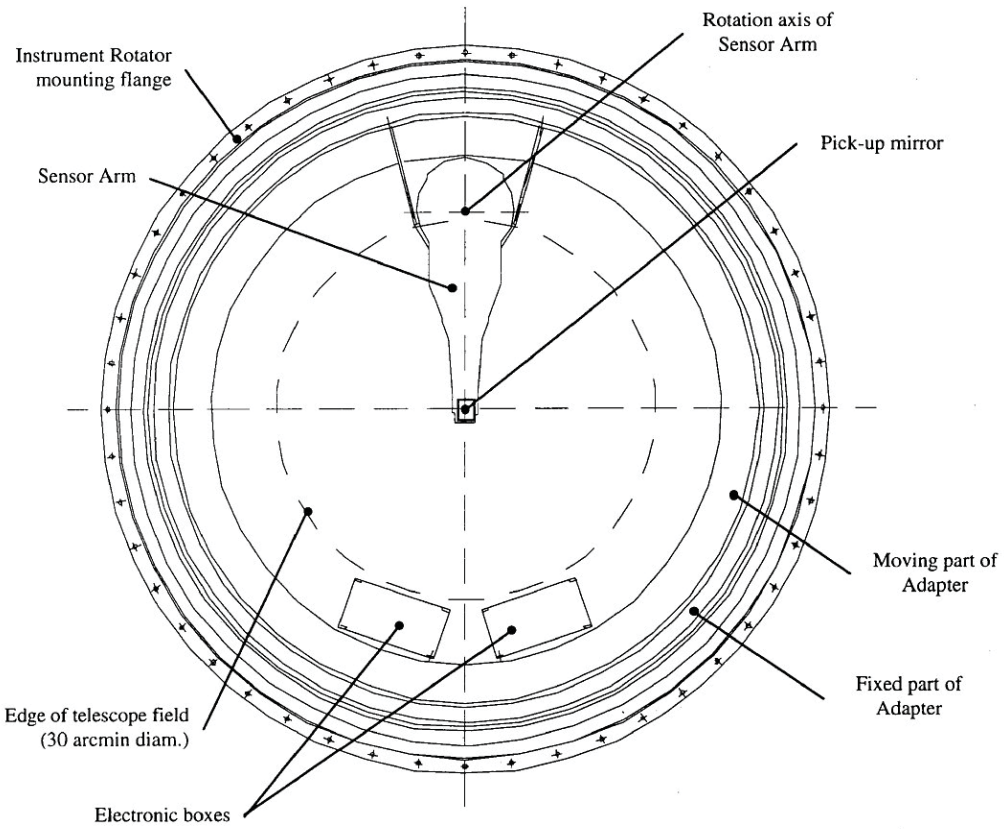

Figure 3.22.:

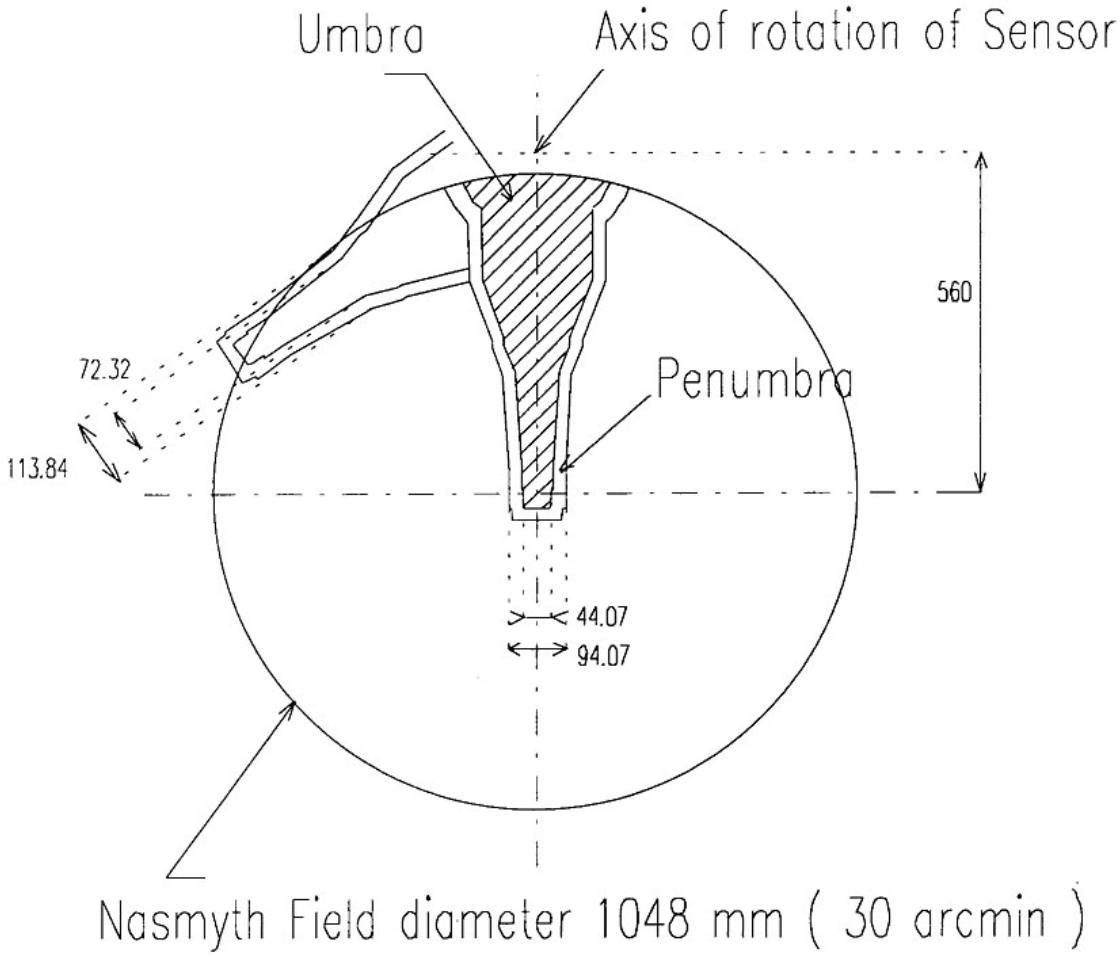
Umbra
Axis of rotation of Sensor
560
72.32
113.84
Penumbra
44.07
94.07
Nasmyth Field diameter 1048 mm (30 arcmin)

Figure 3.23.:

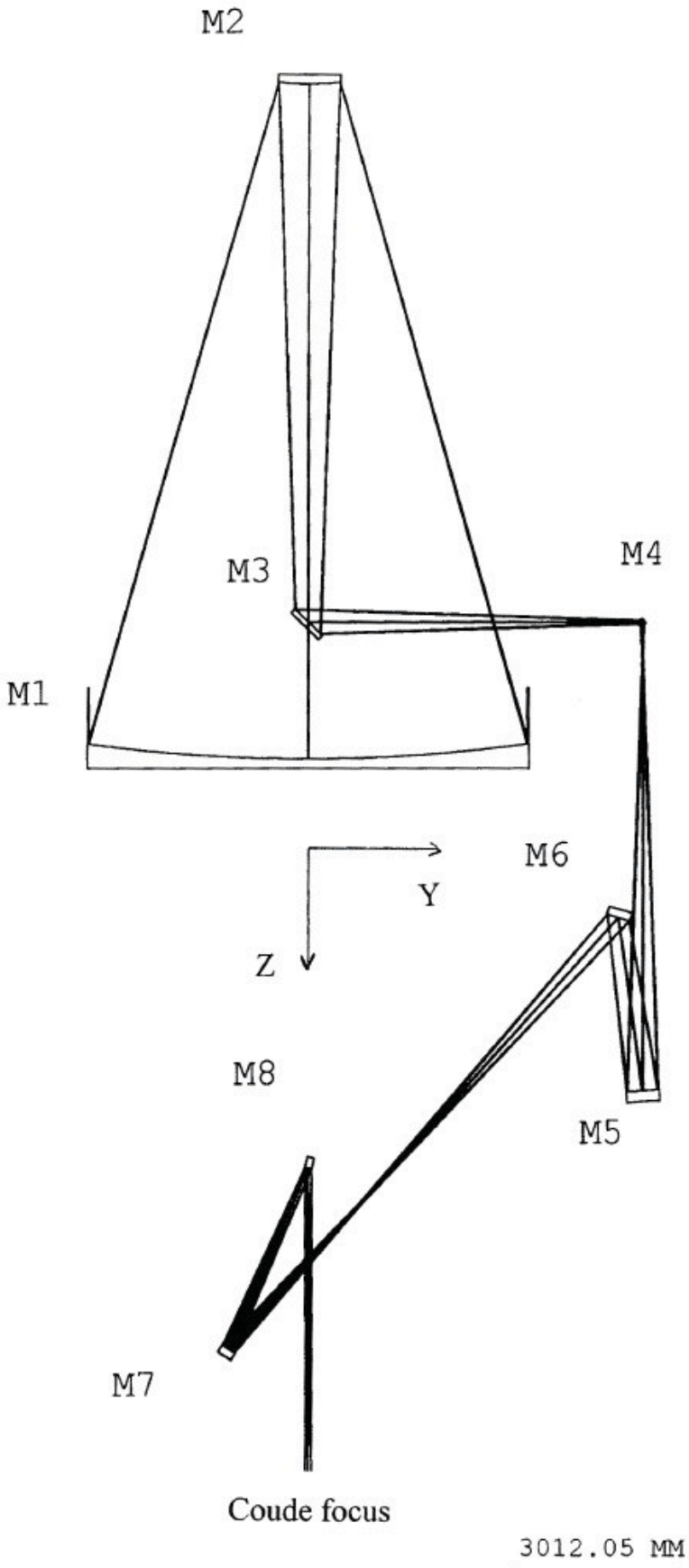

Figure 3.24.:

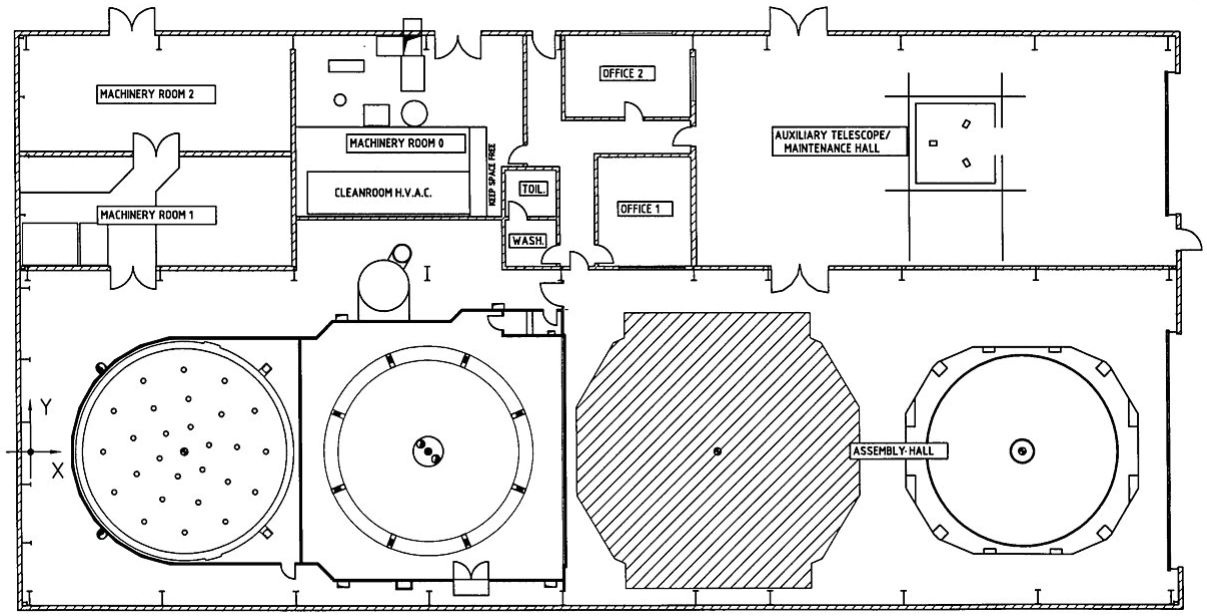

Figure 3.25.:

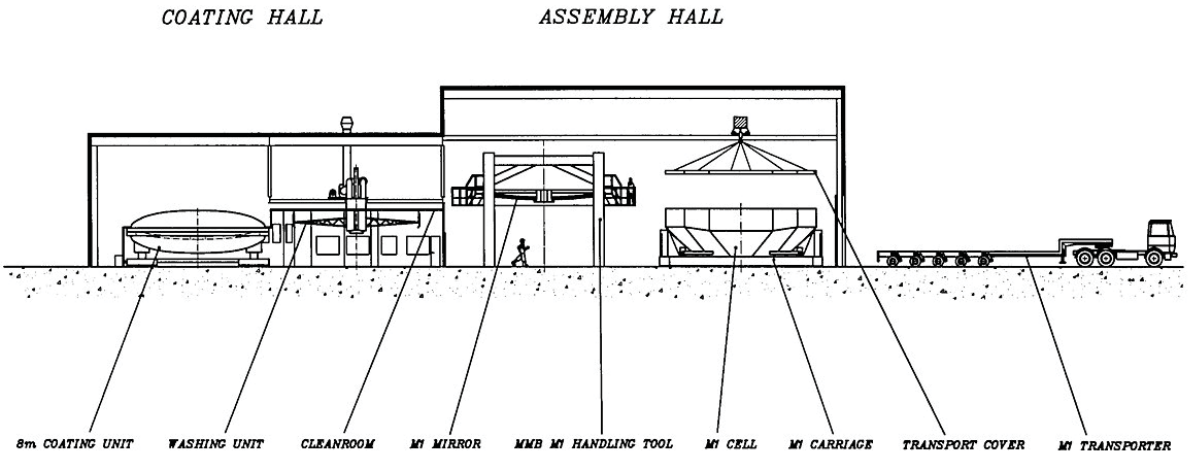

Figure 3.26.:

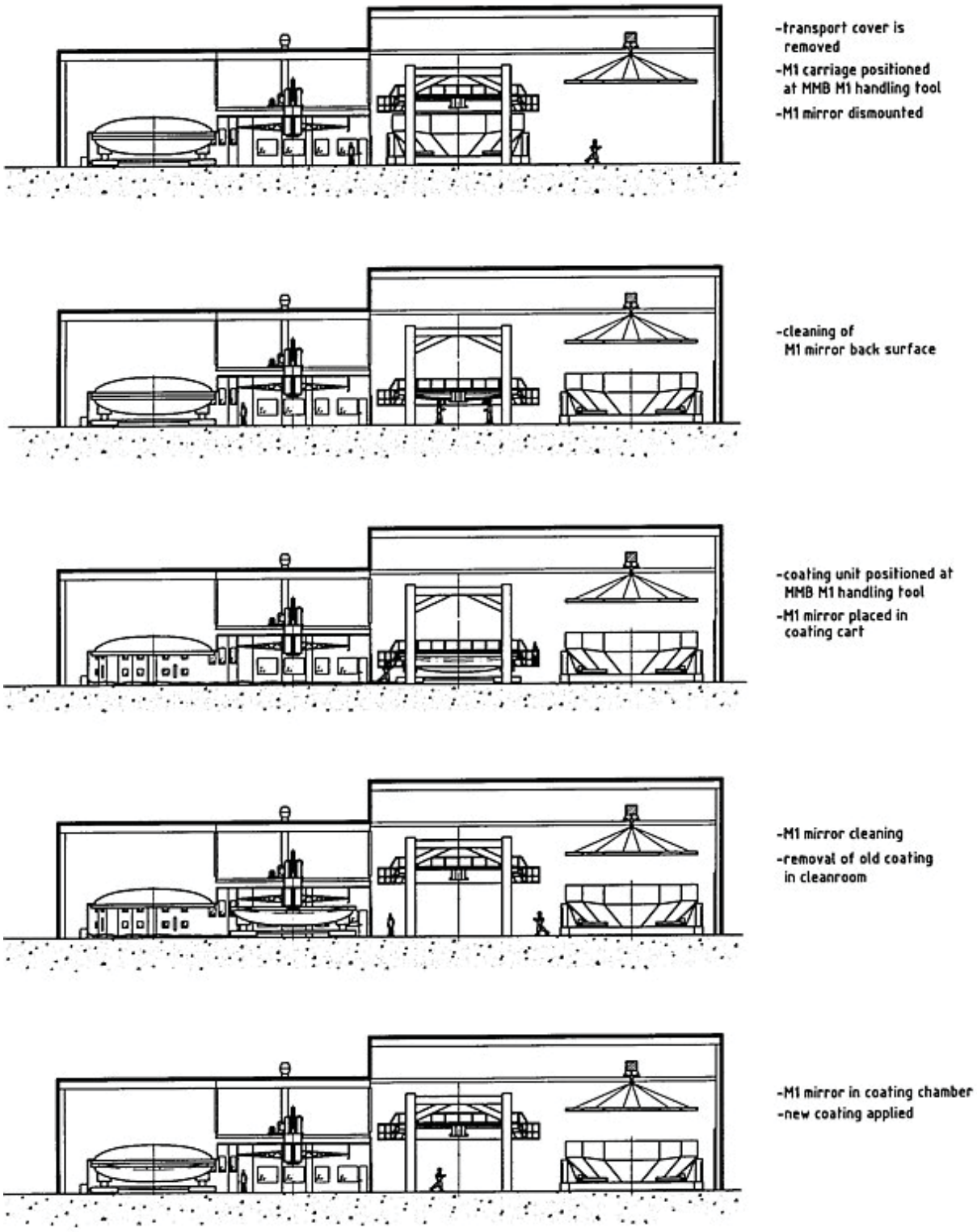
-transport cover is removed
-M1 carriage positioned at MMB M1 handling tool
-M1 mirror dismounted
-cleaning of M1 mirror back surface
-coating unit positioned at MMB M1 handling tool
-M1 mirror placed in coating cart
-M1 mirror cleaning
-removal of old coating in cleanroom
-M1 mirror in coating chamber
-new coating applied

Figure 3.27.:

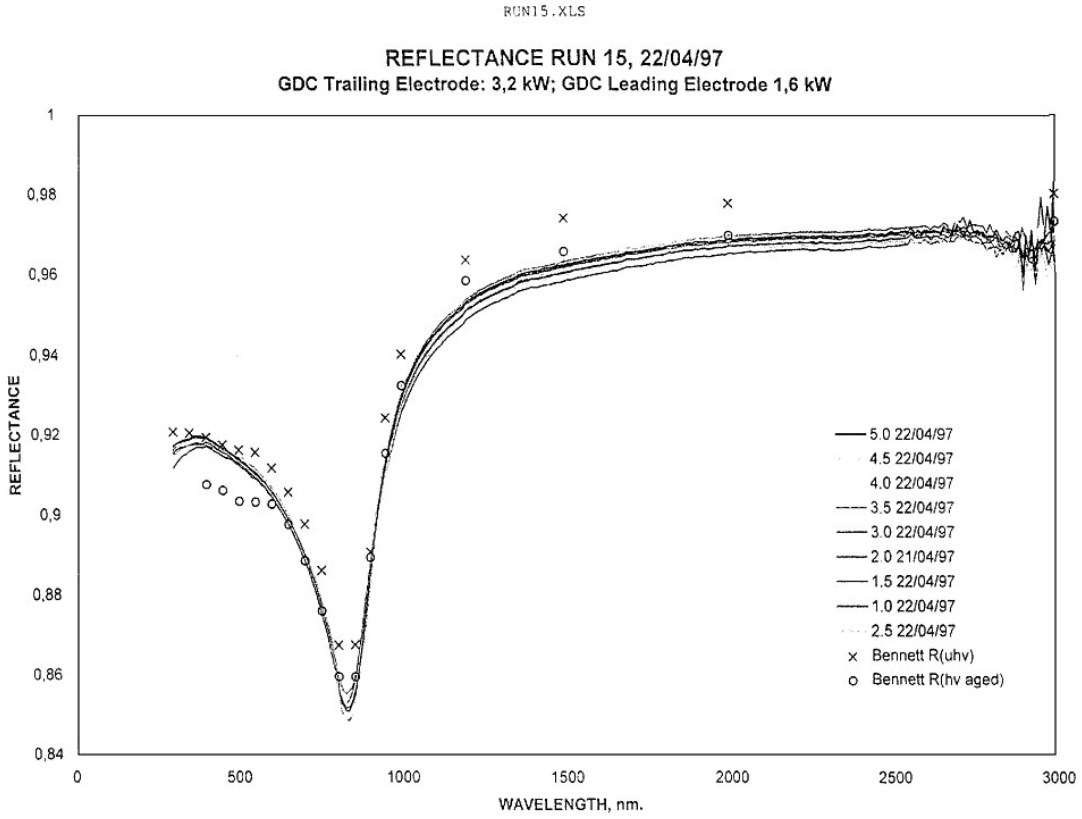

Figure 4.1.:

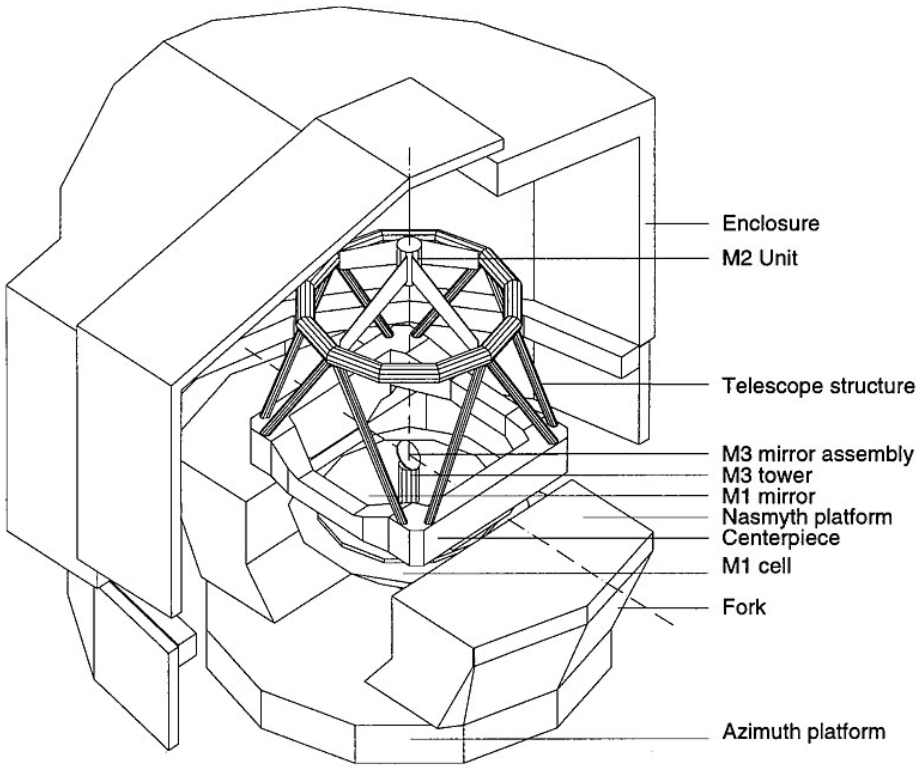

Figure 4.2.:

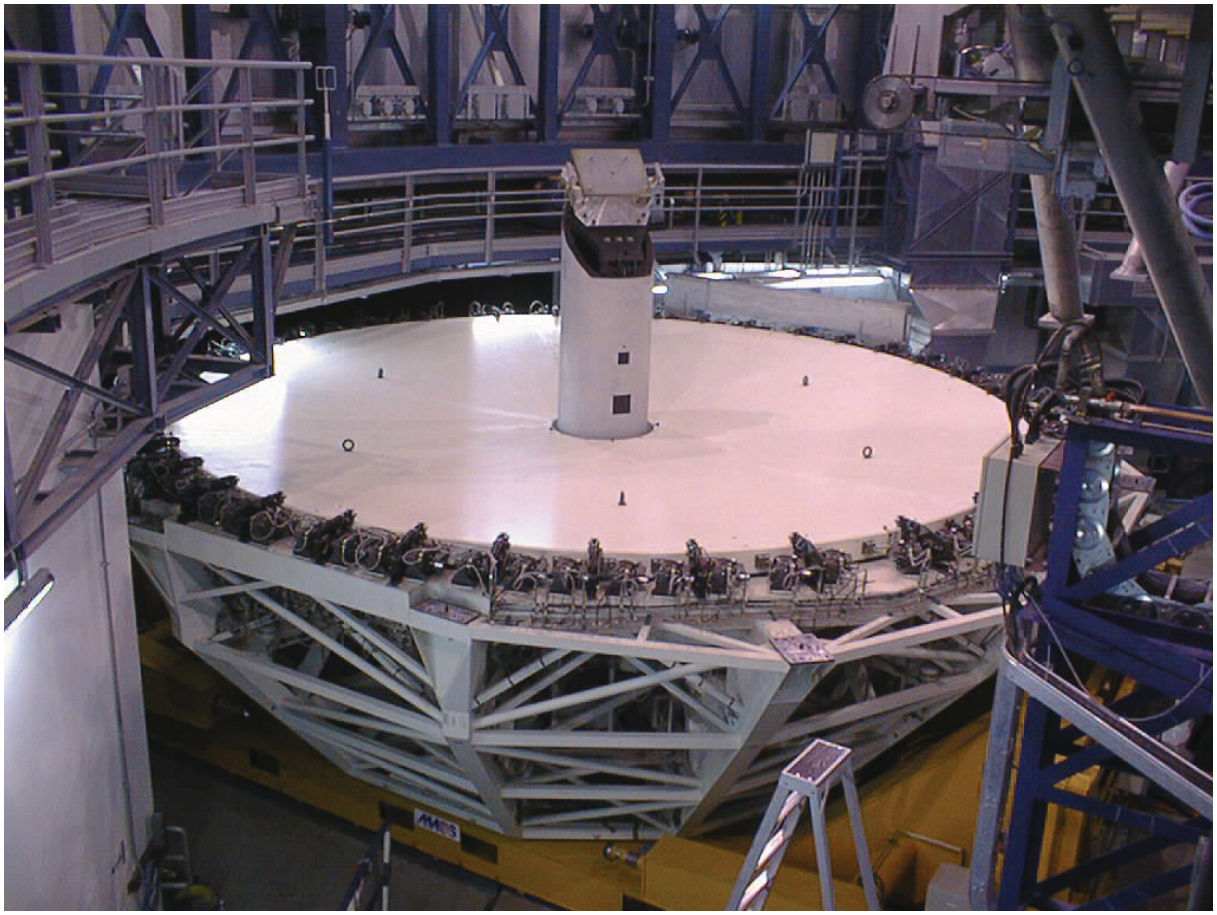

Figure 4.3.:

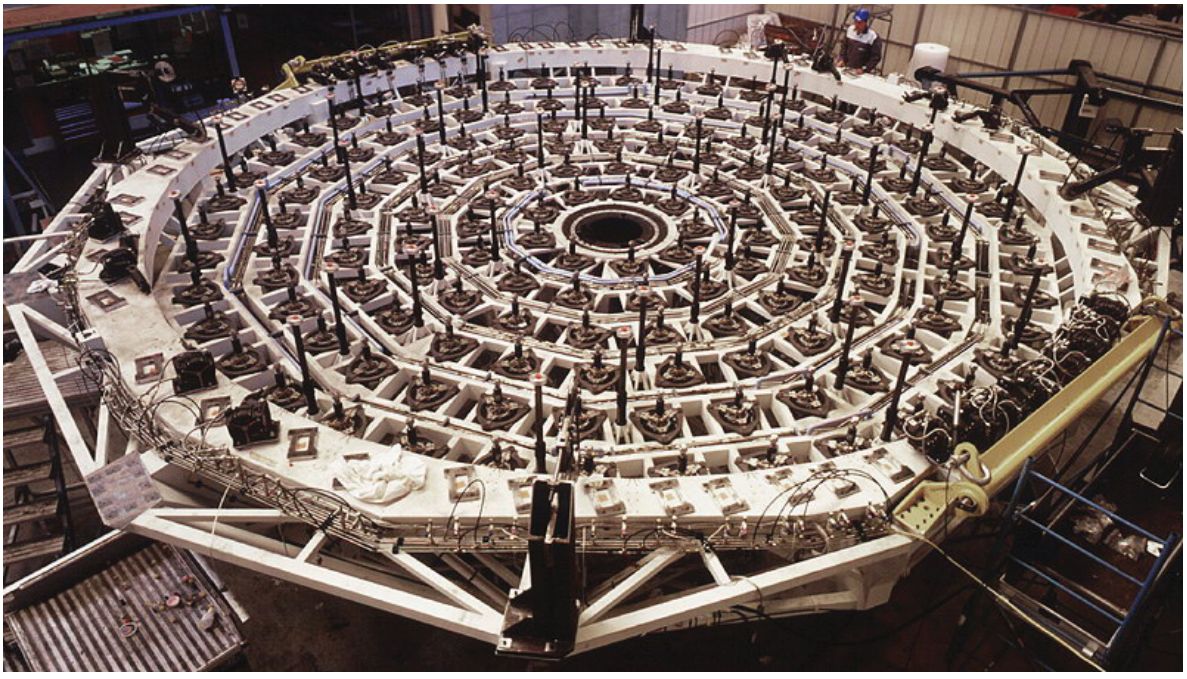

Figure 4.4.:

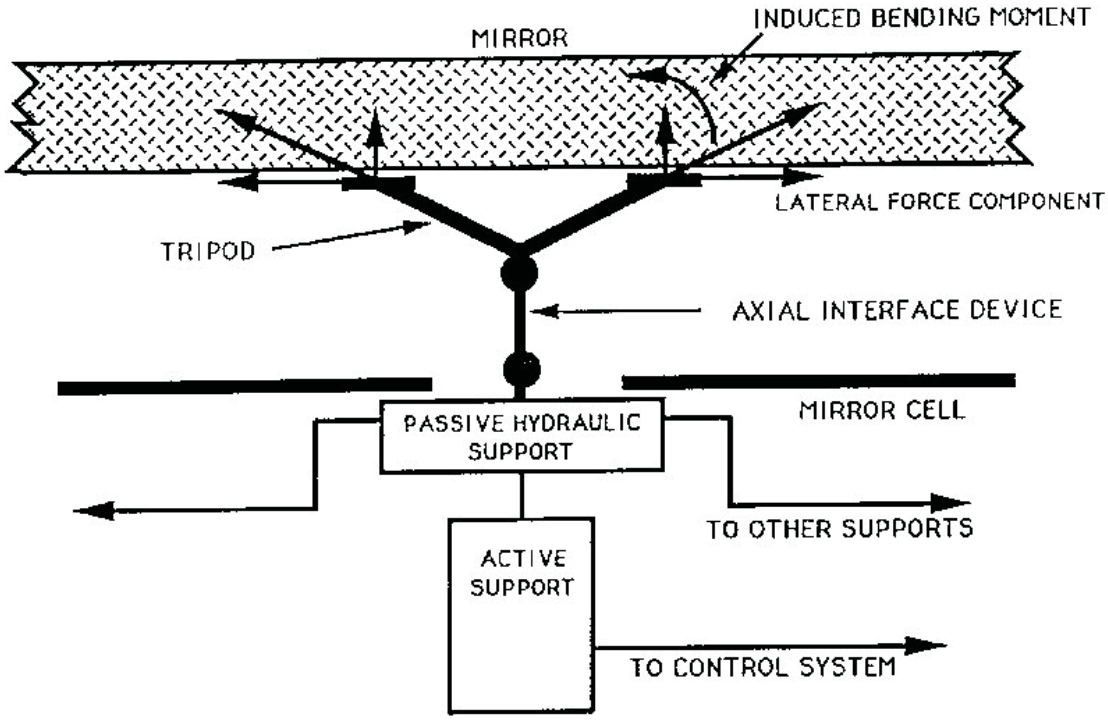

Figure 4.5.:

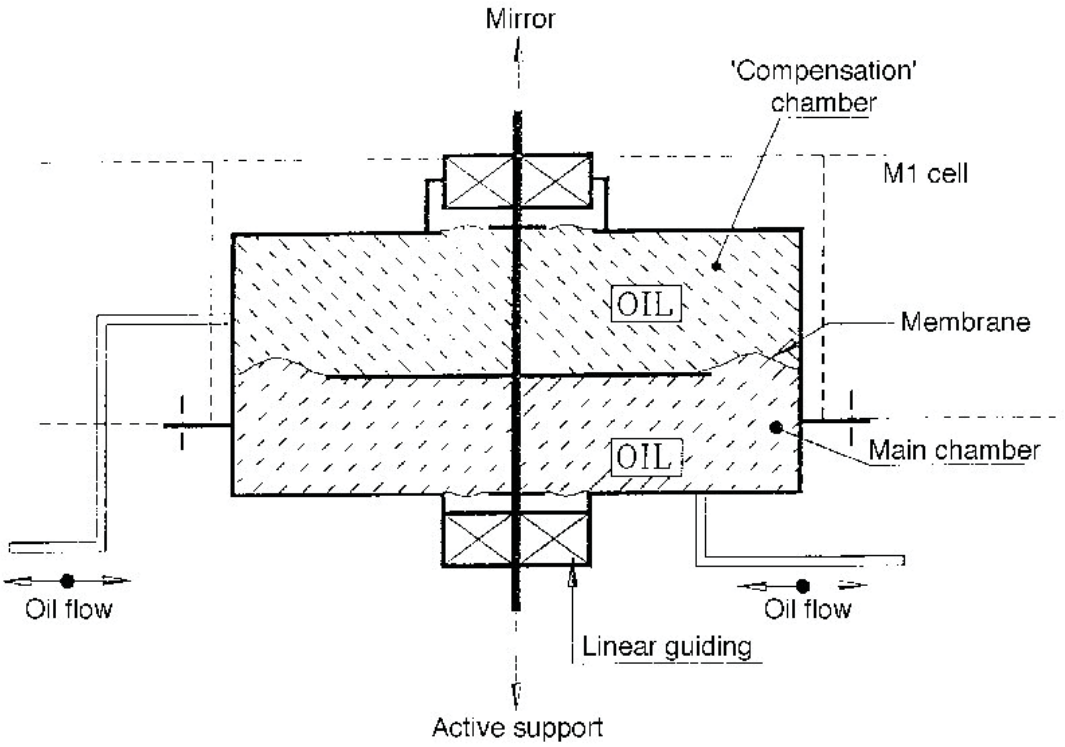

Figure 4.6.:

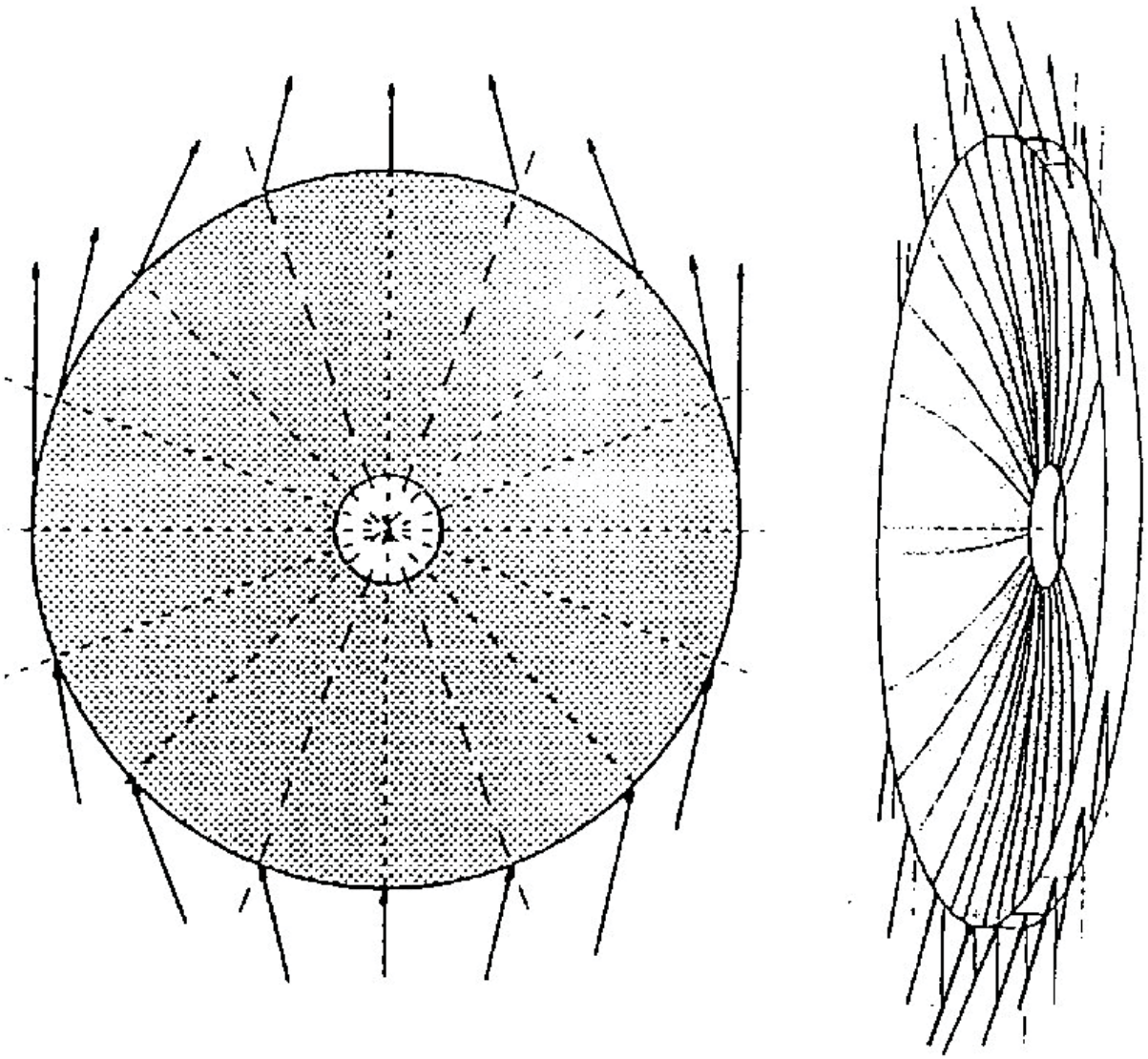

Figure 4.7.:

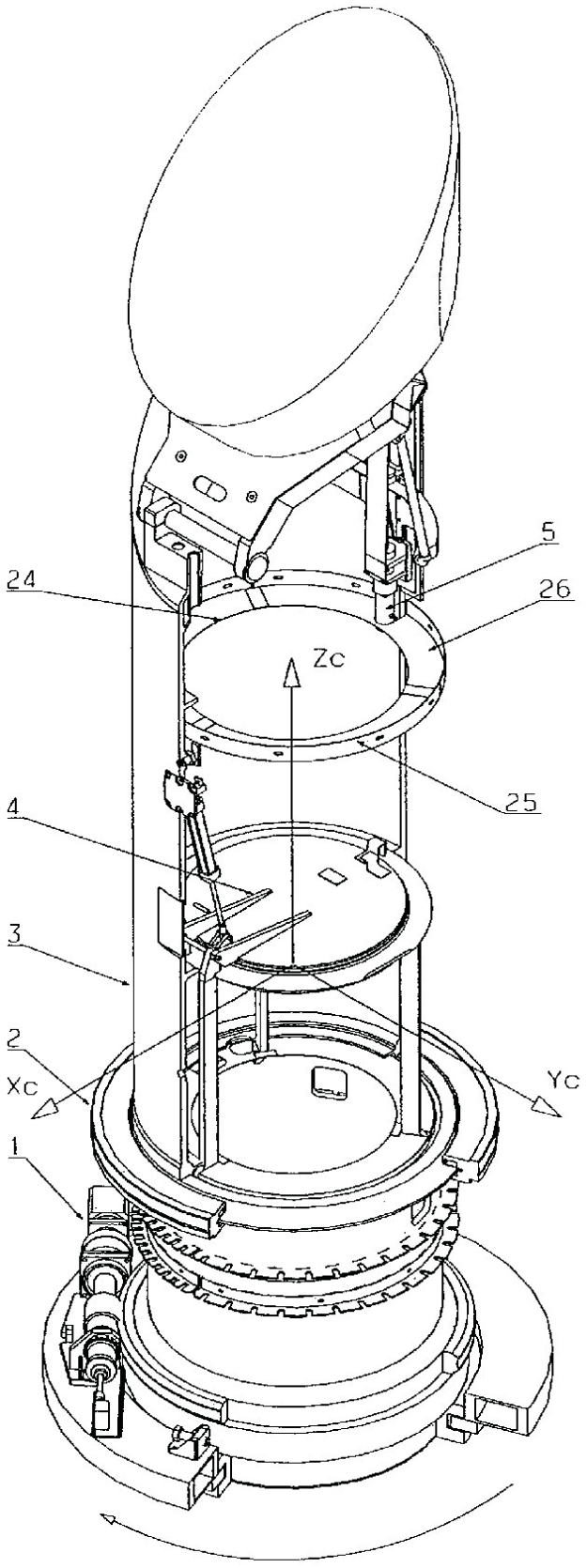

NASMITH B POSITION -

Figure 5.1.:

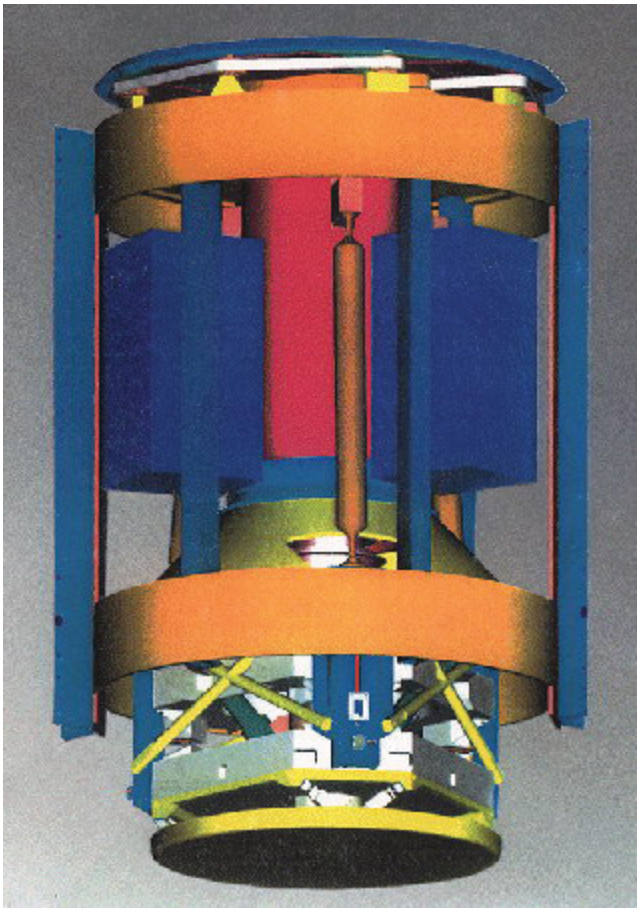

Figure 5.2.:

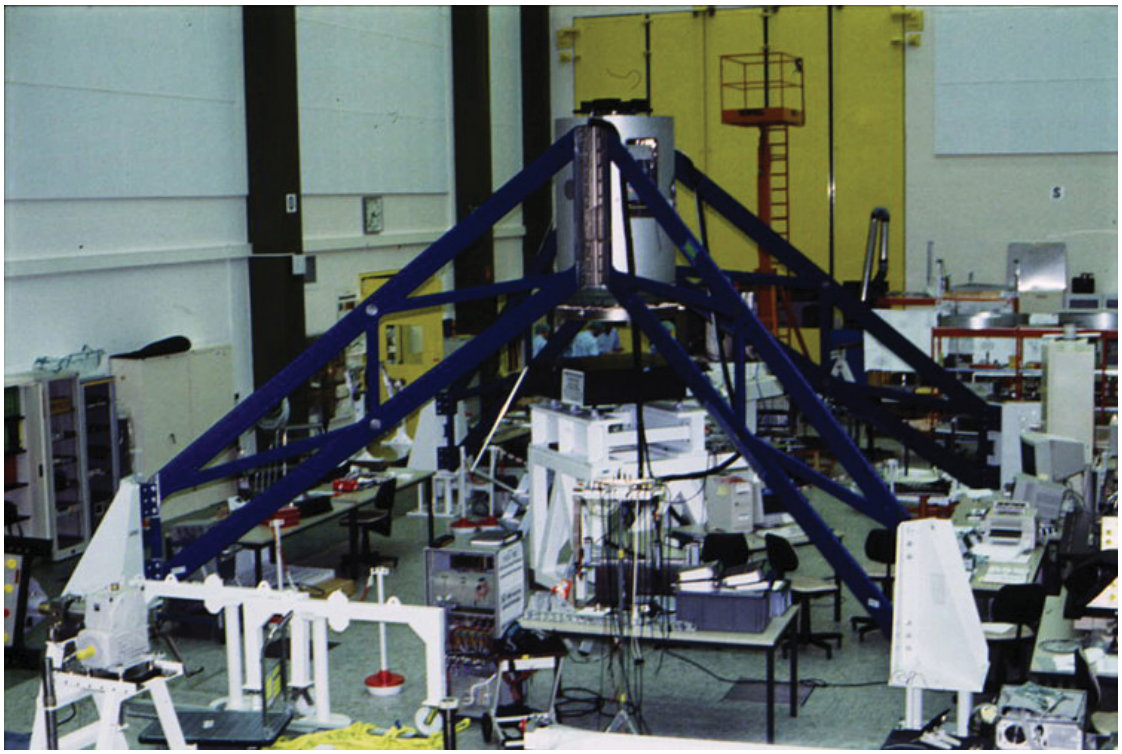

Figure 5.3.:

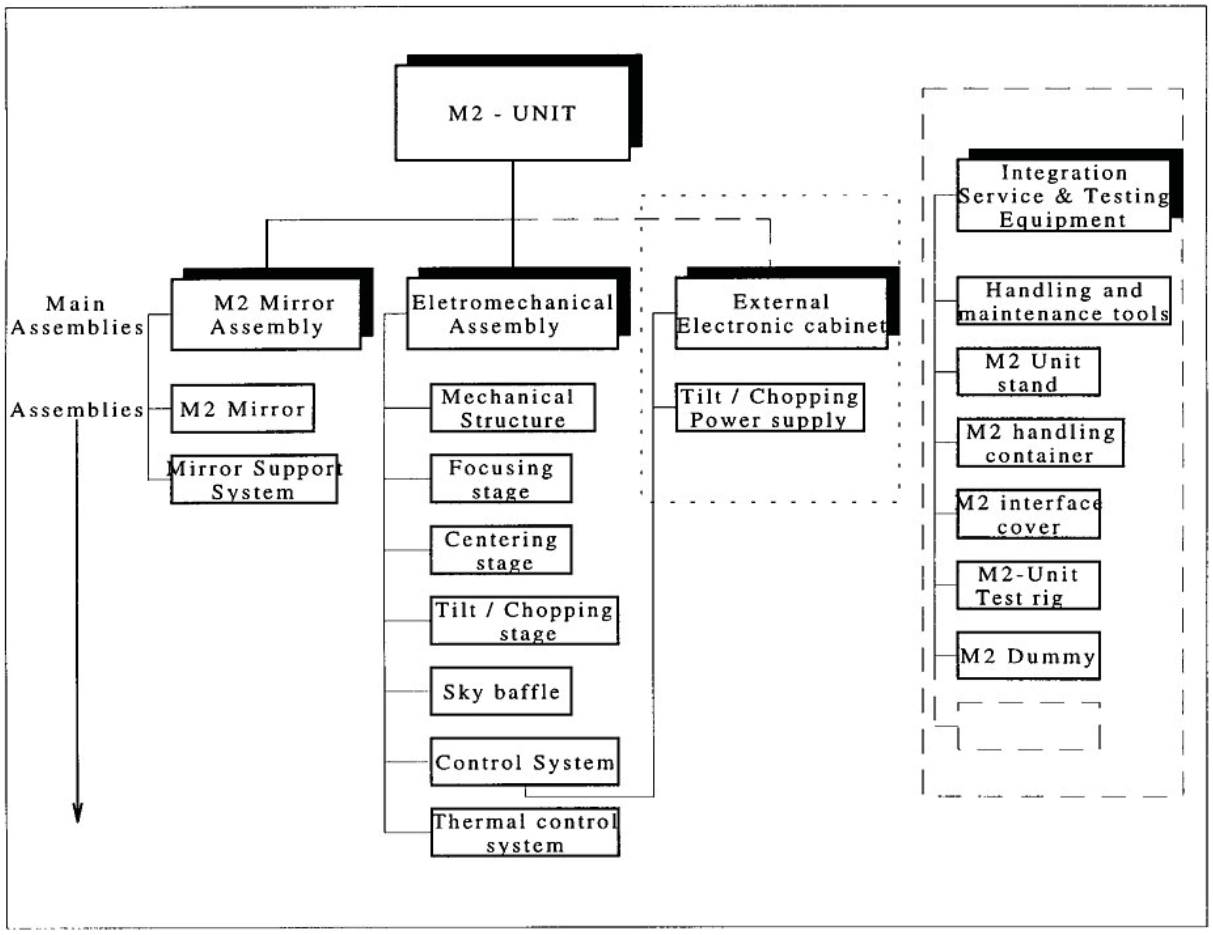
M2 - UNIT
Integration Service & Testing Equipment
Main Assemblies
M2 Mirror Assembly
Eletromechanical Assembly
External Electronic cabinet
Handling and maintenance tools
Assemblies
M2 Mirror
Mirror Support System
Mechanical Structure
Tilt / Chopping Power supply
M2 Unit stand
M2 handling container
Focusing stage
Centering stage
M2 interface cover
Tilt / Chopping stage
M2-Unit Test rig
Sky baffle
M2 Dummy
Control System
Thermal control system

Figure 6.1.:

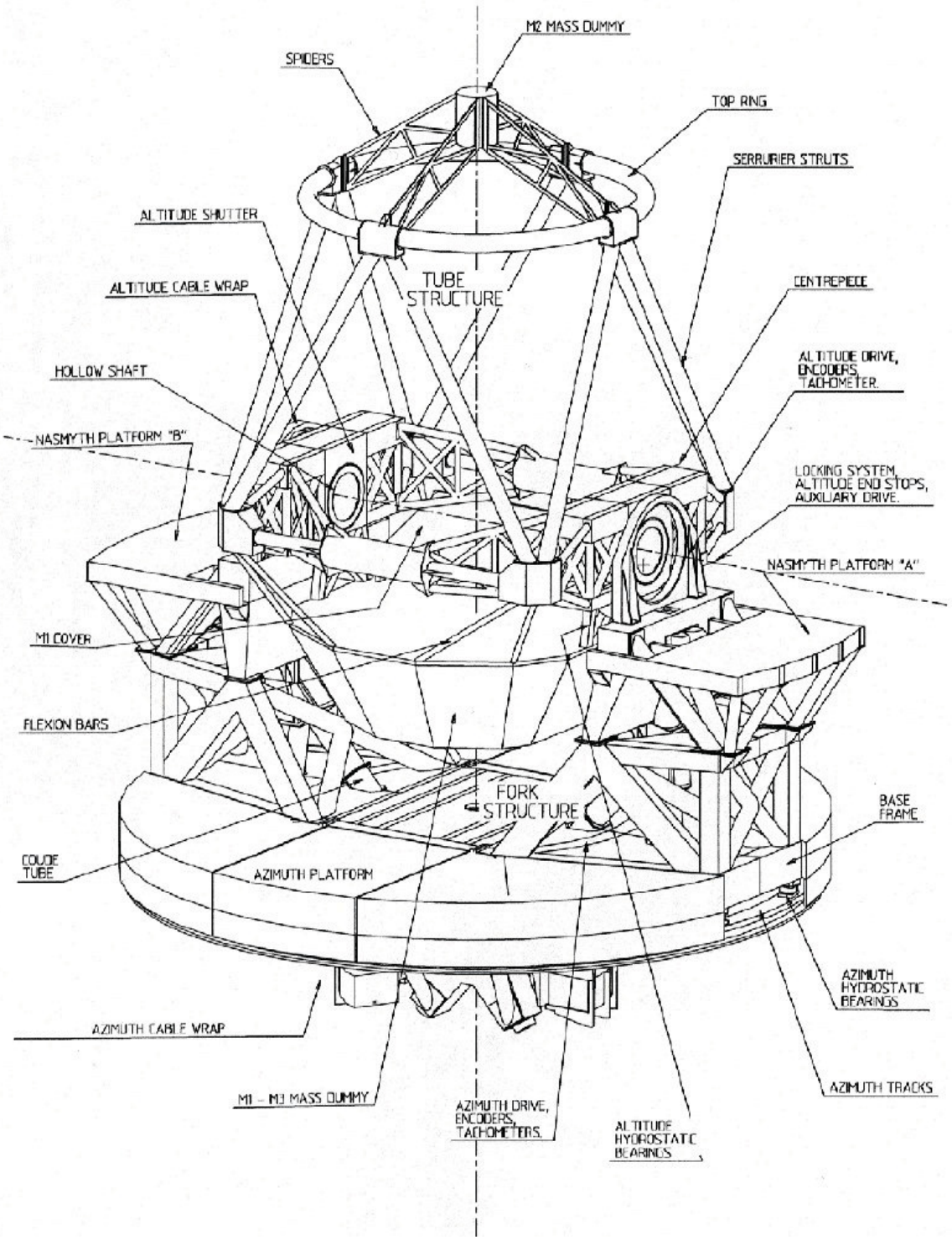
M2 MASS DUMMY
SPIDERS
TOP RING
SERRURIER STRUTS
ALTITUDE SHUTTER
TUBE STRUCTURE
ALTITUDE CABLE WRAP
CENTREPIECE
HOLLOW SHAFT
ALTITUDE DRIVE, ENCODERS, TACHOMETER.
NASMYTH PLATFORM "B"
LOCKING SYSTEM, ALTITUDE END STOPS, AUXILIARY DRIVE.
NASMYTH PLATFORM "A"
M1 COVER
FLEXION BARS
FORK STRUCTURE
BASE FRAME
COUDE TUBE
AZIMUTH PLATFORM
AZIMUTH HYDROSTATIC BEARINGS
AZIMUTH CABLE WRAP
AZIMUTH TRACKS
M1 – M3 MASS DUMMY
AZIMUTH DRIVE, ENCODERS, TACHOMETERS.
ALTITUDE HYDROSTATIC BEARINGS

Figure 6.2.:

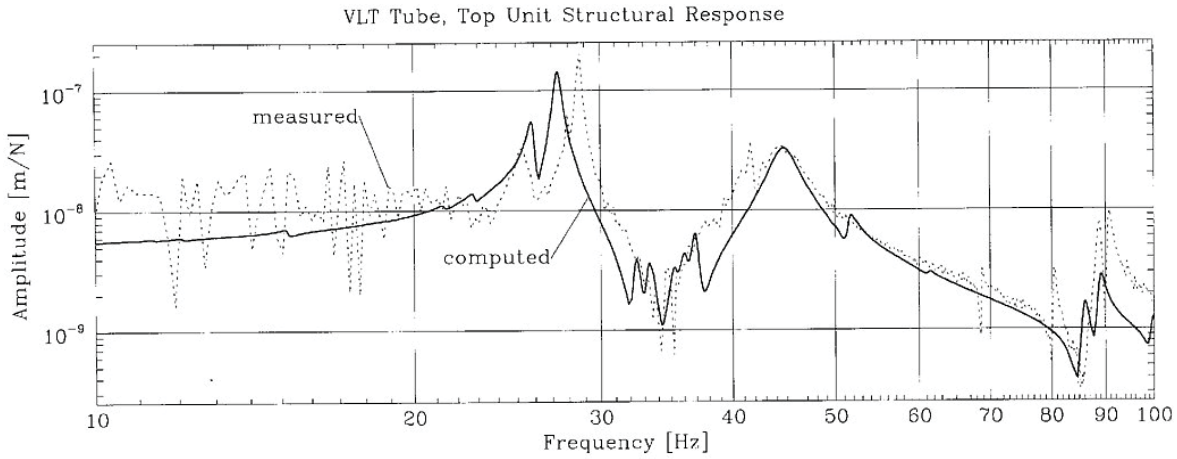

Figure 6.3.:

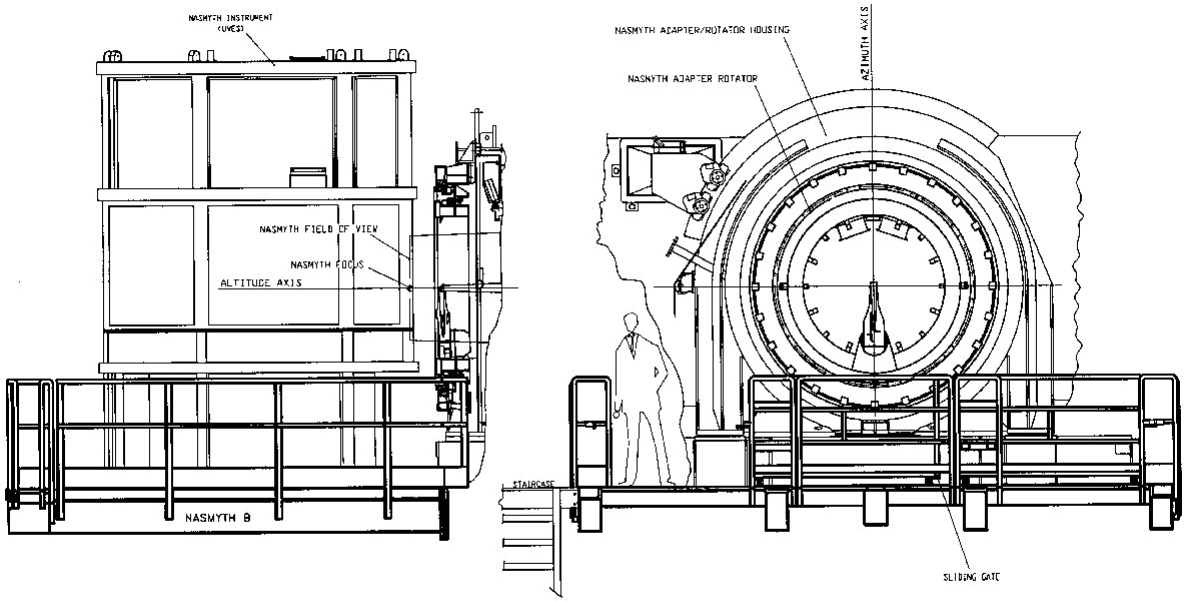

NASMYTH PLATFORM LAYOUT

Figure 7.1.:

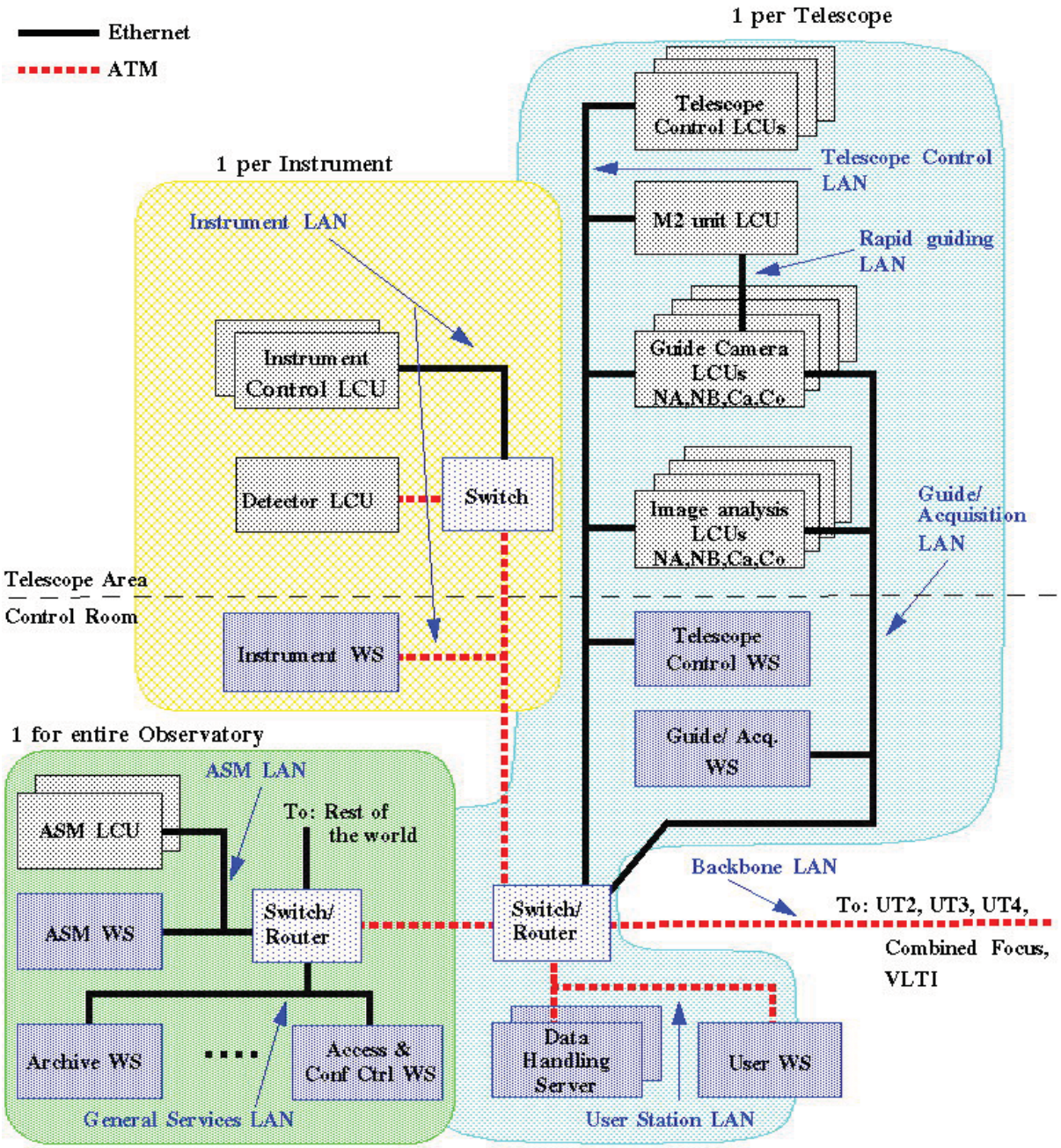
Ethernet
ATM
1 per Telescope
Telescope Control LCUs
Telescope Control LAN
M2 unit LCU
Rapid guiding LAN
Guide Camera LCUs NA,NB,Ca,Co
Image analysis LCUs NA,NB,Ca,Co
Guide/ Acquisition LAN
Telescope Control WS
Guide/ Acq. WS
1 per Instrument
Instrument LAN
Instrument Control LCU
Detector LCU
Switch
Instrument WS
Telescope Area
Control Room
1 for entire Observatory
ASM LAN
ASM LCU
To: Rest of the world
ASM WS
Switch/ Router
Archive WS
Access & Conf Ctrl WS
General Services LAN
Switch/ Router
Backbone LAN
To: UT2, UT3, UT4, Combined Focus, VLTI
Data Handling Server
User WS
User Station LAN

Figure 7.2.:

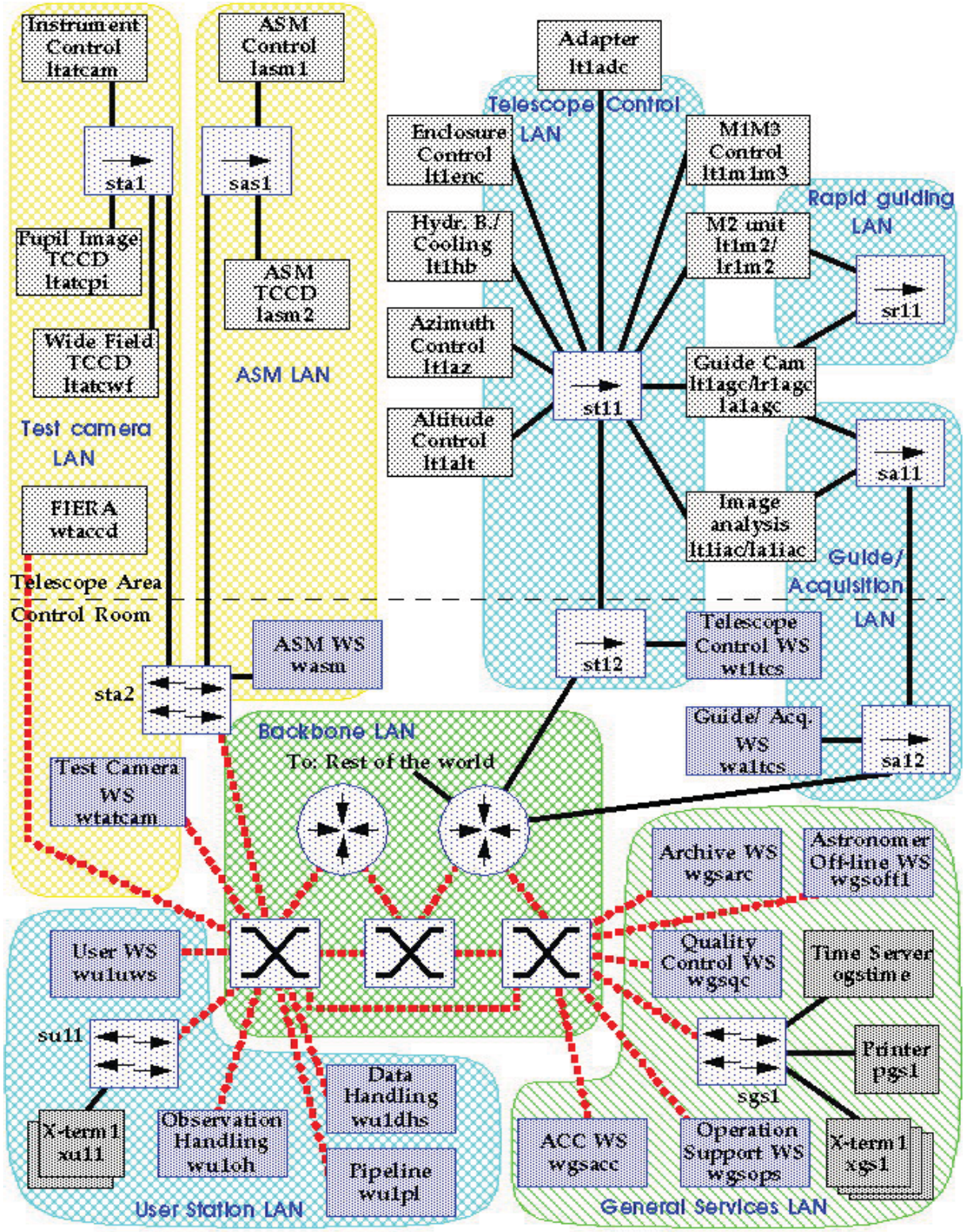
Instrument Control ltatcam
ASM Control lasm1
Adapter lt1adc
Telescope Control LAN
Enclosure Control lt1enc
M1M3 Control lt1m1m3
Rapid guiding LAN
sta1
sas1
Hydr. B./ Cooling lt1hb
M2 unit lt1m2/ lr1m2
sr11
Pupil Image TCCD ltatcpi
ASM TCCD lasm2
Azimuth Control lt1az
Guide Cam lt1agc/lr1agc la1agc
Wide Field TCCD ltatcwf
ASM LAN
st11
Altitude Control lt1alt
Test camera LAN
sa11
FIERA wtaccd
Image analysis lt1iac/la1iac
Guide/ Acquisition LAN
Telescope Area
Control Room
st12
Telescope Control WS wt1tcs
ASM WS wasm
sta2
Guide/ Acq. WS wa1tcs
sa12
Backbone LAN
To: Rest of the world
Test Camera WS wtatcam
Archive WS wgsarc
Astronomer Off-line WS wgsoff1
User WS wu1uws
Quality Control WS wgsqc
Time Server ogstime
su11
Printer pgs1
sgs1
Data Handling wu1dhs
X-term1 xu11
Observation Handling wu1oh
Pipeline wu1pl
ACC WS wgsacc
Operation Support WS wgsops
X-term1 xgs1
User Station LAN
General Services LAN

Figure 7.3.:

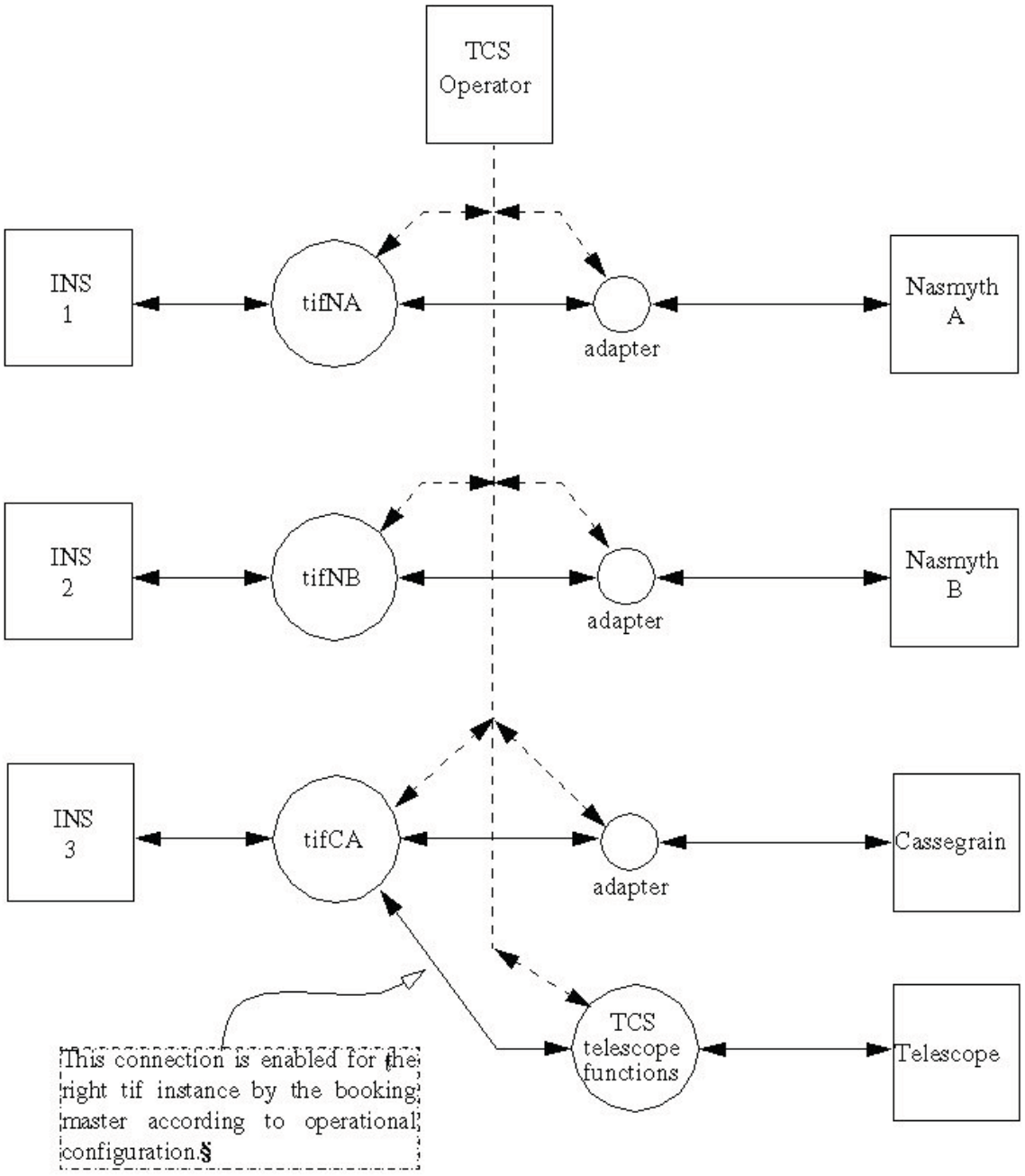
TCS
Operator
INS
1
tifNA
adapter
Nasmyth
A
INS
2
tifNB
adapter
Nasmyth
B
INS
3
tifCA
adapter
Cassegrain
TCS
telescope
functions
Telescope
This connection is enabled for the right tif instance by the booking master according to operational configuration.§

Figure 7.4.:

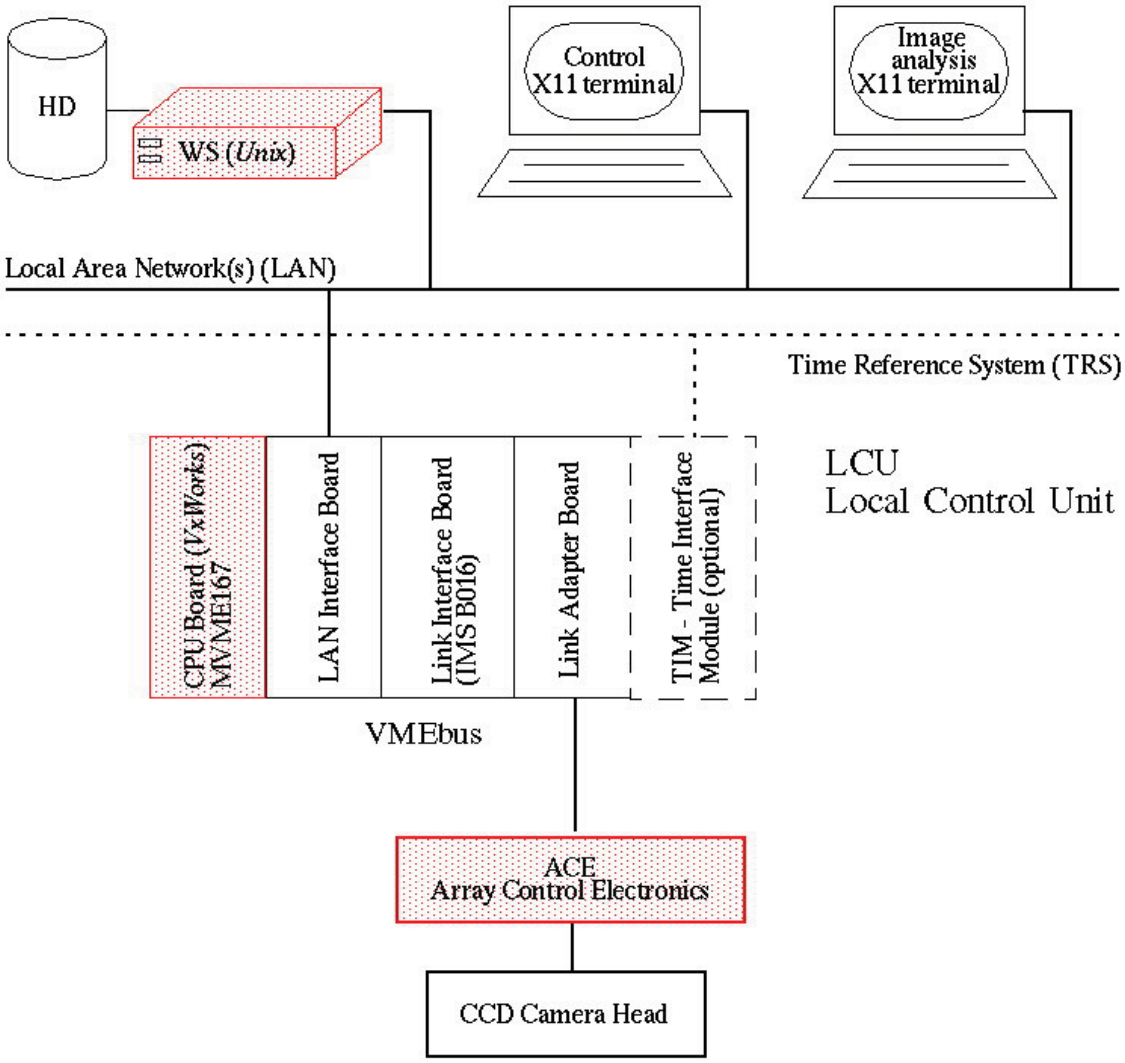
HD
WS (*Unix*)
Control
X11 terminal
Image
analysis
X11 terminal
Local Area Network(s) (LAN)
Time Reference System (TRS)
CPU Board (*VxWorks*)
MVME167
LAN Interface Board
Link Interface Board
(IMS B016)
Link Adapter Board
TIM - Time Interface
Module (optional)
LCU
Local Control Unit
VMEbus
ACE
Array Control Electronics
CCD Camera Head

Figure 7.5.:

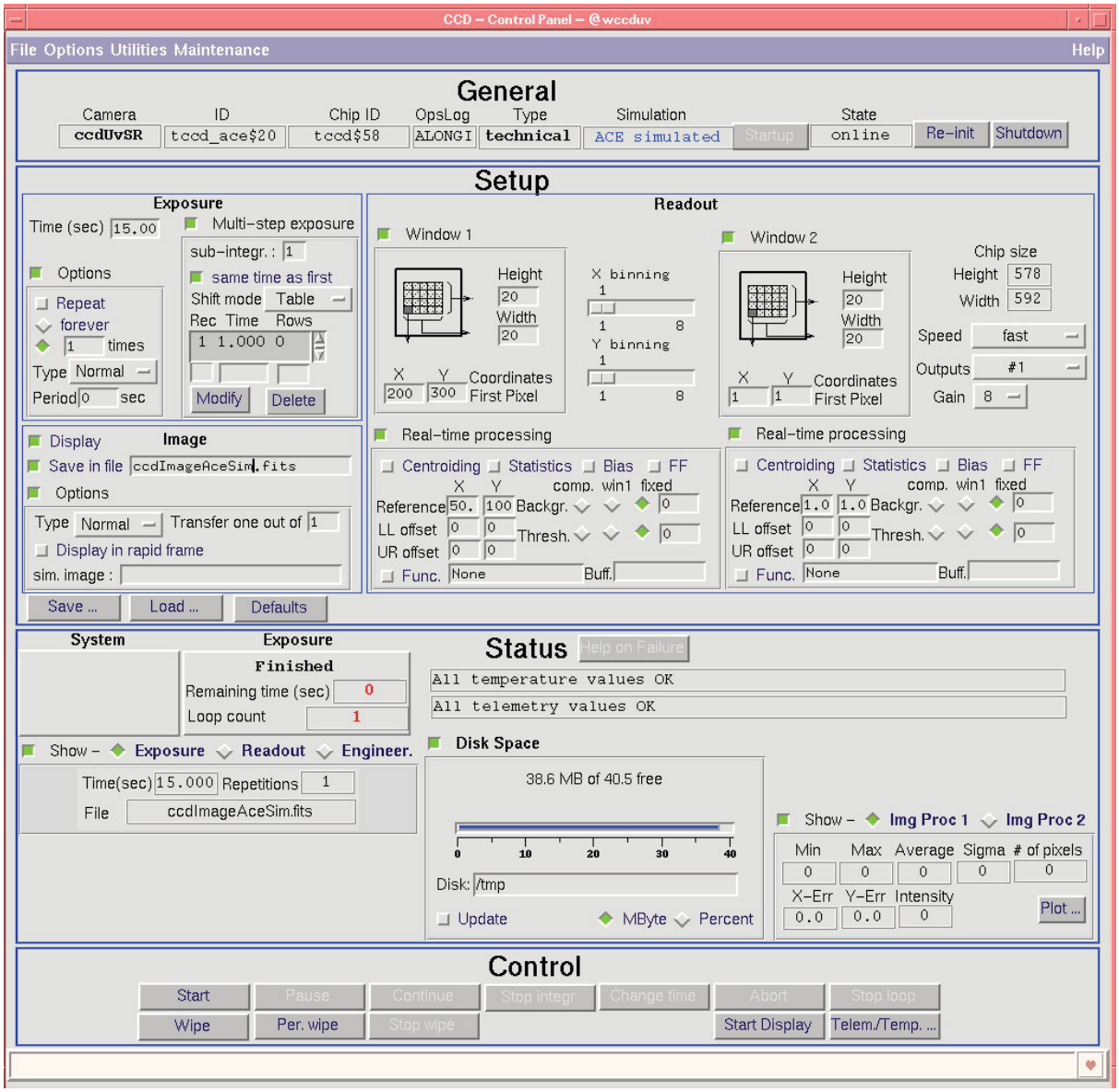
CCD – Control Panel – @wccduv
File Options Utilities Maintenance
Help
General
Camera
ID
Chip ID
OpsLog
Type
Simulation
State
ccdUvSR
tccd_ace$20
tccd$58
ALONGI
technical
ACE simulated
Startup
online
Re-init
Shutdown
Setup
Exposure
Time (sec) 15.00
Multi-step exposure
sub-integr. : 1
same time as first
Shift mode Table
Rec Time Rows
1 1.000 0
Modify
Delete
Options
Repeat
forever
1 times
Type Normal
Period 0 sec
Readout
Window 1
Height 20
Width 20
X binning 1
Y binning 1
X Y Coordinates First Pixel
200 300
Window 2
Height 20
Width 20
1 1
Chip size
Height 578
Width 592
Speed fast
Outputs #1
Gain 8
Display
Image
Save in file ccdImageAceSim.fits
Options
Type Normal
Transfer one out of 1
Display in rapid frame
sim. image :
Real-time processing
Centroiding Statistics Bias FF
X Y comp. win1 fixed
Reference 50. 100 Backgr.
LL offset 0 0
UR offset 0 0
Thresh.
Func. None
Buff.
Real-time processing
Centroiding Statistics Bias FF
X Y comp. win1 fixed
Reference 1.0 1.0 Backgr.
LL offset 0 0
UR offset 0 0
Thresh.
Func. None
Buff.
Save ...
Load ...
Defaults
System
Exposure
Finished
Remaining time (sec) 0
Loop count 1
Status
Help on Failure
All temperature values OK
All telemetry values OK
Show – Exposure Readout Engineer.
Time(sec) 15.000 Repetitions 1
File ccdImageAceSim.fits
Disk Space
38.6 MB of 40.5 free
0 10 20 30 40
Disk: /tmp
Update
MByte Percent
Show – Img Proc 1 Img Proc 2
Min Max Average Sigma # of pixels
0 0 0 0 0
X-Err Y-Err Intensity
0.0 0.0 0
Plot ...
Control
Start
Pause
Continue
Stop integr
Change time
Abort
Stop loop
Wipe
Per. wipe
Stop wipe
Start Display
Telem./Temp. ...

Figure 7.6.:

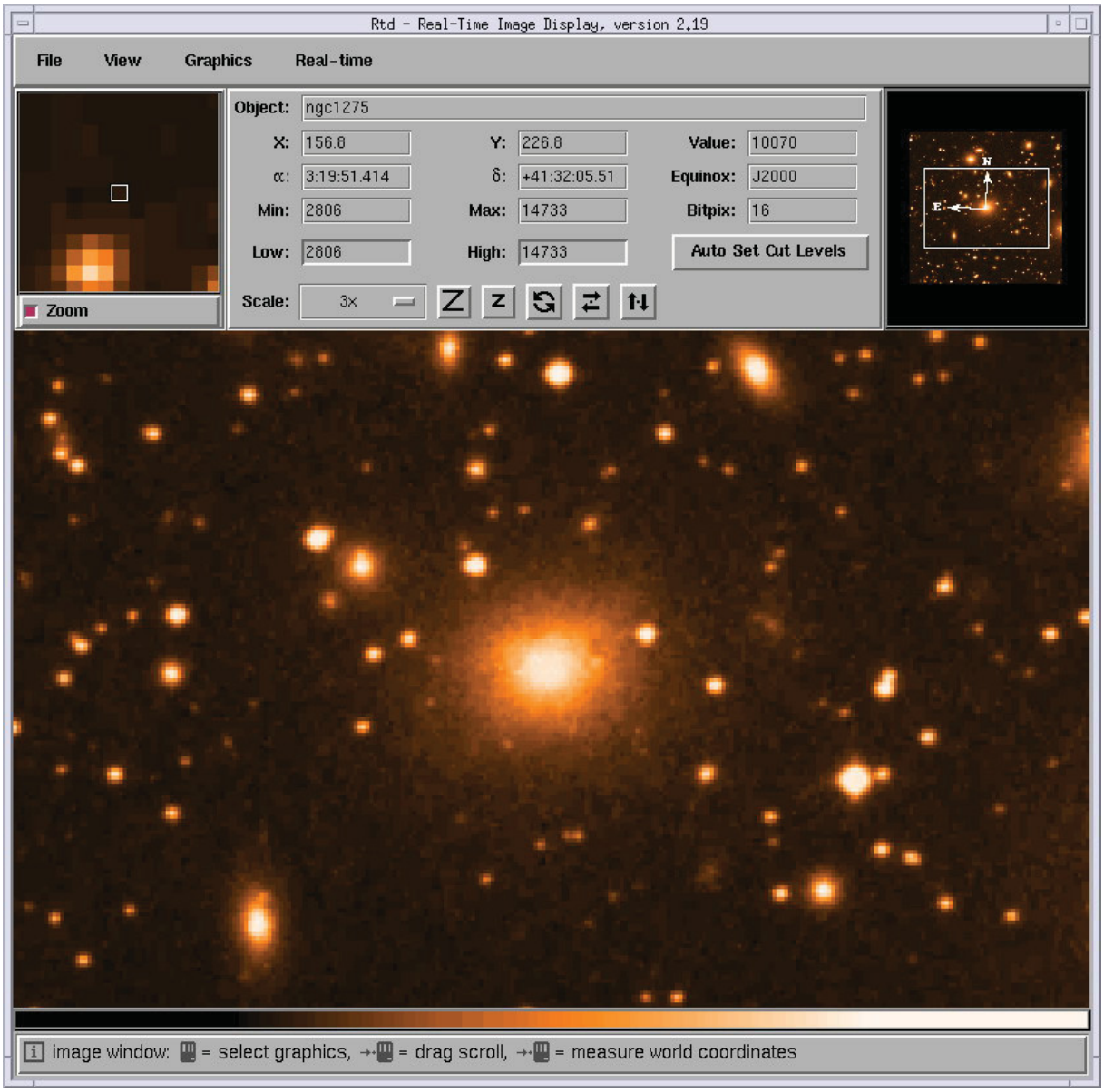
Rtd - Real-Time Image Display, version 2.19
File
View
Graphics
Real-time
Object: ngc1275
X: 156.8
Y: 226.8
Value: 10070
α: 3:19:51.414
δ: +41:32:05.51
Equinox: J2000
Min: 2806
Max: 14733
Bitpix: 16
Low: 2806
High: 14733
Auto Set Cut Levels
Scale: 3x
Zoom
N
E
image window: = select graphics, = drag scroll, = measure world coordinates

Figure 7.7.:

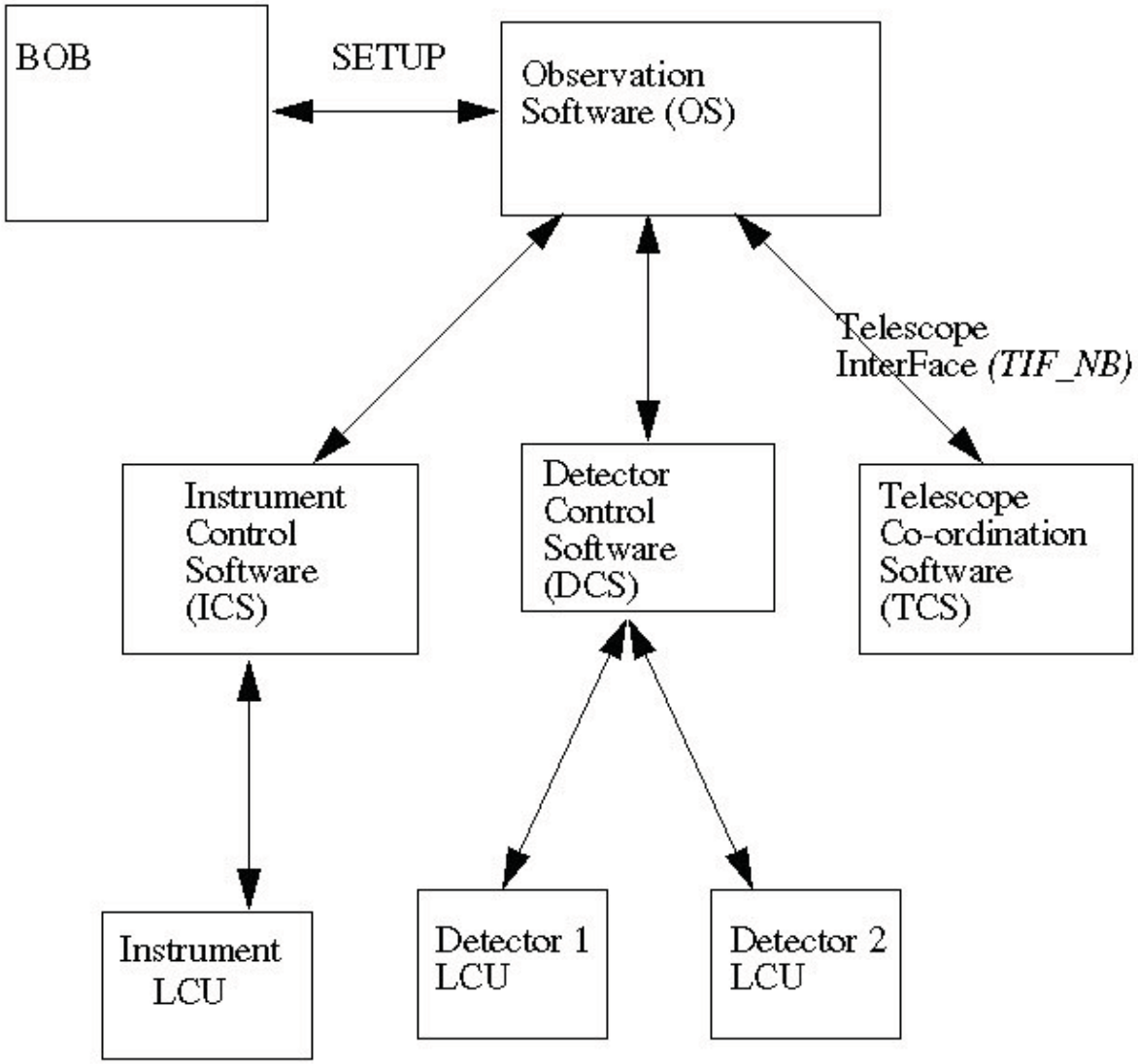
BOB
SETUP
Observation
Software (OS)
Telescope
InterFace (TIF_NB)
Instrument
Control
Software
(ICS)
Detector
Control
Software
(DCS)
Telescope
Co-ordination
Software
(TCS)
Instrument
LCU
Detector 1
LCU
Detector 2
LCU

Figure 7.8.:

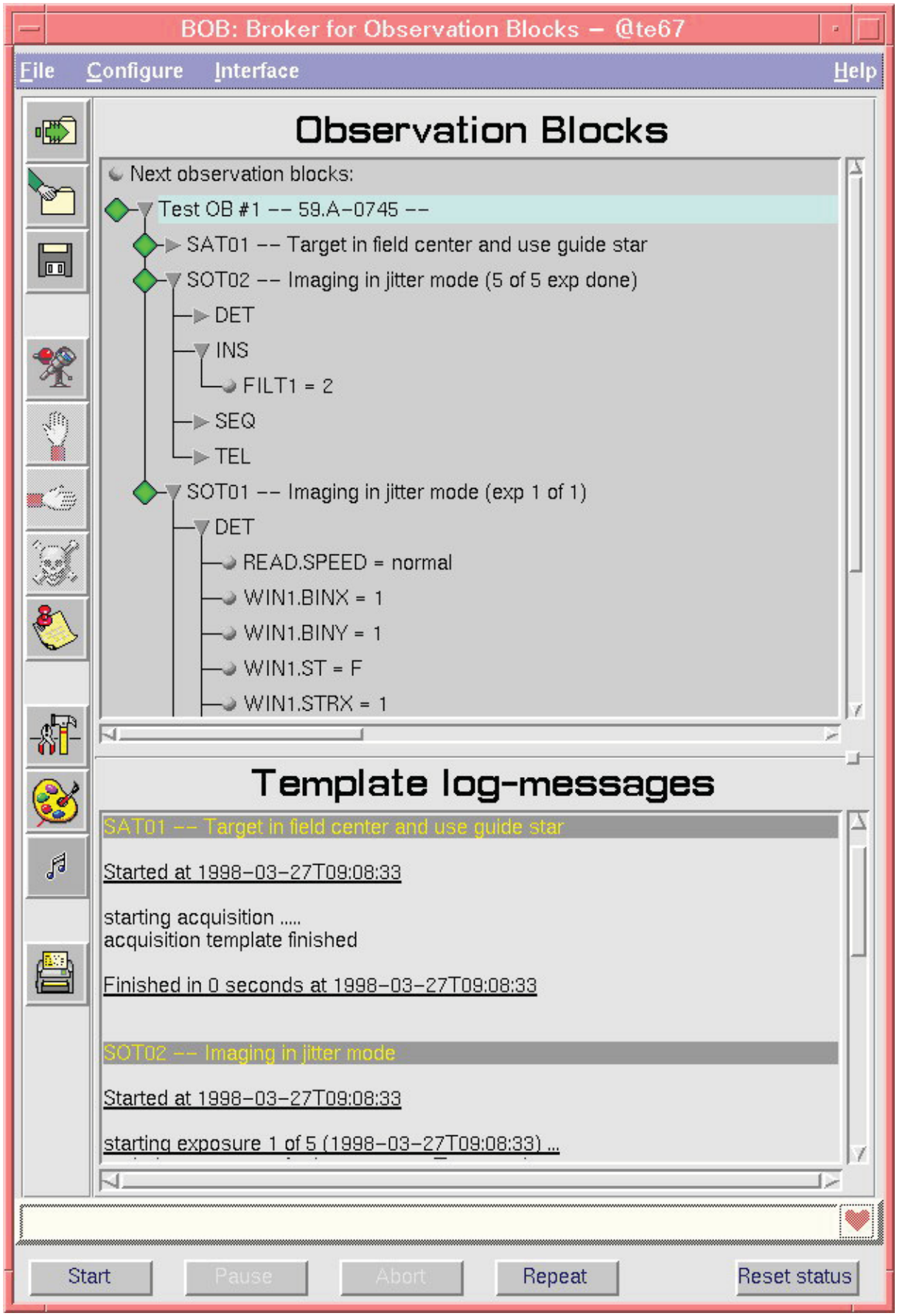
BOB: Broker for Observation Blocks – @te67
File
Configure
Interface
Help
Observation Blocks
Next observation blocks:
Test OB #1 -- 59.A-0745 --
SAT01 -- Target in field center and use guide star
SOT02 -- Imaging in jitter mode (5 of 5 exp done)
DET
INS
FILT1 = 2
SEQ
TEL
SOT01 -- Imaging in jitter mode (exp 1 of 1)
DET
READ.SPEED = normal
WIN1.BINX = 1
WIN1.BINY = 1
WIN1.ST = F
WIN1.STRX = 1
Template log-messages
SAT01 -- Target in field center and use guide star
Started at 1998-03-27T09:08:33
starting acquisition .....
acquisition template finished
Finished in 0 seconds at 1998-03-27T09:08:33
SOT02 -- Imaging in jitter mode
Started at 1998-03-27T09:08:33
starting exposure 1 of 5 (1998-03-27T09:08:33) ...
Start
Pause
Abort
Repeat
Reset status

Figure 8.1.:

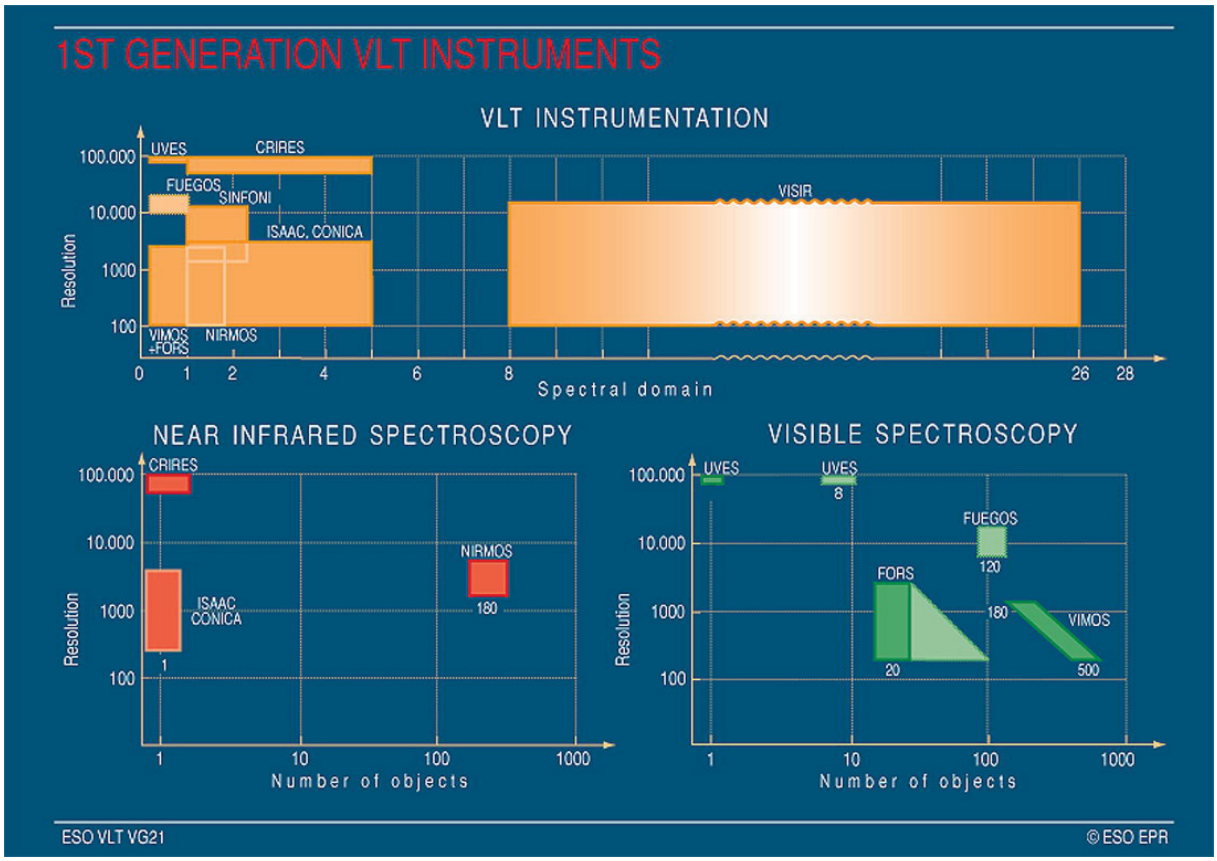

Figure 8.2.:

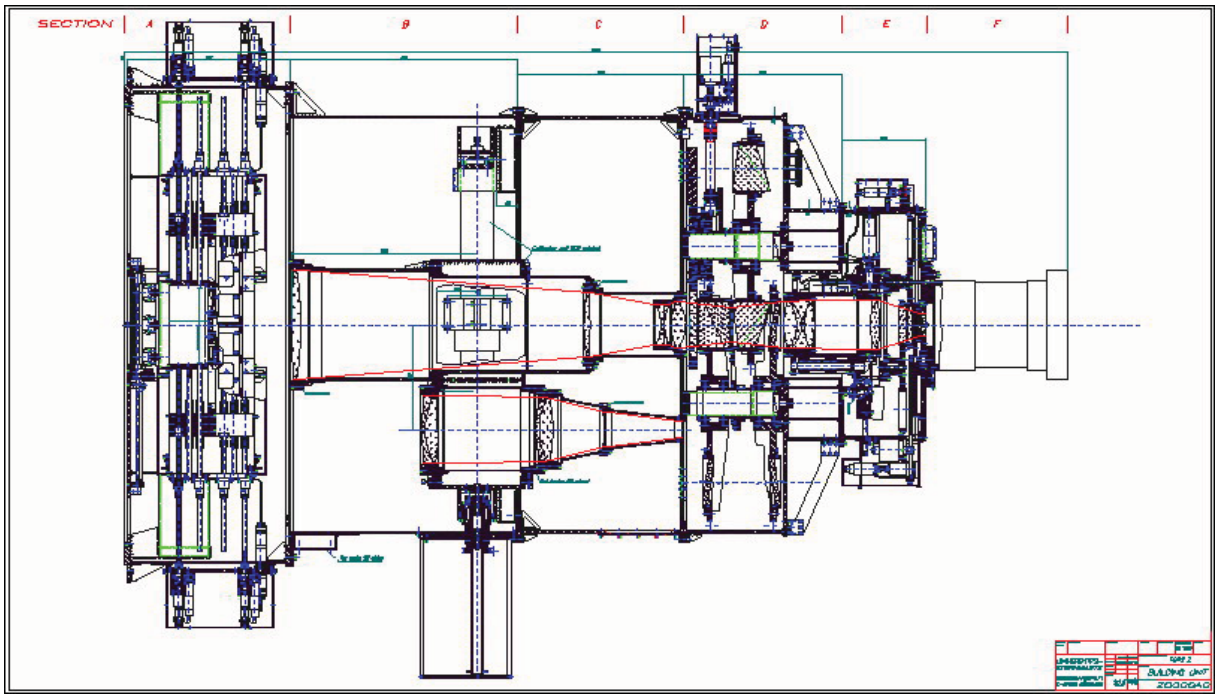

Figure 8.3.:

Figure 8.4.:

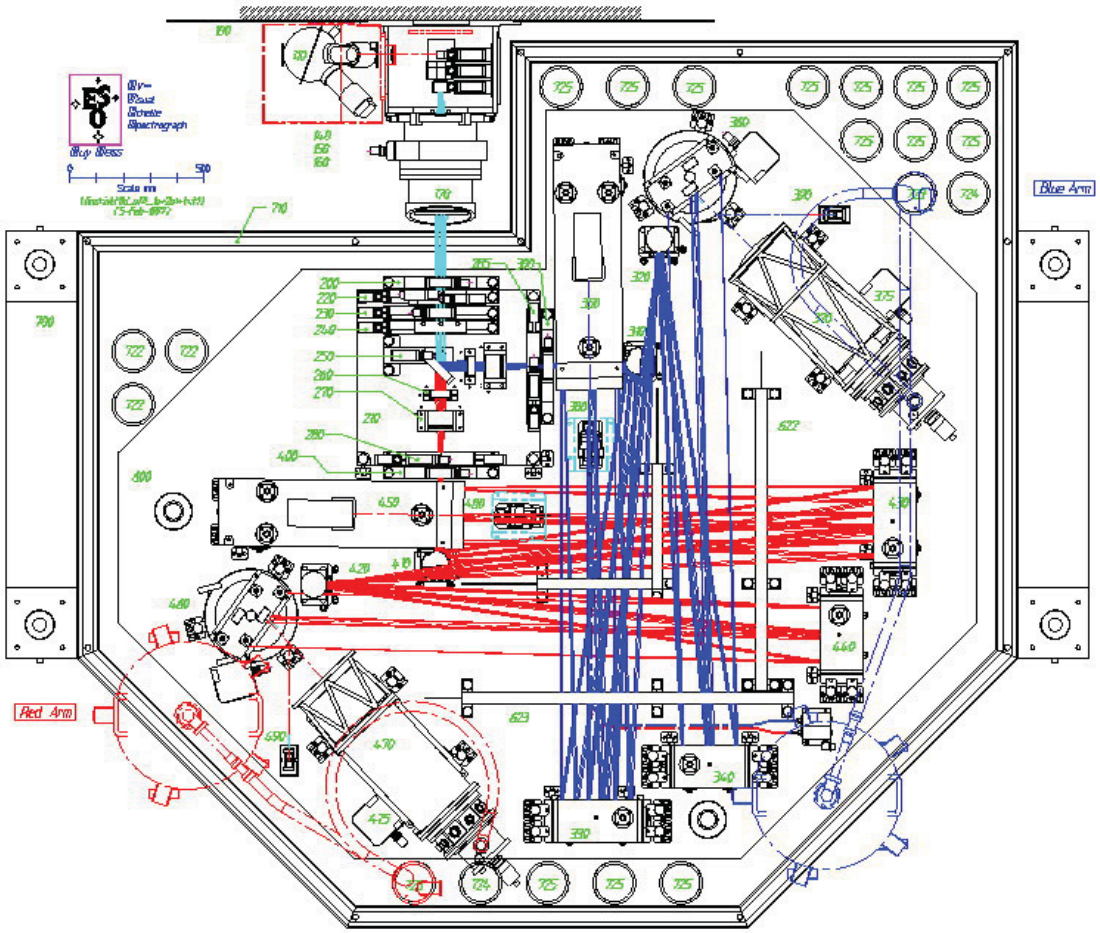

Figure 8.5.:

Figure 8.6.:

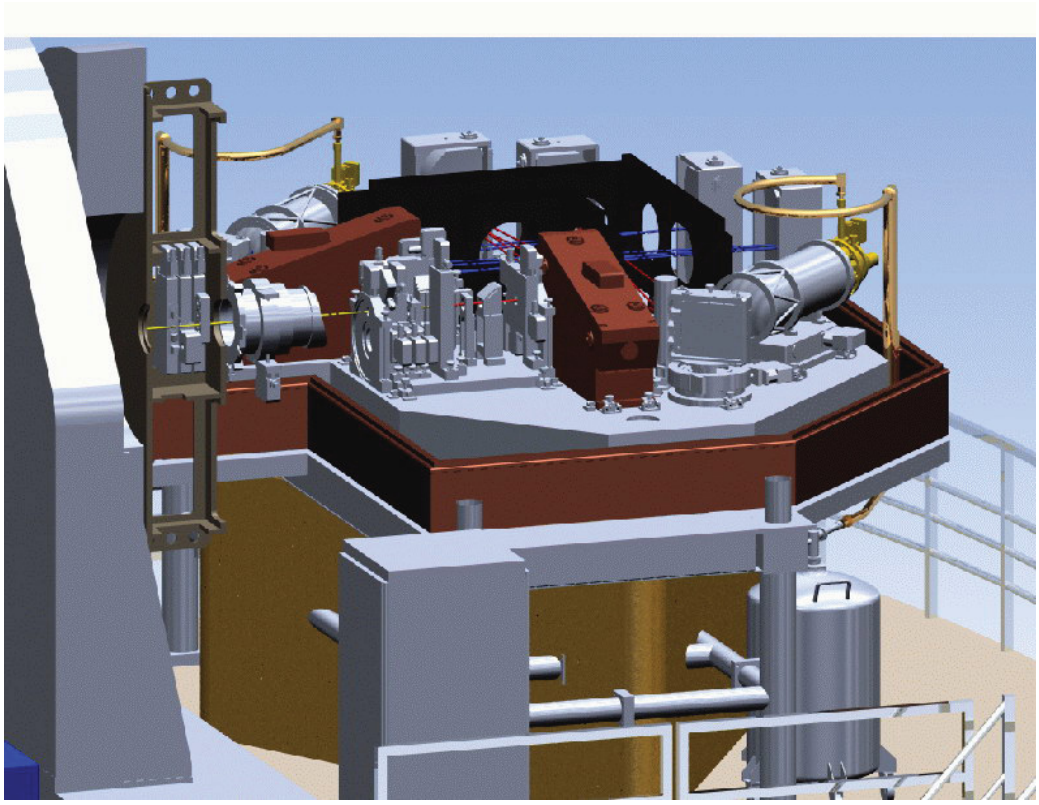

Figure 8.7.:

Figure 8.8.:

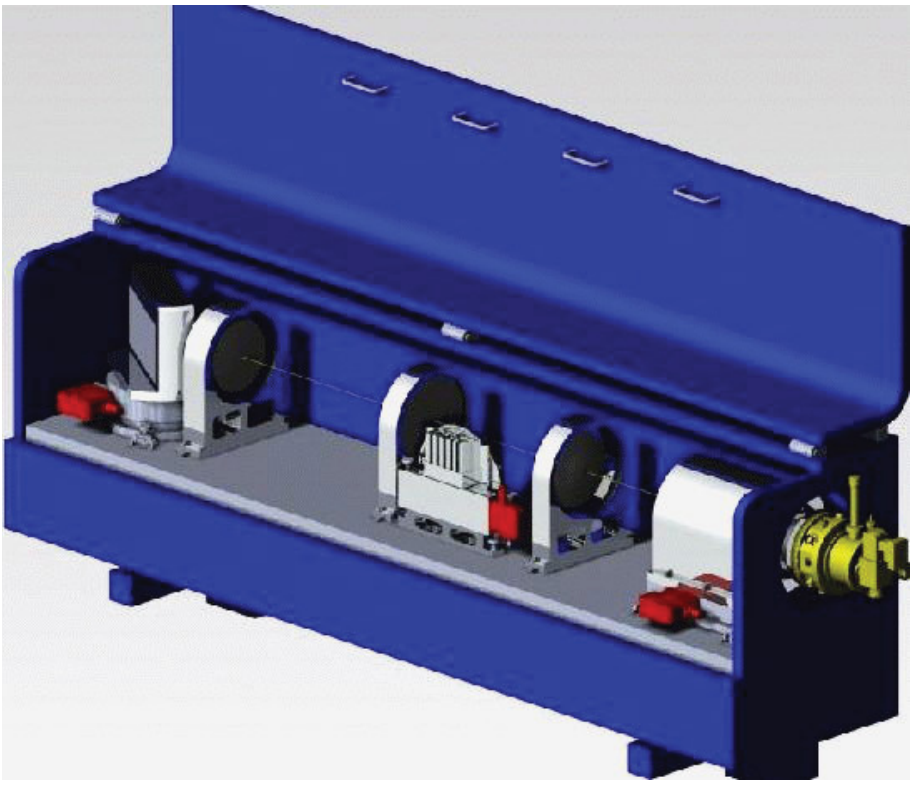

Figure 8.9.:

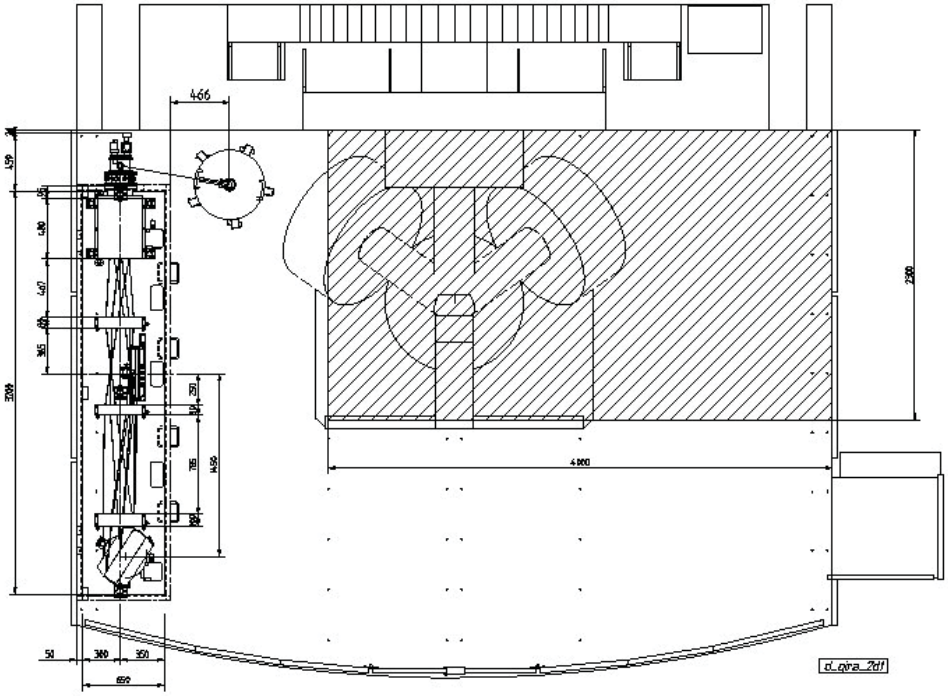

Figure 8.10.:

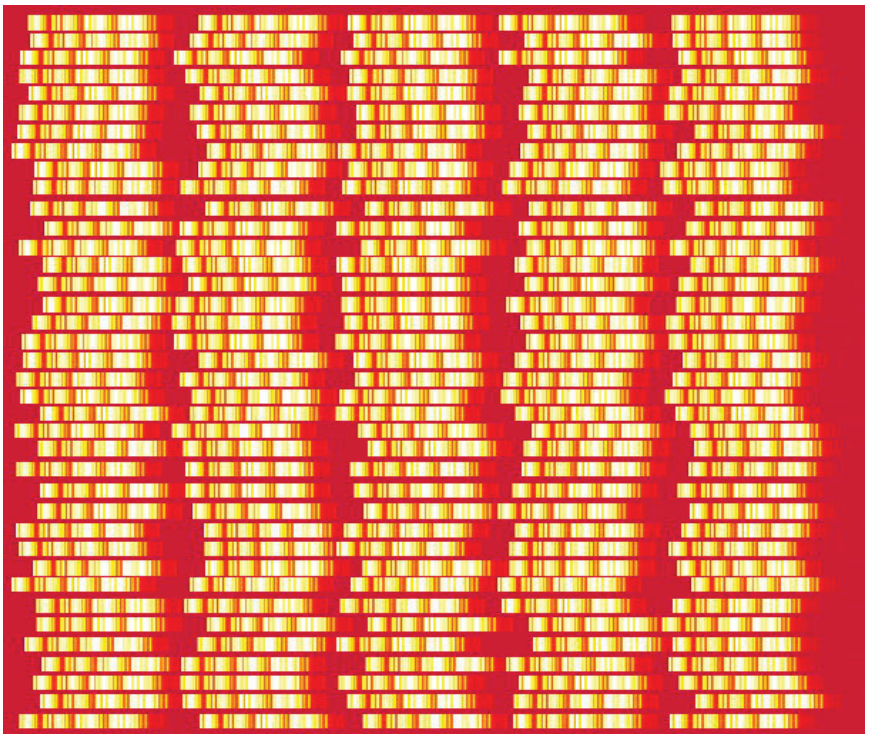

Figure 8.11.:

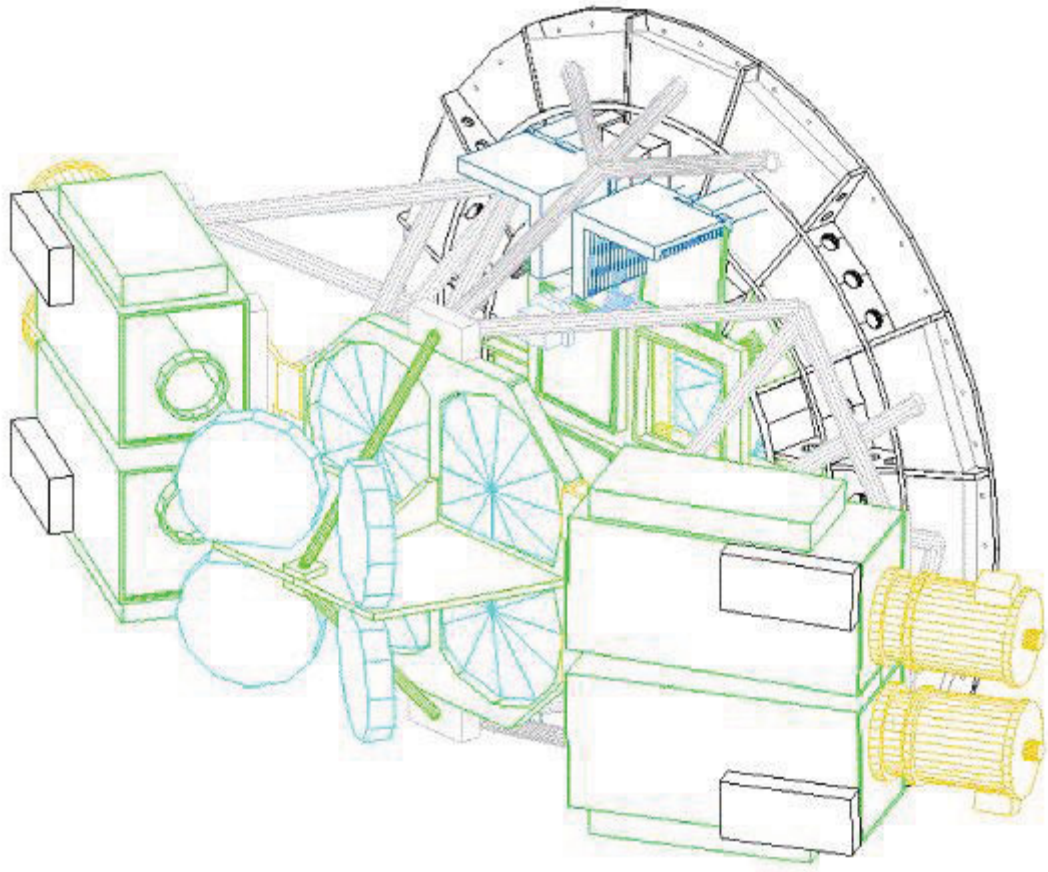

Figure 8.12.:

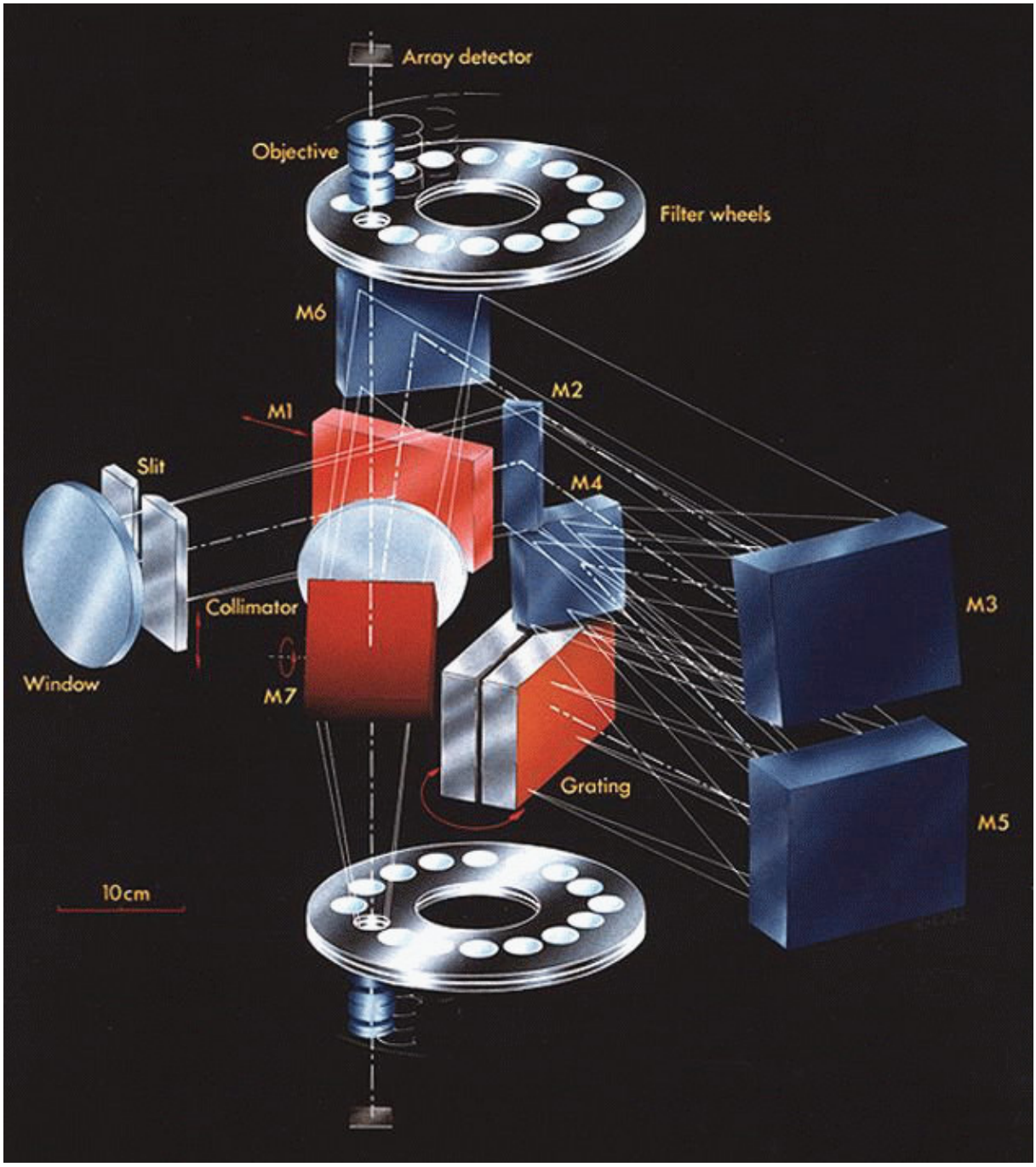
Array detector
Objective
Filter wheels
M6
M2
M1
Slit
M4
M3
Collimator
Window
M7
Grating
M5
10cm

Figure 8.13.:

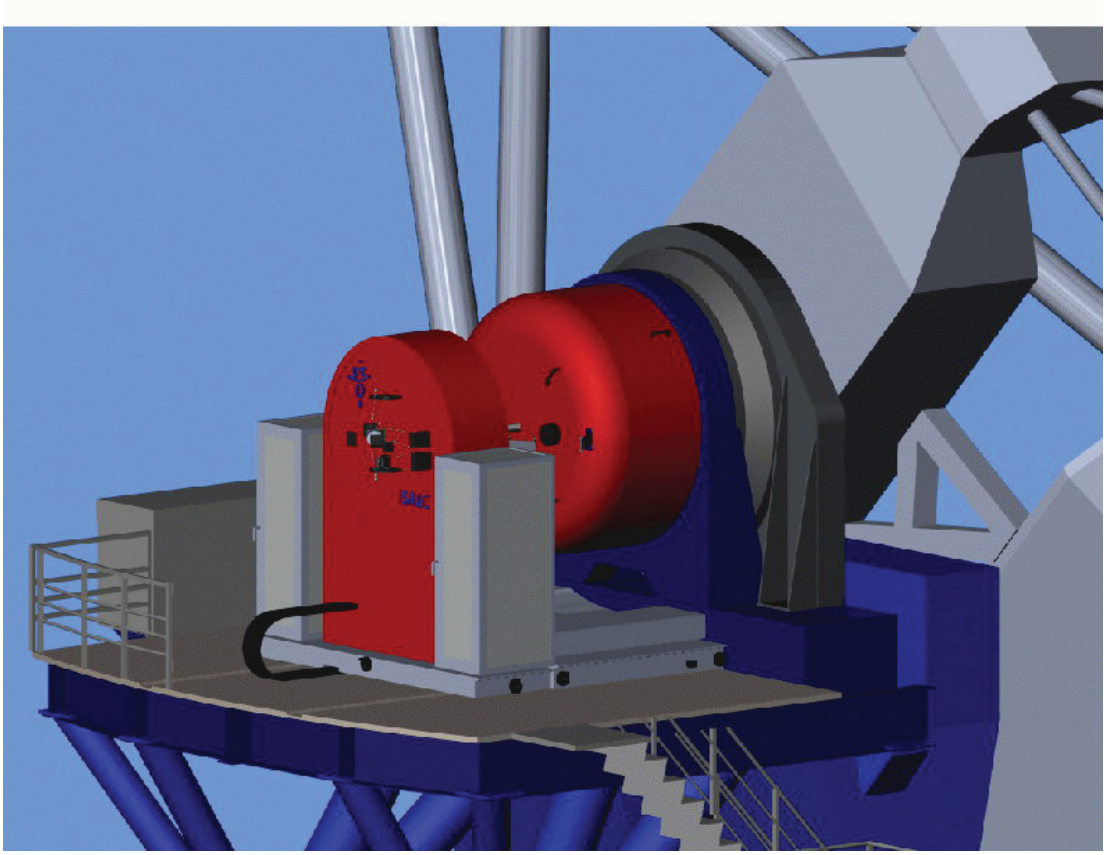

Figure 8.14.:

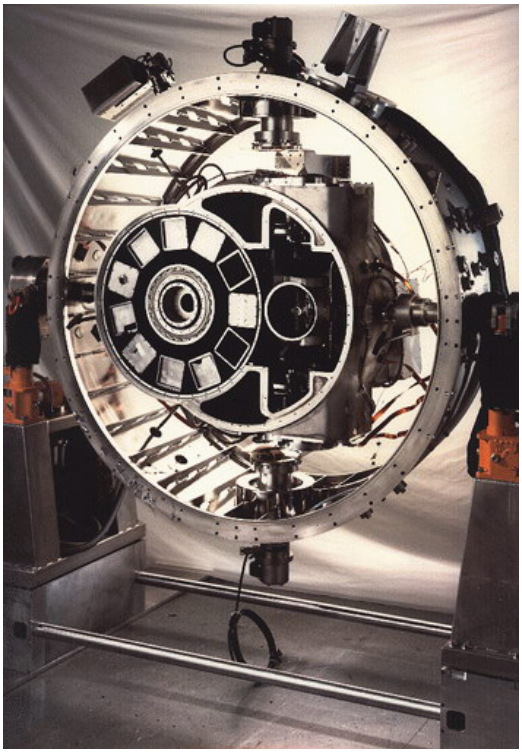

Figure 8.15.:

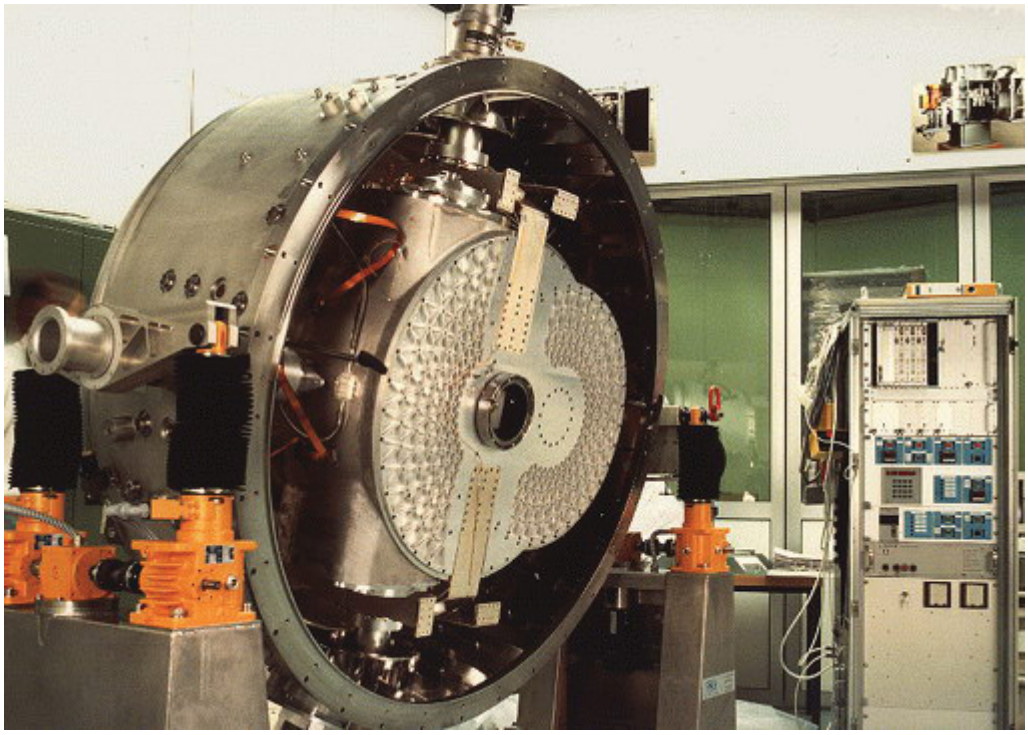

Figure 8.16.:

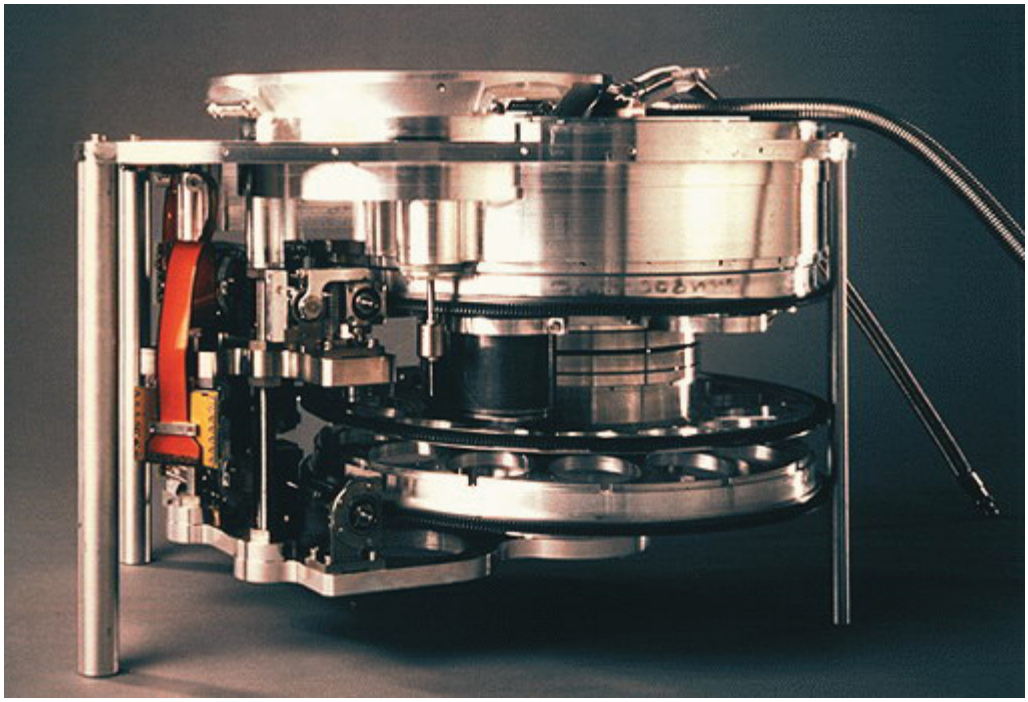

Figure 8.17.:

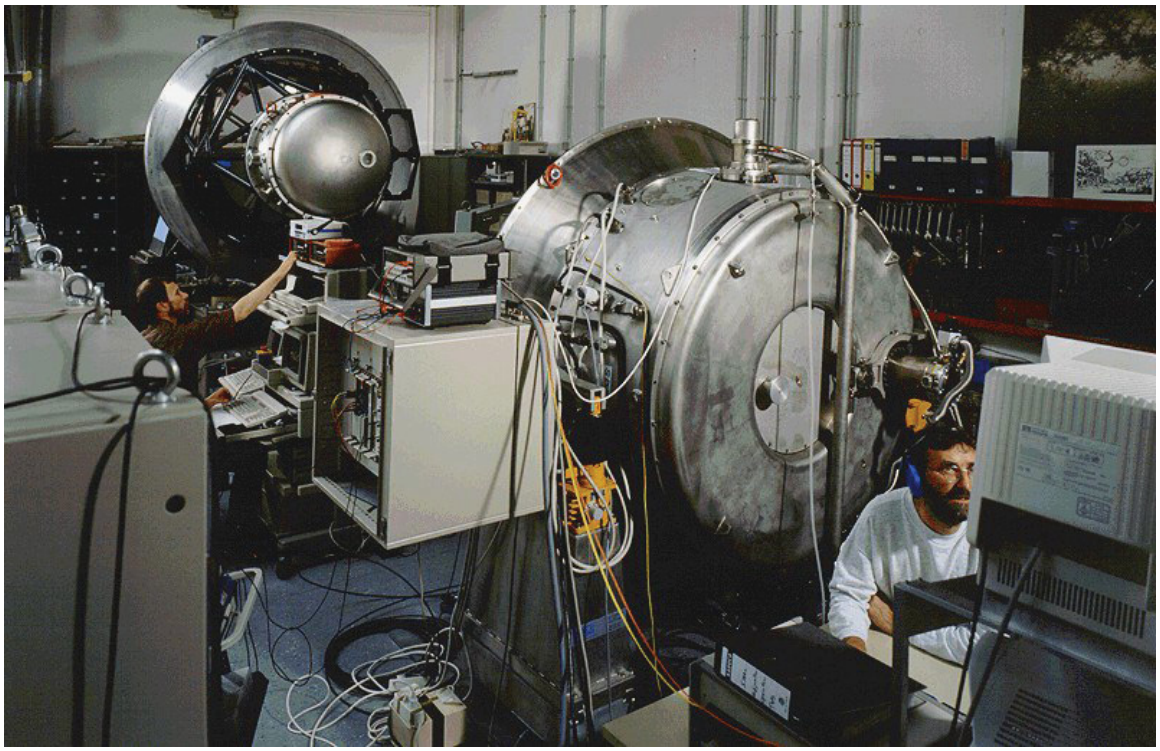

Figure 8.18.:

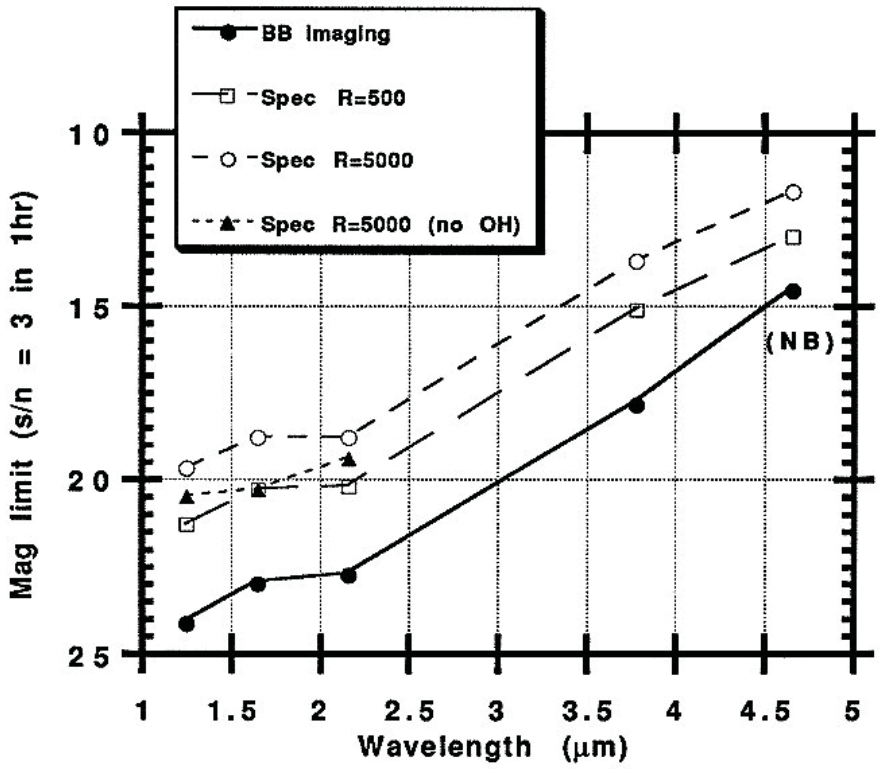

Figure 8.19.:

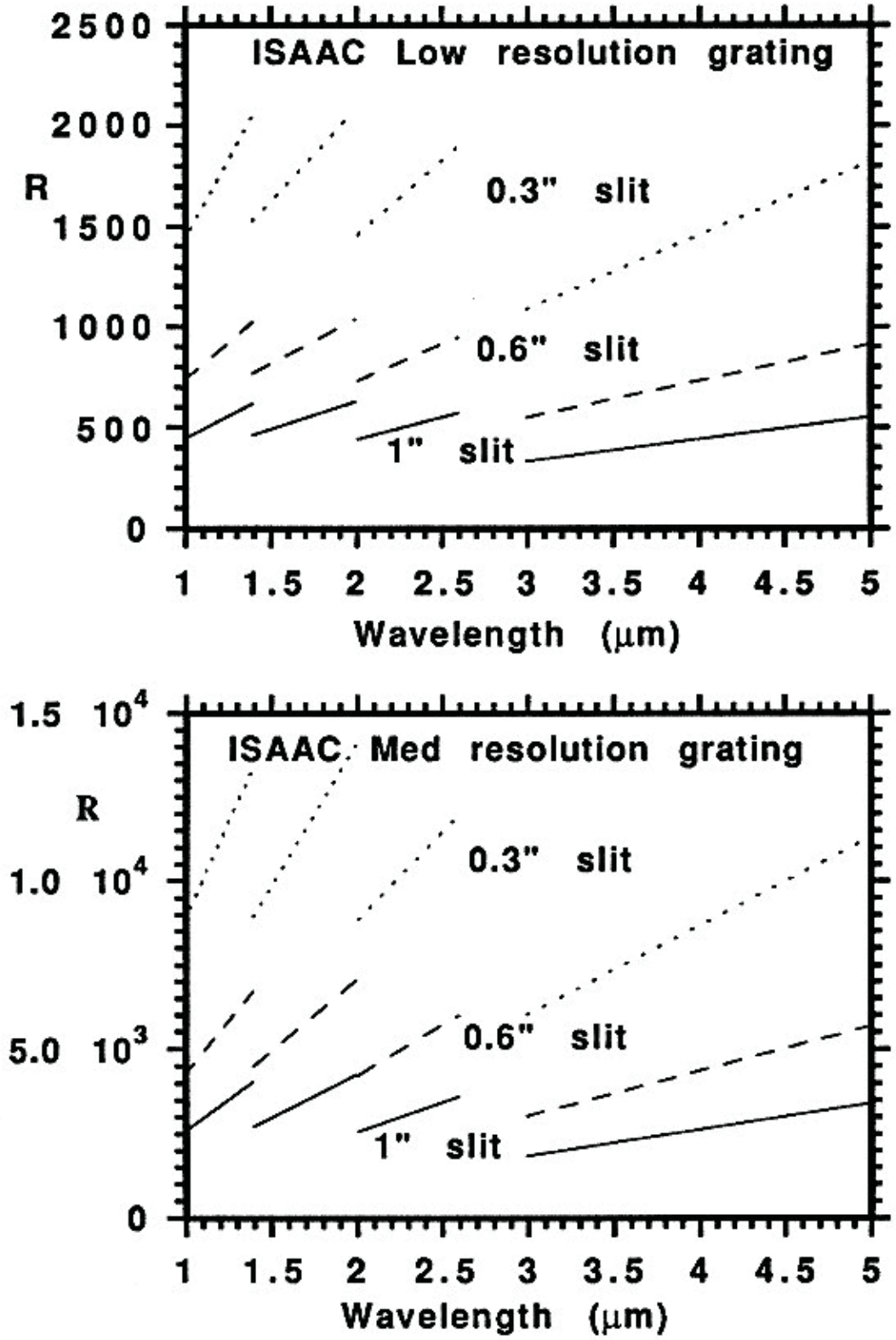
ISAAC Low resolution grating
R
2500
2000
1500
1000
500
0
0.3" slit
0.6" slit
1" slit
1
1.5
2
2.5
3
3.5
4
4.5
5
Wavelength (μm)
ISAAC Med resolution grating
R
1.5 10^4
1.0 10^4
5.0 10^3
0
0.3" slit
0.6" slit
1" slit
1
1.5
2
2.5
3
3.5
4
4.5
5
Wavelength (μm)

Figure 8.20.:

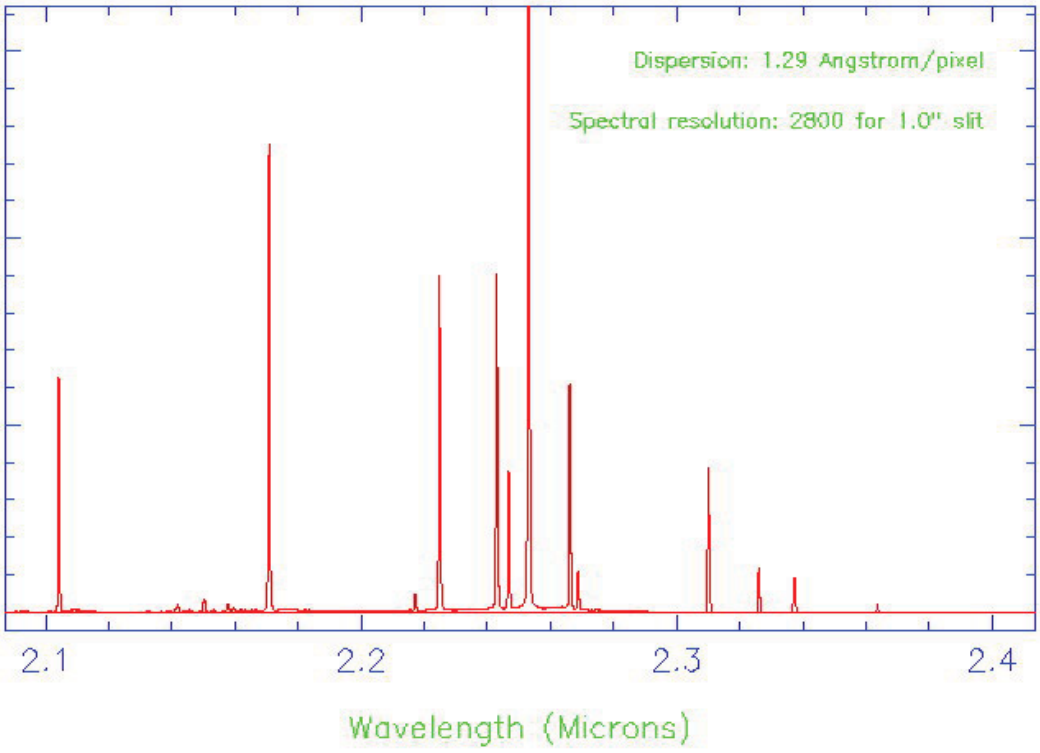

Figure 8.21.:

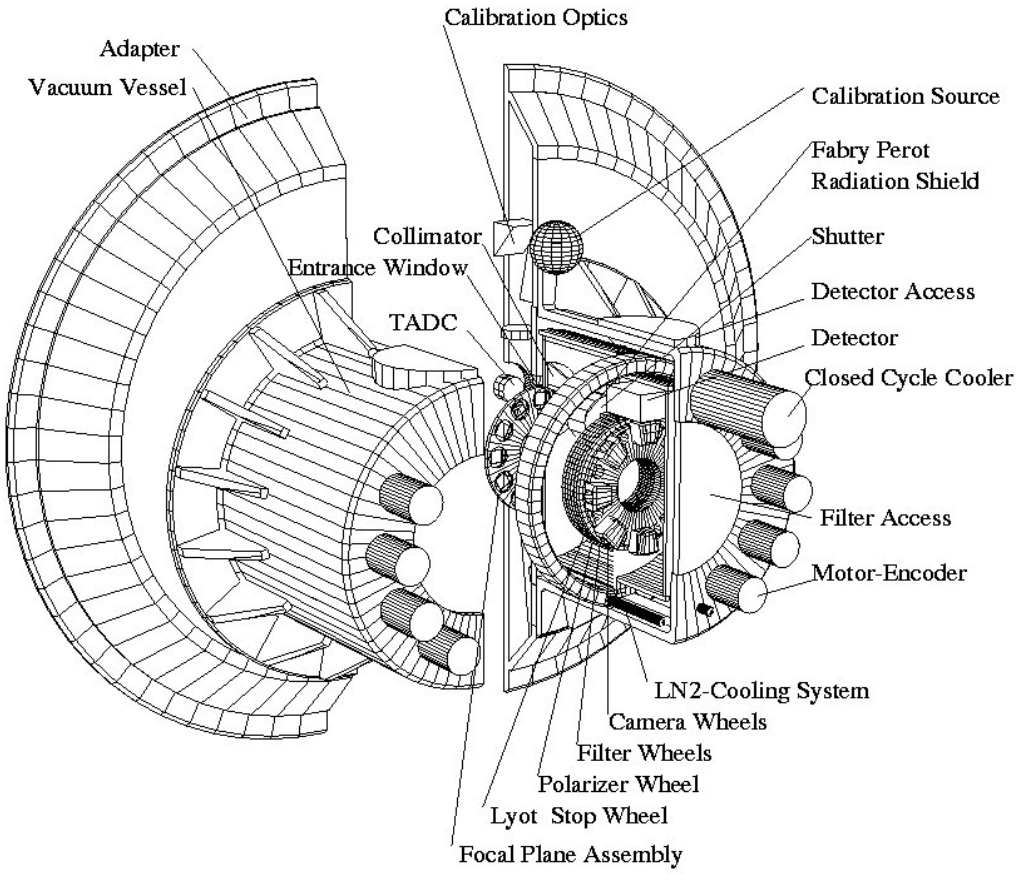

Figure 8.22.:

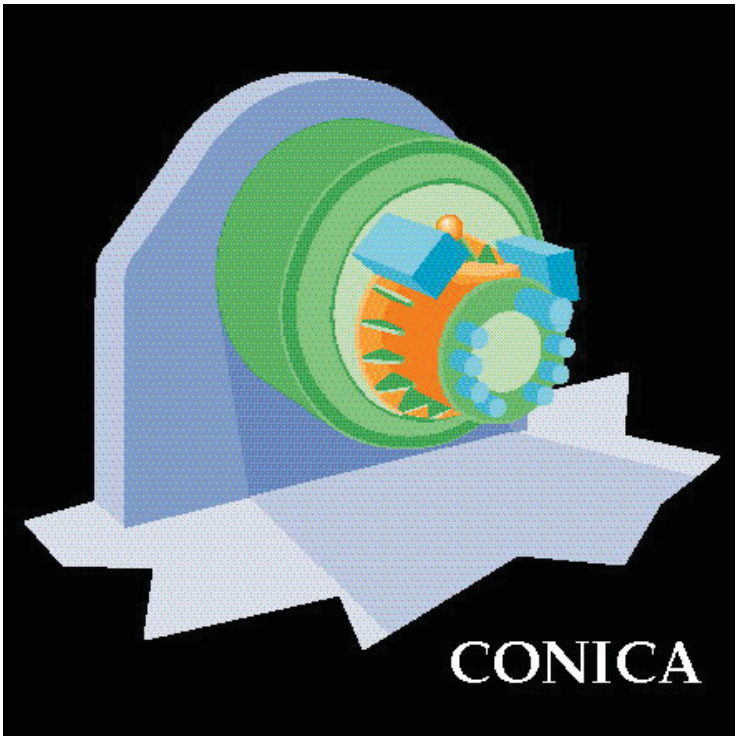

Figure 8.23.:

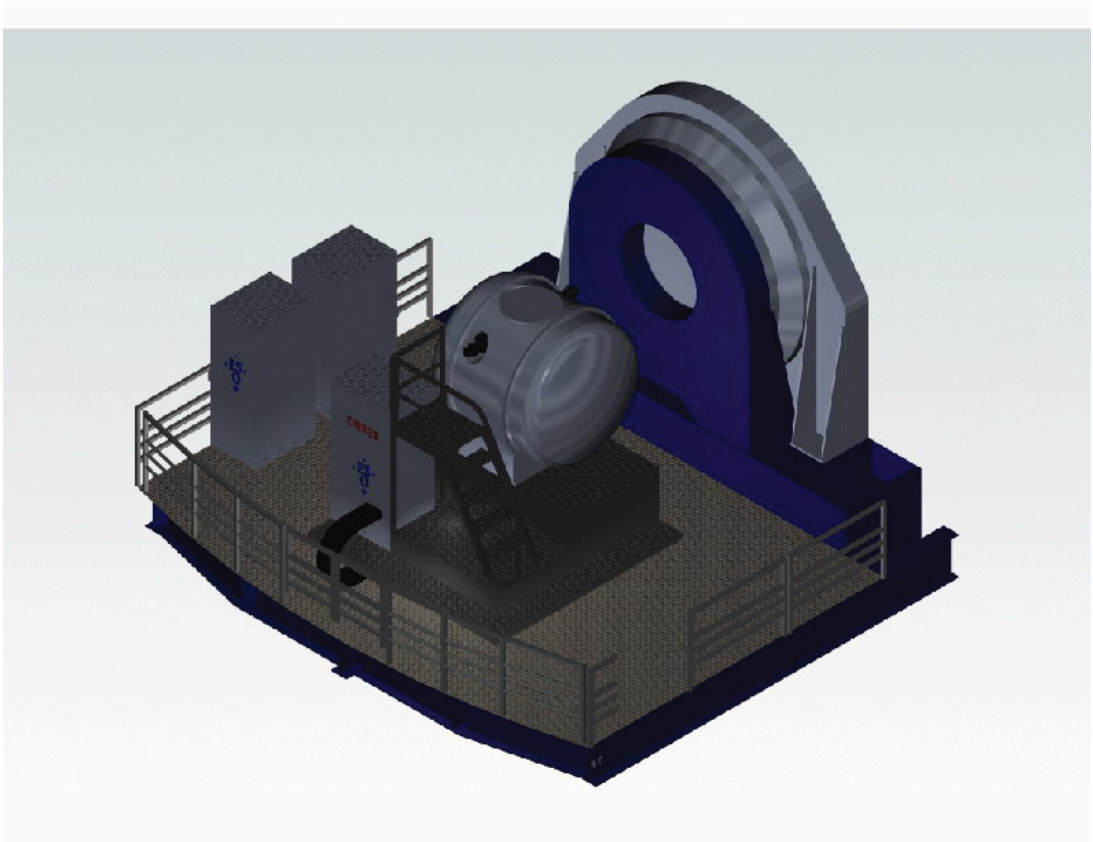

Figure 8.24.:

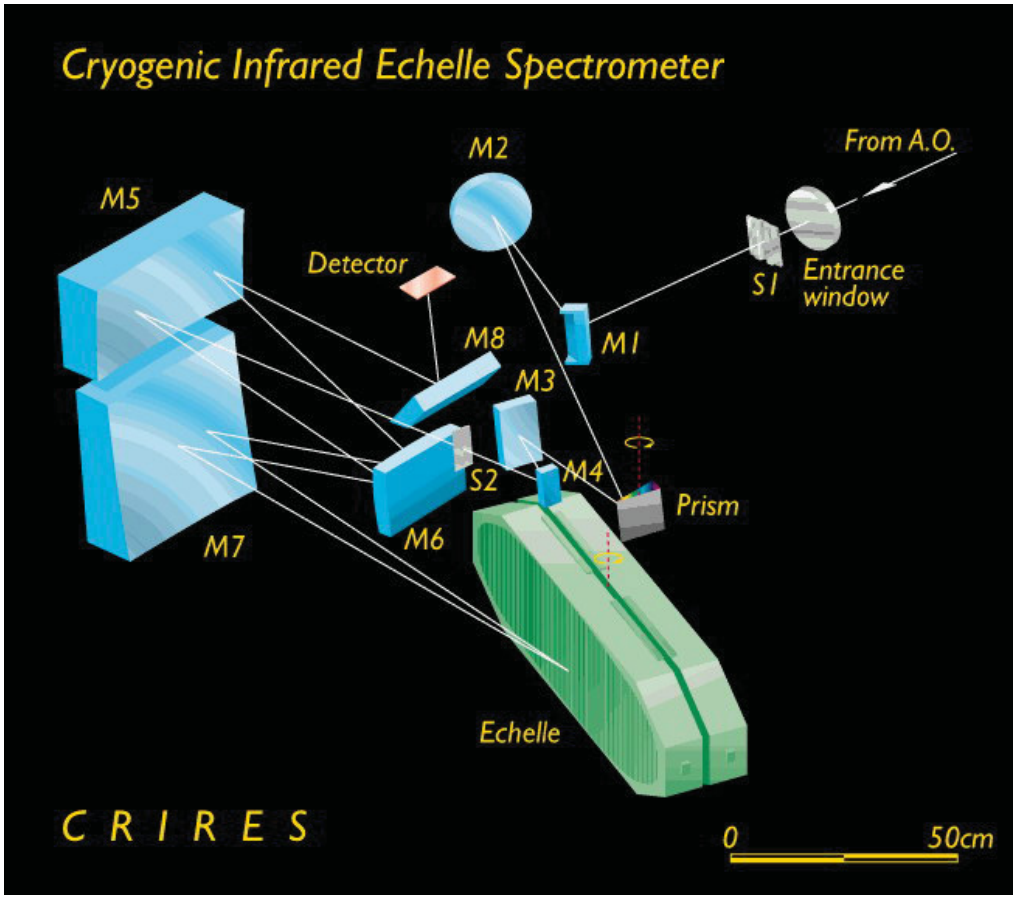

Figure 8.25.:

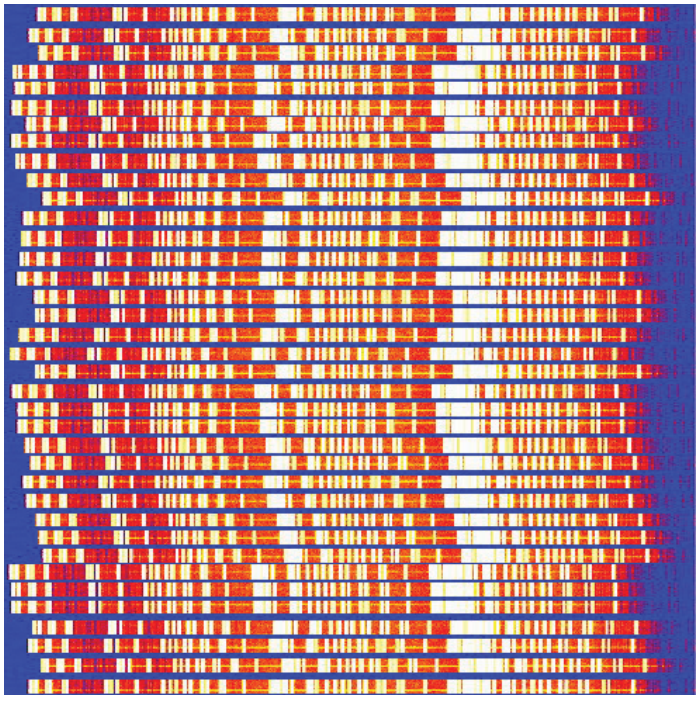

Figure 8.26.:

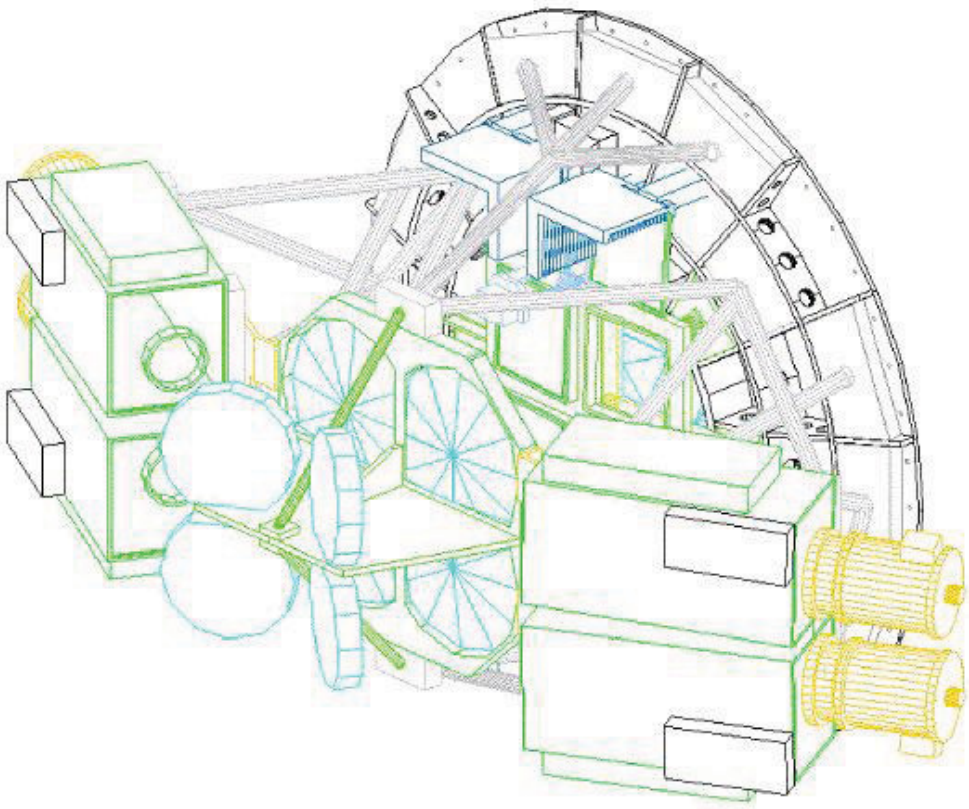

Figure 8.27.:

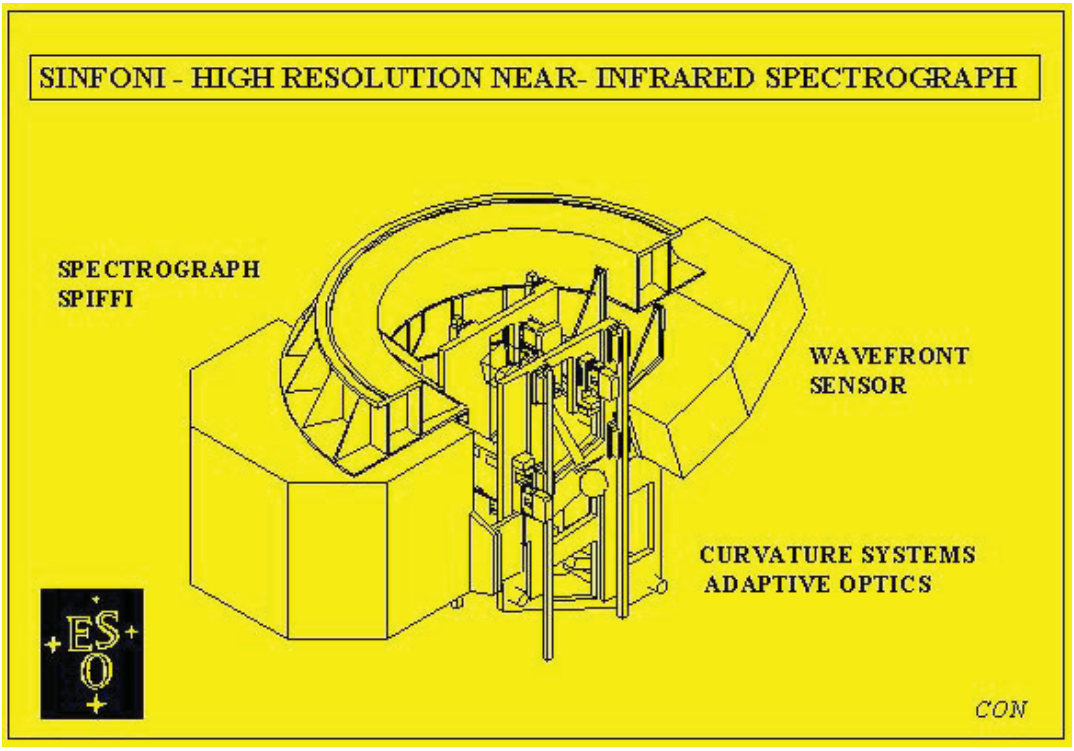

Figure 8.28.:

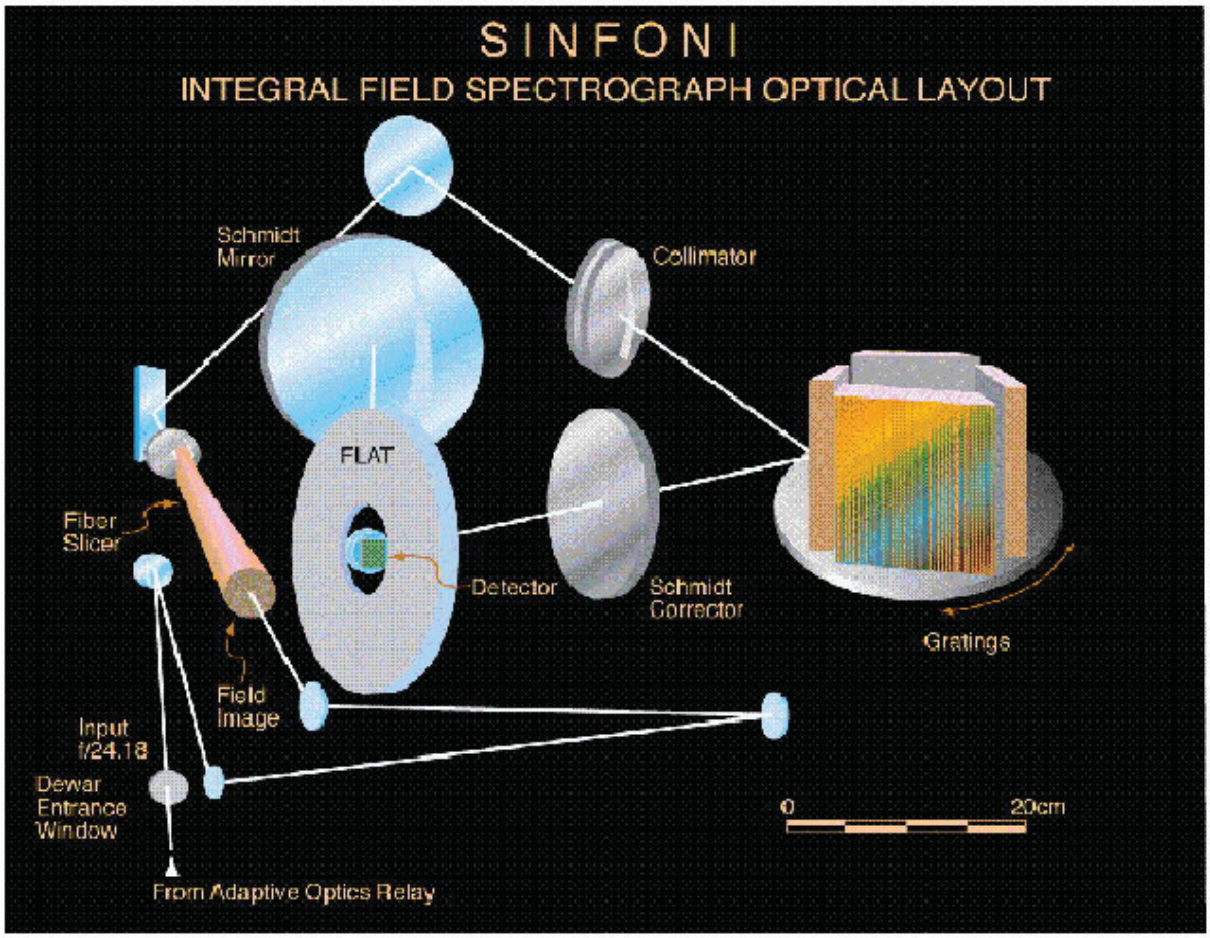

Figure 8.29.:

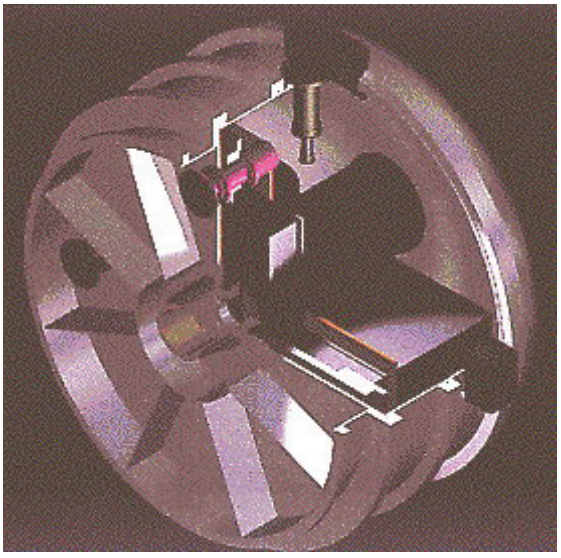

Figure 8.30.:

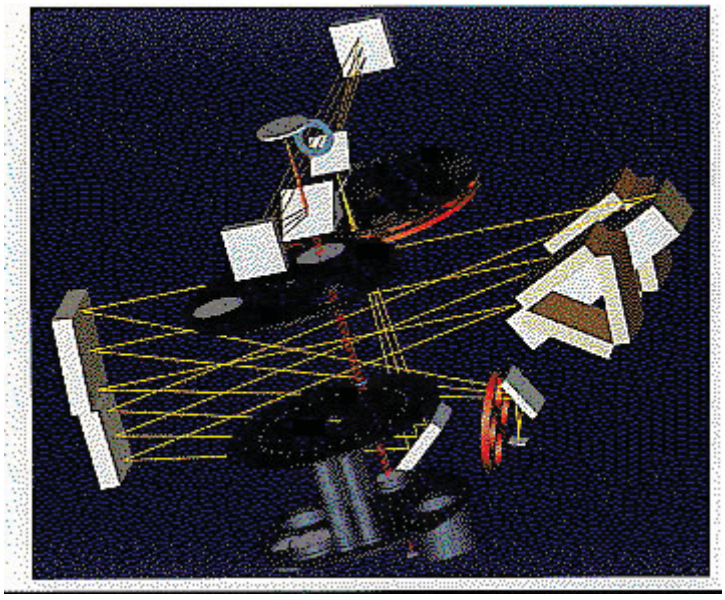

Figure 8.31.:

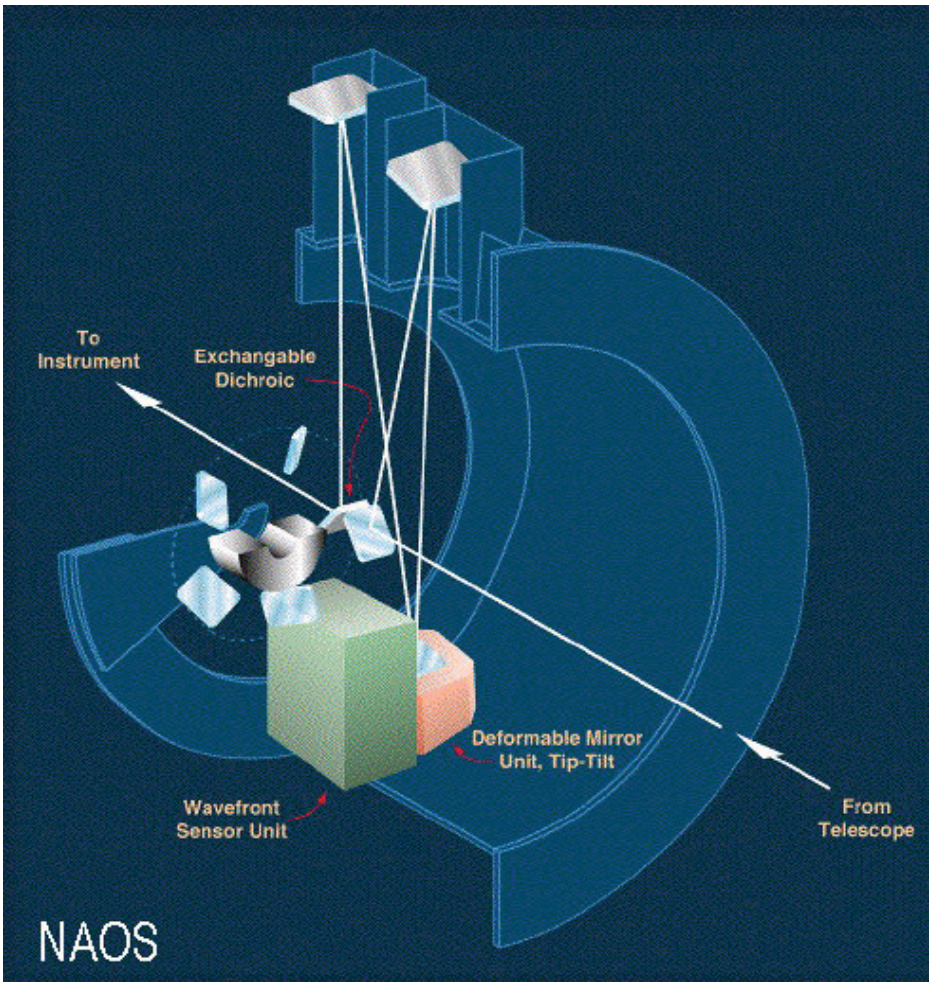

Figure 8.32.:

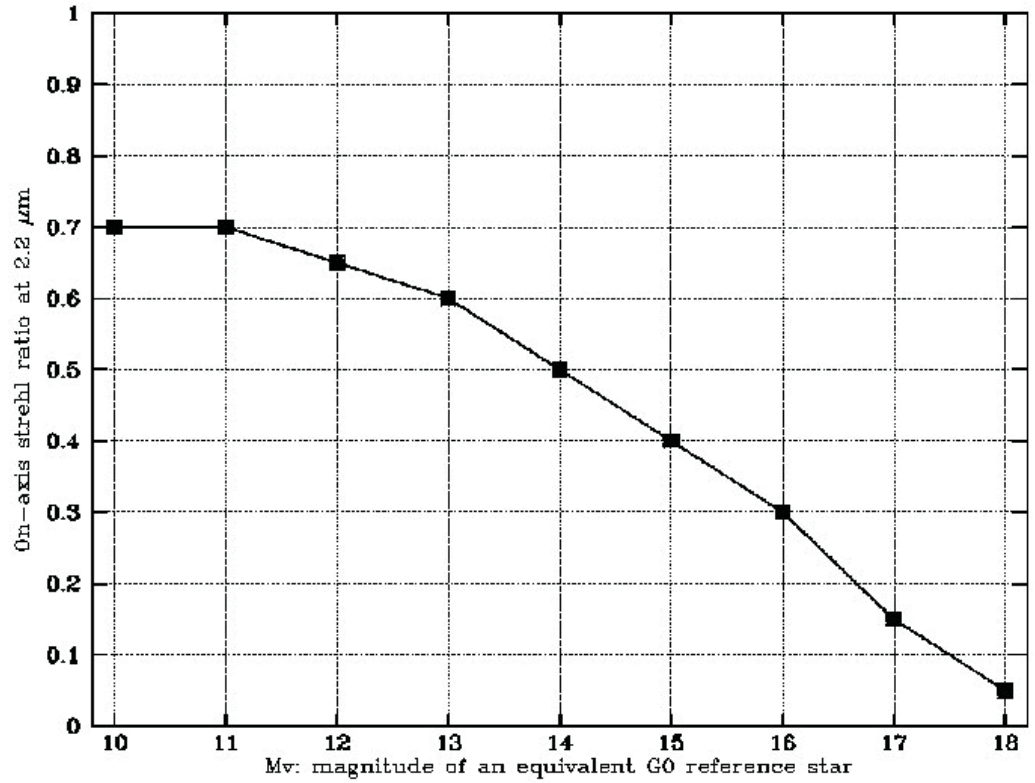

Figure 8.33.:

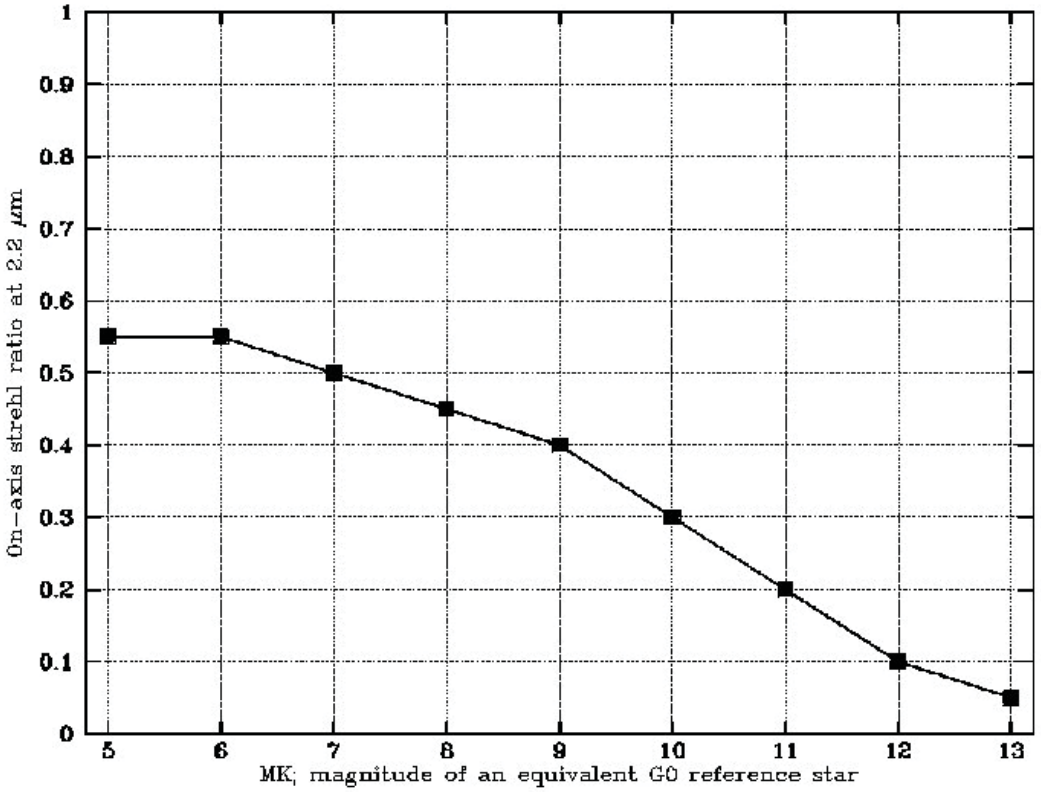

Figure 8.34.:

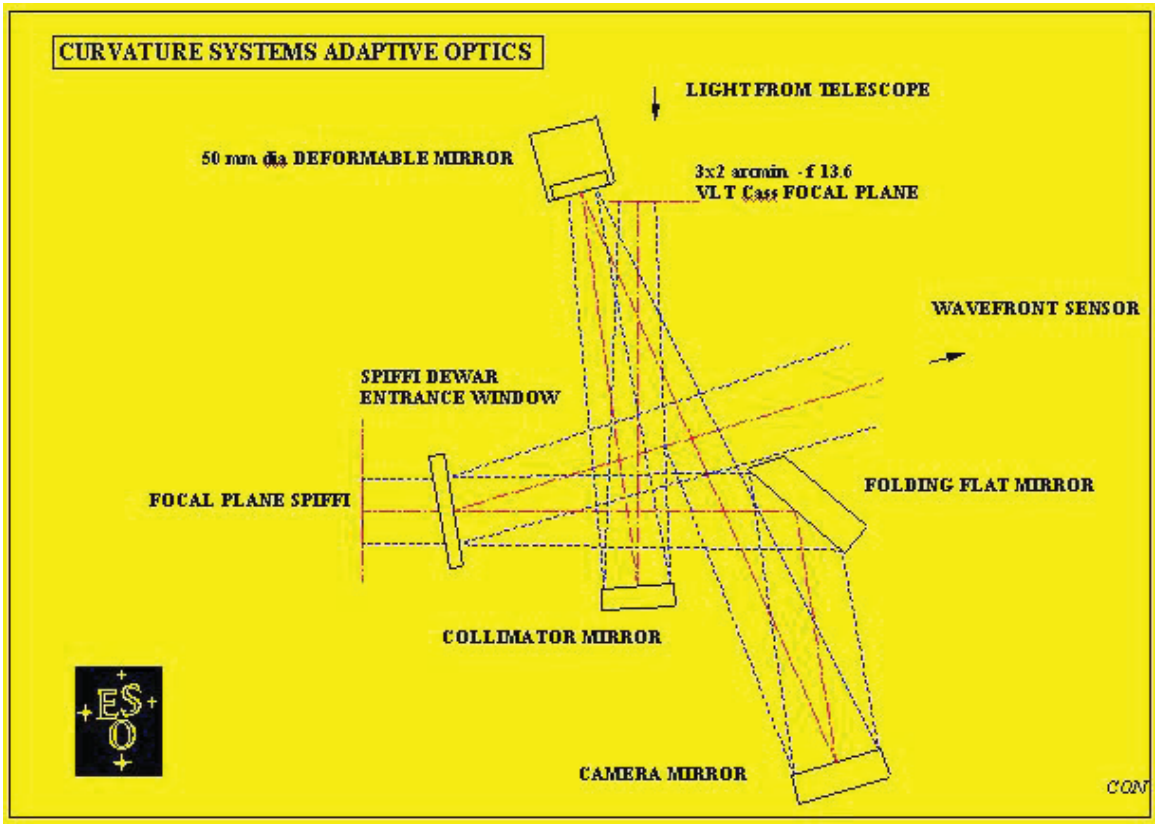

Figure 8.35.:

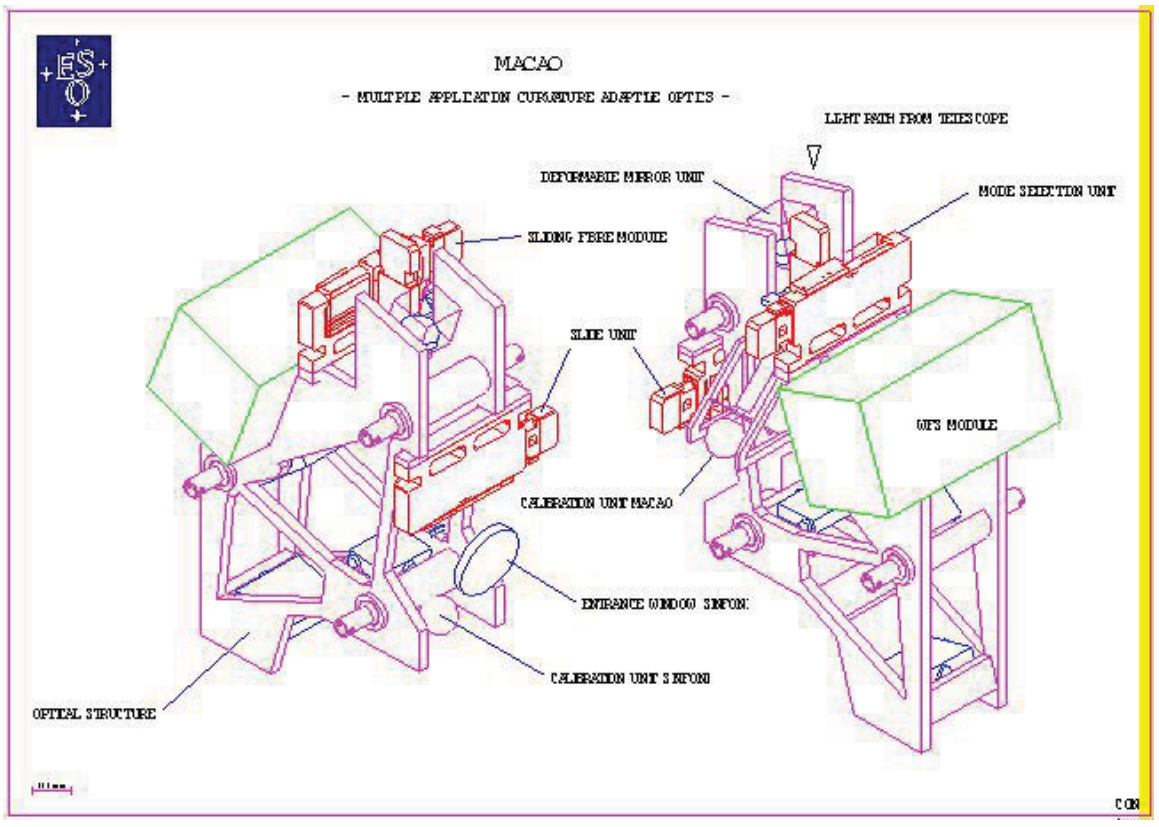

Figure 8.36.:

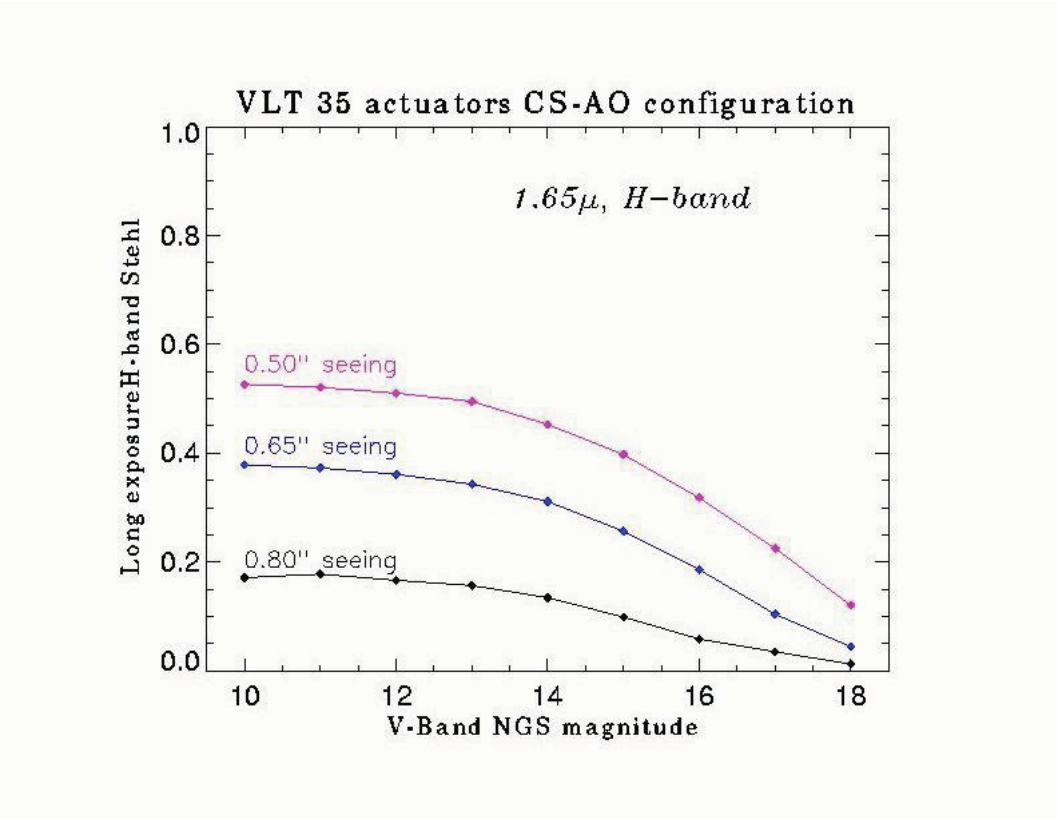

Figure 8.37.:

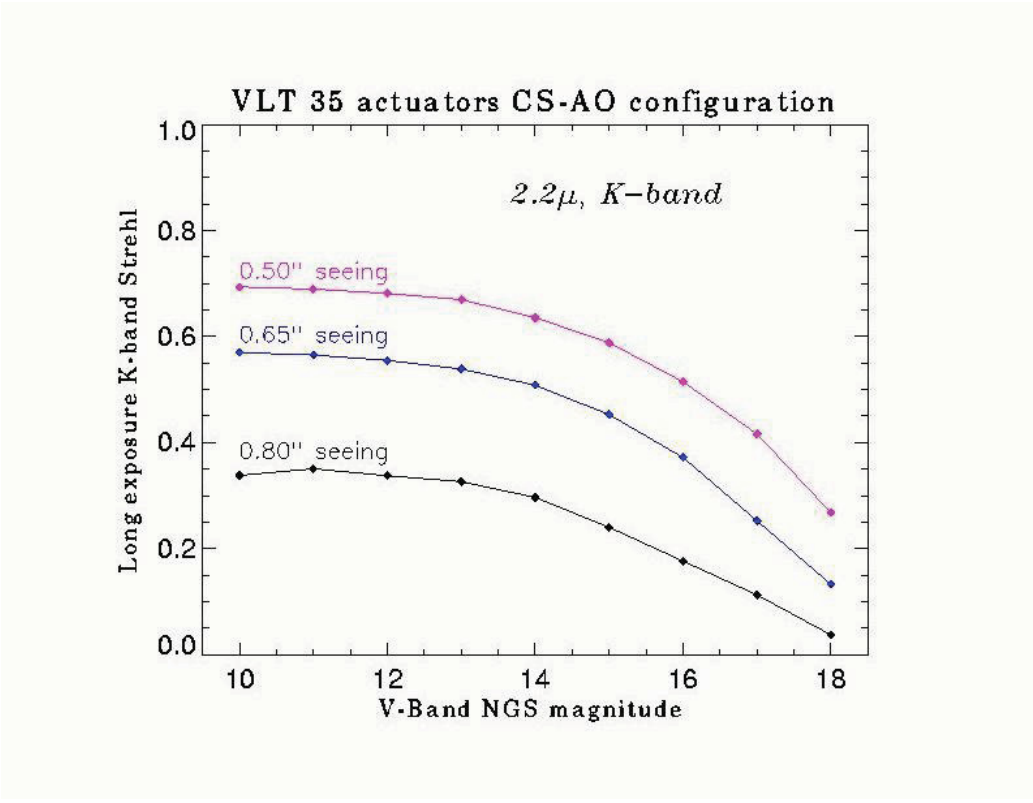

Figure 8.38.:

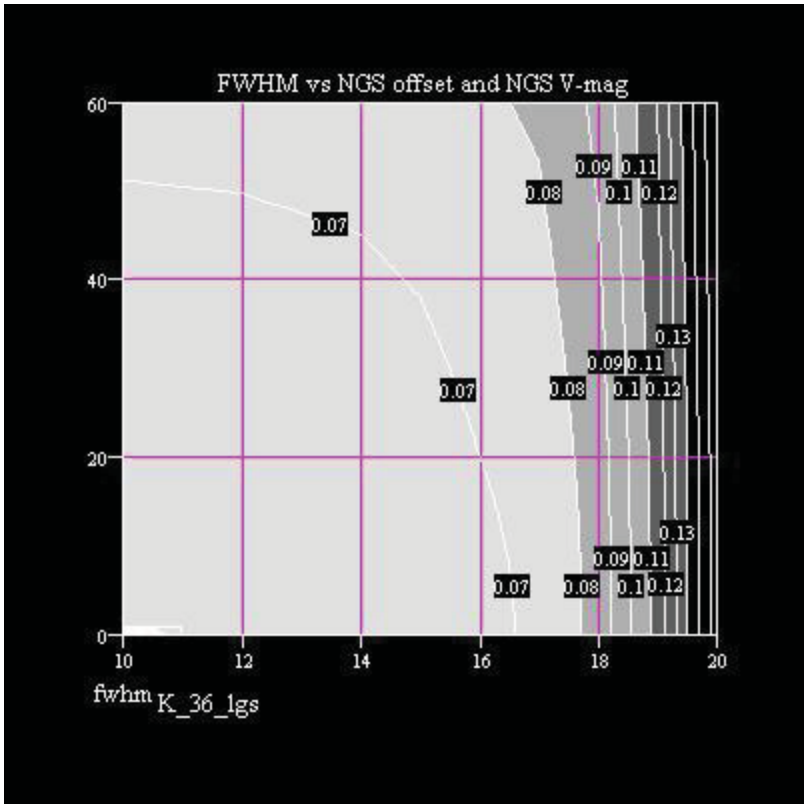

Figure 8.39.:

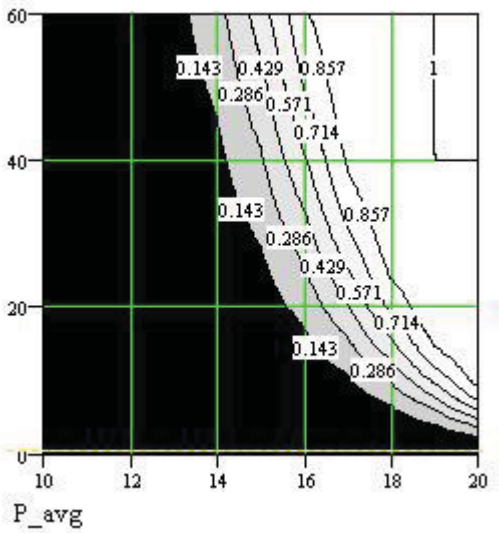

Figure 8.40.:

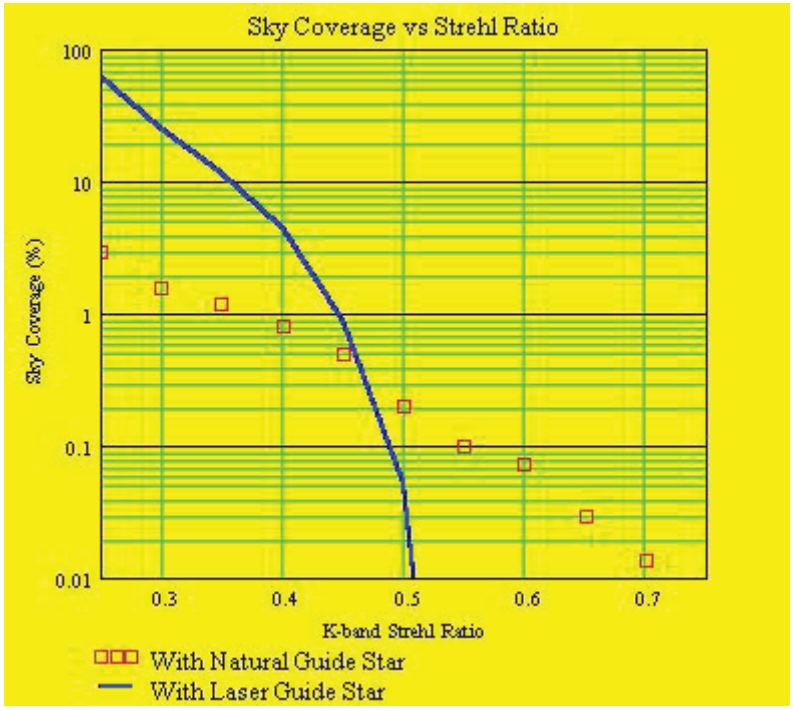

Figure 8.41.:

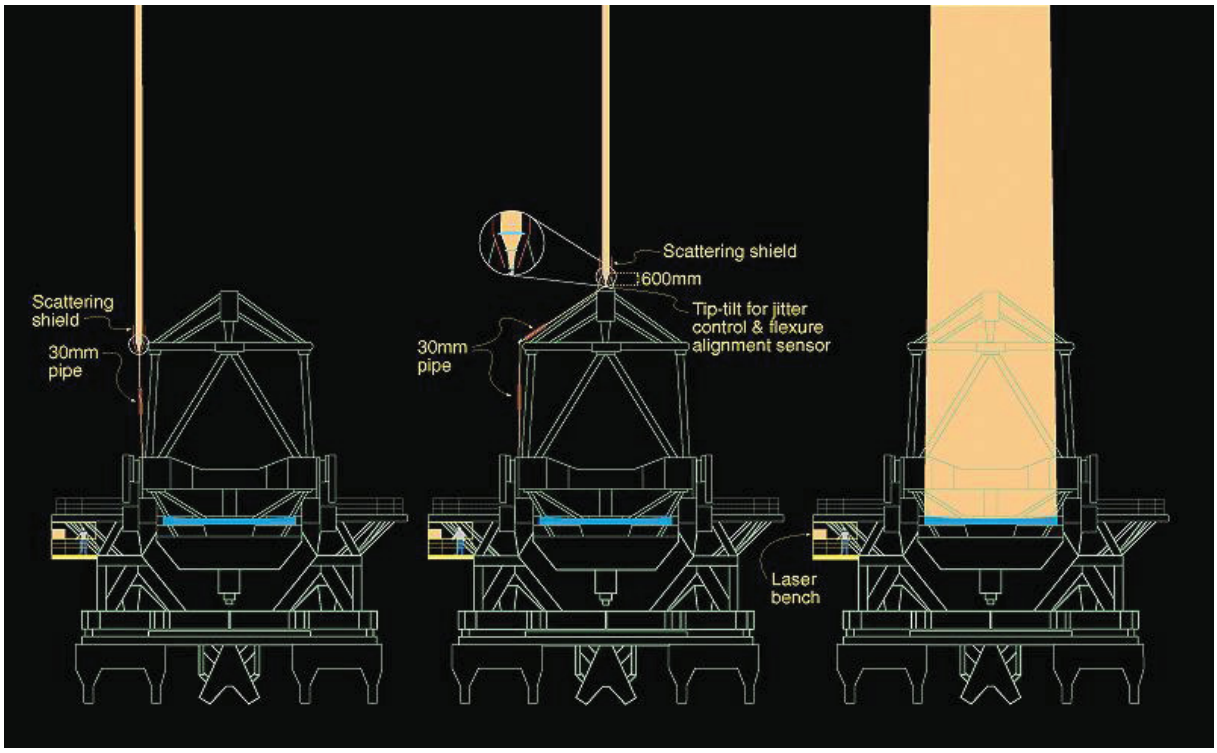

Figure 9.1.:

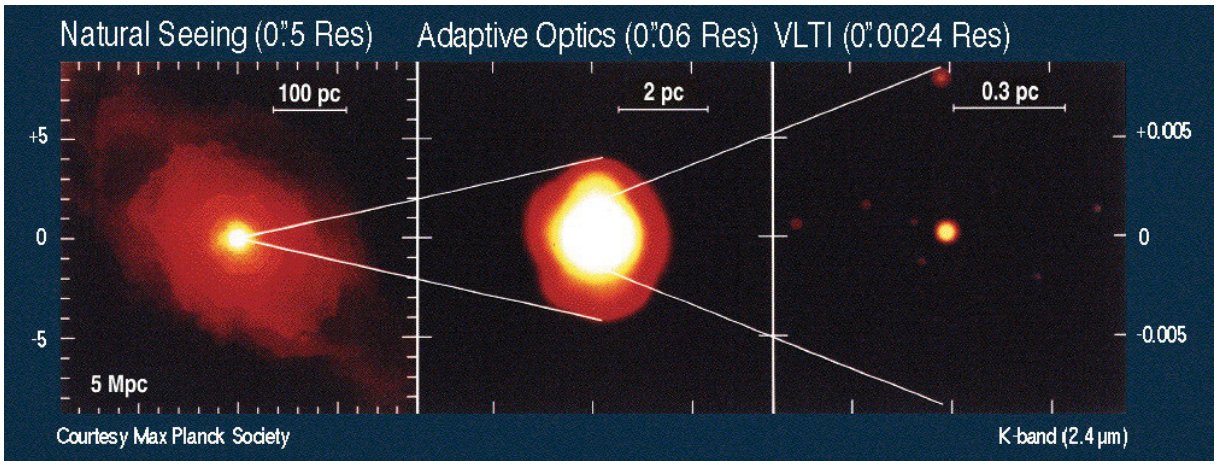

Figure 9.2.:

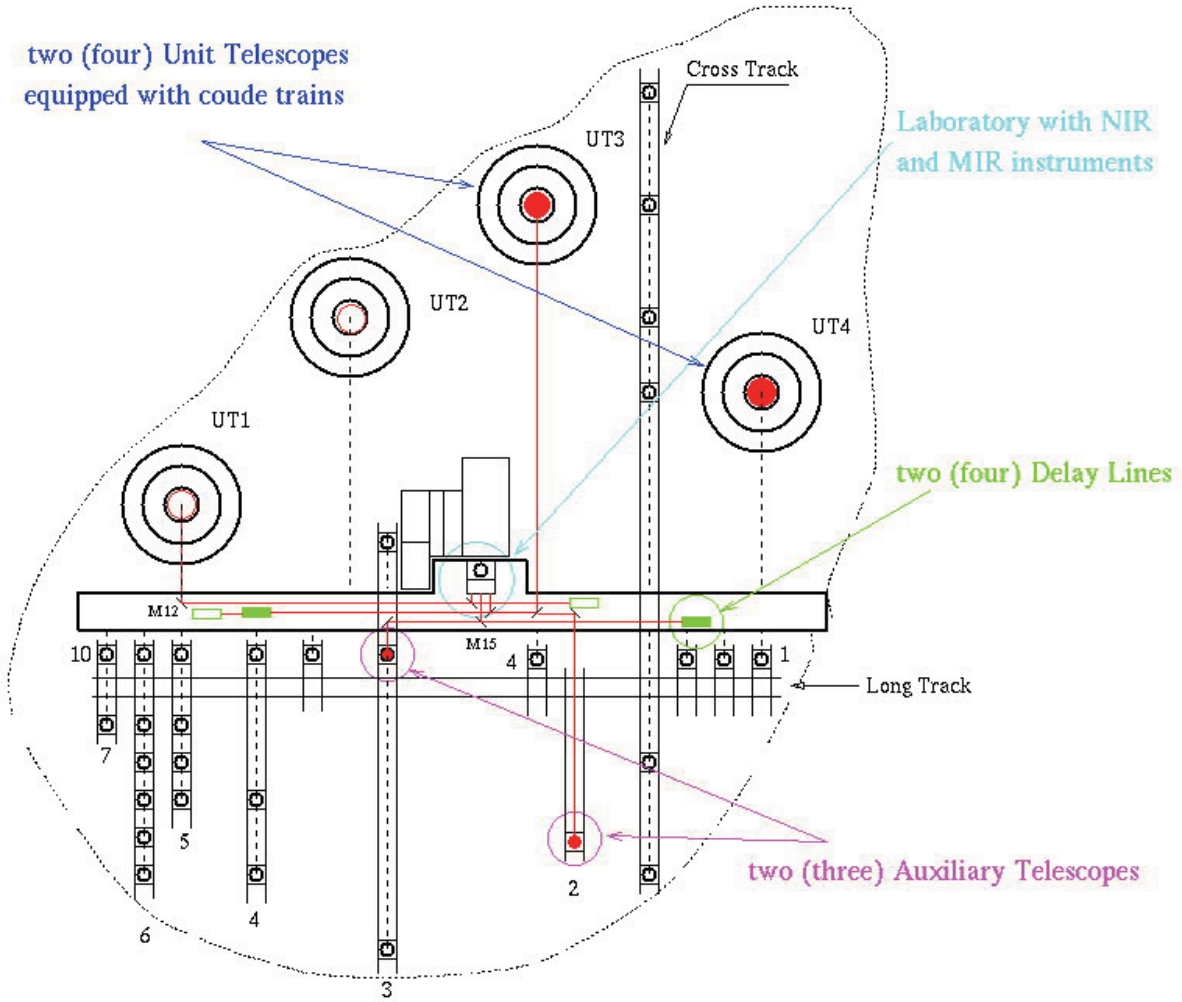

Figure 9.3a.:

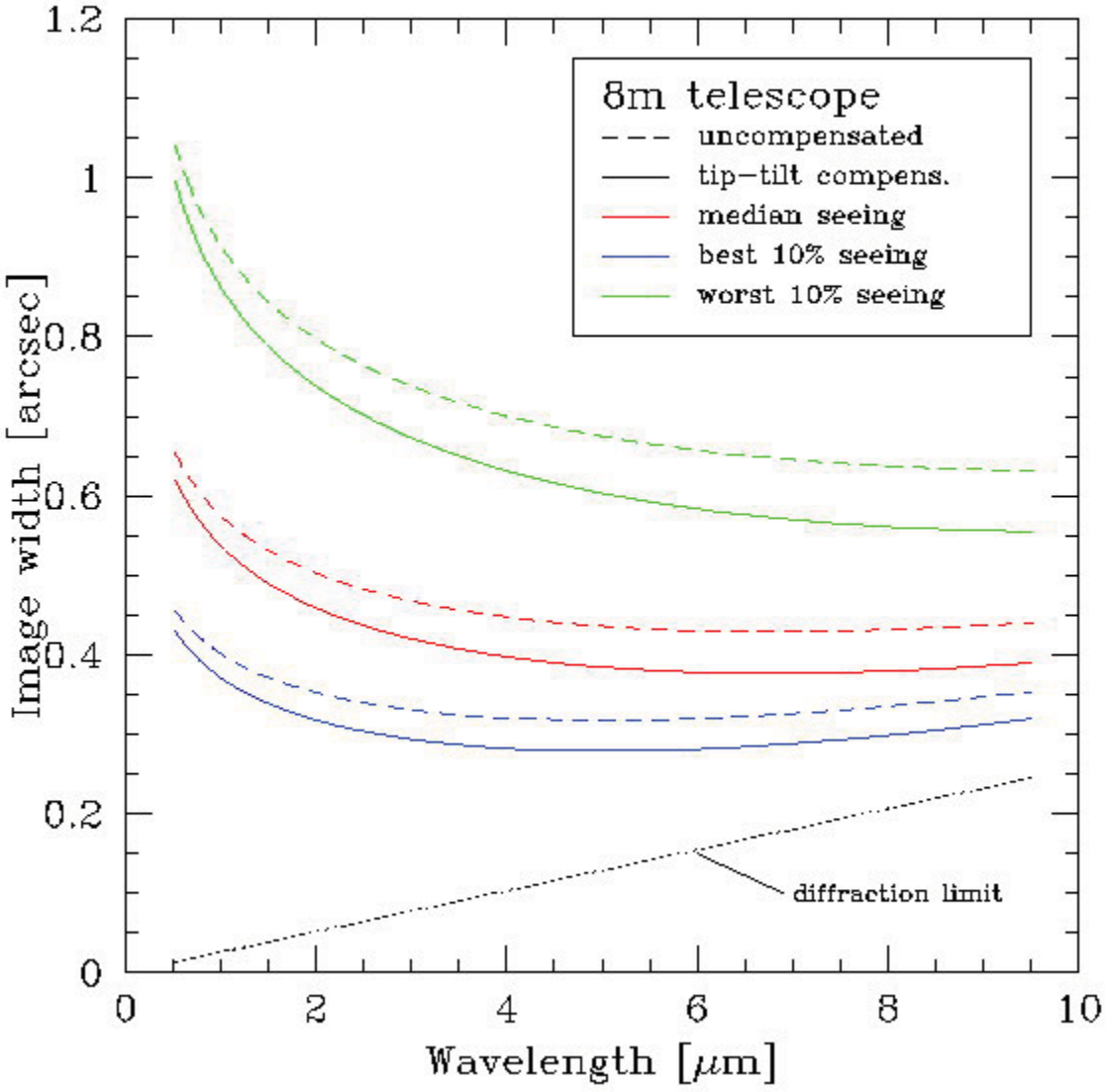
8m telescope
uncompensated
tip–tilt compens.
median seeing
best 10% seeing
worst 10% seeing
diffraction limit
Image width [arcsec]
Wavelength [μm]
0
0.2
0.4
0.6
0.8
1
1.2
0
2
4
6
8
10

Figure 9.3b.:

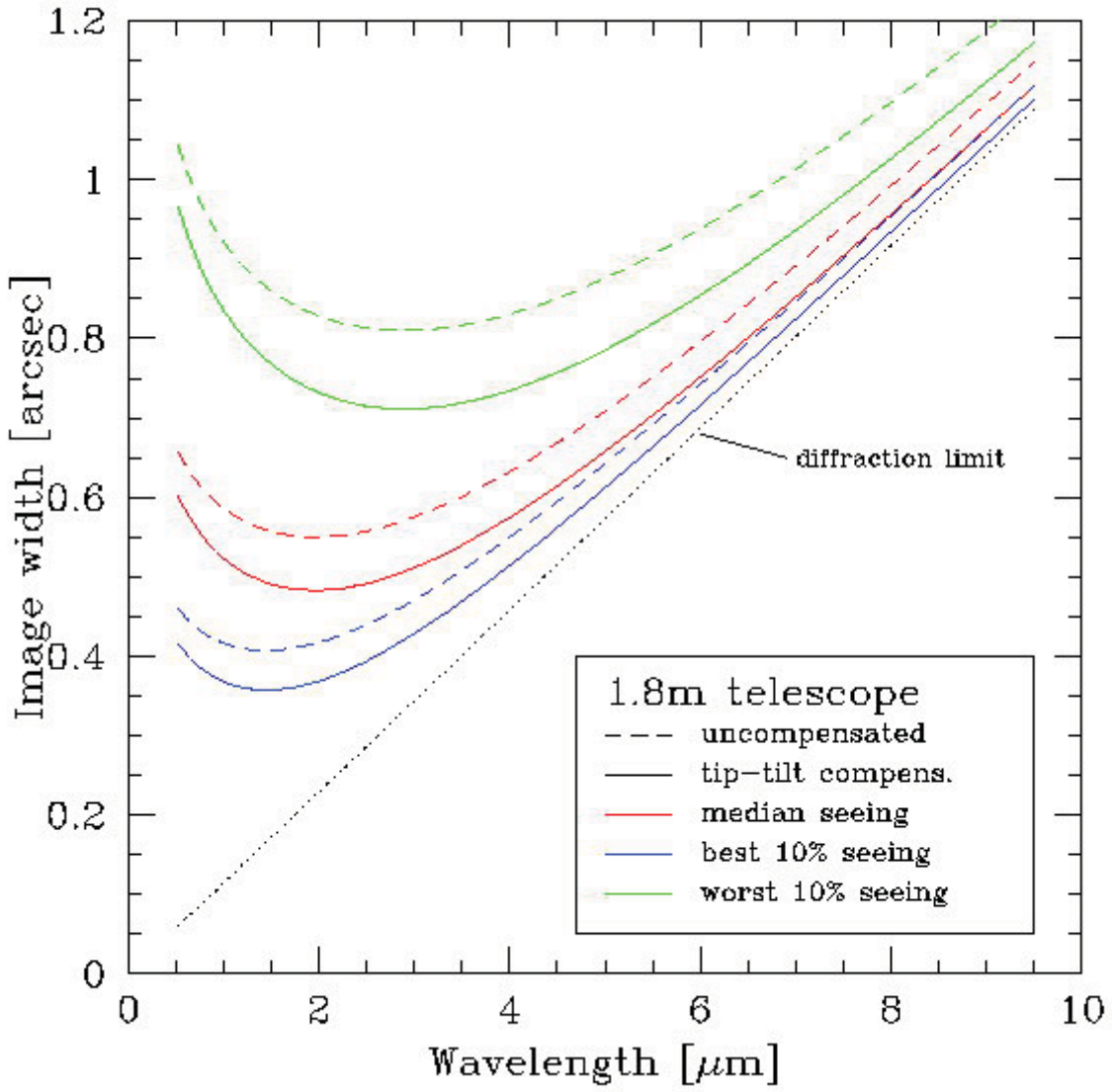
1.2
1
0.8
0.6
0.4
0.2
0
Image width [arcsec]
0
2
4
6
8
10
Wavelength [μm]
diffraction limit
1.8m telescope
uncompensated
tip−tilt compens.
median seeing
best 10% seeing
worst 10% seeing

Figure 9.4.:

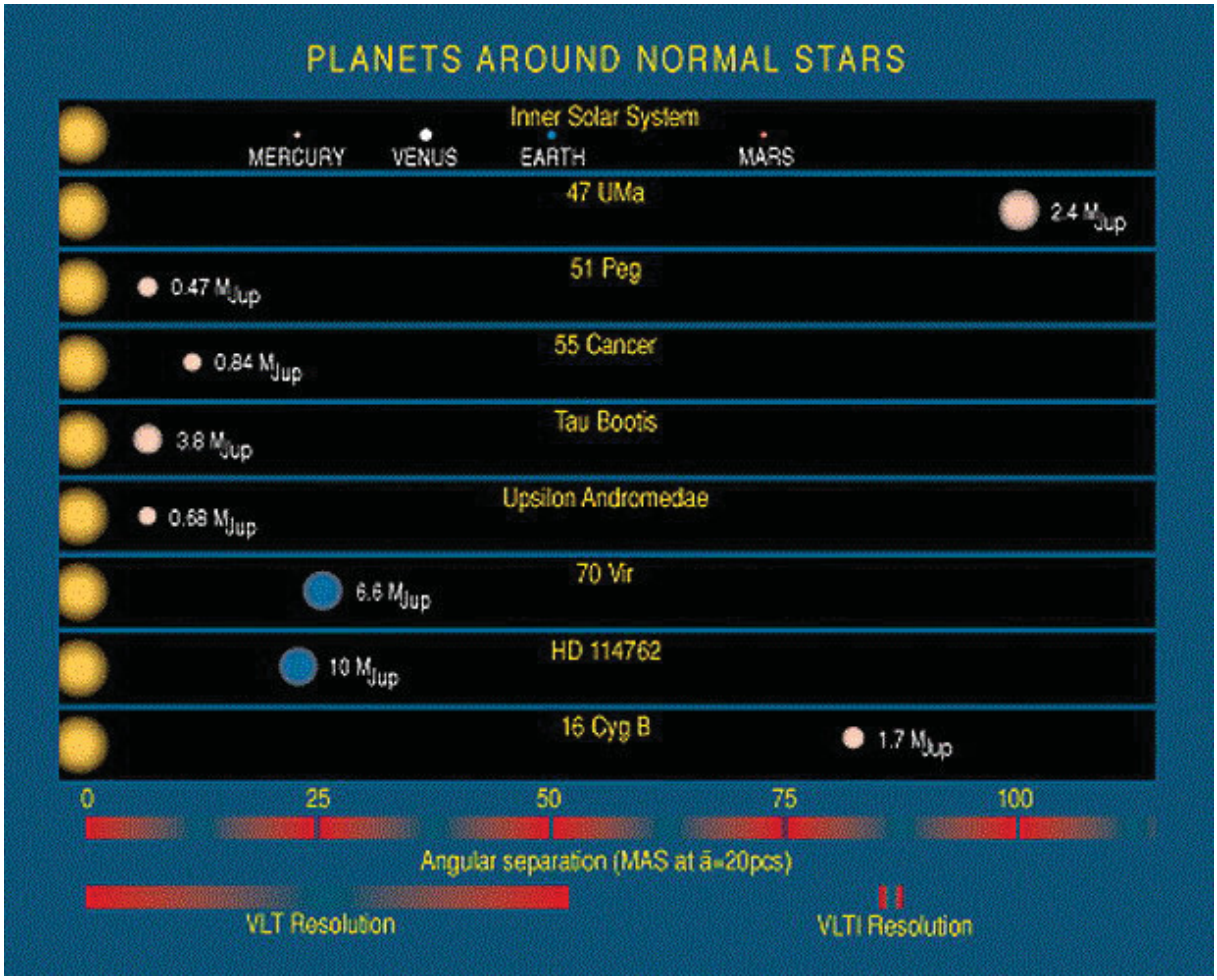
PLANETS AROUND NORMAL STARS
Inner Solar System
MERCURY
VENUS
EARTH
MARS
47 UMa
2.4 MJup
51 Peg
0.47 MJup
55 Cancer
0.84 MJup
Tau Bootis
3.8 MJup
Upsilon Andromedae
0.68 MJup
70 Vir
6.6 MJup
HD 114762
10 MJup
16 Cyg B
1.7 MJup
0
25
50
75
100
Angular separation (MAS at ā=20pcs)
VLT Resolution
VLTI Resolution

Figure 9.5.:

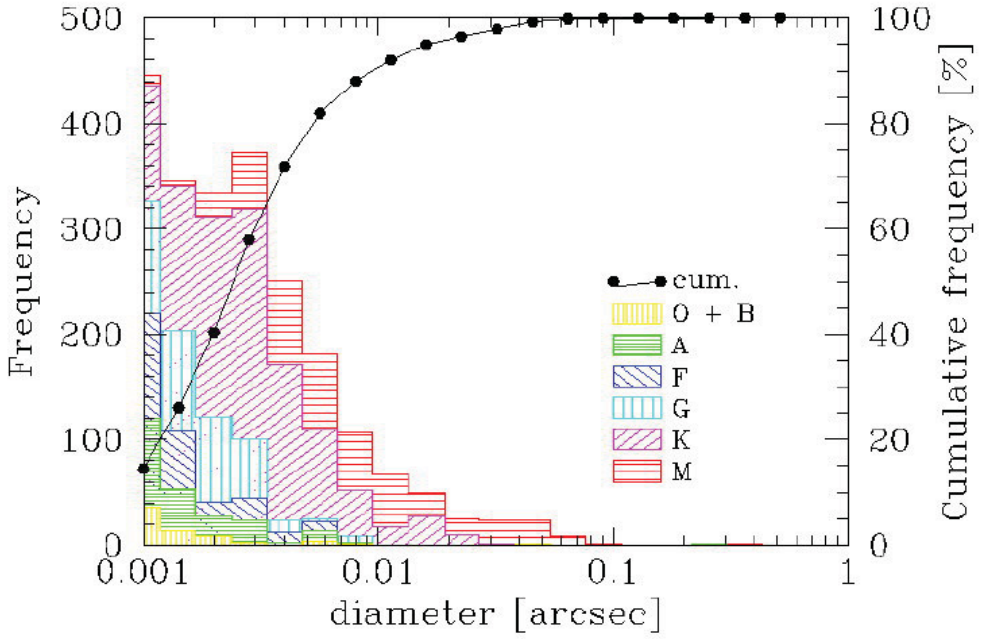
500
400
300
200
100
0
Frequency
100
80
60
40
20
0
Cumulative frequency [%]
0.001
0.01
0.1
1
diameter [arcsec]
cum.
O + B
A
F
G
K
M

Figure 9.6.:

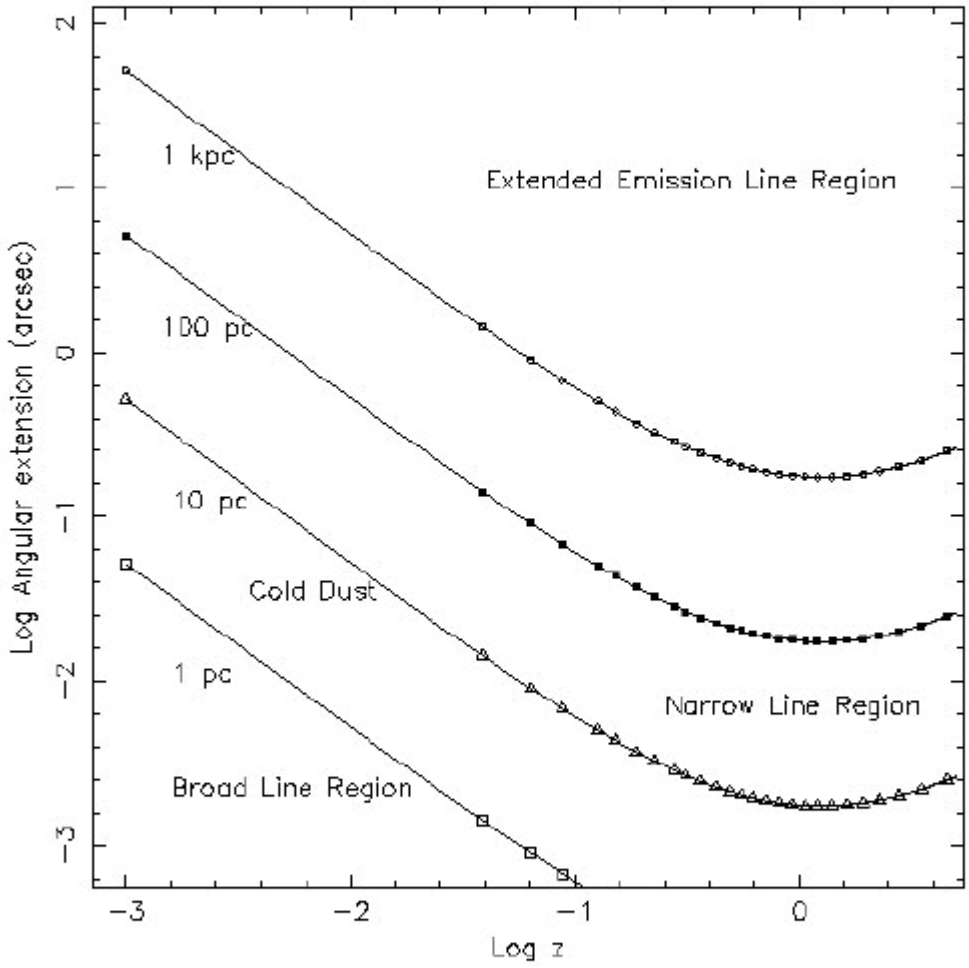
1 kpc
Extended Emission Line Region
100 pc
10 pc
Cold Dust
1 pc
Narrow Line Region
Broad Line Region
Log Angular extension (arcsec)
Log z
2
1
0
−1
−2
−3
−3
−2
−1
0

Figure 9.7.:

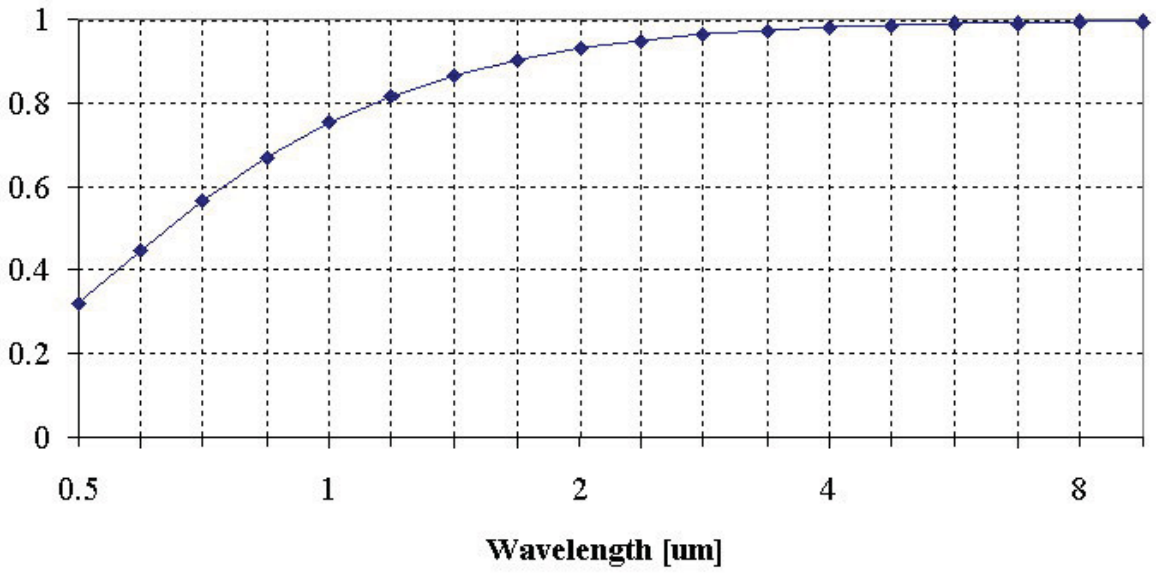

Figure 9.8.:

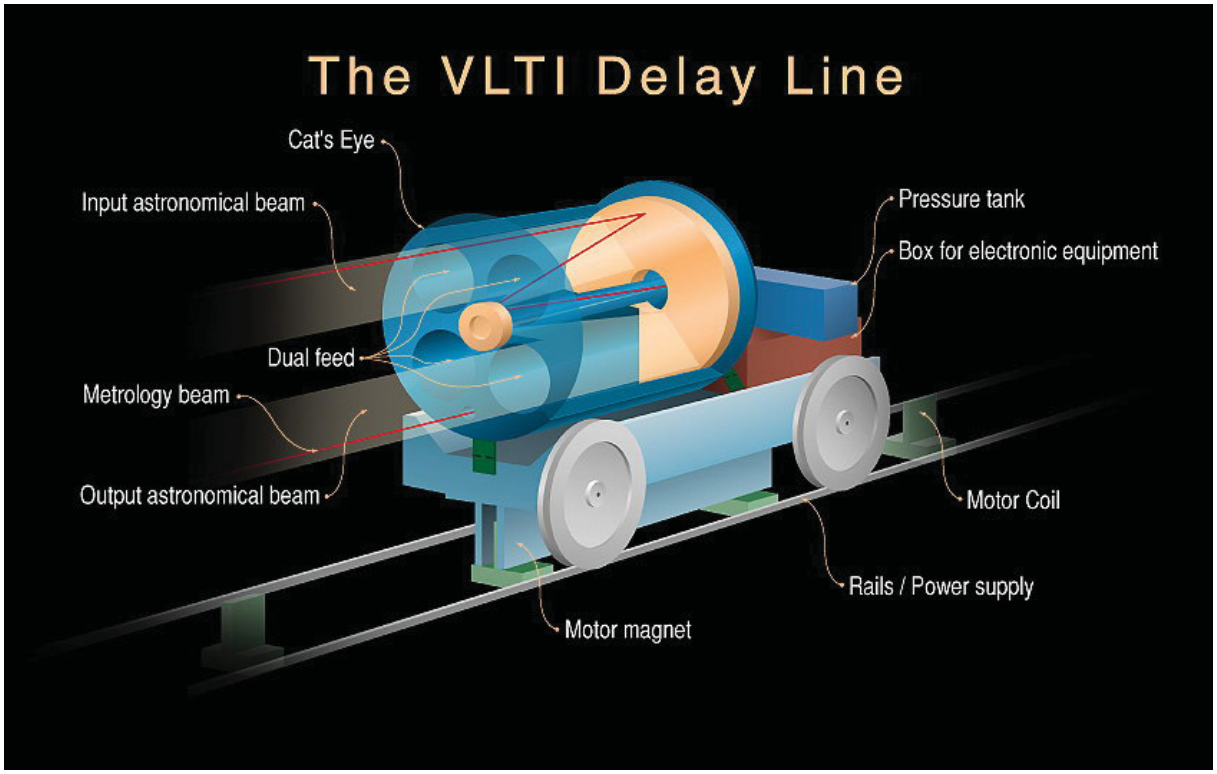

Figure 9.9.:

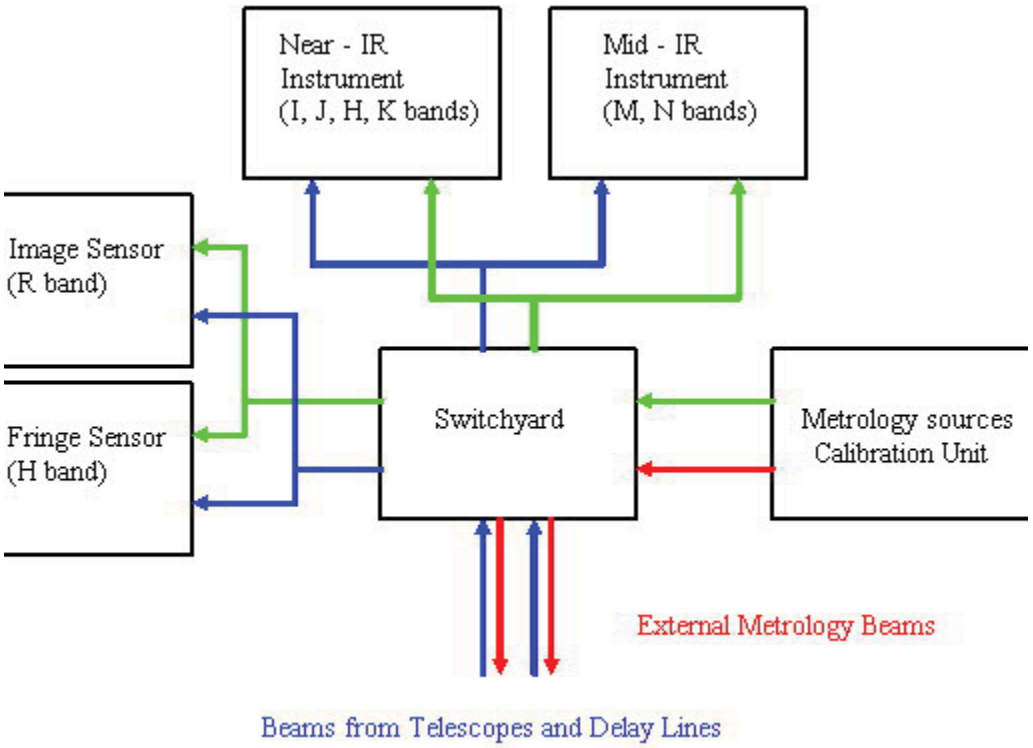

Figure 9.10.:

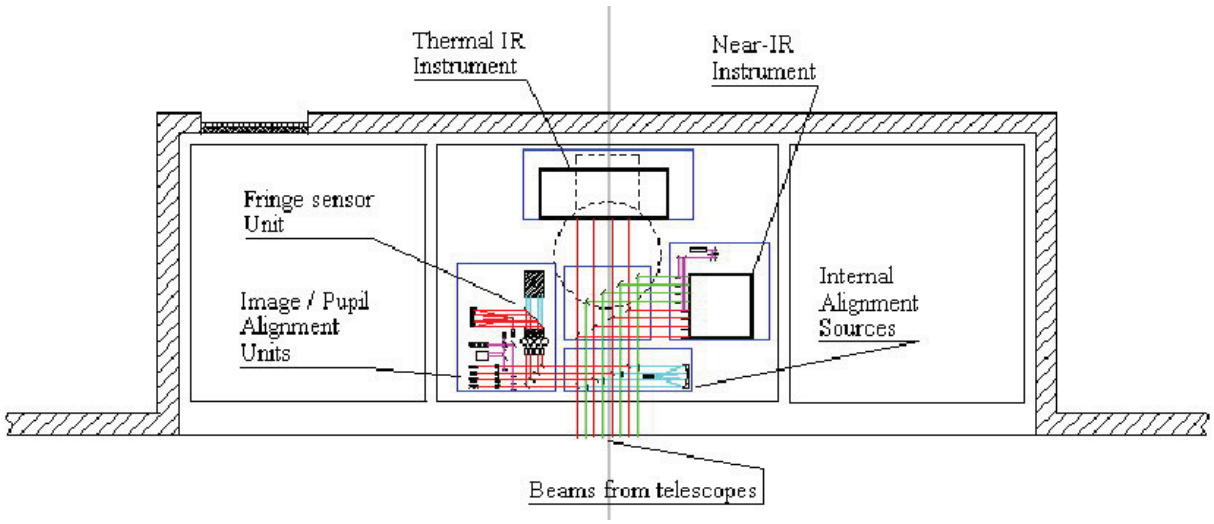

Figure 9.11.:

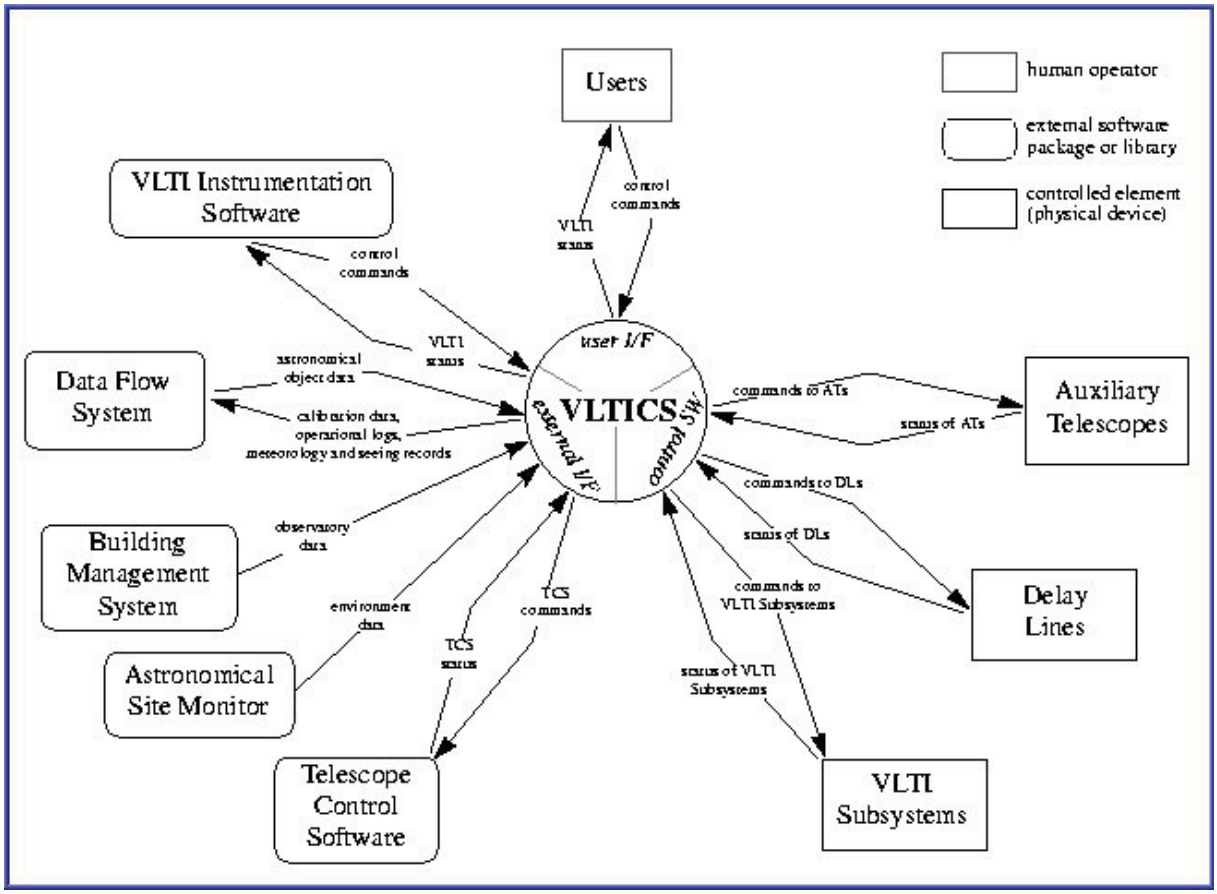

Figure 10.1.:

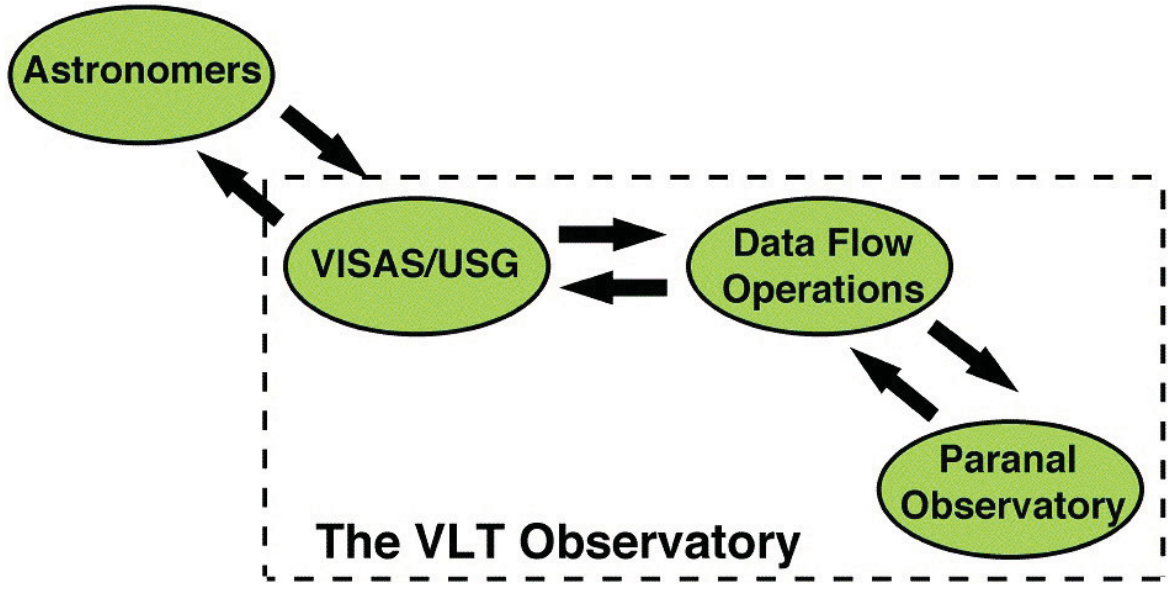

Figure 10.2.:

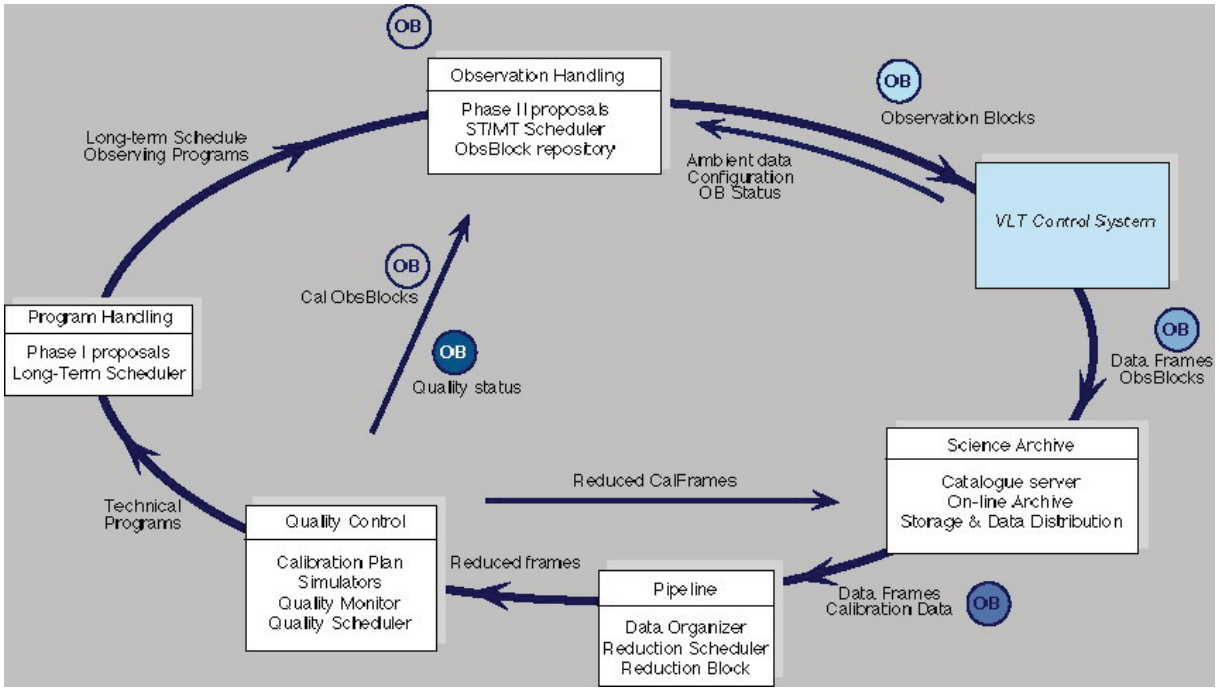

Figure 10.3.:

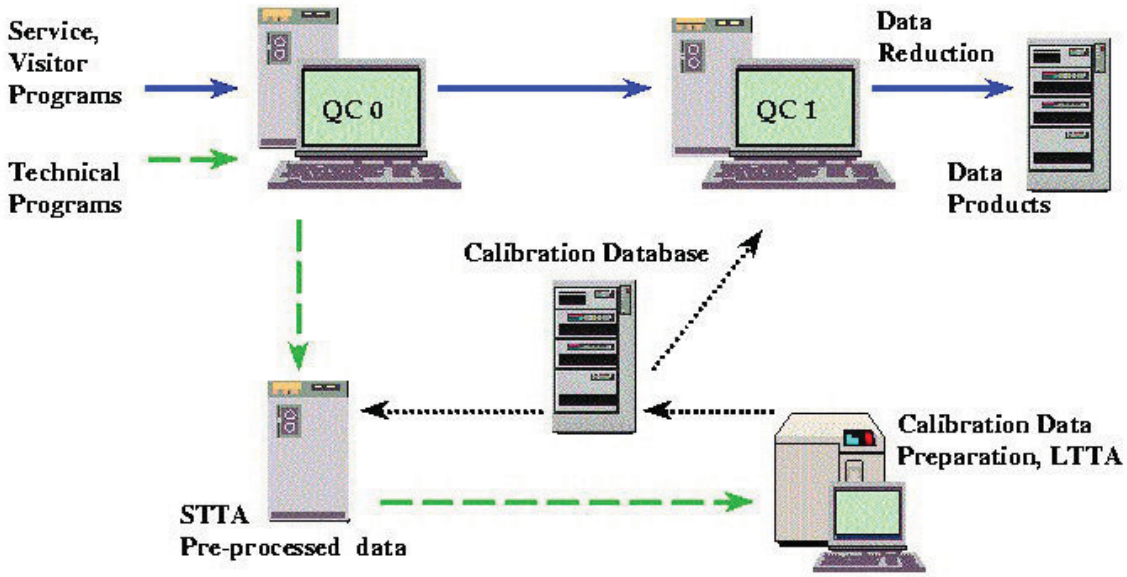

Figure 10.4.:

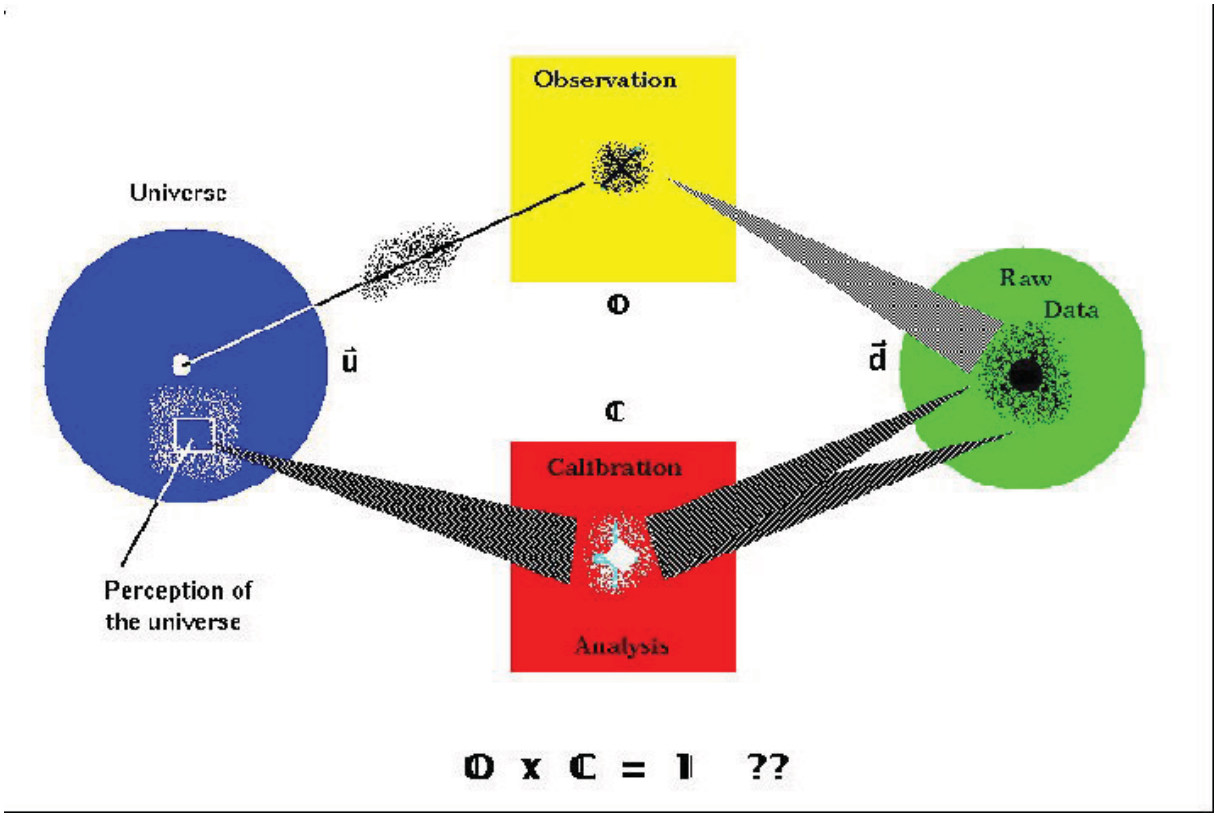

Figure 10.5.:

		1999	2000	2001	2002	2003	2004
UT1	isaac	4	4	4	4	4	4
	fors1	0.5	0.5	0.5	0.5	0.5	0.5
	conica		1.5	1.5	1.5	1.5	1.5
	conica(speckle)		40	40	40	40	40
UT2	TestCam	0.5	0.5				
	uves	2.5	2.5	2.5	2.5	2.5	2.5
	fuegos			2	2	2	2
	fors2		0.5	0.5	0.5	0.5	0.5
UT3	TestCam		0.5	0.5			
	vimos		20	20	20	20	20
	visir			1	1	1	1
UT4	TestCam		0.5	0.5			
	nimos			48	48	48	48
VST	WFI			20	20	20	20
	Typical mix (GB/night)	3.0	19.1	75.6	75.6	75.6	75.6
	TB/Year	1.07	6.80	26.94	26.94	26.94	26.94
	TB cumulative	**1.07**	**7.87**	**34.81**	**61.75**	**88.68**	**115.62**

Figure 10.6.:

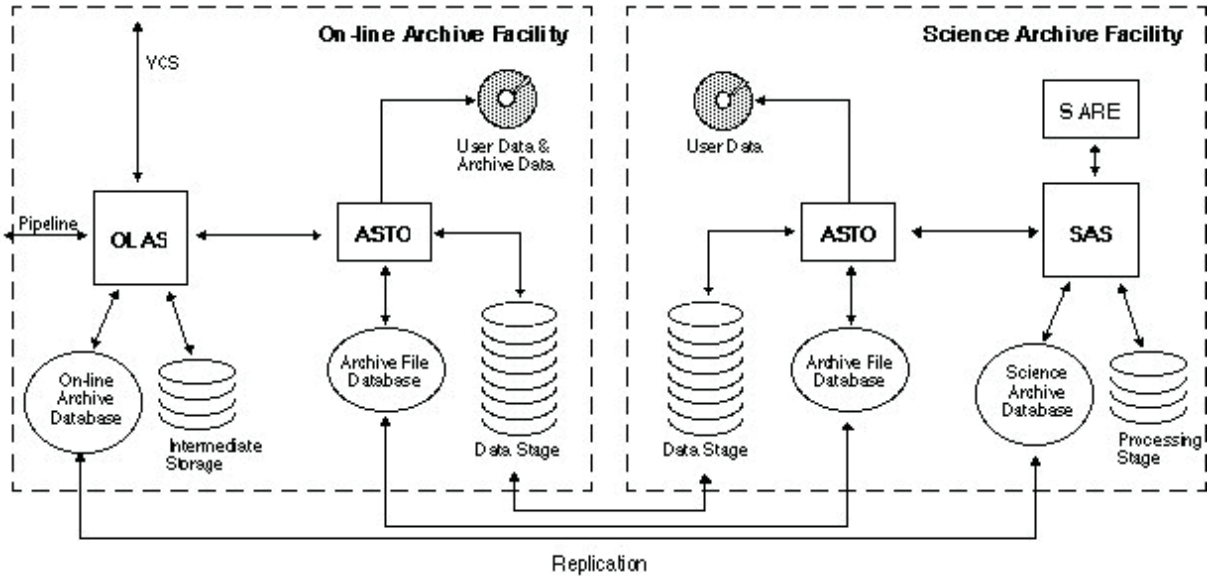
On-line Archive Facility
Science Archive Facility
YCS
User Data &
Archive Data
User Data
S ARE
Pipeline
OLAS
ASTO
ASTO
SAS
On-line
Archive
Database
Intermediate
Storage
Archive File
Database
Data Stage
Data Stage
Archive File
Database
Science
Archive
Database
Processing
Stage
Replication